

SUMOylation and the predicted assembly of a plant NuRD-like repressor complex

Alastair Robert Plant

Submitted in accordance with the requirements for the degree of
Doctor of Philosophy

The University of Leeds
School of Biology

September 2018

The candidate confirms that the work submitted is his/her own and that appropriate credit has been given where reference has been made to the work of others.

This copy has been supplied on the understanding that it is copyright material and that no quotation from the thesis may be published without proper acknowledgement.

The right of Alastair Robert Plant to be identified as Author of this work has been asserted by him in accordance with the Copyright, Designs and Patents Act 1988.

Acknowledgements

I am indebted to all those I have worked with at Leeds for their kindness, patience and wisdom. Thank you to Brendan Davies for giving me this opportunity and for contributing so much time and thought to my project. Special thanks go to Barry Causier for answering more than his fair share of technical questions. Thank you to Jelena Kusakina, Antoine Larrieu and Richa Yeshvekar, as well as past lab members who have made the lab a nice place to work. Thanks also to those around the department who have offered scientific discussion, advice, support and good company, especially Daria Pastok, who always makes me smile and gives me hope for the future.

Thanks go to those who has provided training, technical support and services, including everyone in the Denecke lab for their help with the transient expression assays, the Mass Spectrometry Facility for their work on peptide identification, and Zhu, Zhang et al for sharing their mutant lines. Thank you to the BBSRC for providing financial support for myself and my fellow students. Thank you to those involved in White Rose Doctoral Training Partnership for adding to my opportunities and experiences as a student. Thank you to the staff in the Graduate Office and elsewhere around the university for taking good care of us. To everyone, good luck and have fun! There are more things to discover!

Abstract

TOPLESS and TOPLESS-RELATED protein are members of a conserved family of plant co-repressors. They act as general co-repressors to promote transcriptional repression. Loss of TOPLESS-mediated repression radically affects development and other central processes. Repression via TOPLESS is dependent on the activity of histone deacetylases, but direct interaction between the two has not been observed, although both TOPLESS and HISTONE DEACETYLASE 19 interact with proteins shared with the animal Nucleosome Remodelling and histone Deacetylation complex. Some interactions between co-repressors and histone deacetylases are dependent on the involvement of SMALL UBIQUITIN-LIKE MODIFIERS. TOPLESS and TOPLESS-RELATED proteins are reported to be SUMOylated. The floral phenotype of loss-of-function *tpl-1* mutants is enhanced by the SUMO ligase mutant *siz1-2*. Abnormal *tpl-1* flowers are not seen after crossing *tpl-1* mutants with mutants of the SUMO proteases OVERLY TOLERANT TO SALT 1 and 2. Mutations at predicted SUMOylation sites within TOPLESS affect its ability to complement *tpl-1* embryonic phenotypes and abolish recovery of a high molecular-weight protein, potentially a TOPLESS-SUMO conjugate. Attempts to co-precipitate SUMOylated TOPLESS and NuRD-associated proteins did not recover an intact complex but provided evidence to support heteromeric interactions between TOPLESS and TOPLESS-RELATED proteins. Additionally, the chromatin regulator SPLAYED was identified as a potential interactor or antagonist. Development of novel *topless* and *topless-related* mutant combinations shed light on the functional redundancy of family members and has created a platform for improved complementation assays. Additionally, discovery of an unreported root phenotype in the mutants will allow use of a more quantitative approach to phenotypic scoring. Phylogenetic analysis reveals the absence of a conserved subclade of the TOPLESS family from *Arabidopsis* with implications for evolutionary and functional comparisons with other species, but suggests long-term conservation of a candidate SUMOylation site. SUMO may be involved in regulating TOPLESS function across plants.

Table of Contents

Acknowledgements	iii
Abstract	iv
Table of Contents	v
List of Tables	x
List of Figures	xi
1 Introduction	1
1.1 Gene expression in plant development.....	1
1.1.1 Transcriptional regulation.....	1
1.1.2 The role of chromatin structure and histone modifications in regulating gene expression.....	1
1.1.2.1 Post-translational modifications.....	2
1.1.2.2 Histone acetylation and deacetylation.....	3
1.1.2.3 Histone deacetylation complexes.....	5
1.1.2.4 The Sin3 complex.....	6
1.1.2.5 The NuRD complex.....	7
1.1.2.6 Conservation of Sin3 and NuRD components in plants.....	8
1.2 The TOPLESS family of co-repressors.....	8
1.2.1 The <i>tpl-1</i> phenotype.....	8
1.2.2 The structure and function of TOPLESS and TOPLESS-RELATED proteins.....	10
1.2.2.1 Domain functions.....	11
1.2.3 Evolutionary origins and conservation of TOPLESS.....	12
1.2.4 The TOPLESS interactome.....	13
1.2.5 The putative TOPLESS complex.....	14
1.2.6 The potential role of SUMOylation.....	16
1.2.7 The plant SUMOylation pathway.....	19
1.2.8 SUMO functions.....	21
1.3 Aims of this thesis:.....	23
2 Materials and Methods	24
2.1 Nucleic acids.....	24
2.1.1 DNA extraction.....	24
2.1.2 Oligonucleotide synthesis.....	24

2.1.3 RNA extraction	24
2.1.4 Gel electrophoresis	25
2.1.5 Gel extraction	25
2.1.6 PCR purification	25
2.1.7 PEG precipitation	25
2.1.8 DNA restriction	25
2.1.9 DNA ligation	26
2.2 Cloning	26
2.2.1 Gateway cloning (single and multi-fragment)	26
2.2.2 Transformation of <i>Agrobacterium</i> by electroporation.....	26
2.2.3 Transformation of chemically-competent <i>E. coli</i> by heat shock.....	27
2.2.4 Transformation of chemically-competent <i>Saccharomyces cerevisiae</i> by heat shock	27
2.2.5 Plasmid minipreps	27
2.2.6 Plasmid midipreps	27
2.3 Growth media	28
2.3.1 LB	28
2.3.2 SD	28
2.3.3 YPDA.....	28
2.3.4 MS agar.....	28
2.4 Yeast hybrid assays	29
2.5 Phylogenetic analysis.....	29
2.5.1 Protein sequence alignment.....	29
2.5.2 Phylogeny assembly by Neighbour-joining and UPMGA....	29
2.5.3 Bayesian analysis with MrBAYES3.2.6 via CIPRES	29
2.5.4 Phylogenetic tree drawing with FigTree 1.4.3.....	29
2.6 Plant growth conditions	30
2.6.1 Growth of <i>Arabidopsis thaliana</i> in greenhouse conditions	30
2.6.2 Germination of <i>Arabidopsis thaliana</i> in growth cabinets.....	30
2.6.3 Germination of <i>Arabidopsis thaliana</i> in sterile conditions	30
2.6.4 Growth of <i>Nicotiana benthamiana</i> and <i>tabacum</i> in greenhouse conditions	30
2.6.5 Growth of <i>Nicotiana benthamiana</i> in sterile conditions	30
2.6.6 Heat shock treatment for <i>Arabidopsis thaliana</i>	31

2.7	Plant transformation	31
2.7.1	Floral dip transformation of <i>Arabidopsis thaliana</i>	31
2.7.2	Transient gene expression in <i>Nicotiana tabacum</i> by leaf infiltration	31
2.7.3	Transformation of <i>Nicotiana benthamiana</i> protoplasts	31
2.8	Sequence analysis	31
2.9	Image processing.....	32
2.9.1	Photography	32
2.9.2	Measurement from images.....	32
2.10	Identification of repression domain-containing proteins	32
3	The function of TOPLESS is regulated by SUMOylation	33
3.1	Introduction	33
3.1.1	Co-repressors are regulated via post-translational modifications	33
3.1.2	SUMOylation is a potent modifier associated with protein regulation	34
3.1.3	TOPLESS and associated regulatory proteins are SUMOylated.....	37
3.1.4	Aims	38
3.2	Methods	38
3.2.1	Assembly of mutants by crossing	38
3.2.2	Assembly of constructs for plant transformation.....	39
3.2.3	Protein extraction under mildly denaturing and denaturing conditions	40
3.2.4	Yeast hybrid vector assays.....	41
3.2.5	4-MUG and PNPG assays.....	41
3.2.6	Quantitative PCR.....	42
3.3	Results	42
3.3.1	Identification of candidate SUMOylation sites in TOPLESS.....	42
3.3.2	TOPLESS may have multiple SUMOylation states	43
3.3.3	SUMOylation may facilitate interaction between TOPLESS and HDA19	48
3.3.4	The phenotype of <i>tpl-1</i> mutants is enhanced in a SUMOylation-deficient background.....	52
3.3.5	Complementation of <i>tpl-1</i> with wild type and candidate SUMOylation site mutants.....	59
3.3.6	Repression assays in transient expression systems	63

3.3.7	Repression assays in <i>Arabidopsis thaliana</i>	66
3.4	Discussion	69
3.4.1	Partial complementation of <i>tpl-1</i> by reduction in SUMO turnover supports a model of stabilisation or enhancement of activity for TPL SUMOylation	69
3.4.2	Transient expression assays produce consistent results but may indicate sequestration of repressors	69
3.4.3	The <i>Arabidopsis</i> repression assay system shows that the conserved candidate SUMOylation site, K282, is functionally important for TPL-mediated repression	70
3.4.4	TOPLESS may be SUMOylated at multiple positions	72
4	TOPLESS interacts with TOPLESS-RELATED proteins and chromatin regulators	74
4.1	Introduction	74
4.1.1.1	TOPLESS may act a component of the histone deacetylation complex	74
4.2	Methods	78
4.2.1	Cross-linking with formaldehyde and disuccinyl suberate	78
4.2.2	Protein extraction to preserve SUMOylation	79
4.2.3	SDS-PAGE and Western blotting	79
4.2.4	Peptide analysis by mass spectrometry	81
4.3	Results	81
4.3.1	TOPLESS-RELATED proteins co-precipitate with TOPLESS	81
4.3.2	TOPLESS associates with histones and chromatin regulators	83
4.4	Discussion	87
3.4.5	Co-precipitation of TPRs with TPL	87
3.4.6	TPL co-localises with histone H4	88
3.4.7	Potential interactions between TOPLESS and chromatin remodellers	88
5	Mutants of TOPLESS and TOPLESS-RELATED 1-4 have a phenotypic range resembling <i>tpl-1</i>	91
5.1	Introduction	91
5.1.1	Individual <i>tpl</i> and <i>tpr1/2/3/4</i> mutants lack conspicuous phenotypes	91
5.2	Methods	95
5.2.1	Phylogenetic analysis	95

5.2.2	Assembly of <i>tpr2 tpr3</i> and additional multiple mutants	96
5.2.3	Embryonic and root phenotyping	97
5.2.4	Floral phenotyping	98
5.3	Results	98
5.3.1	Embryonic and vegetative phenotypes	98
5.3.2	Floral phenotypes	100
5.3.3	Root phenotypes	104
5.3.4	Novel mutants display <i>tpl-1</i> -like phenotypes	113
5.3.5	Phylogenetic relationships within the TPL family	118
5.4	Discussion	124
5.4.1	Complementation and redundancy	124
5.4.2	Developmental phenotypes	126
5.4.2.1	Floral development	126
5.4.2.2	Root architecture	127
5.4.3	Evolution of TPL/TPRs	129
6	General Discussion	131
6.1	SUMO as a master regulator	131
6.2	SUMOylation as a positive regulator of TOPLESS-mediated repression	132
6.3	Conclusions	138
	List of References	140
	List of Abbreviations	164
	Appendix A Identification of Repression Domains in annotated transcription factors	169
	Example code	169
	Appendix B Low-scoring proteins represented by peptides co-precipitating with HA-TOPLESS	175
	Appendix C Oligonucleotides used in this thesis	184
	Appendix D Constructs used in this thesis	187

List of Tables

Table 4-1. Proteins co-precipitating with HA-TOPLESS.	81
Table 4-2. Proteins co-precipitating with HA-TOPLESS after cross-linking with 0.1% FA.	83
Table 4-3. Proteins precipitating from anti-HA immunoprecipitation from untransformed wild type <i>Arabidopsis thaliana</i>.....	83
Table 4-4. Proteins co-precipitating with HA-TOPLESS cross-linked with 1% FA.....	83
Table 4-5. Proteins co-precipitating with DSS-cross-linked HA-TOPLESS..	83
Table 5-1. Mutants used to assemble <i>tpl tpr1 tpr3 tpr4</i> and other mutants in Krogan et al. (2012) and to create novel mutant combinations used in this thesis.....	97
Table 5-2. Summary of <i>tpl/tpr</i> mutants described in this thesis and elsewhere.....	99
Table B-0-1. Full list of proteins represented by peptide co-immunoprecipitated by HA-TOPLESS using cross-linking with DSS.	179
Table C-0-1. List of oligonucleotides used in this thesis and their applications.	186
Table D-0-1. List of constructs used in this thesis.....	189

List of Figures

- Figure 1-1. A model of the effect of acetylation and deacetylation on nucleosomes.** Nucleosomes consist of an octamer of histones (two sets of H2A, H2B, H3 and H4) around which the DNA is coiled. Some post-translational histone modifications such as acetylation (-COCH₃) favour an open, euchromatic state by reducing histone-DNA affinity and increasing nucleosome spacing (top). Deacetylation favours a compacted, transcriptionally inactive heterochromatic structure (bottom). 3
- Figure 1-2. The animal Nucleosome Remodelling and histone Deacetylation (NuRD) complex and analogous or homologous components in plants.** (A) The NuRD complex is a multi-protein complex that promotes transcriptional repression via histone deacetylation. Several components of the complex NuRD complex are post-translationally modified with small ubiquitin-like modifiers (SUMOs) (marked 'S'). (B) The plant co-repressor TOPLESS interacts with homologues of NuRD complex components and may form an analogous regulatory complex (colour coding indicates homology). Plants lack analogues of some NuRD proteins, e.g. p66 (purple) and MTA1 (dark blue). TOPLESS could potentially act as an alternative to these missing components but its functions are not directly comparable. As in NuRD, TOPLESS and several of its interacting proteins are SUMO substrates. 6
- Figure 1-3. Early developmental phenotypes of *tpl-1* mutants.** (A) Seedlings exhibit varying degrees of fusion of cotyledons, ranging from formation of a radially symmetrical cup through production of a single cotyledon to wild type phenotypes (the latter not shown). The monocotyledonous phenotype is not universally fatal as some seedlings initiate a shoot apical meristem (A, white arrowhead) and produce leaves. (B) The 'topless' phenotype, where the embryo forms two root axes (white arrows) instead of a root and a shoot is rare (~1/900) (Szemenyei et al., 2008). 9
- Figure 1-4. Domain structure of TOPLESS-like proteins.** LisH, CTLH and CRA domains at the N-terminus are required for binding transcription factors and for dimerisation and tetramerisation between TOPLESS monomers (Ke et al., 2015; Martin-Arevalillo et al., 2017). These domains are folded to form grooves and interaction surfaces for these respective interactions. The C-terminal WD40 repeat clusters are predicted from similar primary protein structures to form two seven-bladed β -propellers (Szemenyei et al., 2008) (not to scale). Residue numbers are annotated according to *Arabidopsis thaliana* TOPLESS (AtTPL). 10

Figure 1-5. Overview of the SUMOylation pathway in plants.

SUMOylation requires a cascade of enzymatic reactions. The precursor SUMO protein is cleaved by ULP class SUMO proteases to remove a C-terminal peptide, exposing a diglycine motif. The mature SUMO is then bound by thioesterification (-S-) to an E1 heterodimer which adenylates the SUMO. The SUMO is transferred to the E2 conjugating enzyme, from which it is conjugated to a lysine residue within the substrate protein, with or without the assistance of an E3 SUMO ligase. Substrate proteins can be deSUMOylated by SUMO proteases. Additionally, *Arabidopsis* SUMOs 1 and 2 can themselves be SUMOylated by PIAL SUMO ligases (E4), allowing for formation of SUMO chains (Tomanov et al., 2018a). DeSUMOylation is performed by ULPs and by Desi proteins. Desi proteins differ in their catalytic site to SP-RING (ULP) type proteases and perform deSUMOylation but not SUMO maturation (Orosa et al., 2018)..... 18

Figure 3-1. Candidate SUMOylation sites in the TOPLESS protein aligned to TPL-like proteins from taxa across the plant kingdom.

No canonical SUMOylation site motifs are present in AtTPL. SUMOplot predicted high-probability SUMOylation sites in AtTPL at K282, K339 and K414, with predicted probabilities of 0.8, 0.74 and 0.82, respectively. K282 has been conserved from algae to flowering plants. AtTPL is phosphorylated at T286, adjacent to the candidate SUMOylation site. This residue (and, potentially, phosphorylation) is also conserved. K339 is present only in AtTPL and its sister protein AtTPR1. K414 is broadly conserved but has been lost in AtTPR4. (At = eudicot; *Arabidopsis thaliana*; Os = monocot *Oryza sativa*; Pp = moss *Physcomitrella patens*; Mp = liverwort *Marchantia polymorpha*; Kn = streptophyte alga *Klebsormidium nitens*; Ps = chlorophycean alga *Picocystis salinarum*.)..... 43

Figure 3-2. Immunoprecipitation of TOPLESS protein.

Immunoprecipitation of HA-tagged TOPLESS proteins from flowering *Arabidopsis thaliana* plants. Western blots for HA-TPL from immunoprecipitation (A, C) and crude extracts (B) from wild type Ler and transgenic Ler and *tpl-1* lines. HA-TPL and versions containing mutations at candidate SUMOylation sites K282 and K339 both generate reproducible fragmentation patterns. Additional high molecular weight bands (black arrows) were observed in one blot and may represent post-translationally modified HA-TPL. No non-specific signal was observed for wild type control precipitations. TOPLESS is phosphorylated (Reiland et al., 2009) and SUMOylated (Miller et al., 2010; Rytz et al., 2018). Rytz et al. (2018) demonstrated that a similar single high-molecular-weight band from TPL-HA immunoprecipitations contained SUMO1/2 proteins. It is unclear if two of the three high-molecular-weight bands are identical in size. Mutation of K282 to prevent SUMOylation may influence other post-translational modifications (e.g. phosphorylation at the neighbouring T286 site) to change the molecular weight of TOPLESS. The failure to recover one band for HA-TPL K282R may indicate abolition of SUMOylation at K282 but may instead reflect low yield of intact protein. Western blotting the same membrane with anti-SUMO1/2 antibody (AB) after stripping the anti-HA AB generated excess background signal and subsequent Western blots using the plant anti-SUMO1/2 AB (ab5316, Abcam) also displayed low target specificity. 46

Figure 3-3. Western blots of SUMOylated *Arabidopsis thaliana* proteins.

SUMOylated proteins were precipitated from wild type Col, *siz1-2* mutants and Col expressing *35S::mCherry-TPL-3xFLAG* ('TPL-FLAG') that had been incubated at room temperature ('Mock') or heat shocked at 37°C. SUMOylated proteins were precipitated from wild type Col, *siz1-2* mutants and Col expressing *35S::mCherry-TPL-3xFLAG* ('TPL-FLAG') that had been incubated at room temperature ('Mock') or heat shocked at 37°C. Low-molecular-weight proteins (likely free SUMO or E1/E1/E3 SUMO conjugates) are not completely captured and are detectable in the fractions discarded from the precipitation (left images, A and B). Additional high-molecular weight bands are detectable with anti-SUMO antibody (AB) in the captured (SUMOylated) fraction for Col and TPL-FLAG but not for *siz1-2*. This effect is more pronounced for heat-shocked protein. Probing TPL-FLAG with anti-FLAG AB identified one high-molecular weight band appearing after heat shock but the molecular weight markers indicate a discrepancy between this band and the expected size of full-length TOPLESS. Marker = Color Prestained Protein Ladder, Broad Range (New England Biolabs). 48

- Figure 3-4. The yeast hybrid system using the bipartite Gal4 activation domain (AD)/binding domain (BD) system.** Transcription of the histidine biosynthesis gene His3 is required for the survival of yeast on histidine-deficient media. Fusion of Gal4BD to a protein of interest (the 'bait') allows its recruitment to the GAL promoter, upstream of His3. Interaction between the bait protein and a 'prey' protein which is fused to Gal4AD induces activation of His3. Where no interaction occurs (A), the yeast is not viable on selective (-H) media. Some proteins may not interact directly (B) but may associate with one another in the presence of an additional protein (e.g. SUMO, 'S') in three-hybrid assays (C). 49
- Figure 3-5. SUMO-conjugating enzyme SCE1 does not enable interaction between TPL/TPR proteins and HDA19 in yeast three-hybrid assays.** Failure to survive on histidine-free selective media with a minimal concentration of His3 inhibitor 3-AT to prevent auto-activation (right panel) indicates absence of interaction. Positive (+) control = BD-UPF1+AD-SMG7; negative (-) control = BD-TPL (control lines kindly provided by B. Causier). 50
- Figure 3-6. Yeast three-hybrid assay for TPL, HDA19 and the transcription factor EPR1.** EPR1, a transcription factor that interacts with all *Arabidopsis* TPL/TPR proteins (Causier et al., 2012a), does not enable interaction between TPL and HDA19 in yeast three-hybrid assays. Positive and negative controls shown in Figure 3-5. 51
- Figure 3-7. Yeast two-hybrid assays for interaction between TPL and HDA19.** TPL and HDA19 do not interact directly. Fusing SUMO to TPL enables only a weak interaction with HDA19. Positive (+) control = BD-UPF1+AD-SMG7; negative (-) control = BD-TPL (control lines kindly provided by B. Causier). 51
- Figure 3-8. Phenotypes of Col, Ler and *tpl-1* plants grown at 27°C.** In addition to floral defects, *tpl-1* often produces a small, disorganised rosette. The transition from vegetative to reproductive growth also occurs earlier in *tpl-1* than wild type plants, hence the presence of siliques. 53
- Figure 3-9. Vegetative and floral phenotypes in *siz1-2* and *siz1-2 tpl-1* mutants grown at 27°C.** The *siz1-2* mutant is dwarfed (A) (n=8) compared to wild type Col and Ler. Dwarfism is retained in *siz1-2 tpl-1*^{+/+} heterozygotes (B) (n=2) and *siz1-2 tpl-1* (C) (n=2), which also produce disordered rosettes as seen in *tpl-1*. While *siz1-2* and *siz1-2 tpl-1*^{+/+} produced small but morphologically normal flowers, *siz1-2 tpl-1* double homozygotes displayed abnormal floral phenotypes more severe than those seen in *tpl-1* mutants (Figure 3-7) grown alongside them. Floral abnormalities were not observed in wild type Ler and Col control plants (Figure 3-8). 56

- Figure 3-10. Phenotypes *ots1 ots2 x tpl-1* crosses at 27°C.** Unlike *ots1 ots2* (n = 8), the *ots1 ots2 tpl-1*^{+/-} (n = 2) and *ots1 ots2 tpl-1* (n = 2) mutants produced a *tpl-1*-like disordered rosette (B, C) but no abnormal floral phenotypes were observed (H, I). Scales for upper images represent 20mm. 57
- Figure 3-11. Complementation of *tpl-1* embryonic phenotypes with *pTPL::TPL* in T1 transformants.** The seedling phenotype of *tpl-1* ranges from the rare double root (DR) phenotype to formation of a radially symmetrical pin, cup or tube (red) to a single cotyledon (green) to morphologically abnormal cotyledons (purple) to wild type (blue) and can be scored based on these categories (Szemenyei et al., 2008). The frequency of severe phenotypes in *tpl-1* seedlings is improved by introduction of the *pTPL::TPL* by transformation. Mutations in candidate SUMO acceptor lysine residues (K282 and K339) diminish this effect. 61
- Figure 3-12. Assay for TOPLESS-mediated repression in infiltrated tobacco leaves.** The *tCUP::TPL-Gal4BD* ('TPL') construct enhances expression of the *2xUAS-35S::GUS* reporter compared to a reporter control ('GUS') in leaf discs sampled from *Nicotiana tabacum* leaves three, six and nine days (DPI) after transformation with both constructs. Catalysis of the substrate 4-MUG yields fluorescent 4-MU (Y-axis). Mutations in candidate SUMOylation sites (K282R K339R K414R) ('-SUMO') diminish this effect at the latter two time points. Values indicate Optical Density of infiltrated cultures at 600nm. Reporter-only controls using increasing concentrations of *Agrobacterium* indicate that fluorescence correlates positively with the number of *Agrobacterium* cells used. This theoretically approximates the number of cells transformed, i.e. the level of expression. Infiltration with TPL constructs alone did not induce GUS-like activity. 64
- Figure 3-13. Assay for TOPLESS-mediated repression in tobacco protoplasts.** Wild type *tCUP::TPL-Gal4BD* ('TPL') enhances expression of the *2xUAS-35S::GUS* ('GUS') reporter in transformed *Nicotiana benthamiana* protoplasts compared to a reporter control ('GUS') but mutations in candidate SUMOylation sites (K282R K339R K414R) ('TPL-SUMO') diminish this effect. The GUS reporter catalyses the transparent substrate PNPG to visible NPG, allowing measurement by spectrophotometry. Bars indicate independent transformations, normalised to the optical density of a reaction mixture lacking the PNPG substrate. 66
- Figure 3-14. *Arabidopsis* GUS reporter activity assay.** A 4-MUG assay to test the TPL-Gal4BD/UAS-GUS system in *Arabidopsis* demonstrated that GUS activity was low in plants transformed with the repressor but also identified variable levels of GUS expression in the control plants. (Light intensity indicates fluorescence of 4-MU produced by GUS catalysis of 4-MUG.) 67

Figure 3-15. QPCR for reporter expression in the TPL-Gal4BD/GUS repression assay. Expression of the TPL-Gal4BD repressor (top chart) with the strong constitutive promoter 35S reduces expression *UAS-UAS-35S::GUS* ('No repressor'). Use of a weaker constitutive promoter, *tCUP*, decreases reporter expression to a lesser extent. A non-synonymous mutation at a candidate SUMOylation site in TPL (K282R) reduces the ability of TPL-Gal4BD to act as a repressor. Intensity of repression was not dependent of the level of expression of the repressor (bottom chart). In fact, an inverse relationship was observed, indicating that an increased dose of TPL-Gal4BD K282R is insufficient to compensate for its reduced ability to repress. 68

Figure 3-16. Models of interactions in the repression assay and potential problems. (A) Wild type TPL-Gal4BD suppresses expression of the *GUS* reporter. (B) Predicted abolition of SUMOylation at K282 decreases the ability of TPL to repress targets. (C) Saturation of HDA19 with excess TPL-Gal4BD interferes with baseline chromatin regulation, leading to a general increase in histone acetylation ('Ac') and gene expression. (D) Reducing SUMOylation of TPL-Gal4BD (e.g. by mutating SUMOylation sites) decreases its affinity for histone deacetylases, allowing them to participate in other regulatory interactions (e.g. binding the co-repressor LEUNIG and the MEDIATOR regulatory complex). 72

Figure 4-1. Unique peptides representing TOPLESS-RELATED proteins co-elute with HA-TOPLESS. Some peptides overlap between TPL family proteins due to sequence conservation but unique peptides were identified for TPL, TPR1 and TPR4. 82

Figure 5-1. Neighbour-joining tree of *Arabidopsis* TOPLESS and TOPLESS-RELATED proteins. *Arabidopsis* TPL/TPRs form two subclades. Branch lengths indicate that AtTPL and AtTPR1 may be the products of a recent gene duplication. Node values indicate bootstrap support expressed as a percentage. Sequences aligned with L-ins-I algorithm on MAFFT 7, bootstrap run with 1000 iterations. 93

Figure 5-2. The floral phenotype of Ler wild type and *tpl-1* flowers at 27°C. Ler flowers (A, C) follow the (4, 4, 4+2, 2) floral plan associated with the wild type while *tpl-1* flowers (B, D) frequently display organ identity defects, e.g. petaloid sepals (red arrowheads); whorls are less tightly arranged and flowers appear more open. 101

Figure 5-3. Floral organ numbers in *tpl/tpr* mutants at 20°C.
Stamen number was significantly reduced in *tpl tpr1 tpr4* mutants compared to the wild type (ANOVA $f = 44.4$, $p < 0.001$; Tukey's HSD $Q = 12$, $p < 0.001$). Sepal number also increased significantly versus wild type Col-0 (ANOVA $F = 8.59$, $p < 0.001$; Tukey's HSD $Q = 5.49$, $p < 0.01$). The *tpr2 tpr3* mutants were not significantly different from wild type. The *tpl-1* mutants displayed morphological abnormalities (splayed floral organs) but did not differ significantly in organ number from other backgrounds. All mutants produced an insignificant minority of floral organs with altered identities, i.e. sepals with petaloid sectors and petaloid stamens 102

Figure 5-4. Floral organ numbers in *tpl tpr1 tpr4* at 20°C and 27°C.
Flowers developing at elevated temperatures did not differ significantly in organ number from those grown at 20°C (t-tests: sepals – $t = -1.00$, $p < 0.16$; petals – $t = -.12$, $p < .67$; stamens – $p < 0.25$), suggesting that temperature sensitivity may specific to the *tpl-1* allele..... 103

Figure 5-5. Root length of *tpl/tpr* mutants grown without sucrose at six days post-germination. Plants were grown on ½ MS agar without sucrose. The primary root of *tpl-1* (Ler background) was shortened by a statistically significant amount (ANOVA $f = 9.03$, $p < 0.001$; Tukey's HSD $Q = 6.38$, $p < 0.01$) whereas *tpl-2* (Ler background) and the multiple *tpl/tpr* mutants (Col-0 background) do not differ significantly from their respective wild types..... 105

Figure 5-6. Primary root length at 7 days post germination on ½ MS agar supplemented with 2% sucrose. The short primary root phenotype of *tpl-1* is complemented by the addition of sucrose to the medium. There is no significant difference between groups (one-way ANOVA; $f = 2.43$; $p < 0.116$; $n = 4$ for each treatment)..... 106

Figure 5-7. Numbers of lateral roots produced by wild type plants and *tpl* mutants at seven days post-germination. ($n = 4$ per treatment.) Plants were grown on ½ MS agar supplemented with 2% sucrose. In both *tpl-1* and the non-dominant mutant *tpl-2*, lateral root number was highly variable. Significant differences between mutants were not detectable due to variance and sample size (ANOVA $f = 0.59$, $p < 0.6325$)..... 107

Figure 5-8. Root hair density in *tpl* mutants. Root hairs per 200µm on primary roots at 7 days post germination on ½ MS agar supplemented with 2% sucrose. No significant difference was observed between groups..... 108

Figure 5-9. Root architecture of <i>tpl/tpr</i> mutants at seven days post-germination. Plants were grown on ½ MS agar supplemented with 2% sucrose. The addition of sucrose increased the length of primary roots in all backgrounds, however, the quadruple mutant exhibited short primary roots and fewer lateral roots. The quadruple mutant may be less capable of founding or maintaining root meristems as its short primary root length is not rescued by the presence of sucrose in the medium, unlike <i>tpl-1</i> . Double and triple mutants do not display this characteristic, although lateral root elongation is compromised in <i>tpl tpr1 tpr4</i>	109
Figure 5-10. Complementation of <i>tpl tpr1 tpr3 tpr4</i>. The short primary root phenotype of <i>tpl tpr1 tpr3 tpr4</i> mutants is complemented by wild type <i>TOPESS</i> expressed from its own promoter (<i>pTPL::TPL</i>). Seedlings were grown on ½ MS agar lacking sucrose as sucrose was previously demonstrated to increase root length in <i>tpl-1</i> seedlings.....	110
Figure 5-11. Complementation of <i>tpl tpr1 tpr3 tpr4</i>. The short primary root phenotype of <i>tpl tpr1 tpr3 tpr4</i> mutants is complemented by <i>pTPL::TPL</i> . T2 mutant seedlings in two lines (L1, L2) showed increased primary root length compared to untransformed sister seedlings at four days post-germination (DPG) on ½ MS agar containing no sucrose. Error bars indicate standard deviation; n = 5, 4, 6, 4 and 6, respectively.	111
Figure 5-12. Expression of auxin and cytokinin signalling gene expression in <i>tpl</i> mutant roots by quantitative PCR. No significant difference is observed in the expression of <i>IAA12</i> , <i>IAA14</i> and <i>GATA23</i> between wild type and mutants, but expression of <i>ARR5</i> , a marker for cytokinin signalling, is significantly increased in <i>tpl-1</i>	112
Figure 5-13. Floral phenotypes of <i>tpr2 tpr3</i>, <i>tpl tpr1 tpr4</i> and <i>tpl tpr1 tpr3 tpr4</i> alongside wild type Columbia. Wild type Col produces flowers with a (4, 4, 4+2, 2) floral pattern and variations in organ number are rare. Flowers of <i>tpr2 tpr3</i> mutants are typically wild type with rare changes in the numbers and identities of perianth organs and stamens (not shown). These defects, e.g. pentapetaly, are more frequent in <i>tpl tpr1 tpr4</i> mutants. Quadruple <i>tpl tpr1 tpr3 tpr4</i> mutants exhibit changes in floral morphology ranging from loss of stamens (above) to changes in organ identity (Figure 5-13).	114

Figure 5-14. Examples of floral phenotypes in novel *tpl/tpr* mutant combinations at 27°C. A and B: *tpl tpr1 TPR2 tpr3 tpr4* flowers display developmental defects including petaloid sectors within sepals (A, arrowhead (dissected to show organs)), ectopic carpels (B, arrow) and petaloid stamens (A and B, arrows). C, D, E and F: *tpl^{+/-} tpr1 tpr2 tpr3 TPR4* flowers also present organ identity defects including ectopic carpels in place of other organs (C and D, arrows) and within the gynoecium (E, arrow) as well as petaloid stamens (F); *TPL tpr1 tpr2 tpr3 TPR4* flowers appear aphenotypic (G (dissected to show organs) and H). 115

Figure 5-15. *TPL tpr1 tpr2^{+/-} tpr3 tpr4* phenotypes. Seedlings bear embryonic and early vegetative mutant phenotypes including asymmetric cotyledons (A, C), asymmetry in early leaves and outgrowth of serration or stipule-like tissue at the base of the leaf blade (B, D; black arrows). Mutants exhibited necrosis at leaf tips (F, red arrows) and produced floral buds early (F, yellow arrow) compared to wild type Col-0 (E). 117

Figure 5-16. Unrooted Bayesian phylogeny of TPL-like proteins across the plant kingdom *Arabidopsis thaliana* TPL/TPRs are underlined. Clade labels denote the narrowest taxonomic group that encompasses all proteins contained therein. Node values indicate posterior probabilities expressed as percentages. Scale indicates branch length (i.e. substitutions per site per unit time). 120

Figure 5-17. Neighbour-Joining phylogeny of TPL- like proteins from algal and basal land plant taxa. Node values indicate bootstrap support values expressed as a percentage (bootstrapped for 1,000 iterations). Sequences for MpTPL (*Marchantia polymorpha*) and PpTPL1 and 2 (*Physcomitrella patens*) were predicted from genomic open reading frames. Predicted algal TPL-like proteins were identified from the OneKP database. Sequence identifiers: *Mesotaenium* – *M. kramstei* NBYP-2056058; *Mougeotia* – *Mougeotia* sp. ZRMT-2005604; *Entransia* – *E. fimbriata*; BFIK-2004708, *Spirogyra* – *Spirogyra* sp. HAOX-2025270, *Cylindrocystis* – *C. cushleckae* JOJQ-2041843; *Coleochaete* – *C. irregularis* QPDY-2006907; Chlorokybus – *C. atrophyticus* AZZW-2021890. 121

Figure 5-18. The proportion of transcription factors of all classes that contain repression domains. Motifs represent repression domains discussed by Kagale and Rozwadowski (**Kagale and Rozwadowski, 2011b**). Protein sequences for transcription factors from the taxa of interest from the Plant Transcription Factor Database v4.0 (Jin et al., 2017) were searched using script based on BioPython libraries (Cock et al., 2009) that identifies regular expressions matching the repression domains. Selected taxa include a chlorophyte alga that lacks TOPLESS-like proteins (*Chlamydomonas reinhardtii*), a streptophyte alga (*Klebsormidium nitens*), mosses (*Sphagnum fallax* and *Physcomitrella patens*) and a lycophyte (*Selaginella*). The appearance of DLNxxP and [R/K]LFGV motifs after the evolution of TOPLESS coincides with the expansion of gene families including APETALA, ETHYLENE RESPONSE FACTOR and LATERAL ORGAN BOUNDARY DOMAIN transcription factors in which these domains are found (Kagale et al., 2010; Kagale and Rozwadowski, 2011b). **122**

1 Introduction

1.1 Gene expression in plant development

1.1.1 Transcriptional regulation

The complexity of plants is a testament to the dynamic regulatory processes that occur within the nucleus of every cell. All life processes, from patterning of the nascent embryo to the determination of the floral primordium, are regulated by closely-controlled patterns of gene expression (Yruela, 2015; Townsley and Sinha, 2012; Wang et al., 2018; Petricka et al., 2012; Lau et al., 2012). Simplistically, expression is regulated at multiple levels. At the most basal level, transcription of messenger RNA provides a template for translation of protein-coding genes; however, to initiate even this process, the chromatin must be structured in a state which is favourable to transcription. Euchromatin, as opposed to compacted heterochromatin, is open and accessible to the transcriptional machinery of the nucleus (Engelhorn et al., 2014). This structure occurs as a consequence of epigenetic marks, nucleosome spacing, nucleosome composition (i.e. histone variants) and histone post-translational modifications (PTMs) (Engelhorn et al., 2014). Such factors are subtle enough even to differ between the promoter, transcriptional start site, coding region and terminator of a gene. The accessibility of the chromatin, and thus the competency of the genes within to be transcribed, depends on a synthesis of these factors (Engelhorn et al., 2014). The dynamism of the system derives from its ability to homeostatically maintain or turn over those factors to adjust chromatin accessibility as required (Reynolds et al., 2013; Krogan et al., 2012).

1.1.2 The role of chromatin structure and histone modifications in regulating gene expression

The basic subunit of the chromatin is the nucleosome-DNA complex. The nucleosome is formed of two histone H2A/H2B and two histone H3/H4 heterodimers, around which approximately 146 base pairs (bp) of DNA are

wound twice. (A single H1 histone interacts with 'linker' DNA between nucleosomes.) The histone itself is a low molecular weight protein, comprising three alpha helices and an unstructured amino terminal tail. Variant histone types, which differ in only a few amino acids, are incorporated as required. In plants, histone H2A may be exchanged for variants H2A.X or H2A.Z, while H3 may be exchanged for H3.3 (Henikoff and Smith, 2015). H2A.Z and H3.3 have been linked to transcriptional activity, while H2A.X facilitates repair of double-strand breaks in the DNA (Henikoff and Smith, 2015). Critically, the N-terminal tail of each histone extends from the face of the nucleosomal disc, presenting a target for functionally important PTMs. Post-translational modifications to the histone core also play a role, affecting dimer-dimer and histone-DNA affinity, as well as nucleosome stability.

1.1.2.1 **Post-translational modifications**

Post-translational histone modifications include phosphorylation, acetylation, mono-, di- and trimethylation, SUMOylation, ubiquitylation and ADP-ribosylation (Bowman and Poirier, 2015). Acetylation is one of the best understood modifications. Acetyl (CH_3COO^-) groups are removed from acetyl-coenzyme A (Shen et al., 2015) and attached to histone lysine amino (NH_3^+) groups (Boycheva et al., 2014; Chen et al., 2017). This negates the positive charge of the lysine and reduces the histone's affinity for the negatively charged DNA strand. Steric hindrance further obstructs histone-DNA interaction. Acetylation also competitively obstructs other modifications that maintain chromatin compaction (Figure 1-1). Acetylation of H3K9, K14, K18, K23 and K56, and H4K16, K77 and K79 has been associated with uncoiling of the DNA from the nucleosome (Shen et al., 2015). The position of these groups on the exterior or at the 'entry' and 'exit' sites of the nucleosome (where the DNA strand joins and leaves the nucleosome core) is believed to be relevant to the rate of winding and unwinding of the DNA strand, and thereby the exposure of the DNA to transcription factors (Tessarz and Kouzarides, 2014; Lu et al., 2015). Conversely, removal of acetyl groups from histone lysine residues has been associated with chromatin compaction, transcriptional repression (Liu et al., 2014) and nucleosome stabilisation (Simon et al., 2011). However, a growing body of

work suggests that the turnover of PTMs is an integral part of regulating or 'resetting' transcription as opposed to constitutively silencing transcription (Reynolds et al., 2013). In addition to altering the chemical nature of histones, PTMs influence the recruitment of chromatin chaperones and remodellers. At least one protein domain, the bromodomain, can recognise and bind to acetylated lysine residues (Dhalluin et al., 1999). Inhibition of histone deacetylation with chemical inhibitors can open facultative chromatin and increase transcription (Watts et al., 2018); however, changes in chromatin structure depend on the specificity of the inhibitors used and the level of inhibition (Sanchez et al., 2018). RNA polymerase II can stall due to increased acetylation, preventing gene expression (Sanchez et al., 2018).

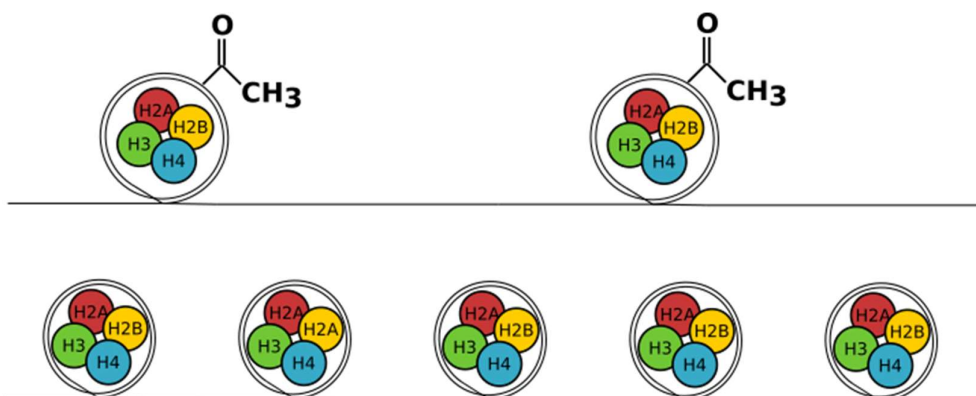


Figure 1-1. A model of the effect of acetylation and deacetylation on nucleosomes. Nucleosomes consist of an octamer of histones (two sets of H2A, H2B, H3 and H4) around which the DNA is coiled. Some post-translational histone modifications such as acetylation (-COCH₃) favour an open, euchromatic state by reducing histone-DNA affinity and increasing nucleosome spacing (top). Deacetylation favours a compacted, transcriptionally inactive heterochromatic structure (bottom).

1.1.2.2 Histone acetylation and deacetylation

In plants, histone acetylation/deacetylation is associated with regulation of (1) growth and development, e.g. seed maturation (Zhou et al., 2013) and germination (Wang et al., 2016), thermomorphogenesis (Tasset et al., 2018), senescence (Chen et al., 2016), leaf development (Luo et al., 2012), flowering time (Yu et al., 2011) and floral patterning (Gonzalez et al., 2007);

(2) homeostasis, e.g. through circadian rhythms (Wang et al., 2013) and metabolism (Liu et al., 2017); (3) stress responses, including drought (Song, 2005), salt (Luo et al., 2012; Song and Galbraith, 2006; Ueda et al., 2017) and pathogen responses (Latrasse et al., 2017a; Wang et al., 2017); and (4) signalling via phytohormones including auxin (Szemenyei et al., 2008), brassinosteroids (Hao et al., 2016), abscisic acid (Perrella et al., 2013), gibberellins (Li et al., 2017) and ethylene (Han et al., 2016; Zhang et al., 2018). For further examples, please consult the review by Liu et al. (Liu et al., 2014). Histones are acetylated and deacetylated by two respective families of enzymes, histone acetyltransferases and histone deacetylases. Nucleus-associated (type A) histone acetyltransferases include the General Non-Derepressible 5 (GCN5), MOZ-YBF2/SAS3-SAS2/TIP60 (MYST) and p300/cAMP-responsive element binding (CREB) families, plus TATA-binding protein Associated Factor 1 (Boycheva et al., 2014; Shen et al., 2015). Cytoplasmic (free) histones are acetylated by type B enzymes, of which one has been characterised in *Zea mays* and one is predicted to be expressed in *Arabidopsis* (Boycheva et al., 2014). Plants deacetylate histones using three distinct groups of histone deacetylases (HDACs): reduced potassium dependency 3/ histone deacetylase 1 (RPD3/HDA1)-like; HD-tuin (HDT)-like; and silent information regulator 2 (Sir2)-like. *Arabidopsis* has six, four and two members of each family, respectively (Hartl et al., 2017). HDTs are unique to the plant kingdom while Sir2s are conserved between prokaryotes and eukaryotes. RPD3/HDA1-like deacetylases are conserved across eukaryotes. The latter group can be further divided into three classes: Class I/RPD3-like, which includes *Arabidopsis* HDA 7, 9, 10, 17 and 19; Class II/HDAC1-like, represented by *Arabidopsis* HDA 5, 8, 14, 15 and 18; and Class IV (in *Arabidopsis*, HDA2) (Shen et al., 2015; Alinsug et al., 2009). This scheme differs from an earlier classification by Hollender and Liu (Hollender and Liu, 2008). Within classes, members differ in their tissue localisation and intensity of expression, although there is a general trend of increased expression in reproductive tissues (Hollender and Liu, 2008). The classes exhibit differential sensitivity to inhibitors (Bradner et al., 2010). The activity of both Class I and Class II enzymes can be inhibited by the chemical inhibitor Trichostatin A (TSA). Another inhibitor, apicidin, acts

specifically upon Class I (Gallo et al., 2008). While the proteins in both classes are named as histone deacetylases, it is unlikely that this is their sole function. Though they are predicted to contain nuclear localisation signals (Alinsug et al., 2009) and nuclear localisation has been reported for HDA15 and HDA19 (Shen et al., 2015), histone deacetylases localise in both the nucleus and cytosol (Hartl et al., 2017). Additionally, HDA14 is localised specifically in the chloroplasts (Hartl et al., 2017). As a result, HDACs are now frequently described with the broader term lysine deacetylases, or KDACs (Füßl et al., 2018).

1.1.2.3 Histone deacetylation complexes

To regulate transcription at specific loci (or patterns of loci), histone deacetylases must be directed to those loci. HDACs do not possess intrinsic sequence specificity; instead, they are incorporated into multi-protein complexes (Liu et al., 2014). These complexes couple the discrete functions of their components, for example, DNA sequence recognition, chromatin mark binding and enzymatic activity. Some regulatory complexes are composed of functional modules that are interchangeable with other modules (Samanta and Thakur, 2015; Merini et al., 2017). The core complex can recruit modules with different regulatory functions, potentially regulating a single pathway in two different ways, or regulating antagonistic pathways (Samanta and Thakur, 2015). The assembly of a complex itself provides additional layers of regulatory control – components must be available in stoichiometric ratios, must co-localise and must have undergone any necessary post-processing, e.g. PTMs. Subunits may induce conformational changes in other subunits that affect function or competence to bind to other factors. The stability of the complex, which may depend on the presence or absence of PTMs, inhibitors or other factors, can also determine the making and maintenance of histone modifications.

Several major histone deacetylation complexes have been characterised in animals and yeast. These groups use a number of different, conserved co-repressor complexes to carry out histone deacetylation and thereby repress gene expression. Some of these complexes share components, but their

overall compositions are distinct. Class I histone deacetylases have been associated with three types of chromatin modifying/remodelling complex: CoREST (Corepressor for element-1-silencing transcription factor) or LCH (LSD1/CoREST/HDAC; Barrios et al., 2014), Sin3 (Switch-independent 3) and NuRD (Nucleosome Remodelling and Histone Deacetylation) (Seto and Yoshida, 2014). The Sin3 and NuRD complexes are better characterised and can be described in some detail.

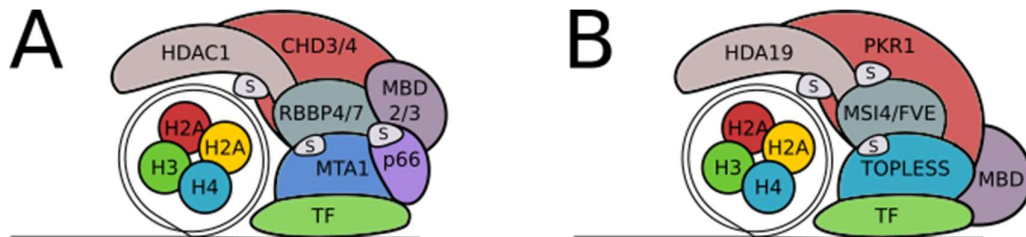


Figure 1-2. The animal Nucleosome Remodelling and histone Deacetylation (NuRD) complex and analogous or homologous components in plants. (A) The NuRD complex is a multi-protein complex that promotes transcriptional repression via histone deacetylation. Several components of the complex NuRD complex are post-translationally modified with small ubiquitin-like modifiers (SUMOs) (marked 'S'). (B) The plant co-repressor TOPLESS interacts with homologues of NuRD complex components and may form an analogous regulatory complex (colour coding indicates homology). Plants lack analogues of some NuRD proteins, e.g. p66 (purple) and MTA1 (dark blue). TOPLESS could potentially act as an alternative to these missing components but its functions are not directly comparable. As in NuRD, TOPLESS and several of its interacting proteins are SUMO substrates.

1.1.2.4 The Sin3 complex

In animals and yeast, Sin3 complexes contain a common core of seven subunit types. HDAC1 and 2 perform histone deacetylation. Sin3a/b themselves act as scaffolding proteins, binding transcription factors via four Paired Amphipathic Helix (PAH) domains and retaining HDACs via an HDAC Interaction Domain (HID) (Saunders et al., 2017). Sin-associated protein (SAP) 18 is a co-repressor (Zhang et al., 1997) associated with transcription factor binding (Song and Galbraith, 2006) and regulation of splicing (Singh et al., 2010) while SAP30 may be involved in nucleic acid binding (Xie et al., 2011). Methyl CpG binding protein (MeCP) 2 is a member of the methyl

binding domain (MBD) family. Originally characterised for its role in repressive DNA methylation, it is thought to recruit histone deacetylases and has been shown to interact with histone methyltransferases (Fuks et al., 2003). Retinoblastoma-associated Binding Proteins (RBBP) 4 and 7 (also known as RETINOBLASTOMA ASSOCIATED PROTEIN (RbAp) 46 and 48) are WD40 proteins that are found in several nucleosome modifying and remodelling complexes, where they are believed to function in histone recognition (Millard et al., 2016). Lastly, suppressor of defective silencing 3 homolog (SDS3, AKA SUDS3) is capable of binding to DNA and may be able to recruit HDACs in a Sin3-dependent manner (Alland et al., 2002; Clark et al., 2015). Interestingly, the complex has been associated with gene activation as well as gene repression (Saunders et al., 2017). Sin3 complexes also co-localise with other post-translational histone modifiers (de Castro et al., 2017).

1.1.2.5 The NuRD complex

The NuRD complex is equally intricate (Figure 1-2A). (Please consult Torchy et al. (Torchy et al., 2015) for an extensive review of the NuRD complex.) The 1MDa complex contains seven subunit types. CHROMODOMAIN, HELICASE, DNA BINDING DOMAIN (CHD) 3/4 (also known as Mi-2 α and Mi-2 β in *Drosophila melanogaster*) bind to histone H3 tails and provide ATP-dependent helicase activity. METHYL CpG BINDING DOMAIN (MBD) 2/3 recognise CpG islands, which are associated with transcriptional start sites (Morey et al., 2008). HISTONE DEACETLYASE (HDAC) 1/2 modify histone tail lysine residues. Additional subunits include METASTASIS ASSOCIATED (MTA) 1/2/3, a central structural component that binds to HDACs in an inositol phosphate-dependent manner (Millard et al., 2013); RETINOBLASTOMA BINDING PROTEIN (RBBP) 4/7, which bind to histones and to MTA1; DELETED IN ORAL CANCER (DOC) 1, and GATAD2A/B (also known as p66 α/β) (Figure 1-2A). The complex contains multiple copies of some subunits and some subunit types (MTA 1, 2 or 3) appear to be mutually exclusive (Zhang, 2006).

1.1.2.6 Conservation of Sin3 and NuRD components in plants

Over the last two decades, evidence has emerged to suggest that some but not all of these complexes are conserved in plants. Proteins homologous to components of histone deacetylation complexes have been identified in plants, including LSD1 (CoREST complex (Spedaletti et al., 2008)), Sin3-like (Bowen et al., 2010) and SAP18 (Song and Galbraith, 2006). These complexes are required for essential cellular processes in animals, e.g. cell division (Sims and Wade, 2011), so it is interesting to note that some components of the canonical NuRD complex are not found in plants. In *Arabidopsis thaliana*, the proteins PICKLE and PICKLE-RELATED 1, AtMBD5/6/7 and MULTICOPY SUPPRESSOR OF IRA1 4 (also known as FVE) are homologous to CHD3/4, MBD2/3 and RBBP4/7, respectively. Homologues of MTA1 have not yet been identified, although *Arabidopsis* proteins containing MTA1's conserved Egl-27 and MTA1 homology domain 2 (ELM2) domain have been found (Yao and Yang, 2003). Proteins p66 α and β also appear to be absent from plants. Analogues may yet be identified. Alternatively, components of the canonical complexes may now incorporate neofunctionalised or entirely novel co-repressors. Several plant-specific co-repressors have arisen since the last common ancestor of plants and animals, including LEUNIG (Conner and Liu, 2000) and TOPLESS (Long et al., 2006). Evidence exists which suggests that these interact with ancestral chromatin-associated complexes (or, at least, components of those complexes) (Gonzalez et al., 2007; Causier et al., 2012a).

1.2 The TOPLESS family of co-repressors

1.2.1 The *tpl-1* phenotype

TOPLESS was first identified from a semi-dominant mutant, *tpl-1* (Long et al., 2002). While the knockout mutant *tpl-2* causes no obvious phenotype, *tpl-1* has a pleiotropic, temperature sensitive phenotype affecting growth, development, fertility and stress responses (Long et al., 2002, 2006). Embryonic development is profoundly affected (Smith and Long, 2010) (Figure 1-3). In rare cases, the apical domain is replaced with a second root,

hence 'topless' (Long et al., 2002). More frequently, the cotyledons are partially or fully fused and the primary root is truncated. Other phenotypic defects, such as delayed flowering (Causier et al., 2012a) and defects in floral organ identity (Long et al., 2002), manifest later in development. The severity of this phenotype is increased at elevated temperatures; embryos developing at 27°C are more likely to display the double root phenotype than at 20°C (Long et al., 2002). Even at high temperatures, however, penetrance of the phenotype is incomplete. Subsequent studies have created multiple mutants of *TOPLESS* (*TPL*) and *TOPLESS-RELATED* (*TPR*) genes that recapitulate this phenotype (Krogan et al., 2012), indicating that *tpl-1* causes a family-wide loss of function.

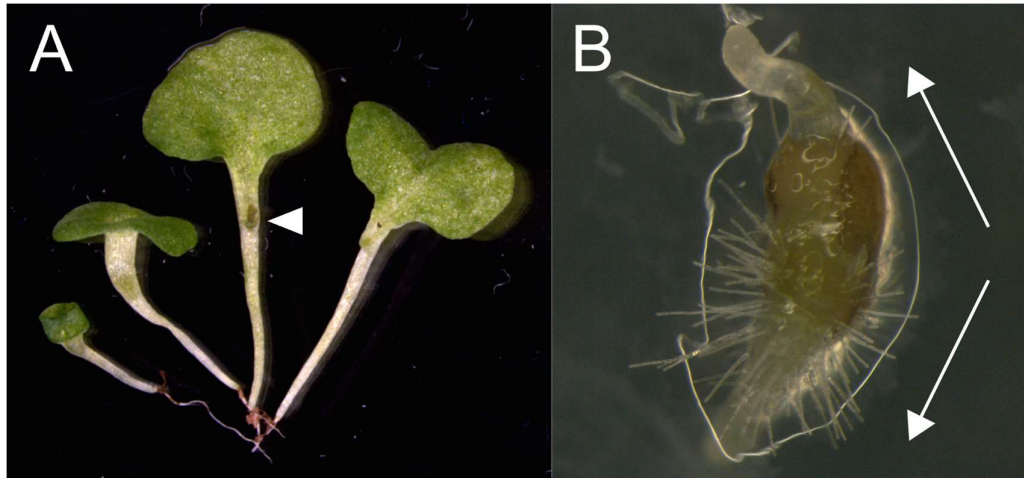


Figure 1-3. Early developmental phenotypes of *tpl-1* mutants. (A) Seedlings exhibit varying degrees of fusion of cotyledons, ranging from formation of a radially symmetrical cup through production of a single cotyledon to wild type phenotypes (the latter not shown). The monocotyledonous phenotype is not universally fatal as some seedlings initiate a shoot apical meristem (A, white arrowhead) and produce leaves. (B) The 'topless' phenotype, where the embryo forms two root axes (white arrows) instead of a root and a shoot is rare (~1/900) (Szemenyei et al., 2008).

Recent data supports the hypothesis that the *tpl-1* mutation (N176H; Figure 1-4) stabilises an aberrant binding surface, allowing TPL N176H proteins to aggregate with non-mutant TPR proteins to form less- or non-functional

aggregates (Ma et al., 2017). TPL N176H remains capable of interacting conventionally with TPL/TPR proteins and histone deacetylase HDA19 but cannot bind transcription factors (Krogan et al., 2012). Depletion of free TPL/TPR monomers (and potentially co-associated proteins, e.g. transcription factors) may diminish TPL/TPR mediated repression, resulting in ectopic expression of target genes.

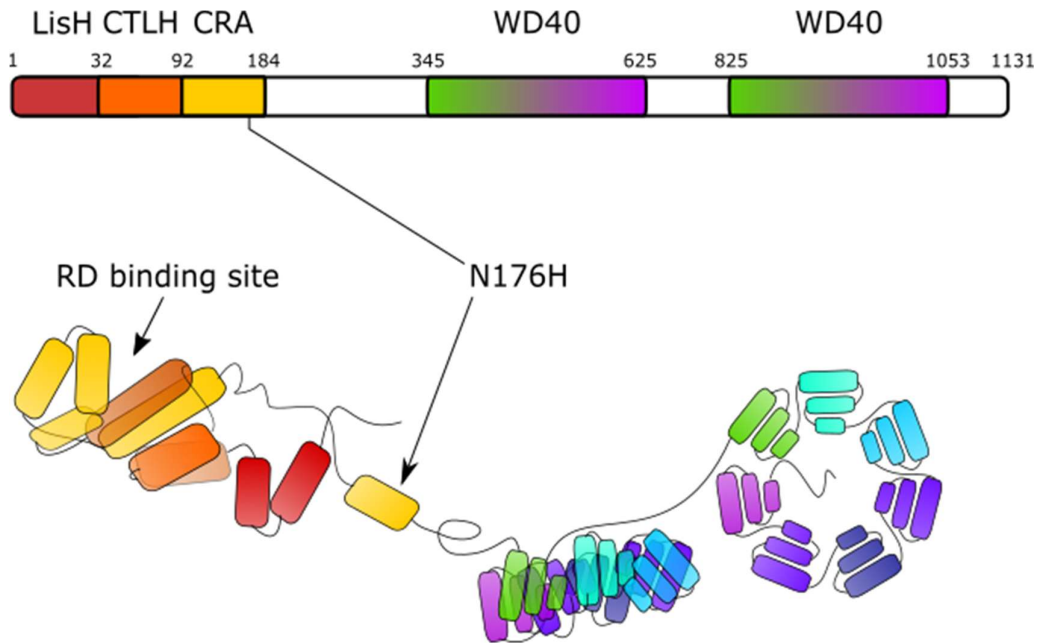


Figure 1-4. Domain structure of TOPLESS-like proteins. LisH, CTLH and CRA domains at the N-terminus are required for binding transcription factors and for dimerisation and tetramerisation between TOPLESS monomers (Ke et al., 2015; Martin-Arevalillo et al., 2017). These domains are folded to form grooves and interaction surfaces for these respective interactions. The C-terminal WD40 repeat clusters are predicted from similar primary protein structures to form two seven-bladed β -propellers (Szemenyei et al., 2008) (not to scale). Residue numbers are annotated according to *Arabidopsis thaliana* TOPLESS (AtTPL).

1.2.2 The structure and function of TOPLESS and TOPLESS-RELATED proteins

Soon after TOPLESS and its relatives were discovered, they were identified as co-repressors through their interactions with AUX/INDOLE ACETIC ACID (AUX/IAA) transcription factors (Szemenyei et al., 2008; Long et al., 2002, 2006). TPL/TPR proteins were assigned to a broader class of co-repressors

(Long et al., 2006), varyingly called Groucho/TLE (Transducin-Linked Enhancer of Split), Groucho/Tup1 and other titles (Liu and Karmarkar, 2008). Groucho (from *Drosophila melanogaster*), TLE (from mammals) and Tup1 (*Saccharomyces cerevisiae*) plus others including LEUNIG and LEUNIG HOMOLOG (*Arabidopsis thaliana*) contain C-terminal repeats of the WD40 domain (also known as β -transducin domains), coupled to N-terminal domains involved in protein-protein interactions (Liu and Karmarkar, 2008). Like TPL/TPRs, they couple DNA sequence recognition by transcription factors to histone deacetylation by HDACs (Liu and Karmarkar, 2008). Recent publications have highlighted mechanistic differences (Ke et al., 2015; Martin-Arevalillo et al., 2017) and phylogenetic separation (Copley, 2016) of TPL/TPRs and Groucho/TLE co-repressors, but as analogous co-repressors the comparison remains useful.

1.2.2.1 Domain functions

TPL/TPR proteins are composed of four types of known protein domain: Lisencephaly Homolog 1 (LisH); C-terminal to LisH (CTLH); CT11-RanBPM (CRA); and WD40 domains (Figure 1-4). The N-termini of *Arabidopsis thaliana* TOPLESS and *Orzya sativa* TPR2, which includes the LisH, CTLH and CRA domains, have been structurally characterised. The CRA domain distinguishes TOPLESS from related LisH-CTLH-WD40 proteins such as AtSMU1 (Ulrich et al., 2016). LisH and CTLH domains are conserved eukaryotic domains with identified roles in transcriptional regulation, DNA replication and repair and RNA splicing. In TOPLESS, the LisH-CTLH-CRA arrangement forms a loop that contains three exposed grooves.

Transcription factors binding occurs at the third groove, although some transcription factors contain an auxiliary RD-like motif that interacts with the second groove (Ma et al., 2017). This region of the protein also facilitates dimerisation and tetramerisation between TPL monomers (Ke et al., 2015). Heteromerisation of different TPL family members has not been directly observed but has been predicted by yeast two-hybrid assays (Causier et al.,

2012a). Heteromerisation is likely to occur due to high N-terminal sequence conservation in the regions of the protein responsible for multimerisation (Ke et al., 2015; Martin-Arevalillo et al., 2017).

No structure is available for the C-terminus of TOPLESS. We can infer from crystal structures of other WD40 repeat proteins that each of the twin C-terminal clusters of WD40 repeats in TOPLESS would form a seven-bladed β -propeller structure. This structure has been associated with a number of activities in repressive complexes. For example, in Groucho the β -propeller binds WRPY motifs in Runt family TFs (Aronson et al., 1997) and WRPW motifs in Hairy family TFs (Fisher et al., 1996). Runt and Hairy TFs bind to the dorsal face of the central pore, respectively (Jennings et al., 2006). In RBBP5, a member of the histone-methylating WRAD complex, the β -propeller binds to nucleic acids (Mittal et al., 2018). RBBP4 and 7 (both members of the Sin3 and NuRD complexes) bind to histone H4 (Murzina et al., 2008) and to the NuRD cofactor FOG1 (Lejon et al., 2011) on the outside edge and dorsal face of the β -propeller, respectively. TOPLESS possesses a different mechanism of transcription factor binding but may conserve other protein-protein interactions mediated by the β -propeller. However, no protein-protein interactions have been ascribed to the β -propellers of TPL thus far.

1.2.3 Evolutionary origins and conservation of TOPLESS

The *TOPLESS* gene is unique to plants (Causier et al., 2012b). The presence of *TOPLESS* in the charophycean alga *Klebsormidium nitens* (Martin-Arevalillo et al., 2017) indicates an early origin prior to major events in the natural history of plants, e.g. terrestrialisation. From a single gene in algae (Martin-Arevalillo et al., 2017) and basal land plants (Flores-Sandoval et al., 2015; Causier et al., 2012b), the family has expanded (see Chapter 3). In angiosperms, *Arabidopsis thaliana* (a rosid species) possesses five *TPL*-like genes. These are named *TPL* and *TOPLESS-RELATED 1-4*. *Solanum lycopersicum* (tomato), an asterid, has six genes (*SITPL1-6*) (Hao et al., 2014). The model monocot rice (*Oryza sativa*) has three: *ABERRANT SPIKELET AND PANICLE (ASP1)*, *ASP-RELATED 1 (ASPR1)* and *ASPR2*,

also referred to as *OsTPL*, *OsTPR1* and *OsTPR2* (Causier et al., 2012b; Ke et al., 2015). Key mechanistic characteristics of TOPLESS-like proteins, e.g. mode of transcription factor binding, are conserved between these species (Ke et al., 2015; Martin-Arevalillo et al., 2017). *TOPLESS*-like genes exhibit some degree of redundancy in their expression, functions and interactions (Long et al., 2006; Causier et al., 2012a); however, incomplete redundancy between family members has been reported. In *Arabidopsis*, loss of *TOPLESS*, *TPR1* and *TPR4* causes an incremental loss of pathogen resistance (Zhu et al., 2010) while in tomato individual SITPLs differ in their binding affinity for certain AUX/IAAs (Hao et al., 2014). In monocots, *TPL*-like genes exhibit greater independence. Loss of function of *ASP1* in rice causes an early transition to flowering, prolonged inflorescence growth and derepression of axillary bud development (Yoshida et al., 2012). Loss of the maize homologue *RAMOSA ENHANCING LOCUS2 (REL2)* results in increased branching of the inflorescence and prolonged indeterminacy (Gallavotti et al., 2010). Whether or not these orthologues have been neofunctionalised or subfunctionalised is unclear but similarity to *tpl-1* (early flowering and altered floral development) indicates conservation of function, perhaps through common interactions with transcription factors.

1.2.4 The TOPLESS interactome

TOPLESS is recruited by a diverse range of transcription factors. Yeast two-hybrid (Y2H) library screens revealed interactions between TPL and transcription factors from the AUX/INDOLE ACETIC ACID (AUX/IAA), *ARABIDOPSIS* RESPONSE FACTOR (ARF), ETHYLENE RESPONSE FACTOR (ERF), APETALA2 (AP2), LATERAL ORGAN BOUNDARY DOMAIN (LOB/LBD), JASMONATE-ZIM (JAZ), TEOSINTE BRANCHED 1/CYCLOIDEA/PCF (TCP), NAM/ATAF/CUC2 (NAC), MYELOBLASTOSIS (MYB), WUSCHEL/ WUSCHEL HOMEODOMAIN (WOX), BASIC LEUCINE ZIPPER (bZIP) and other families (*Arabidopsis* Interactome Mapping Consortium, 2011; Causier et al., 2012a).

As a result, TPL controls a variety of regulatory pathways. It has been implicated in the control of embryo polarity (Smith and Long, 2010)(Negin et

al., 2017), meristem maintenance (Kieffer, 2006), lateral root development (Stoeckle et al., 2018), branching (Soundappan et al., 2015), leaf lamina growth (Gonzalez et al., 2015), flowering time (Graeff et al., 2016), floral patterning (Krogan et al., 2012), sperm cell division and differentiation (Borg et al., 2014), ovule development (Chen et al., 2014), circadian rhythms (Wang et al., 2013) and defence against pathogens (Zhu et al., 2010). TPL is also involved in signalling pathways for phytohormones including auxin (Szemenyei et al., 2008), jasmonic acid (Pauwels et al., 2010), strigolactones (Soundappan et al., 2015), gibberellic acid (Fukazawa et al., 2014), brassinosteroids (Oh et al., 2014) and abscisic acid (Espinosa-Ruiz et al., 2017).

The majority of interacting transcription factors contain repression domains (RDs), short consensus motifs that bind to a hydrophobic groove at the N-terminus of the TPL protein. Although all known plant repression domains are represented in TPL-interacting proteins (Kagale and Rozwadowski, 2011a; Causier et al., 2012a), the most common is L-x-L-x-L, the Ethylene-responsive element binding factor-associated Amphiphilic Repression (EAR) motif (Kagale and Rozwadowski, 2011a). The TPL interactome has been broadened by the discovery that adaptor proteins such as NINJA (Pauwels et al., 2010), KIX8 and KIX9 (Gonzalez et al., 2015) and ROXY19 (Uhrig et al., 2017) are able to recruit TOPLESS on behalf of other transcription factors that lack the necessary RDs to bind TOPLESS.

1.2.5 The putative TOPLESS complex

TPL's mode of transcription factor binding has been described, but information regarding its broader interactome is sparse. To act as a co-repressor, TPL must couple transcription factors to histone deacetylases. Although histone deacetylases co-localise with TPL and can be captured by TPL via semi-*in vivo* pulldowns (Krogan, Hogan, & Long, 2012), a direct interaction has never been observed (Causier, Ashworth, Guo, & Davies, 2012). Additional co-factors or post-translation modifications of one or both may be required for interaction. In a Y2H library screen, TPL was found to interact with homologues of two NuRD complex components (Causier et al.,

2012a). These interactions are outlined in Figure 1-2B. MULTICOPY SUPPRESSOR OF IRA4/FVE (MSI4/FVE) is homologous to RBBP4 and 7, WD40 proteins thought to recognise histone proteins. PICKLE-RELATED1 (PKR1) is homologous to the mouse ATP-dependent chromatin remodellers Chromodomain Helicase Domain 3 and 4 (CHD3/4). Additionally, TPL has been recovered by co-immunoprecipitation using transcription factors and coregulators as bait. Clavel et al. (Clavel et al., 2015) co-precipitated TPL, MSI4/FVE, MBD10 (homologous to MBD2/3) and SWI3a using DOUBLE-STRANDED RNA BINDING 2 (DRB2), a repressive chromatin regulator, as bait. Similarly, Zheng et al. (Zheng et al., 2017) recovered TOPLESS alongside the co-repressor SAP18, the chromatin remodellers SIN3-LIKE 4 (SNL4), BRAHMA (BRM) and SPLAYED (SYD) and the methylation-associated proteins METHYL BINDING DOMAIN 2 (MBD02), METHYLTRANSFERASE 1 (MET1) and DNA METHYLTRANSFERASE DRM2. Furthermore, TOPLESS has been associated with the Mediator complex (Ito et al., 2016). The Mediator complex is a modular transcriptional regulatory complex that interacts with RNA Polymerase II (Yang et al., 2016). It is broadly conserved across all eukaryotes (Yang et al., 2016). In *Arabidopsis*, the transcription factors AUXIN RESPONSE FACTORS (ARF) 7 and 19 are antagonised by IAA14. TOPLESS couples the transcription factor IAA14 to a CDK8 kinase module (CKM) which binds to the core Mediator complex (Ito et al., 2016). This is thought to prevent recruitment of RNA Polymerase II, ensuring that targets of ARF7 and 19 remain silent (Ito et al., 2016). Thus, association with at least one conserved, multi-protein complex is believed to facilitate TPL-mediated repression and TPL may also associate with a plant analogue of the Sin3 and/or NuRD complex (Mazur and van den Burg, 2012). How TPL is recruited to these complexes (or *vice versa*) is unclear, but it has been proposed that SUMOylation is important for complex assembly, as many components of these complexes, TPL included, are SUMOylated (Mazur and van den Burg, 2012). TPL is “highly SUMOylated” under heat and hypoxic stress (Miller et al., 2010). TPR1, TPR2, TPR4, HDA19 and PICKLE RELATED 1 show increased SUMOylation under the same stress conditions, as are the related plant co-repressors LEUNIG and LEUNIG HOMOLOG and their co-factor SEUSS

(Miller et al., 2010). SUMOylation may play a role in the regulation of TOPLESS activity and complex formation (Mazur and van den Burg, 2012).

1.2.6 The potential role of SUMOylation

Regulatory complexes and their constituent co-repressors are not mere switches. They vary in their localisation, their modular configuration and their mode of regulation by post-translational modification. They compete with antagonistic complexes and with variants of themselves for access to the chromatin. In the case of histone modifications such as acetylation/deacetylation, turnover itself may be necessary for maintenance of normal gene regulation (Hazzalin and Mahadevan, 2005). Attention has increasingly focused on the assembly and stability (or turnover) of regulatory complexes. Post-translational modifications (PTMs) of proteins have been identified as an effective, inducible and reversible means of regulating protein-protein and protein-nucleic acid interactions in these complexes. The myriad of protein PTMs includes phosphorylation, methylation, ubiquitylation, glycosylation, acetylation, acylation, adenylation, myristoylation, nitrosylation and SUMOylation. I will focus on the last of these, SUMOylation.

SUMOylation is the addition of small ubiquitin-like modifiers (SUMOs).

SUMOs are a conserved class of proteins that have been recognised as potent, post-translational modifiers of other proteins (and each other). Over a thousand plant proteins are SUMOylated (Rytz et al., 2018). SUMOs are one class of ubiquitin-like (UBL) protein; other classes prevalent in plants include NEDD8/RELATED TO UBIQUITIN1 (the most similar of these to ubiquitin (van der Veen and Ploegh, 2012; Mergner and Schwechheimer, 2014)), AUTOPHAGY-RELATED PROTEINS 8 and 12 (ATG8/12), HOMOLOGY TO UBIQUITIN (HUB) and MEMBRANE-ANCHORED UB-FOLD (MUB) (Hua et al., 2018; Saracco et al., 2007). UBLs are similar in size to one another (100 amino acids) and have a similar 'β-grasp' tertiary structure. This structure is sometimes referred to as the ubiquitin fold (Cappadocia and Lima, 2018).

The enzymatic pathway by which different UBLs are conjugated to their targets is broadly similar (Figure 1-5). E1 activating enzymes adenylate the UBL as an intermediate step before forming a thioester bond. Next, the UBL

is transferred by trans-thioesterification to the E2 conjugating enzyme. From the E2, the UBL is either transferred directly to the primary amine group of a lysine residue in the substrate protein or is transferred to an E3 enzyme for subsequent conjugation to a target (Cappadocia and Lima, 2018). E3 enzymes increase conjugation efficiency and provide greater substrate specificity than E2 enzymes, which may justify this apparent redundancy (Cappadocia and Lima, 2018). SUMOs also undergo pre-processing of their C-terminal tail by proteases including ESD4 (Murtas et al., 2003) to leave a terminal diglycine motif.

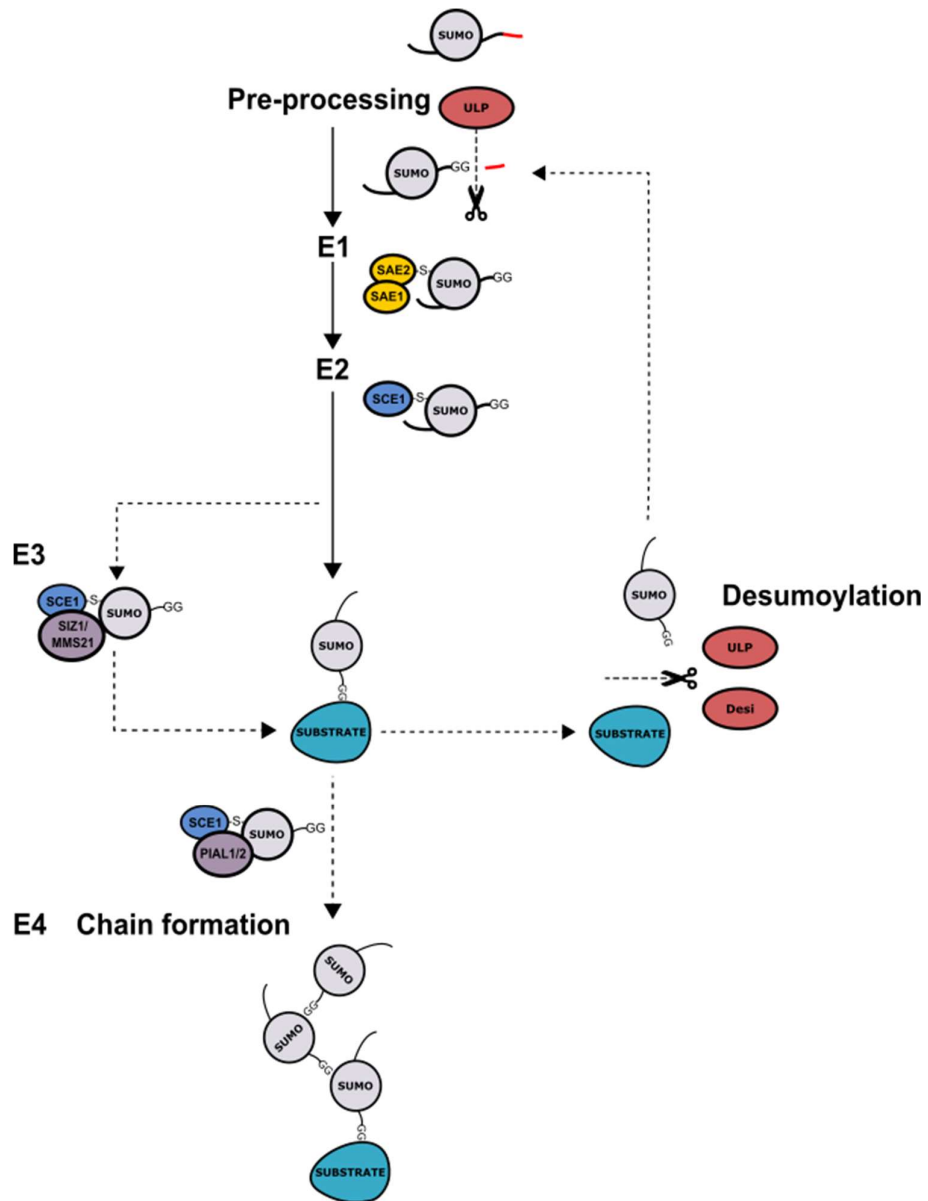


Figure 1-5. Overview of the SUMOylation pathway in plants.

SUMOylation requires a cascade of enzymatic reactions. The precursor SUMO protein is cleaved by ULP class SUMO proteases to remove a C-terminal peptide, exposing a diglycine motif. The mature SUMO is then bound by thioesterification (-S-) to an E1 heterodimer which adenylates the SUMO. The SUMO is transferred to the E2 conjugating enzyme, from which it is conjugated to a lysine residue within the substrate protein, with or without the assistance of an E3 SUMO ligase. Substrate proteins can be deSUMOylated by SUMO proteases. Additionally, *Arabidopsis* SUMOs 1 and 2 can themselves be SUMOylated by PIAL SUMO ligases (E4), allowing for formation of SUMO chains (Tomanov et al., 2018a). DeSUMOylation is performed by ULPs and by Desi proteins. Desi proteins differ in their catalytic site to SP-RING (ULP) type proteases and perform deSUMOylation but not SUMO maturation (Orosa et al., 2018).

1.2.7 The plant SUMOylation pathway

In *Arabidopsis thaliana*, there are eight SUMO-encoding genes (*AtSUMO1-8*; a pseudogene, *AtSUMO9*, is also present) (van den Burg et al., 2010). Of these, *AtSUMO1*, 2, 3 and 5 are known to be expressed (van den Burg et al., 2010). The SUMO conjugation pathway in plants has also been well characterised (Kurepa et al., 2003) (Figure 1-5). SUMO ACTIVATING ENZYMEs (SAE) 1a/b form a heterodimeric E1 complex with SAE2 (Castaño-Miquel et al., 2013). E2 activity is performed by a lone enzyme, SUMO E2 CONJUGATING ENZYME 1 (SCE1) (Lois et al., 2003). Both SAE2 and SCE1 are essential for viability (Saracco et al., 2007) while loss of *SAE1a* causes plants to accumulate fewer SUMO-conjugated proteins under heat stress (Castaño-Miquel et al., 2013). There are four *Arabidopsis* E3 ligases: HIGH PLOIDY 2 (HPY2), also known as MMS21 (Huang et al., 2009; Ishida et al., 2012); SAP and MIZ1 1 (SIZ) 1 (Miura et al., 2005); PROTEIN INHIBITOR OF ACTIVATED STAT LIKE (PIAL) 1 and PIAL2 (Tomanov et al., 2014). The ligases exhibit differences in substrate specificity degree of specificity (Tomanov et al., 2014; Rytz et al., 2018). A recent profile of plant protein SUMOylation revealed that while HPY2/MMS21 may target only a small number of proteins, 112 proteins show decreased SUMOylation in *siz1-2* mutants, and that this group is enriched for transcription factors and chromatin remodellers (Rytz et al., 2018). PIAL 1 and 2 are upregulated under heat or salt and osmotic stress, respectively, and are capable of ligating poly-SUMO chains to substrate proteins (Tomanov et al., 2014; Knipscheer et al., 2007). Chain formation appears to occur preferentially at a subset of acceptor lysine residues (Tomanov et al., 2018a).

DeSUMOylation is performed by two families of cysteine proteases, ubiquitin-like proteases (ULPs) and DeSUMOylating isopeptidases (Desi). There are eight known ULPs in *Arabidopsis thaliana* (Castro et al., 2018), divided into three classes: Class I encompasses proteases similar to *Saccharomyces cerevisiae* ULP1: At4g15880 (encoding EARLY IN SHORT DAYS4 (ESD4)), At3g06910 (ESD4-LIKE SUMO PROTEASE 1 (ELS1)) and At4g00690 (ESD4-LIKE SUMO PROTEASE 2 (ELS2)). Classes II, III and IV contain those SUMO proteases that are similar to *Saccharomyces*

cerevisiae ULP2. Class II contains At1g60220 (OVERLY TOLERANT TO SALT 1 (OTS1)) and At1g10570 (OVERLY TOLERANT TO SALT 2 (OTS2)). Class III contains At1g09730 (encoding SUMO PROTEASE RELATED TO FERTILITY1 (SPF1)) and At4g33620 (SUMO PROTEASE RELATED TO FERTILITY2 (SPF2)). Class IV has one representative in *Arabidopsis* (At3g48480, encoding FOURTH ULP GENE CLASS 1 (FUG1)) and is unique to spermatophytes. These proteases differ in their relative affinities for individual SUMOs (Hermkes et al., 2011; Conti et al., 2009; Castro et al., 2016). Desi proteins were first identified in mammals as SUMO proteases that perform deSUMOylation but not SUMO maturation (Shin et al., 2012). Recently, eight predicted Desi proteins were identified in *Arabidopsis thaliana* through their sequence homology to human Desi-1 within the catalytic domain (Orosa et al., 2018). Owing to their recent discovery, the substrate range and specificity and the subcellular localisation of these proteins has not yet been fully described, but Orosa et al. (2018) revealed that Desi3a localises to plasma membranes and has deSUMOylating activity on the SUMOylated flagellin receptor FLS2.

What determines if a protein is SUMOylated? Bioinformatic analysis of SUMOylated proteins and of known SUMO-accepting peptides has elucidated a consensus motif for the SUMO attachment site – ψ -K-x-E/D, where ψ is a large, hydrophobic residue (Rodriguez et al., 2001). Inverted consensus motifs have also been shown to be valid binding sites (Matic et al., 2010). However, not all SUMOylation occurs at consensus motifs; for example, the co-repressor KAP1 recruits the NuRD complex with a non-canonical motif, Q-E-K-L (Ivanov et al., 2007). Additionally, SUMOylation depends on SUMO ligases which may differ in their expression patterns and their specificity (Rytz et al., 2018).

SUMOylation has been strongly associated with stress responses. In *Arabidopsis thaliana*, the number of detectable SUMO-conjugated proteins rapidly doubles in response to heat shock (Rytz et al., 2018). Colignon et al. also report changes to patterns of protein SUMOylation in response to infection by pathogens (Colignon et al., 2017b). Though SUMO substrates are diverse (Rytz et al., 2018; Hendriks and Vertegaal, 2016), many of these are involved in promoting responses to stress. Stress-responsive

transcription factors, co-regulators such as TPL and chromatin remodellers have been revealed as targets of SUMOylation (Rytz et al., 2018; Miller et al., 2010). SUMOylation may transduce stress signals, promoting changes in transcription-regulating complexes and enabling a shift in gene expression as part of the stress response.

We might also ask, what determines if a protein *remains* SUMOylated? In the ubiquitylation pathway E3 ligases have radiated, permitting subfunctionalisation and enhancing regulatory control at the point of ubiquitin attachment. In contrast, the model plant *Arabidopsis* has only two E3 SUMO ligases. Instead, regulatory control may be exerted at the deSUMOylation step (Yates et al., 2016). *Arabidopsis* has seven ubiquitin-like proteases, of which three (ESD4, OVERLY TOLERANT TO SALT1 and OVERLY TOLERANT TO SALT2) have been functionally characterised (Yates et al., 2016). Recent research on OVERLY TOLERANT TO SALT (OTS) 1 and 2 in *Arabidopsis* has revealed a role in salt and copper tolerance (Conti et al., 2009; Zhan et al., 2018). In rice, OsOTS1 has been implicated in regulation of salt tolerance (Srivastava et al., 2016b), germination (Srivastava et al., 2016a) and drought responsiveness, the latter via destabilisation of the transcription factor OsbZIP23 (Srivastava et al., 2017). DeSUMOylation therefore fine-tunes a range of genetic pathways. The discovery of an additional class of deSUMOylating proteins, the Desi family (Shin et al., 2012; Orosa et al., 2018), revealed additional tools available to plants to regulate SUMO substrates at the deSUMOylation step.

1.2.8 SUMO functions

SUMOylation has a range of functional consequences. SUMOylation has been associated with enhanced (Lin et al., 2016a) or diminished transcriptional activity (Bies et al., 2002; Zheng et al., 2012; Hansen et al., 2017), stability (Zheng et al., 2012), degradation (Zhang et al., 2017) and promotion of further post-translational modification (Saleh et al., 2015) in plants. SUMO chains have been identified as recognition sites for SUMO-Targeted Ubiquitin Ligases (STUbLs), which ligate ubiquitin to the protein, marking it for degradation through the 26S proteasome pathway (Elrouby,

2015). SUMO can also compete with other post-translational modifications of lysine residues, including ubiquitylation, methylation and acetylation. Outside of plants, there are also examples of SUMO influencing sub-cellular (Wang et al., 2011) and sub-nuclear (Maarifi et al., 2018) localisation, and of SUMOylation stabilising (Shen et al., 2015; Klenk et al., 2006) or blocking (Rouvière et al., 2018) protein-protein interactions. SUMO is a potent regulator of protein activity. It is unsurprising that it is recruited to regulate similar co-repressors to TPL. Groucho is positively and negatively regulated by SUMOylation. SUMOylation at K282 and K279 enhances interaction with histone deacetylase HDAC1 (Ahn et al., 2009). Mutations in the HDAC1 decreased its affinity for SUMOylated Groucho *in vitro* (Ahn et al., 2009). Conversely, SUMOylation recruits the SUMO-targeted ubiquitin ligase (StUbl) Degringolade, which also targets the Groucho-interacting transcription factor Hairy (Abed et al., 2011). Abed et al. propose that SUMOylation is necessary for Groucho activity, but that SUMOylation induces rapid turnover to place a time limit on Groucho-mediated repression. Another example is the yeast co-repressor Tup1. Mutations at SUMOylation sites K229 and K270 enhanced expression of target genes ARG1 and CPA2 and weakened Tup1's association with histone H3 (Ng et al., 2015). Additionally, loss of Tup1 SUMOylation appeared to diminish SUMOylation of H3-associated proteins, suggesting that SUMOylation of these proteins is interdependent or occurs as part of a cascade of modification (Ng et al., 2015). Other substrates include the NuRD subunits MTA1, which undergoes SIM-dependent SUMOylation (Cong et al., 2011), p66 (Gong et al., 2006) and HDAC1 (David et al., 2002). These examples demonstrate that SUMOylation is employed to regulate the activity, stability and interactions of co-repressors and their constituent regulatory complexes. As TOPLESS is similarly modified, what effect does SUMOylation have on the activity of TOPLESS? Why is it "highly SUMOylated" under stress conditions? Furthermore, is SUMOylation important for interaction with known interacting partners which are also SUMOylated? This thesis aims to explore these questions, with the following aims.

1.3 Aims of this thesis:

- 1.) To determine the role of SUMOs in the regulation of the plant co-repressor TOPLESS
- 2.) To explore the concept of a TOPLESS regulatory complex
- 3.) To expand our understanding of TOPLESS family and its functions in *Arabidopsis thaliana*

2 Materials and Methods

2.1 Nucleic acids

2.1.1 DNA extraction

Plant DNA was extracted from leaf tissue. One leaf was removed and transferred to a 2ml microcentrifuge tube (Eppendorf). The tissue was homogenised with a pestle at room temperature in 400ul DNA extraction buffer (100mM tris-HCl, 50mM EDTA, 100mM NaCl and 10mM β -mercaptoethanol). After homogenisation, the extract was clarified by centrifugation at 13,000 x g for two minutes. The supernatant was transferred to a new tube mixed with 0.9 volumes of isopropanol by pipetting. The extract was chilled at -20°C for ten minutes to maximise precipitation, then centrifuged at 13,000 x g for ten minutes. The centrifuge was discarded and the pellet washed with 70% ethanol made with sterile, distilled water, then centrifuged again at 13,000 x g for five minutes. The ethanol was removed and the centrifuge tube left uncapped to evaporation of any remaining ethanol for ten minutes. The dry pellet was resuspended in 100ul sterile, distilled water and its concentration quantified using a Nanodrop ND1000 microvolume spectrophotometer (Thermo Scientific).

2.1.2 Oligonucleotide synthesis

Oligonucleotides were designed using A Plasmid Editor (Ape) (Davis, 2018) and Primer3 and purchased from Integrated DNA Technologies (IDT). Oligonucleotides used for cloning, genotyping and other purposes are described in Appendix C. The *tCUP* promoter fragment was synthesised and cloned by Generon.

2.1.3 RNA extraction

RNA was extracted using a High Capacity RNA Extraction Kit (Applied Biosystems). Where available, 50mg of leaf tissue was used per extraction. The recommended protocol was followed with the exception of reduction of the final elution volume to 40 μ l.

2.1.4 Gel electrophoresis

DNA fragments were separated by gel electrophoresis through agarose gel made with Hi-Res Standard Agarose (Geneflow), Tris-Borate EDTA (TBE) buffer (from 50x concentrate; Severn Biotech) containing 5 μ l of Midori Green (Nippon Genetics) per 100ml of gel. Standard gels were made to 1% concentration. Gels requiring resolution of low molecular weight bands were made to 1.2% concentration. Those for high molecular weight fragments were made to 0.8% concentration.

2.1.5 Gel extraction

DNA fragments were separated. Gel bands were viewed with a blue light transilluminator and excised with a razor blade. Gel fragments were processed with a Qiaquick gel extraction kit (Qiagen) and eluted from the purification column with a minimal volume of the provided elution buffer (typically 25 μ l).

2.1.6 PCR purification

5 μ l of each PCR reaction was mixed with 1 μ l of 6x DNA gel loading dye (Thermo Scientific) and checked by gel electrophoresis through agarose gel (see Gel Electrophoresis). The remainder of the PCR reaction with processed with a QiaQuick PCR Purification kit (Qiagen) as per the recommended protocol.

2.1.7 PEG precipitation

PEG precipitation was used as an alternative method of purifying PCR reactions prior to Gateway recombination reactions. PCR reactions were diluted with 125 μ l Tris-EDTA (TE) buffer then mixed with 100 μ l PEG-400 and centrifuged at 16,000 x g for ten minutes. The supernatant was removed and the pellet resuspended in 25 μ l TE buffer.

2.1.8 DNA restriction

Purified plasmid DNA or purified linear DNA fragments were digested with FastDigest enzymes (NEB). The DNA was digested for no less than ten minutes at 37°C in a 10 μ l reaction volume, with the volume of enzyme not exceeded 1.5 μ l to limit the glycerol content of the reaction. For simultaneous

digestion with two or more enzymes, the incubation time was extended to 20 minutes. Where the reaction contained a plasmid vector backbone for use in subsequent ligation reactions, the reaction mixture was supplemented with 2µl FastAP alkaline phosphatase (NEB), which is compatible with the FastDigest reaction buffer.

2.1.9 DNA ligation

The majority of DNA fragments were ligated using Rapid Ligase (ThermoFisher Scientific) using the recommended protocol. Where the expected size of the assembled vector would exceed 10,000 base pairs, the ligation was performed using T4 DNA ligase (NEB), incubated at 16°C for 16 hours. To assemble a complete plasmid, insert and vector backbone fragments were ligated in a ratio of ligatable fragment ends of 3:1.

2.2 Cloning

2.2.1 Gateway cloning (single and multi-fragment)

Gateway-compatible DNA fragments were created by amplifying sequences of interest from cDNA by polymerase chain reaction using primers that included the appropriate Gateway recombination sequences, as described in the Thermo Fisher Gateway cloning manual. Constructs intended for single fragment Gateway recombination were cloned into the entry vectors pDONR201 or pDONR 207 (Invitrogen via Thermo Fisher) while those intended for multi-fragment assembly were cloned into appropriate pDONR221 vectors (Invitrogen via Thermo Fisher). Gateway cloning was performed using BP Clonase II and LR Clonase II recombinases (Invitrogen) according to the manufacturers protocol.

2.2.2 Transformation of *Agrobacterium* by electroporation

Aliquots of electrocompetent *Agrobacterium tumefaciens* GV3101 were thawed on ice. Of these, 50µl was transferred to a 1.5ml microcentrifuge tube (Eppendorf) that have been pre-cooled on ice. The aliquot was inoculated with 0.1µl plasmid then gently pipetted into a pre-cooled electroporation cuvette (Cell Projects) and immediately shocked at 1.8kV. 450µl LB was added to each cuvette to resuspend the transformation

mixture. The whole volume was then transferred to a 2ml microcentrifuge tube (Eppendorf) and incubated at 37°C for one hour. Aliquots of 50µl and 100µl were spread under onto LB agar plates with antibiotic selection using sterile technique. Plates were incubated at 37°C for 16 hours to allow colony growth.

2.2.3 Transformation of chemically-competent *E. coli* by heat shock

50µl aliquots of electrocompetent DH5-α *E. coli* were thawed on ice, inoculated with 0.1µl plasmid and incubated on ice for 20 minutes, then heat shocked in a 42°C water bath for 45 seconds. The aliquots were place back on ice for two minutes before resuspension in LB media. Cells were incubated for one hour at 37°C to allow recovery before plating of 50µl and 100µl aliquots on LB agar plates with appropriate antibiotics for selection. Plates were incubated overnight at 37°C to allow colony growth.

2.2.4 Transformation of chemically-competent *Saccharomyces cerevisiae* by heat shock

Chemically competent yeast was transformed by heat shock at 42°C, as described in Causier and Davies (Causier and Davies, 2002).

2.2.5 Plasmid minipreps

5ml liquid LB cultures containing appropriate antibiotics for selection were inoculated with a sterilised wire loop from plate-grown colonies under sterile conditions. Cultures were grown overnight at 37°C (*E. coli*) or for 24 hours at 28°C (*Agrobacterium*) in an orbital shaker at 200rpm. Plasmids were miniprepped from 2ml aliquots of each culture using a QIAprep Spin Miniprep kit (Qiagen) as per the manufacturers recommended protocol.

2.2.6 Plasmid midipreps

10ml bacterial cultures were grown overnight at 37°C with orbital shaking then midiprepped using a Qiagen Plasmid Midi kit, following the manufacturers protocol

2.3 Growth media

2.3.1 LB

LB broth for overnight cultures and bacterial transformations was prepared using 10g dm⁻³ tryptone (Fisher), 5g dm⁻³ yeast extract (Fisher) and 10g dm⁻³ sodium chloride (Fisher) dissolved in sterile, distilled water. LB agar was prepared in the same manner but included 15g dm⁻³ Bacto-agar (Oxoid) as a gelling agent. LB media was sterilised after preparation by autoclaving.

2.3.2 SD

SD medium is a minimal growth medium for yeast that lacks amino acids. SD was made with 6.7g dm⁻³ yeast nitrogen base with 15g dm⁻³ Bacto-agar (Oxoid) if required for plates. To make selective media lacking amino acids (-WL, -WLA and -WLAH), the medium was supplemented with appropriate amino acid dropout solution made from stock powder (Clontech) and 2% sucrose (weight:volume). The pH of the medium was adjusted to 6.5 if necessary.

2.3.3 YPDA

YPDA was used for non-selective growth of yeast. YPDA was made with 20g dm⁻³ peptone (Fisher), 10g dm⁻³ yeast extract (Fisher) and 20g dm⁻³ Bacto-Agar (Oxoid). The medium was supplemented with 200mg dm⁻³ adenine hemisulphate (Clontech) and the pH was adjusted to 5.8 if necessary. N.b. This version of YPDA lacks the titular dextrose component.

2.3.4 MS agar

MS agar used for sterile germination of seeds were made from Murashige and Skoog basal medium with Gamborg's vitamins (Sigma) at half the concentration recommended by the manufacturer (½ MS) plus 6.5g dm⁻³ plant agar (Duchefa) and an appropriate percentage of sucrose if required. MS agar was sterilised by autoclaving.

2.4 Yeast hybrid assays

Yeast hybrid assays were performed as described by Causier and Davies with the exception that YPD growth medium was supplemented with adenine (Clontech) to make YPDA (Causier and Davies, 2002).

2.5 Phylogenetic analysis

2.5.1 Protein sequence alignment

Nucleotide and amino acid sequences were submitted to the MAFFT 7 online server and automatically aligned using the L-ins-I algorithm. Alignments were exported in NEXUS format and manually edited with Bioedit (Hall, 1999). NEXUS alignments were edited to remove the header table to comply with MrBayes formatting requirements then uploaded to the CIPRES Gateway.

2.5.2 Phylogeny assembly by Neighbour-joining and UPMGA

Alignments generated by MAFFT 7 (Kato et al., 2017) were reviewed for accuracy then submitted to the MAFFT server, specifying Neighbour-Joining including Bootstrap with 1000 repetitions or UPMGA. The outputted tree was reviewed using Phylo.io (Robinson et al., 2016).

2.5.3 Bayesian analysis with MrBAYES3.2.6 via CIPRES

NEXUS format alignments were submitted to the CIPRES Gateway (Miller et al., 2011) and run on the 'MrBayes 3.2.6 on XCEDE' tool with the following custom parameters. Number of generations (ngen) = 1,000,000; rates = invgamma; sumt burnin = 0.25; sump burnin = 0.25; number of hours (on four cores) = 4. Where necessary, outgroup was placed as the last taxon in the alignment and was specified by number in the tool's parameters.

2.5.4 Phylogenetic tree drawing with FigTree 1.4.3

Trees were rendered as cladograms from NEXUS format consensus trees generated by MrBayes and imported directly into Figtree. Post-processing of taxon labels and branch colours was performed using Inkscape.

2.6 Plant growth conditions

2.6.1 Growth of *Arabidopsis thaliana* in greenhouse conditions

Plants were grown in long day conditions (16 hours of light, 18 hours of dark) at under halogen lamps with exposure to natural light. Greenhouses were set to 20°C, typically maintaining a temperature range of 18-22°C over a 24-hour period.

2.6.2 Germination of *Arabidopsis thaliana* in growth cabinets

Plants were grown in long day conditions (16 hours of light, 18 hours of dark) at under fluorescent lamps in a Sanyo cabinet at either 21°C or 27°C as required.

2.6.3 Germination of *Arabidopsis thaliana* in sterile conditions

Seeds were sieved to be free of chaff then stratified in non-sterile water for two days at 4°C. After stratification, the seeds were sterilised in 20% household bleach (Clorox; approximately 1% sodium hypochlorite) for ten minutes then washed once with sterile distilled water. Bleached seeds were then immersed in 70% ethanol for one minute then washed three times with sterile distilled water and resuspended in sterile 0.1% agar suspended in distilled water. The seeds were pipetted onto plates containing 2.2g dm⁻³ Murashige and Skoog salts (Sigma), 6.5g dm⁻³ plant agar (Duchefa) and 2% molecular-grade sucrose (Serva).

2.6.4 Growth of *Nicotiana benthamiana* and *tabacum* in greenhouse conditions

Plants were germinated as described for *Arabidopsis* for two weeks then transplanted to potting compost and grown in greenhouse conditions for two weeks under 16-hour light/8-hour dark conditions.

2.6.5 Growth of *Nicotiana benthamiana* in sterile conditions

N. benthamiana seeds were sown without stratification onto sterile media supplemented with 10mM iron citrate in sterilised glass jars (Weck) and grown under 24-hour lighting at 21°C for two weeks.

2.6.6 Heat shock treatment for *Arabidopsis thaliana*

Arabidopsis seedlings required for heat shock experiments were sterilised as described in section in this chapter and plated onto similar plates covered with a nylon sheet (VWR) sterilised by autoclaving. (This excludes the seedlings from the medium and prevent carryover of agarose to the protein extraction.) Plates were placed into a dark 37°C cabinet for 5 minutes or two hours as required. Control plates were placed into a dark, unheated cabinet for an equal period of time.

2.7 Plant transformation

2.7.1 Floral dip transformation of *Arabidopsis thaliana*

Floral dipping was performed as described in by Bent (Bent, 2006).

2.7.2 Transient gene expression in *Nicotiana tabacum* by leaf infiltration

Nicotiana tabacum leaf infiltration was performed as described by J. Denecke (Denecke, 2018, personal communication) with the assistance of Jonas Alvim and Fernanda Silva-Alvim.

2.7.3 Transformation of *Nicotiana benthamiana* protoplasts

Protoplasts were prepared according to the protocols described by Silva-Alvim et al., Foresti et al. and Gershlick et al. (2012) with the assistance of Jonas Alvim and Fernanda Silva-Alvim (Silva-Alvim et al., 2018; Foresti, 2006; Gershlick et al., 2014).

2.8 Sequence analysis

Sequences located in the databases on the *Arabidopsis* Information Resource (Lamesch et al., 2012), Genbank (Benson, 2004) and Phytozome (Goodstein et al., 2012) websites. (TAIR, 2018; and downloaded in FASTA format for alignment using MAFFT 7 (Kato et al., 2017). A Plasmid Editor (Ape) was used for sequence annotation (Davis, 2018).

2.9 Image processing

2.9.1 Photography

Photographs were taken using a Panasonic TZ6 digital camera. Microscopic images were captured using two systems, a Leica binocular microscope equipped with a DFC480 digital camera and a KL1500 LCD lighting system, and a Keyence VHX6000 digital microscope equipped with 5-50x or 20-200x magnification lenses.

2.9.2 Measurement from images

Measurements were made directly from images taken with the Keyence VHX6000 digital microscope using the software tools included with the system.

2.10 Identification of repression domain-containing proteins

The script used to identify repression domains in algal transcription factors was written in Python 3.6.2. The script utilises the Biopython module (version 1.70). Regular expressions and file names were hard-coded for convenience. FASTA format sequence files and tabulated transcription factor family annotations were downloaded from the Plant Transcription Factor Database (PlantTFDB, now version 4.0) (Jin et al., 2017). An example script can be found in Appendix A.

3 The function of TOPLESS is regulated by SUMOylation

3.1 Introduction

3.1.1 Co-repressors are regulated via post-translational modifications

Post-translational modifications (PTMs) enable fine regulation of substrate proteins by influencing their localisation, conformation, function, stability and other characteristics (Bowman and Poirier, 2015; Friso and van Wijk, 2015). Known PTMs include low-molecular-weight chemical modifiers such as phosphate, methyl, acetyl, glycosyl and lipid groups, but also higher-molecular-weight peptides and proteins such as ubiquitin-like proteins (Bowman and Poirier, 2015). Substrate proteins often receive multiple PTMs, allowing them to integrate upstream signal via cross-talk. PTMs may be competitive, either allosterically or functionally, or may be co-operative (Skelly et al., 2016). Modifications may also be prerequisites for further modifications to the host protein (Hietakangas et al., 2006). Some modifications are themselves targeted for modifications (e.g. methylation of methyl groups) (Friso and van Wijk, 2015). The inducible and reversible nature of many PTMs makes them adept at regulating transient events, e.g. stress responses (Augustine and Vierstra, 2018; Lyzenga and Stone, 2012; Song and Walley, 2016). As stress responses often involve post-translational modification of proteins in diverse regulatory pathways, systemic changes can be made by modulating that pathway, e.g. by altering the activity of enzymes or the availability of the modifier itself.

PTMs facilitate some protein-protein interactions (Friso and van Wijk, 2015). PTMs can abolish or create topological or biochemical features such as grooves and binding pockets that facilitate or obstruct quaternary interactions (Friso and van Wijk, 2015). PTMs are important for the assembly and disassembly of some multi-protein complexes (Clapier and

Cairns, 2009). Protein complexes are often modular and exist in different configurations depending on factors such as post-translational modification (or lack thereof) that favour association or disassociation of the complex (Clapier and Cairns, 2009). Several authors have recognised that components of transcriptional regulatory complexes are modified with small ubiquitin-like modifiers (SUMOs), a class of ubiquitin-like protein, and have proposed SUMOylation as a regulator of these complexes (Garcia-Dominguez and Reyes, 2009; Miller et al., 2010; Mazur and van den Burg, 2012). TOPLESS and TOPLESS-RELATED proteins, a class of conserved plant co-repressors, have been described as “highly SUMOylated” (Miller et al., 2010). SUMOylation may regulate the interaction between TOPLESS and other transcriptional regulators.

3.1.2 SUMOylation is a potent modifier associated with protein regulation

SUMOs were first identified in 1997, when the interaction between the human proteins Ran GTPase-activating protein 1 (RanGAP1) and Ran-GTP-binding protein 2 (RanBP2) was found to be stabilised by the ATP-dependent conjugation of SUMO-1 to RanGAP1 (Mahajan et al., 1997). Since this discovery, SUMOs were found to be conserved across eukaryotes. An array of processes is subject to regulation via post-translational modification with SUMOs (SUMOylation). In plants, SUMOylation has been implicated in responses to biotic (Saleh et al., 2015; Lee et al., 2007) and abiotic stress (Mishra et al., 2018; Catala et al., 2007; Miura et al., 2005; Benlloch and Lois, 2018), growth (Catala et al., 2007), hormone signalling and responses (Miura et al., 2009; Pauwels et al., 2010; Srivastava et al., 2018), temperature sensitivity (Hammoudi et al., 2018), frost resistance (Miura et al., 2007), thermomorphogenesis (Lin et al., 2016b) and maintenance of circadian rhythms (Hansen et al., 2017). Key regulators of photosynthesis, oxidative phosphorylation and the TCA cycle are SUMO substrates (Colignon et al., 2017a).

SUMOylation has a variety of effects: protein stabilisation (Kwak et al., 2016; Guo and Sun, 2017), marking proteins for degradation (Saleh et al., 2015)

and disruption of protein-protein interaction (Liu et al., 2016, 21). The effects of SUMOylation are substrate-specific, due partly to SUMO-SUMO interactions. SUMOs interact in a non-covalent manner with SUMO interaction motifs (SIMs) found in proteins including *Arabidopsis thaliana* SUMO1 and 2 (Hecker et al., 2006). SUMOylation and deSUMOylation are rapid processes, allowing responsive protein regulation under varying environmental conditions (Miller et al., 2010).

An interesting aspect of SUMOylation has been described as the 'SUMO enigma' (Hay, 2005). A given protein may depend on SUMOylation for its activity. Loss of SUMOylation, e.g. due to mutation of the substrate protein, causes loss of function. However, only a fraction of proteins of that type need be SUMOylated at any one time. Hay hypothesised that SUMO is necessary to initiate protein-protein interactions, e.g. complex formation. SUMOylation may not be needed for retention. Once the protein has associated with its interacting partners, it can be deSUMOylated without loss of function.

Several reviews have provided a detailed description of the SUMOylation cycle (Novatchkova et al., 2012; Mazur and van den Burg, 2012; Augustine and Vierstra, 2018). (The cycle is illustrated in Chapter 1, Figure 1-5.) Here I will give a brief overview of the pathway in *Arabidopsis thaliana*.

SUMOylation is the covalent attachment of a SUMO protein to a substrate lysine residue of another protein. The process is reversible as bound SUMOs can be removed from the SUMO by SUMO proteases (also known as ubiquitin-like proteases) (Li and Hochstrasser, 1999; Kurepa et al., 2003). Initially, SUMO proteases cleave C-terminal peptide from the SUMO precursor protein to expose a diglycine motif. (The terminal glycine residue will bind to the side chain of the target lysine.) E1 SUMO activating enzymes adenylate the SUMO. The SUMO is transferred to an E2 SUMO conjugating enzyme. *Arabidopsis thaliana* possesses a single E2 enzyme, SUMO CONJUGATING ENZYME 1 (SCE1). From SCE1, it is transferred to the substrate or to an E3 SUMO ligase. There are four SUMO ligases in *Arabidopsis thaliana*: SAP and Miz1 (SIZ1), HIGH PLOIDY2/METHYL METHANESULFONATE-SENSITIVITY PROTEIN 21 (HPY2/MMS21) and PROTEIN INHIBITOR OF ACTIVATED STAT 1 and 2 (PIAL1 and 2). These

enzymes differ in their functions and substrate ranges (Ishida et al., 2012; Tomanov et al., 2014; Rytz et al., 2018). SIZ1 is the most promiscuous ligase with over a thousand known targets (Rytz et al., 2018). HPY2/MMS21 SUMOylates a narrower range of proteins including several that are associated with DNA damage repair (Rytz et al., 2018). PIAL1 and 2 were found to form SUMO chains by SUMOylating SUMO proteins themselves, as part of a mechanism that can recruit SUMO-targeted ubiquitin ligases (StUbls) (Tomanov et al., 2014).

SUMOylation appears to be essential for viability. It is not possible to recover homozygous *sce1* mutants (Saracco et al., 2007), implying that SUMO conjugation is an essential process. SUMOylation is not completely abolished by mutations in individual SUMO ligases due to the availability of other SUMO ligases and to direct attachment by SUMO conjugating enzyme SCE1; however, significant changes in SUMOylation occur in response to loss of SUMOylation pathway enzymes. Mutations in *SIZ1* cause growth and metabolic phenotypes, as the *Arabidopsis thaliana* mutants *siz1-2* and *siz1-3* exhibit dwarfism, drought sensitivity and early flowering (Catala et al., 2007; Miura et al., 2005; Jin and Hasegawa, 2008). *Arabidopsis siz1* mutants accumulate salicylic acid and have increased resistance to bacterial infection due to derepression of salicylic acid-mediated systemic acquired resistance (Lee et al., 2007), have impaired basal thermotolerance leading to high temperature sensitivity (Yoo et al., 2006) and have increased sensitivity to phosphate starvation (Miura et al., 2005). In *Glycine max*, RNAi of the *SIZ1* homologues *GmSIZ1a* and *b* does not lead to salicylic acid accumulation or early flowering but does cause dwarfism (Cai et al., 2017). SIZ1 has been exploited as a master regulator of stress responses; in *Oryza sativa*, overexpression of *OsSIZ1* resulted in improved abiotic stress tolerance (Mishra et al., 2018). Key proteins involved in the regulation of stress responses such as TOPLESS appear to be substrates for SIZ1 SUMO ligation (Rytz et al., 2018). The abundance of SUMOylated TOPLESS, TOPLESS-RELATED 2, PICKLE and numerous other regulatory proteins is decreased in the *Arabidopsis thaliana* mutant *siz1-2* compared to wild type (Rytz et al., 2018). Deficiencies in deSUMOylation also affect plant growth and metabolism. OVERLY TOLERANT TO SALT1 (OTS1) was discovered

through an activation tagging screen where enhancement of *OTS1* expression increased salinity resistance (Conti et al., 2008; Gou and Li, 2012). *OTS1* and *OTS2* are partially redundant (Conti et al., 2008). Single *ots1* and *ots2* mutants are wild type in appearance, but double mutants have increased sensitivity to salt and flower early compared to wild type plants (Conti et al., 2008). Overexpression of *OTS1* decreases the abundance of SUMO conjugates and increases salt tolerance (Conti et al., 2008).

3.1.3 TOPLESS and associated regulatory proteins are SUMOylated

TOPLESS interacts with a diverse group of transcription factors. Its ability to also bind to core chromatin regulatory proteins (*MSI4/FVE*, *PKR1*) (Causier et al., 2012a) and to interact indirectly with histone deacetylases (Krogan et al., 2012) makes TOPLESS a strong candidate to couple the two groups together into the same complex. Stabilisation of TOPLESS could ensure that association between transcription factors and chromatin modifiers is maintained, while degradation of TOPLESS would decouple these proteins, enabling turnover or rearrangement of this pseudo-complex. In 2010, Miller et al. reported that *Arabidopsis* transcriptional regulators are among the most highly SUMOylated proteins under heat stress. Co-repressors from the TOPLESS, LEUNIG and SIN3-like families, HISTONE DEACETYLASE 19 (*HDA19*), HISTONE ACETYLTRANSFERASE 1 (*HAC1*) and chromatin regulators including PICKLE and PICKLE-RELATED 1 (*PKR1*) were identified as SUMO substrates (Miller et al., 2010). The relevance of SUMOylation to the function of these proteins is unknown. Studies of other co-repressors have revealed roles for SUMOs in transcriptional repression, including histone deacetylase-mediated repression. Two co-repressors with structural similarity to TOPLESS, Groucho (from the fly *Drosophila melanogaster*) and Tup1 (from the yeast *Saccharomyces cerevisiae*) are both SUMO substrates (Ahn et al., 2009; Ng et al., 2015). Interaction between Groucho and histone deacetylase *HDA1* depends on interaction between their respective SUMO moieties and SIMs (Ahn et al., 2009) Tup1 also interacts with histone deacetylases (Watson, 2000) and is SUMOylated

under stress conditions (Ng et al., 2015, 1; Oeser et al., 2016) to enhance its repressive activity and to stabilise it (Ng et al., 2015, 1) and possibly to prevent its aggregation (Oeser et al., 2016). It has been postulated that SUMOylation plays an important role in the regulation of co-repressors and repressive complexes in plants as many plant transcriptional regulators are SUMOylated (Mazur and van den Burg, 2012).

3.1.4 Aims

SUMOylation is an important post-translational modification used to regulate proteins associated with numerous essential processes occurring in plants. TOPLESS and TOPLESS-RELATED proteins are co-repressors that interact with an equally broad range of genetic pathways. TPL/TPRs have been identified as substrates for SUMOylation, but the importance of SUMOylation to these proteins was unknown. Additionally, no evidence was available to show which residues within these proteins were SUMOylated. My aims were:

- To determine whether (and how) SUMOylation influences the function of TOPLESS in terms of its ability to repress gene expression
- To identify where the TOPLESS protein is SUMOylated, to gain insight into how SUMO moieties affect its interactions

3.2 Methods

3.2.1 Assembly of mutants by crossing

The *tpl-1* mutant was provided by Jeff Long (UCLA). Harold van den Burg (University of Amsterdam) provided *ots1 ots2* along with sequences for appropriate genotyping primers. The *siz1-2* mutant was supplied by the National *Arabidopsis* Stock Centre (Nottingham). *Siz1-2* and *ots1 ots2* were genotyped by PCR fragment analysis while *tpl-1* was genotyped by sequencing. Crosses were made using *tpl-1* pollen and emasculated *ots1 ots2/siz1-2* flowers. This allowed rapid screening for weak *tpl-1*-like phenotypes to confirm successful crossing before genotyping.

3.2.2 Assembly of constructs for plant transformation

Constructs described in this section are listed alongside additional descriptive information in Table D-0-1 (Appendix D). The *TOPLESS* genomic sequence and its promoter region were amplified from DNA extracted from *Arabidopsis thaliana* (Landsberg erecta) leaf tissue by polymerase chain reaction (PCR) with a high-fidelity DNA polymerase (Phusion; Thermo Scientific) using gene-specific primers flanked with Gateway cloning sequences attB1 and attB2. The product was gel purified and cloned into pDONR201 using the Gateway recombination system (pDONR201-*pTPL::TPL*). Sequencing identified an introduced nonsense mutation (Q164STOP). This position is flanked by PstI restriction sites. The region was excised by PstI restriction digestion and cloned into pUC19 (pUC19-*TPL* Q164STOP). Conveniently, the cloned fragment included candidate SUMOylation sites. The mutation was restored to the wild type sequence by site-directed mutagenesis and the fragment was ligated back into the original vector. To assemble versions of pDONR201-*pTPL::TPL* with mutations at candidate SUMOylation sites, pUC19-*TPL* was mutated by site-directed mutagenesis. All permutations of the SUMOylation site mutations were attained by sequential mutagenesis. At each step, multiple clones were selected for the next round of mutagenesis. Each fragment was wholly sequenced prior to excision and ligation into the full construct to prevent carry-over of mutations introduced during PCR. Constructs were cloned into Alligator plant expression vectors downstream of a constitutive 35S promoter (Bensmihen et al., 2004).

For expression of haemagglutinin (HA)-tagged TOPLESS, the TOPLESS coding sequence was cloned by Gateway recombination from pDONR207 into the binary transformation vector Alligator II (Bensmihen et al., 2004) in-frame with its N-terminal HA repeats. Vectors were transformed into *Agrobacterium tumefaciens* strain GV3101 by electroporation at 1.8kV. Plants were transformed using the improved floral dip method (Bent, 2006) and transformed seeds were selected based on expression of the GREEN FLUORESCENT PROTEIN seed coat marker using a fluorescence microscope (Bensmihen et al., 2004). Single copy lines were obtained for

GUS reporter transformants by selecting lines segregating according to ratios predicted for monohybrid (single gene) inheritance.

3.1.1 Protein extraction under mildly denaturing and denaturing conditions

Ler seedlings expressing *35S::3xHA-TPL* were sterilised by immersion in 1% sodium hypochlorite for ten minutes then immersion in 70% ethanol for one minute, followed by washing three times in sterile distilled water. Sterile seed were sown on agar plates containing half the recommended concentration of Murashige and Skoog basal medium with Gamborg's vitamins (Sigma) with 6.5g dm⁻³ plant agar (Duchefa) as a gelling agent. Seedlings were harvested two weeks after sowing. Roots were removed to avoid contamination of the protein extracts with growth medium. The remaining tissue was flash frozen in liquid nitrogen then homogenised using a pestle and mortar to yield 13g of powdered tissue. From this point until the immunoprecipitation, the protein was kept at 4°C. The powder was resuspended in 50ml extraction buffer consisting of 100mM tris-hydrochloride (tris-HCl) at pH7.5, 150mM sodium chloride (NaCl), 0.5% (volume) NP-40 detergent, 1mM phenylmethane sulfonyl fluoride (PMSF) and one cOMplete protease inhibitor cocktail tablet (Roche). For denaturing extractions, the buffer was supplemented with 2% (mass to volume) sodium dodecyl sulphate (SDS) and was kept at 10°C to avoid SDS precipitation. (N.b. The PMSF and protease inhibitors were added to the buffer immediately prior to resuspension of the powdered tissue.) The extract was vortexed briefly, filtered through Miracloth (Merck Millipore) and then clarified by centrifugation at 4,500 x g for five minutes. The supernatant was filtered using 0.2µm disc filters. To reduce the total volume, the extract was concentrated to a total volume of 5ml by centrifugation at 4,500 x g through concentrator columns with a 50kDa molecular weight cut-off (Pierce).

Capture of HA-tagged proteins: 100µl of µMACS anti-HA-conjugated magnetic beads (Miltenyi Biotec) was added to the extract and incubated for 30 minutes with end-to-end shaking. The magnetic beads were captured on µMACS columns using a magnetic separator. The beads were washed

according to the manufacturer's protocol and the isolated proteins were recovered with elution buffer pre-heated to 65°C. Samples were digested in-solution or excised from SDS-polyacrylamide gels after electrophoresis at 200V for 30 minutes. Processing of solutions and gel fragments was performed by the Mass Spectrometry Facility at the University of Leeds. SUMOylated proteins were captured using recombinant SUMO-interacting motif agarose (Boston Biochem) using the recommended protocol.

3.2.3 Yeast hybrid vector assays

Two hybrid assays were performed as described by Causier and Davies using pGBKT7 (binding domain) and pGADT7 (activation domain) vectors modified to replace the multiple cloning sites with Gateway cloning cassettes (reading frame A) (Thermo Fisher). TPL, HDA19 and SCE1 vectors were kindly provided by Barry Causier. The EPR1 coding sequence was amplified from Ler complementary DNA (cDNA) by polymerase chain reaction and cloned into the pDONR207 entry vector, then cloned into the three-hybrid expression vector pTFT by single fragment Gateway recombination. The TPL-SUMO fusion was assembled in pGBKT7 by two fragment Gateway recombination using an existing clone of SUMO1 in pDONR221 (kindly provided by Barry Causier) and a pDONR221 vector containing the TPL coding sequence minus the stop codon, cloned by polymerase chain reaction from wild type Ler complementary DNA.

3.2.4 4-MUG and PNPG assays

4-MUG and PNPG assays were performed in flat bottomed, optically clear (UV compatible) 96-well plates, according to the protocol described by Francis and Spiker (Francis and Spiker, 2005) using 4-Methylumbelliferyl- β -D-glucuronide hydrate (4-MUG) (Sigma-Aldrich) or 1-(4-Nitrophenyl)glycerol (PNPG) (Sigma) as a substrate, respectively. Fluorescence was imaged using a G:Box gel imager (Syngene) with UV illumination and quantified using FLUO-star Omega F384 optical plate reader (BMG Labtech) with excitation at 355nm and 400nm, respectively.

3.2.5 Quantitative PCR

To measure expression of the GUS reporter and TOPLESS repressor constructs in the repression assay, RNA was extracted from seedling leaf tissue using an RNeasy Plant RNA extraction kit (Qiagen). Reverse transcription of RNA to cDNA was performed using a High-Capacity cDNA Reverse Transcription Kit (Applied Biosystems) using an oligo-dT primer with 1 µg RNA as template. Quantitative PCR was CFX Connect Real-Time PCR System (Bio-Rad) performed according to the protocol in the General Methods section using one-step amplification at 60°C

3.3 Results

3.3.1 Identification of candidate SUMOylation sites in TOPLESS

SUMOylation is reported to occur at higher frequency in lysines within consensus sequences ψ -K-x-E/D (where ψ is a large, hydrophobic residue) than at other lysine residues (Rodriguez et al., 2001). B. Causier (University of Leeds) previously screened TOPLESS and TOPLESS-RELATED proteins for consensus sequences using the bioinformatic program SUMOplot (Abgent, 2018). I also performed regular expression searches using the RegExr v3.4 website (Skinner, 2018) with the search term $[V/L/I/M/P/F/V]K.[E/D]$ to identify any consensus sequences. No consensus sequences were identified, however, SUMOplot and SUMOSP identified the most probable candidate SUMOylation sites as K282, K339 and K414. These motifs were matched to aligned TPL/TPR protein sequences from angiosperms, bryophytes and algae (**see Chapter 3**). Two of these sites, K282 and K414, are broadly conserved across plant TOPLESS-like proteins, while a third (K339) is specific to *Arabidopsis* TPL and TPR1 (Figure 3-1).

Residue (AtTPL)	282	286	339	414
AtTPL	A L K H P	R T P	A F K A P D	L V K E P V
AtTPR1	A L K H P P	R T P P	T F K A P D D	L V K E P V A
PpTPL1	L L K R P P	R T P P	N N V S P D D	L L V K D P P A
PpTPL2	L L K R P P	R T P P	N N V S P D D	L L V K D P P A
MpTPL2	L L K R P P	R T P P	N A Y T P D D	L L V K D P P A
OsASP1	F L K H P	R T P	N I Y T Q D	L M K D A A T
AtTPR4	M L K R E R P	R T P P	A T Y S T D D	L A S E Y T S
AtTPR2	E L K H P P	R A P P	P P A S L D D	I V K E P S S
AtTPR3	I L K H P P	R T P P	A P W S L E D	I A K E T S S
KnTPL	T S K R P P	R T P P	P P N L D D	I V H D T S
PsTPL	Q M S H M	A Q P	Q M S H M D	L V E N

Figure 3-1. Candidate SUMOylation sites in the TOPLESS protein aligned to TPL-like proteins from taxa across the plant kingdom. No canonical SUMOylation site motifs are present in AtTPL. SUMOplot predicted high-probability SUMOylation sites in AtTPL at K282, K339 and K414, with predicted probabilities of 0.8, 0.74 and 0.82, respectively. K282 has been conserved from algae to flowering plants. AtTPL is phosphorylated at T286, adjacent to the candidate SUMOylation site. This residue (and, potentially, phosphorylation) is also conserved. K339 is present only in AtTPL and its sister protein AtTPR1. K414 is broadly conserved but has been lost in AtTPR4. (At = eudicot; *Arabidopsis thaliana*; Os = monocot *Oryza sativa*; Pp = moss *Physcomitrella patens*; Mp = liverwort *Marchantia polymorpha*; Kn = streptophyte alga *Klebsormidium nitens*; Ps = chlorophycean alga *Picocystis salinarum*.)

3.3.2 TOPLESS may have multiple SUMOylation states

TOPLESS was identified as a SUMO substrate by Miller et al. (2010). Miller et al. transformed plants with a histidine-tagged SUMO1/2-like protein that had been modified to enable easy cleavage by trypsin for mass spectrometry (MS), then captured and identified SUMOylated proteins by MS. The data did not reveal where TOPLESS was SUMOylated. I aimed to advance this report by assaying immunoprecipitated TOPLESS protein with an anti-SUMO1/2 antibody. Ler plants were transformed to constitutively express haemagglutinin-tagged TOPLESS (35S::3xHA-TPL). Whole protein extracts were purified under weakly denaturing conditions. While HA-TPL could be precipitated using immobilised anti-HA antibody (Figure 3-2A), subsequent Western blotting with anti-SUMO1/2 lacked specificity (Figure 3-2C). In spite of this, I reasoned that it should be possible to distinguish SUMOylated and non-SUMOylated TPL by mass. Heat shock was used to induce SUMOylation (Miller et al., 2010). The discovery of low-abundance,

high-molecular-weight bands (Figure 3-2B, arrowheads) suggested that TPL protein was present in a modified form. The increase in molecular weight could result from the addition of SUMO moieties. Recently, Rytz et al. (2018) have shown that these bands are indeed SUMOylated TPL. I attempted to abolish SUMOylation by mutating candidate SUMOylation sites within TOPLESS, but was able to recover similar high-molecular-weight bands for HA-TPL K282R and HA-TPL K339R. These sites may not be *bona fide* SUMOylation sites; however, the presence of multiple bands suggests that SUMOylation may occur at multiple residues, and that elimination of a single site may be insufficient to abolish SUMOylation completely.

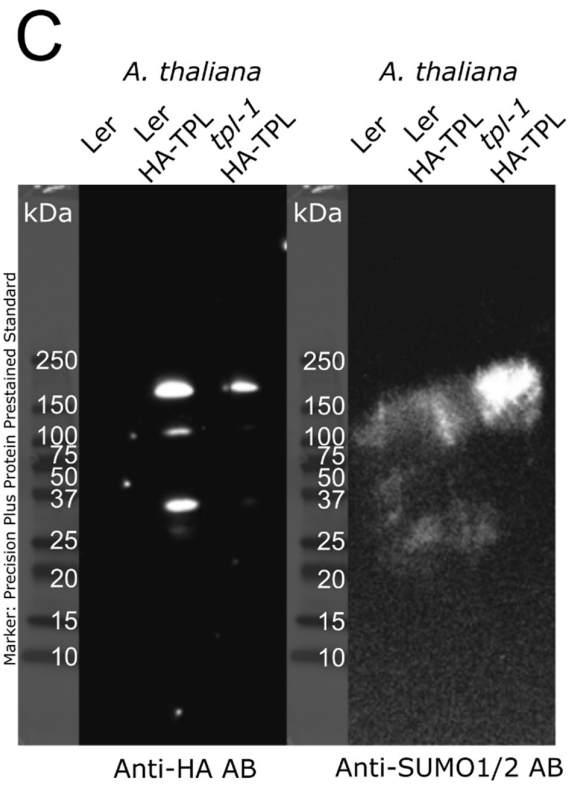
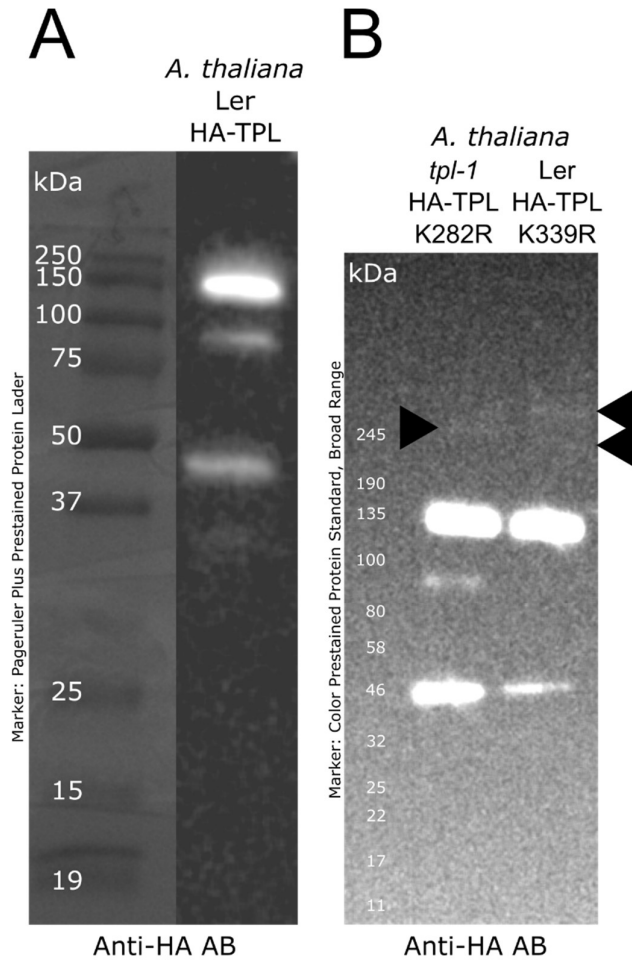


Figure 3-2. Immunoprecipitation of TOPLESS protein.

Immunoprecipitation of HA-tagged TOPLESS proteins from flowering *Arabidopsis thaliana* plants. Western blots for HA-TPL from immunoprecipitation (A, C) and crude extracts (B) from wild type Ler and transgenic Ler and *tpl-1* lines. HA-TPL and versions containing mutations at candidate SUMOylation sites K282 and K339 both generate reproducible fragmentation patterns. Additional high molecular weight bands (black arrows) were observed in one blot and may represent post-translationally modified HA-TPL. No non-specific signal was observed for wild type control precipitations. TOPLESS is phosphorylated (Reiland et al., 2009) and SUMOylated (Miller et al., 2010; Rytz et al., 2018). Rytz et al. (2018) demonstrated that a similar single high-molecular-weight band from TPL-HA immunoprecipitations contained SUMO1/2 proteins. It is unclear if two of the three high-molecular-weight bands are identical in size. Mutation of K282 to prevent SUMOylation may influence other post-translational modifications (e.g. phosphorylation at the neighbouring T286 site) to change the molecular weight of TOPLESS. The failure to recover one band for HA-TPL K282R may indicate abolition of SUMOylation at K282 but may instead reflect low yield of intact protein. Western blotting the same membrane with anti-SUMO1/2 antibody (AB) after stripping the anti-HA AB generated excess background signal and subsequent Western blots using the plant anti-SUMO1/2 AB (ab5316, Abcam) also displayed low target specificity.

In a final attempt to verify that TPL is SUMOylated, I used a SUMO-targeted approach. I heat shocked wild type Col plants, SUMO ligase mutant *siz1-2* plants, and Col plants expressing FLAG-tagged TOPLESS (Col *35S::mCherry-TPL-3xFLAG*, kindly provided by Antoine Larrieu) at 37°C for five minutes. TOPLESS is one of many proteins that exhibits increased SUMOylation under heat stress (Miller et al., 2010; Rytz et al., 2018). SUMOylated proteins were captured from heat-shocked plants using SUMO-interacting motif (SIM) peptides bound to agarose beads (Figure 3-3). Western blotting with anti-FLAG antibody (Figure 3-3B) detected multiple protein bands for the discarded protein fractions and a single, high-molecular weight band for the SIM-captured fractions (Figure 3-3). Heat shock increased the abundance of captured mCherry-TPL-3xFLAG. This supports prior research by Miller et al. which shows that TPL is SUMOylated *in planta* and that more TPL proteins are SUMOylated under heat stress. This experiment also serves as a proof-of-concept. Capture of SUMOylated proteins with SIM agarose had not previously been demonstrated for plant

proteins, and its success underlines the conservation of SUMO-SIM interactions in plants.

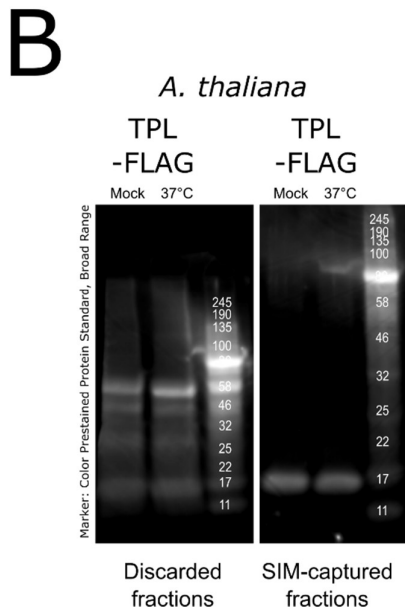
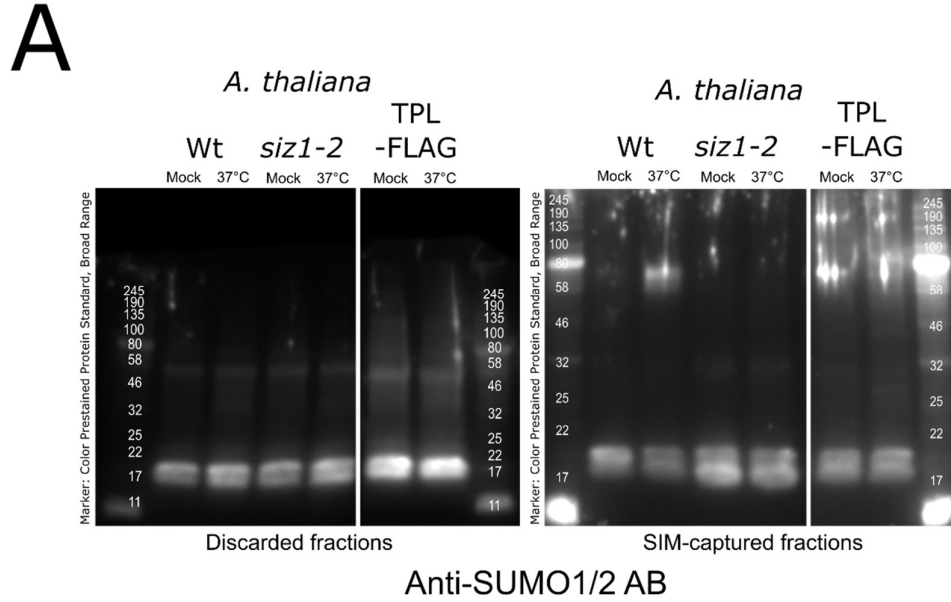
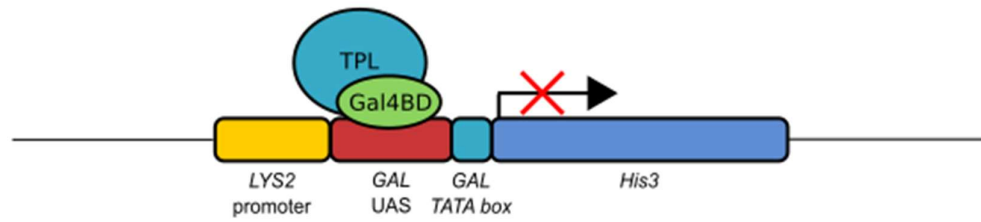


Figure 3-3. Western blots of SUMOylated *Arabidopsis thaliana* proteins. SUMOylated proteins were precipitated from wild type Col, *siz1-2* mutants and Col expressing *35S::mCherry-TPL-3xFLAG* ('TPL-FLAG') that had been incubated at room temperature ('Mock') or heat shocked at 37°C. SUMOylated proteins were precipitated from wild type Col, *siz1-2* mutants and Col expressing *35S::mCherry-TPL-3xFLAG* ('TPL-FLAG') that had been incubated at room temperature ('Mock') or heat shocked at 37°C. Low-molecular-weight proteins (likely free SUMO or E1/E1/E3 SUMO conjugates) are not completely captured and are detectable in the fractions discarded from the precipitation (left images, A and B). Additional high-molecular weight bands are detectable with anti-SUMO antibody (AB) in the captured (SUMOylated) fraction for Col and TPL-FLAG but not for *siz1-2*. This effect is more pronounced for heat-shocked protein. Probing TPL-FLAG with anti-FLAG AB identified one high-molecular weight band appearing after heat shock but the molecular weight markers indicate a discrepancy between this band and the expected size of full-length TOPLESS. Marker = Color Prestained Protein Ladder, Broad Range (New England Biolabs).

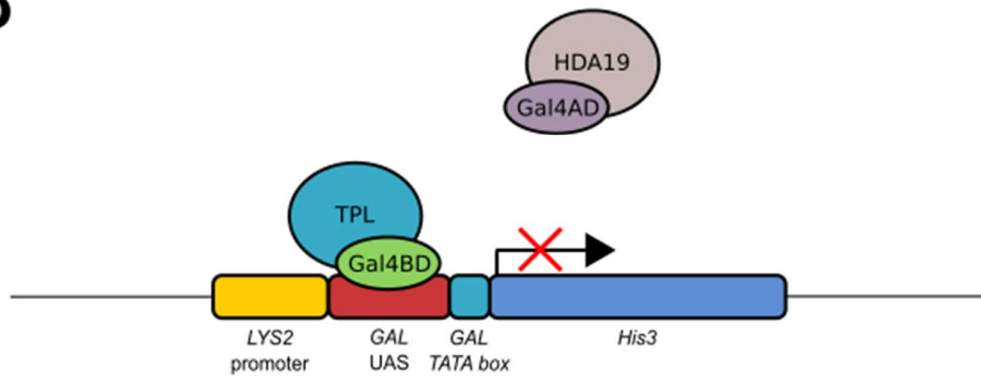
3.3.3 SUMOylation may facilitate interaction between TOPLESS and HDA19

Although TOPLESS-mediated repression depends on histone deacetylation (Long et al., 2006), a direct interaction between TPL and histone deacetylases has not been convincingly shown. Weak signals from yeast two-hybrid assays for TPR1 and HDA19 (HDA1) (Cheng et al., 2018) suggest that the two have low affinity or that any interaction has low stability. Unpublished data from the Davies Laboratory had suggested that SCE1 acts as a bridge between TPL and HDA19, based on a yeast three hybrid assay (yeast hybrid assay model shown in Figure 3-4). Repetition of this experiment did not support the earlier finding, as SCE1 was unable to induce interaction between TPL and HDA19 (Figure 3-5). I also attempted to induce interaction using the transcription factor EARLY PHYTOCHROME RESPONSIVE 1 (EPR1). EPR1 was selected as it interacts with all *Arabidopsis thaliana* TPL-like proteins (Causier et al., 2012a) and may generally represent TPL-interacting transcription factors. EPR1 was insufficient to induce interaction (Figure 3-6). Additional proteins are likely required for the assembly of this complex.

A



B



C

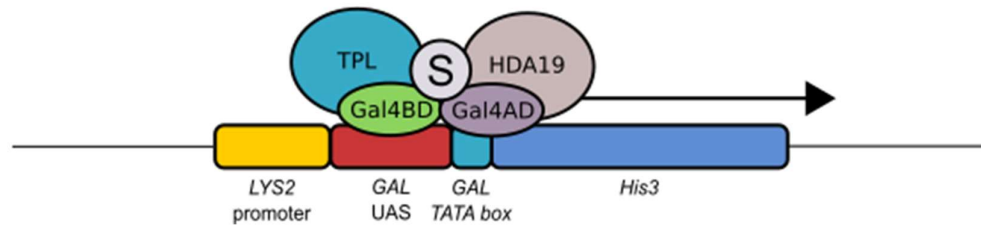


Figure 3-4. The yeast hybrid system using the bipartite Gal4 activation domain (AD)/binding domain (BD) system. Transcription of the histidine biosynthesis gene *His3* is required for the survival of yeast on histidine-deficient media. Fusion of Gal4BD to a protein of interest (the 'bait') allows its recruitment to the GAL promoter, upstream of *His3*. Interaction between the bait protein and a 'prey' protein which is fused to Gal4AD induces activation of *His3*. Where no interaction occurs (A), the yeast is not viable on selective (-H) media. Some proteins may not interact directly (B) but may associate with one another in the presence of an additional protein (e.g. SUMO, 'S') in three-hybrid assays (C).

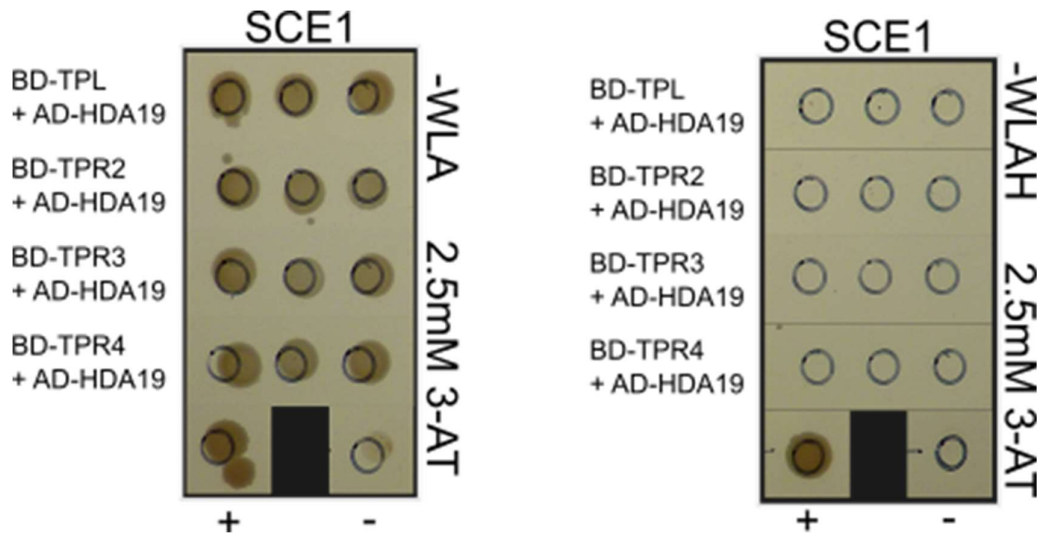


Figure 3-5. SUMO-conjugating enzyme SCE1 does not enable interaction between TPL/TPR proteins and HDA19 in yeast three-hybrid assays. Failure to survive on histidine-free selective media with a minimal concentration of His3 inhibitor 3-AT to prevent auto-activation (right panel) indicates absence of interaction. Positive (+) control = BD-UPF1+AD-SMG7; negative (-) control = BD-TPL (control lines kindly provided by B. Casier).

TPL-HDA19 interaction may not be detectable in yeast if the interaction is SUMO-dependent, as the two proteins may not be recognised or appropriately modified by the yeast SUMOylation machinery. I next attempted to induce interaction between TPL and HDA19 by directly fusing the SUMO1 protein to the C-terminus of TPL. The yeast two-hybrid assay indicates no interaction between TPL and HDA19 but a weak interaction occurs between the TPL-SUMO fusion and HDA19 (Figure 3-7). This result must be approached cautiously. This interaction is not occurring in its native context. Additionally, TOPLESS may be SUMOylated at other positions rather than the C-terminus. (Newly published data indicates that SUMOylation does in fact occur within the C-terminal WD40 repeats (Rytz et al., 2018)). Although HDA19 may be interacting with SUMO independently of TOPLESS, the interaction would imply that SUMO- SIM-mediated recruitment of Class I HDACs is conserved between plants and animals (Ahn et al., 2009).

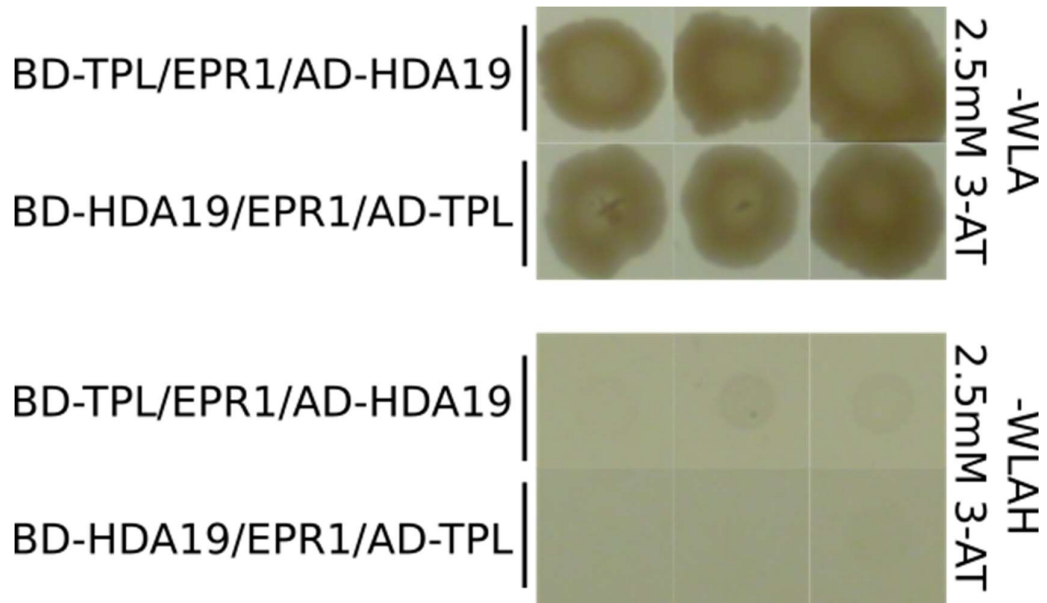


Figure 3-6. Yeast three-hybrid assay for TPL, HDA19 and the transcription factor EPR1. EPR1, a transcription factor that interacts with all *Arabidopsis* TPL/TPR proteins (Causier et al., 2012a), does not enable interaction between TPL and HDA19 in yeast three-hybrid assays. Positive and negative controls shown in Figure 3-5.

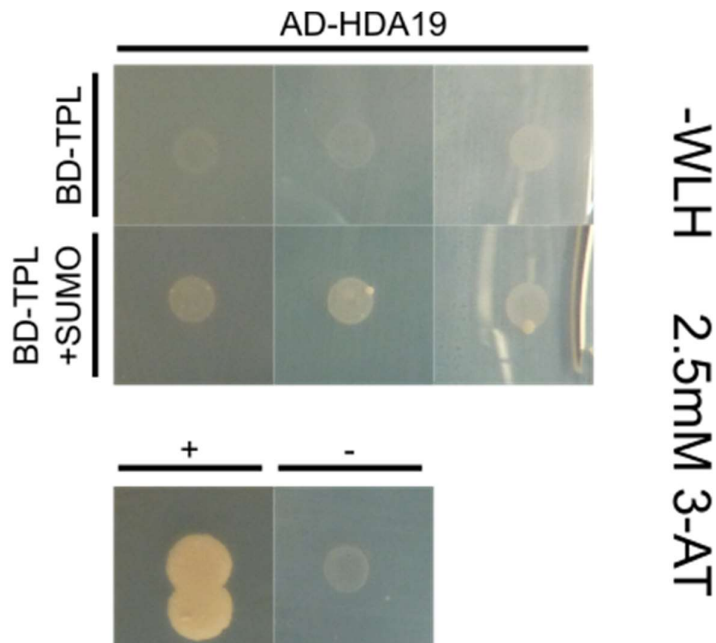


Figure 3-7. Yeast two-hybrid assays for interaction between TPL and HDA19. TPL and HDA19 do not interact directly. Fusing SUMO to TPL enables only a weak interaction with HDA19. Positive (+) control = BD-UPF1+AD-SMG7; negative (-) control = BD-TPL (control lines kindly provided by B. Causier).

3.3.4 The phenotype of *tpl-1* mutants is enhanced in a SUMOylation-deficient background

TOPLESS and TOPLESS-RELATED proteins are “highly SUMOylated” (Miller et al., 2010) but the purpose of this SUMOylation is unknown. We can gain insight by examining how changes in protein SUMOylation impact upon mutants of *TPL/TPR* genes. Loss of key SUMOylation pathway enzymes causes systemic changes in SUMOylation. The E3 SUMO ligase mutant *siz1-2* and the SUMO protease double mutant *ots1 ots2* show decreased and increased SUMOylation of substrate proteins, respectively. Crossing these mutants with the loss-of-function *tpl-1* mutant allows us to see whether or not changes in SUMOylation enhance or complement deficiencies in TPL/TPR function.

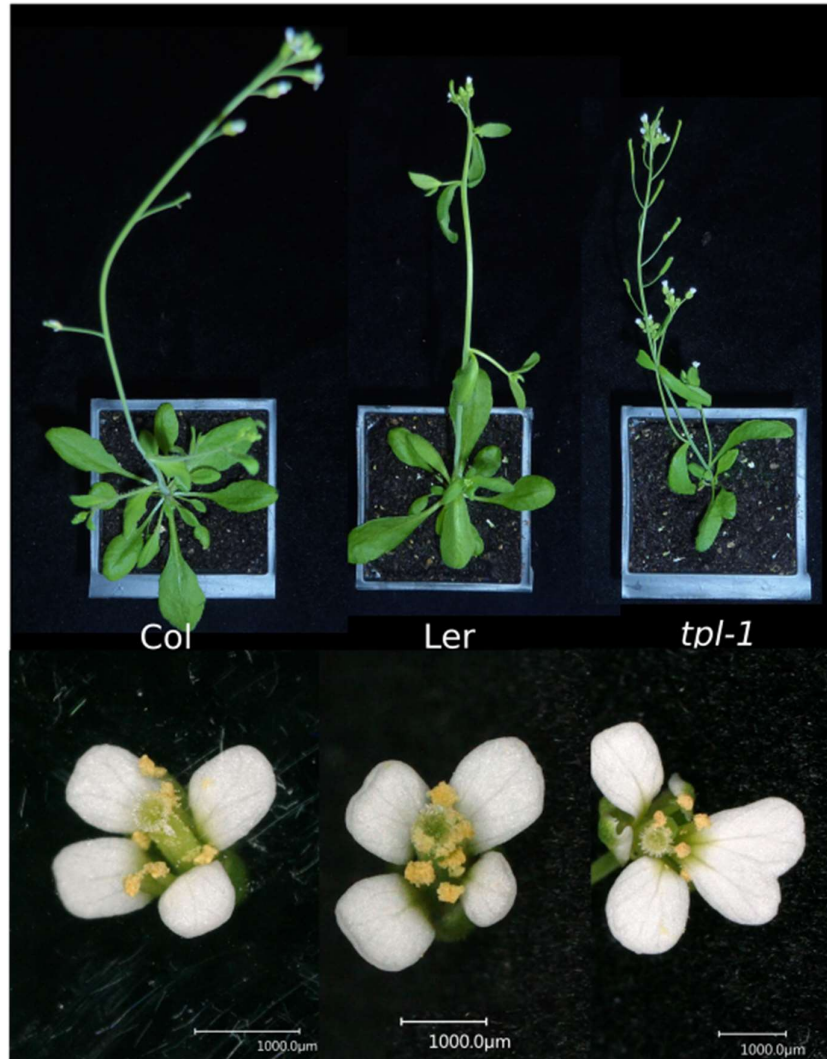


Figure 3-8. Phenotypes of Col, Ler and *tpl-1* plants grown at 27°C. In addition to floral defects, *tpl-1* often produces a small, disorganised rosette. The transition from vegetative to reproductive growth also occurs earlier in *tpl-1* than wild type plants, hence the presence of siliques.

The *tpl-1* mutant has conspicuous morphological phenotypes in embryonic development growth habit and floral development (Figure 3-8) resulting from a point mutation in *TPL*. Single *tpr1*, 2, 3 and 4 mutants are superficially wild type (Long et al., 2006). The *siz1-2* and *ots1 ots2* do not exhibit these same defects in morphological development. The mutant TPL-1 protein is thought to aggregate with wild type TOPLESS-RELATED protein monomers, diminishing the pool of free, functional proteins (Ma et al., 2017). Changes in global SUMOylation or deSUMOylation could alter the activity of the wild type TOPLESS-RELATED proteins, aggravating or mitigating the effects of

tpl-1. I crossed *tpl-1* with *siz1-2*. SIZ1 is one of four SUMO ligases in *Arabidopsis thaliana* and is the most prolific in terms of target range (Rytz et al., 2018). Mutant *siz1-2* plants progress through vegetative development slowly, remain dwarfed and have low fertility (Figure 3-9) compared to wild type Col control plants (Figure 3-8).

siz1-2

siz1-2 tpl-1^{+/-}

siz1-2 tpl-1

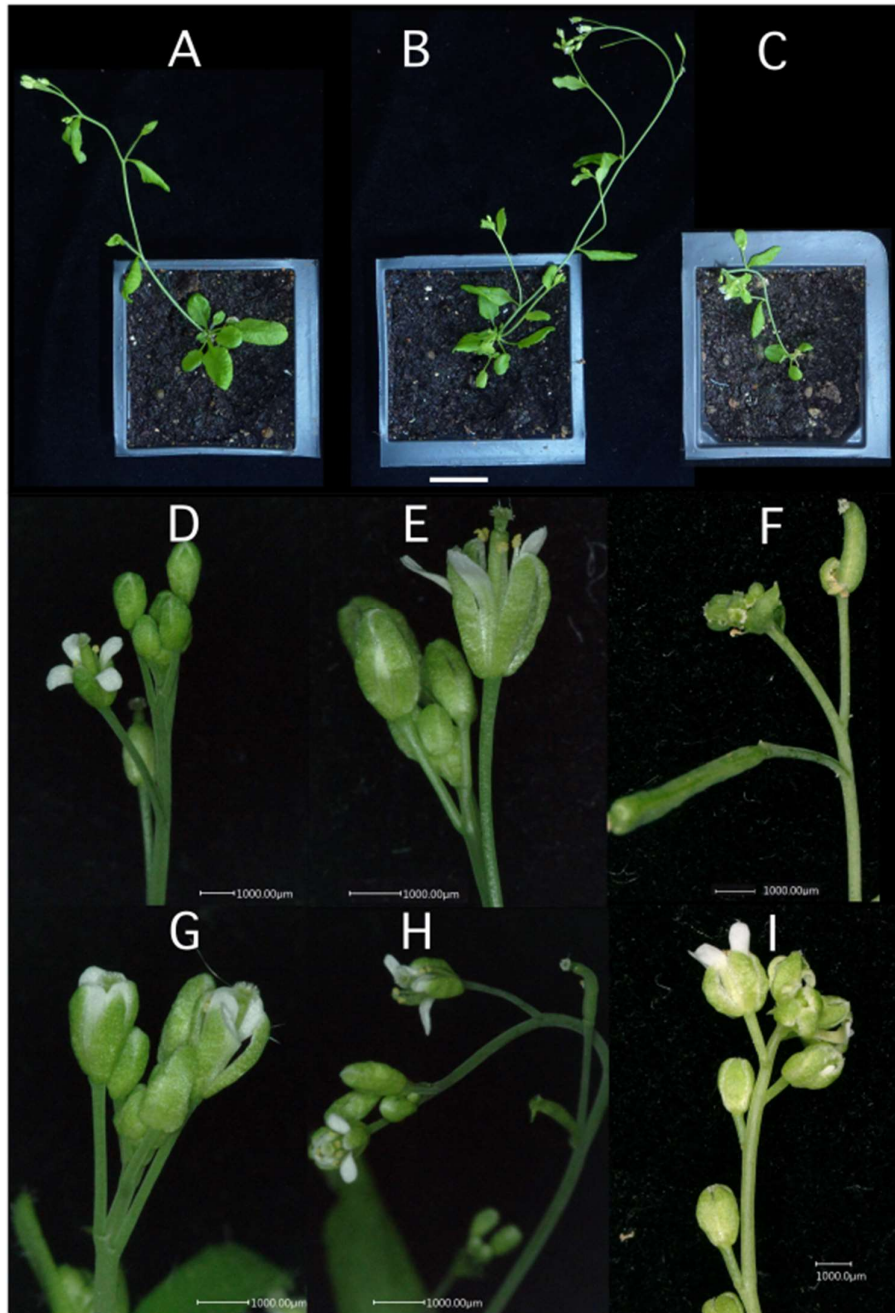


Figure 3-9. Vegetative and floral phenotypes in *siz1-2* and *siz1-2 tpl-1* mutants grown at 27°C. The *siz1-2* mutant is dwarfed (A) (n=8) compared to wild type Col and Ler. Dwarfism is retained in *siz-1 tpl-1^{+/-}* heterozygotes (B) (n=2) and *siz1-2 tpl-1* (C) (n=2), which also produce disordered rosettes as seen in *tpl-1*. While *siz1-2* and *siz-1 tpl-1^{+/-}* produced small but morphologically normal flowers, *siz1-2 tpl-1* double homozygotes displayed abnormal floral phenotypes more severe than those seen in *tpl-1* mutants (Figure 3-7) grown alongside them. Floral abnormalities were not observed in wild type Ler and Col control plants (Figure 3-8).

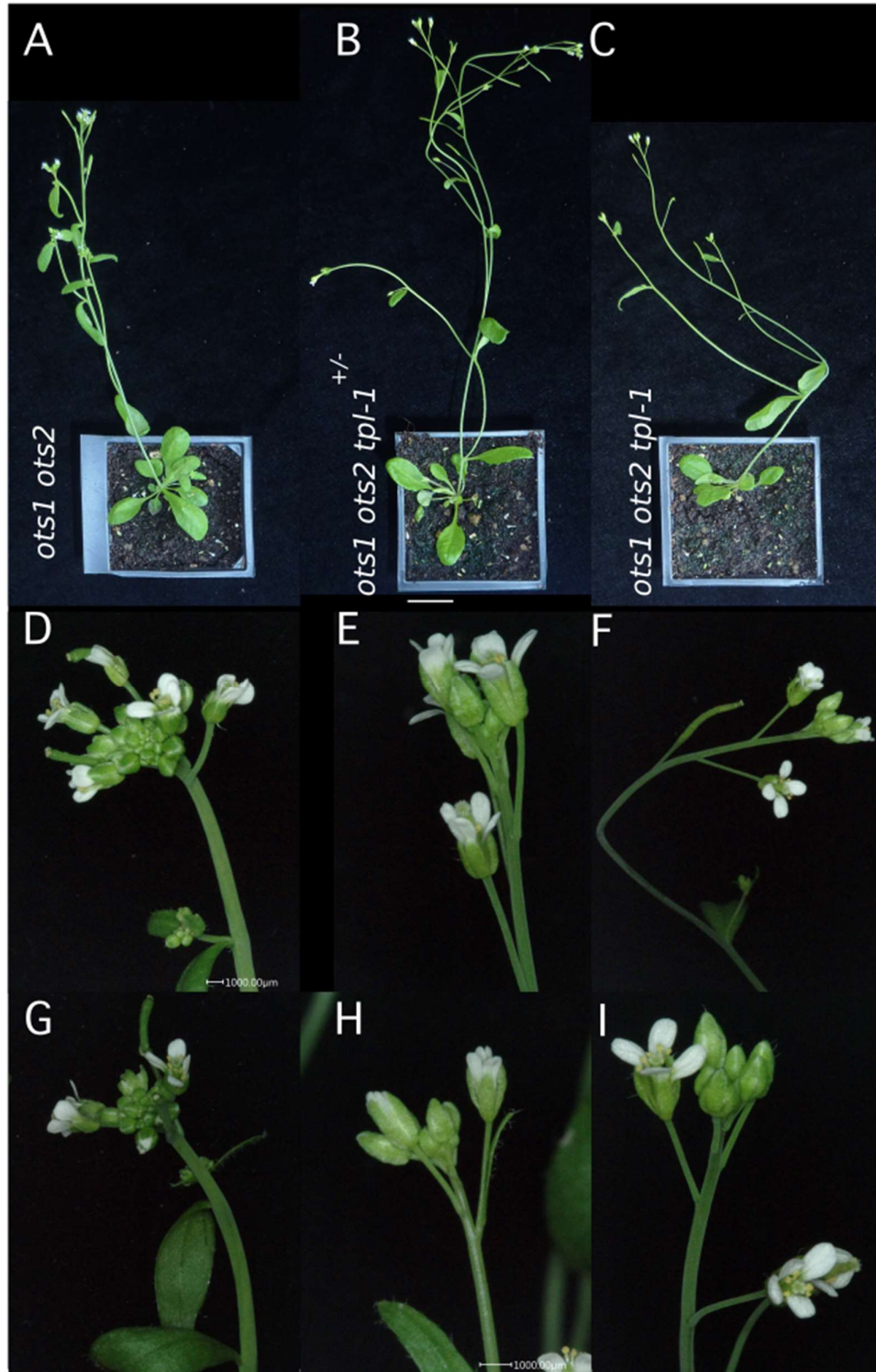


Figure 3-10. Phenotypes *ots1 ots2* x *tpl-1* crosses at 27°C. Unlike *ots1 ots2* (n = 8), the *ots1 ots2 tpl-1*^{+/-} (n = 2) and *ots1 ots2 tpl-1* (n = 2) mutants produced a *tpl-1*-like disordered rosette (B, C) but no abnormal floral phenotypes were observed (H, I). Scales for upper images represent 20mm.

The progeny of *siz1-2 tpl-1^{+/-}* mutants exhibited a mixture of wild type and *tpl-1*-like early developmental phenotypes. The seedlings were transplanted to soil trays for growth at 20°C or 27°C after developing two pairs of true leaves. Abnormal floral phenotypes were not observed in *siz1-2 tpl-1^{+/-}* and *siz1-2 tpl-1* mutants grown at 20°C. At 27°C, *siz1-2 tpl-1^{+/-}* produces wild type flowers while *siz1-2 tpl-1* produced some flowers with an abnormal phenotype (Figure 3-9). Flowers produced ectopic carpelloid tissue or exhibited loss of petals and stamens (Figure 3-9, F and I). Control *siz1-2* plants produce small but developmentally wild-type flowers, although a small number of flowers with minor defects were observed later in senescent plants. We do not have enough information to determine if these rare abnormal flowers result from loss of SUMOylation of TPL/TPRs and their interacting partners or through disruption of an independent SUMO-regulated pathway. However, the heterozygous *siz1-2 tpl-1^{+/-}* mutant had no conspicuous mutant phenotype, suggesting that the phenotype observed in the double homozygous mutant is dependent on loss of TPL function rather than being an enhancement of an existing phenotype. Additionally, the observed floral phenotype of *siz1-2 tpl-1* plants was more severe than phenotypes observed in control *tpl-1* plants grown alongside. The observed phenotypes indicate that loss of SUMO ligase activity in *siz1-2* enhances the mutant phenotype of *tpl-1*.

SUMO moieties can be actively removed from substrates by SUMO proteases. We hypothesised that the loss-of-function of the SUMO proteases that facilitate this process would prolong (perhaps indefinitely) the period for which a protein is SUMOylated, once it has become SUMOylated. *Arabidopsis* SUMO proteases include OVERLY TOLERANT TO SALT 1 and 2 (OTS1/2) (Kurepa et al., 2003; Conti et al., 2008). An *ots1 ots2* double mutant was kindly provided to us by Harold van den Burg (University of Amsterdam). These mutants undergo normal embryonic development and do not produce morphologically aberrant flowers. I crossed *ots1 ots2* and *tpl-1* and obtained a single recombinant heterozygote (*ots1 ots2 tpl-1^{+/-}*) which was selfed to give a segregating progeny. Embryonic *tpl-1*-like phenotypes were commonly observed among the progeny. Developmentally altered (but

viable) seedlings were transplanted to soil and grown at 20°C or 27°C alongside the aforementioned *siz1-2* crosses plus crossed *siz1-2*, *ots1 ots2*, *tpl-1*, Ler and Col controls plants after developing two pairs of true leaves. Like *siz1-2 tpl-1* homozygotes and heterozygotes, *ots1 ots2 tpl-1* flowered earlier than wild type controls under both permissive and elevated temperature conditions. No abnormal floral phenotypes were observed in *ots1 ots2* crosses or in *ots1 ots2* control plants (Figure 3-10), indicating that loss of deSUMOylation in *ots1 ots2* rescues the floral phenotype of *tpl-1* but not the embryonic phenotype. Enhanced SUMOylation may allow TOPLESS-RELATED proteins or other relevant transcriptional regulators to compensate for TPL-1. Alternatively, SUMOylation may be driving the mutant TPL-1 towards degradation via SUMO-targeted ubiquitin ligases and the 26S proteasome and faster or more frequent turnover may prevent the deleterious effects of TPL-1 aggregation.

3.3.5 Complementation of *tpl-1* with wild type and candidate SUMOylation site mutants

Long et al. (Long et al., 2006) and Gallavotti et al. (Gallavotti et al., 2010) have reported that transformation of *tpl-1* with an additional wild type *TPL* gene is sufficient to complement the *tpl-1* mutant phenotype. Unpublished research from the Davies Laboratory indicated that a construction using the *TPL* coding sequence alone with a constitutive promoter (CaMV 35S) was insufficient to completely rescue some transformants. To replicate the published experiments more closely, I cloned a 10.2kb kilobase (kb) fragment of DNA comprising the gene and approximately 4.5kb of DNA upstream of the start codon. This was intended to ensure that the entire endogenous promoter was included in the construct. This differs from the constructs used by Long et al. (2006), who complemented *tpl-1* with TPL-GFP, and Gallavotti et al. 2010, who complemented *tpl-1* with REL2-YFP (REL2 being the maize *TPL* paralogue *RAMOSA ENHANCER LOCUS 2*). In both cases, 4.1kb of upstream DNA sequence was used as a promoter (Long et al., 2006; Gallavotti et al., 2010).

To prevent SUMOylation at candidate acceptor lysines, I made non-synonymous (lysine to arginine) mutations within the relevant codon. Lysine

and arginine share similar chemical properties; both are positively charged, basic, hydrophobic, can be methylated and have similar pK_a values.

However, arginine is not a substrate for SUMOylation. Transformants were scored categorically according to their phenotype one week after sowing. Seeds/seedling were categorised as (a) non-germinating (where the radicle had not emerged from the seed coat); (b) double-rooted; (c) pin-like (radially symmetrical shoot axis with no cotyledons); (d) tubular (where cotyledons were fused to form a radially symmetrical cup); (e) monocotyledonous (a single cotyledon or two cotyledons fused on one edge along >50% of the lamina); (f) dicotyledonous (with two distinct cotyledons separated along $\leq 50\%$ of lamina edge, but with partial fusion, cotyledons not opposite one another or with abnormal positioning of the first pair of true leaves); (g) wild type.

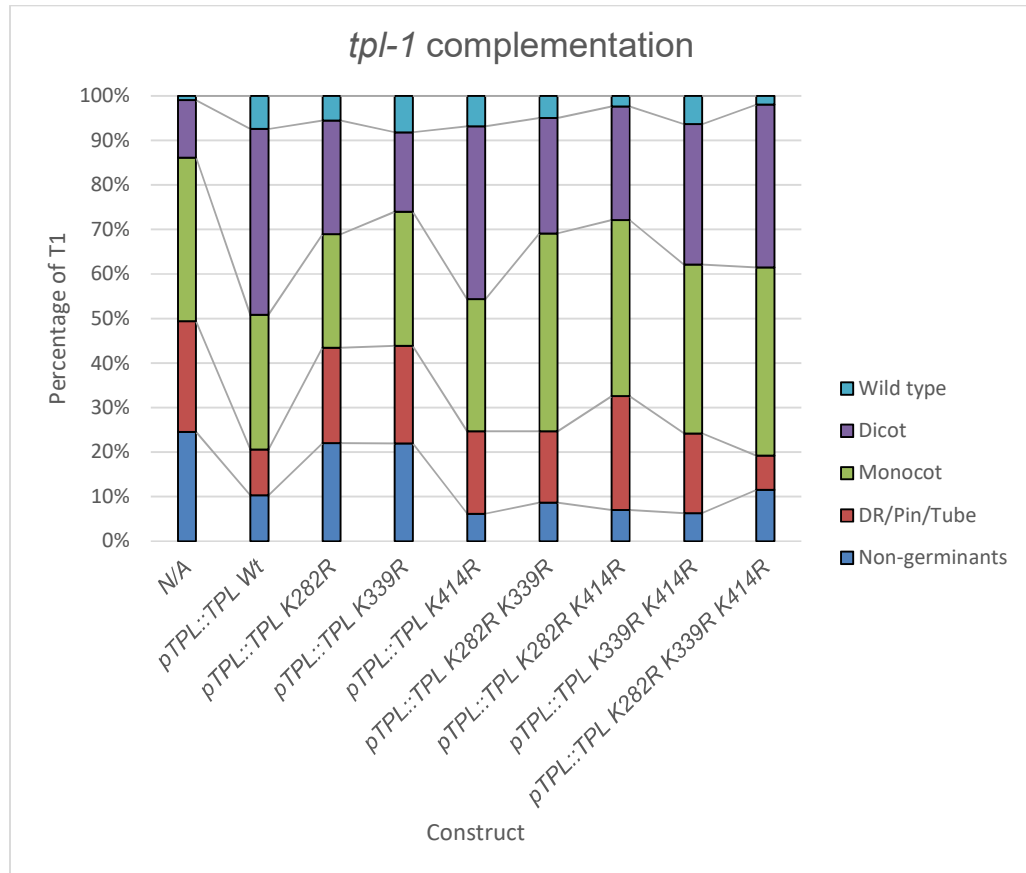


Figure 3-11. Complementation of *tpl-1* embryonic phenotypes with *pTPL::TPL* in T1 transformants. The seedling phenotype of *tpl-1* ranges from the rare double root (DR) phenotype to formation of a radially symmetrical pin, cup or tube (red) to a single cotyledon (green) to morphologically abnormal cotyledons (purple) to wild type (blue) and can be scored based on these categories (Szemenyei et al., 2008). The frequency of severe phenotypes in *tpl-1* seedlings is improved by introduction of the *pTPL::TPL* by transformation. Mutations in candidate SUMO acceptor lysine residues (K282 and K339) diminish this effect.

At 20°C, the most prevalent phenotype (37%) in untransformed *tpl-1* seedlings is the single cotyledon (Figure 3-11). The ‘topless’ double root phenotype is rare (<2%). Wild type individuals are also rare (<1%) and the frequency of non-germinants is significantly higher than for wild type Ler seeds produced and germinated under identical conditions.

Transformation with wild type *pTPL::TPL* partially complements *tpl-1* in T1 transformant seedlings. Germination frequency is increased relative to *tpl-1* (Figure 3-11). The frequency of milder phenotypes (wild type and dicotyledonous) is also increased and the most severe phenotypes were absent. *TPL K282R* and *TPL K339R* constructs were less effective at complementing *tpl-1*. Both constructs improved the *tpl-1* phenotype with regard to the germination rate and the frequency of dicotyledonous and wild type seedlings. However, they did so less effectively than wild type *TPL* and *TPL K414R*. It is unclear which of these two sites has greater the greater influence on function, as K282R transformants were less likely to present a wild type phenotype but more likely to present the dicotyledonous phenotype. Mutation of a second candidate site had minor effects on the efficiency of complementation. Constructs in which K282 is mutated were less able to achieve complete complementation (wild type phenotype). Unexpectedly, germination frequency was improved by constructs containing two mutations compared to the single mutation constructs K282R and K339R. However, this improvement yielded more seedlings with poor phenotypes (monocots) rather than leading to complementation seedlings. Mutation of all three candidate sites further reduced the frequency of the wild type phenotype in transformants (1.9% versus 7.4% for wild type *TPL*). The construct did, however, significantly improve the phenotypic range of *tpl-1*, i.e. a greater proportion of seedlings produced two cotyledons.

I had anticipated that making mutations at multiple SUMOylation sites in *TPL* would additively decrease complementation efficiency, as had been reported for similar experiments on the *Drosophila* co-repressor Groucho (Ahn et al., 2009) and the *Saccharomyces* co-repressor Tup1 (Ng et al., 2015, 1). Changes in complementation efficiency were inconsistent (Figure 3-11). Survivorship bias may increase the number of T1 transformants obtained, as more effective constructs may partially rescue embryos that would otherwise be aborted. The sample sizes for *TPL* transformants with multiple mutations were small (43 – 95 transformants per construct) versus single site mutants (123 – 175 transformants per construct). All available transformants were screened. While transformation efficiency depends on many factors not controlled for here, it this difference may reflect differences in

complementation efficiency. As sample sizes are lower for the multiple mutant constructs, we approach the data with caution. This is particularly important with regard to the ends of the phenotypic spectrum (e.g. double root and wild type phenotypes) which are already represented at low frequency. Overall, *tpl-1* is a difficult system in which to conduct complementation studies due to the variability in its phenotype. Furthermore, the mechanism by which the mutant TPL-1 interferes with wild type TPR proteins has only been partially explained (Krogan et al., 2012; Ma et al., 2017). To create a more amenable mutant background for further studies, I have developed novel *tpl/tpr* mutant combinations (Chapter 3).

3.3.6 Repression assays in transient expression systems

The mutant TPL-1 protein is thought to act in a dominant manner by interacting with wild type TPL and TPR proteins. The phenotype of *tpl-1* can be partially rescued by addition of wild type TPL protein, presumably by competing with TPL-1 for interaction with wild type TPL/TPRs. It would be preferable to assess the impact of SUMOylation on TPL without having this confounding factor. Both Szemenyei et al. (2008) and Krogan et al. (2012) have exploited reporter systems as assays for TOPLESS-mediated repression (Figure 3-16). These systems depend on (a) the expression of a reporter gene and (b) a repressor that modulates the expression of the reporter. The repressor is fused to a DNA binding domain. The target sequence for that domain is added to the promoter of the reporter gene. Thus, the repressor can be recruited to repress expression of the reporter, and the reduction in expression can be quantified by biochemical or quantitative PCR assay. In this case, *TPL* was fused to the Gal4 DNA binding domain (Gal4BD) and expressed from a constitutive promoter (*tCUP*). Upstream Activation Sequences (UAS) were fused to a minimal 35S promoter which was used to express a GUS reporter gene. Two methods of expression were tested: *Agrobacterium*-mediated leaf infiltration and electroporation of protoplasts. Wild type TPL was compared to a version harbouring mutations at all three candidate SUMOylation sites; multiple mutations may have antagonistic effects, but may also counteract redundancy between functional sites.

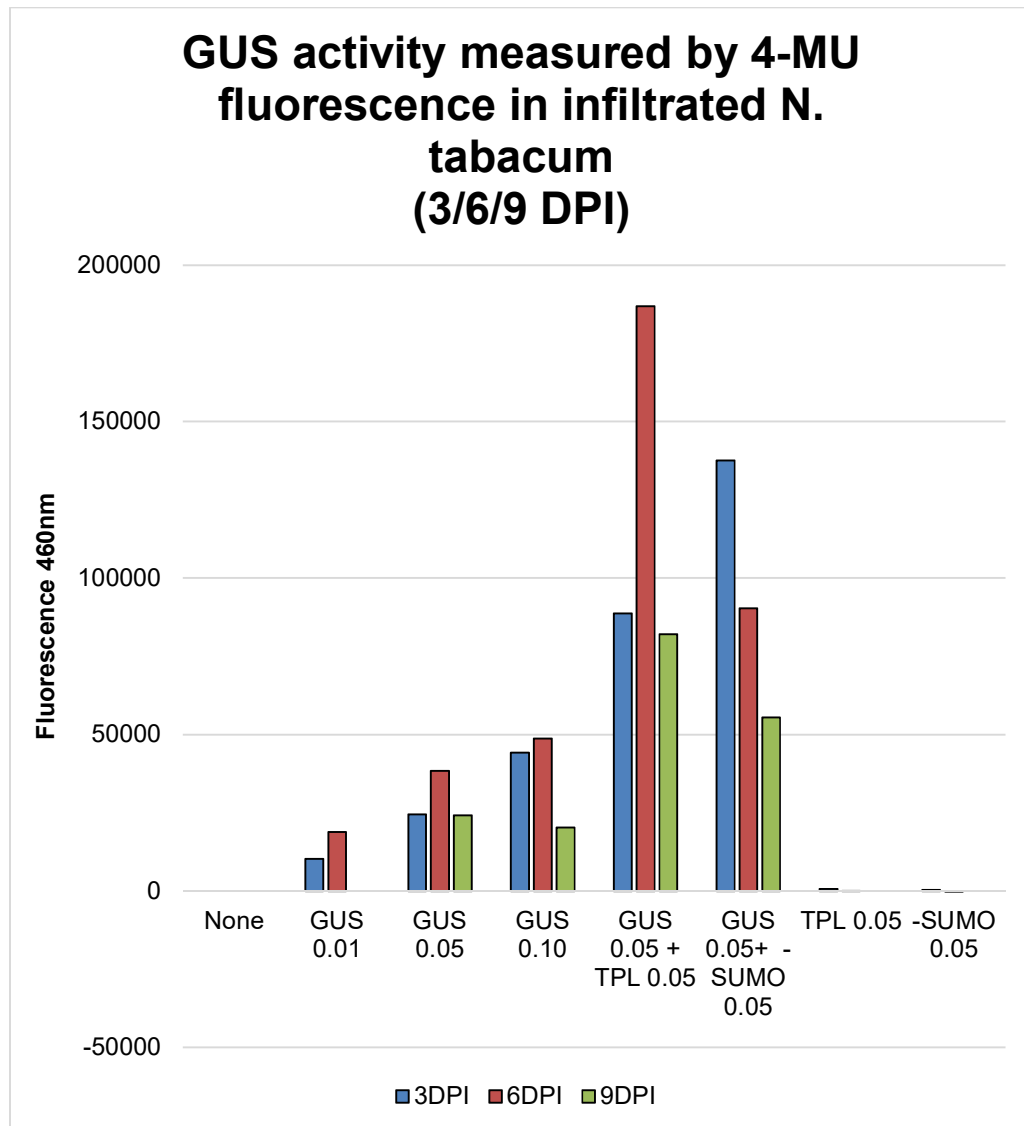


Figure 3-12. Assay for TOPLESS-mediated repression in infiltrated tobacco leaves. The *tCUP::TPL-Gal4BD* ('TPL') construct enhances expression of the *2xUAS-35S::GUS* reporter compared to a reporter control ('GUS') in leaf discs sampled from *Nicotiana tabacum* leaves three, six and nine days (DPI) after transformation with both constructs. Catalysis of the substrate 4-MUG yields fluorescent 4-MU (Y-axis). Mutations in candidate SUMOylation sites (K282R K339R K414R) ('-SUMO') diminish this effect at the latter two time points. Values indicate Optical Density of infiltrated cultures at 600nm. Reporter-only controls using increasing concentrations of *Agrobacterium* indicate that fluorescence correlates positively with the number of *Agrobacterium* cells used. This theoretically approximates the number of cells transformed, i.e. the level of expression. Infiltration with TPL constructs alone did not induce GUS-like activity.

Wild type and K282R K339R K414R versions of the *tCUP::TPL-Gal4BD* constructs were transiently expressed in *Nicotiana tabacum*. *N. tabacum* leaves were infiltrated with *Agrobacterium tumefaciens* GV3101 carrying the *UAS-UAS-35S::GUS* reporter construct plasmid and a repressor plasmid. The same constructs were transformed into *Nicotiana benthamiana* protoplasts by electroporation. For leaf infiltration assays, leaf punches were taken at infiltration sites and assayed for GUS activity using the substrate 4-methylumbelliferyl- β -D-glucuronide hydrate (4-MUG). Catalysis of 4-MUG yields the fluorescent compound 4-methylumbelliferone (4-MU). For protoplasts, the substrate PNPG was used; catalysis of PNPG yields the pigmented compound NPG which can be quantified by spectrophotometry. Data for assays of leaf infiltrations and protoplast transformations are presented in Figures 3-12 and 3-13, respectively. For the leaf infiltrations, GUS expression controls indicate that the reporter was expressed correctly and in proportion to the concentration of *Agrobacterium* used per infiltration while negative controls (repressor only) were clear. Unexpectedly, co-infiltration of the reporter and repressor generated reporter expression opposite to prior expectations. Addition of the 'repressor' increased *GUS* expression. The mutated repressor also elevated reporter expression, but to a lesser degree. 4-MUG assays of leaf punches taken from the same infiltration sites supported these data (Figure 3-13). For protoplast assays, transformed protoplasts were harvested, lysed and assayed using PNPG. The results were consistent with those from leaf infiltrations. The two assays indicated that addition of TPL-Gal4BD increased expression of the reporter and that mutations at the three candidate SUMOylation sites diminished this effect.

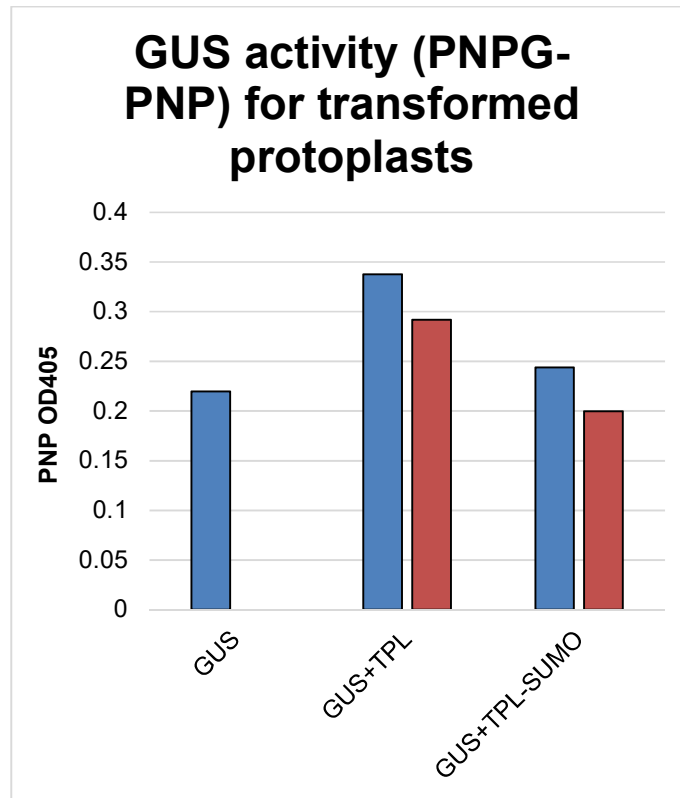


Figure 3-13. Assay for TOPLESS-mediated repression in tobacco protoplasts. Wild type *tCUP::TPL-Gal4BD* ('TPL') enhances expression of the *2xUAS-35S::GUS* ('GUS') reporter in transformed *Nicotiana benthamiana* protoplasts compared to a reporter control ('GUS') but mutations in candidate SUMOylation sites (K282R K339R K414R) ('TPL-SUMO') diminish this effect. The GUS reporter catalyses the transparent substrate PNPG to visible NPG, allowing measurement by spectrophotometry. Bars indicate independent transformations, normalised to the optical density of a reaction mixture lacking the PNPG substrate.

3.3.7 Repression assays in *Arabidopsis thaliana*

Unexpected results for repression assays in *Nicotiana* may be due to the use of a heterologous system (*Nicotiana*) for expression (see discussion). As an alternative to transient expression, I developed single copy *2xUAS-35S::GUS* (Figure 3-14) reporter line in *Arabidopsis thaliana* in wild type Ler and *tpl-1* and transformed them with a *pTPL::TPL-Gal4BD* wild type repressor construct. Expression of the reporter in T2 transformants was quantified by 4-MUG assay. Substantial variability was observed in controls but reporter activity was reduced in transformed lines (Figure 3-15). Protein

expression may inaccurately represent transcriptional activity, as the stability of GUS allows the protein to accumulate, potentially masking subtle differences.

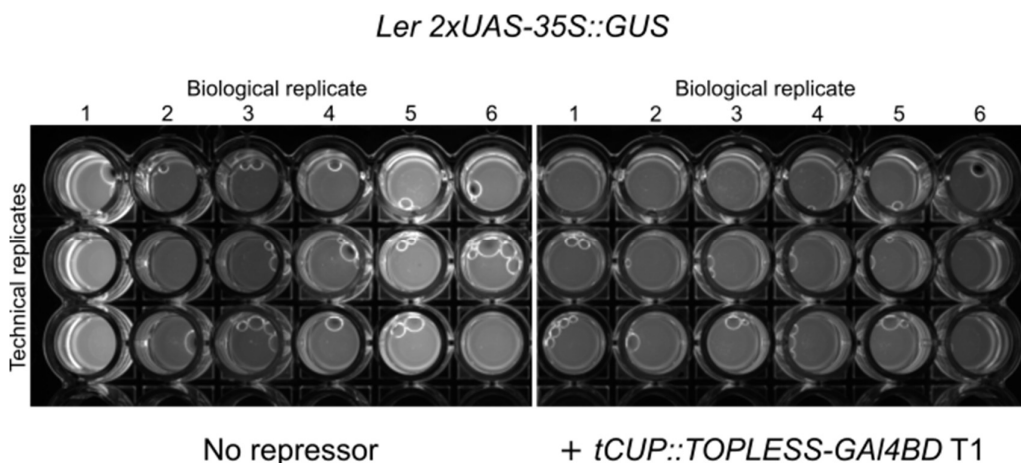


Figure 3-14. *Arabidopsis* GUS reporter activity assay. A 4-MUG assay to test the TPL-Gal4BD/UAS-GUS system in *Arabidopsis* demonstrated that GUS activity was low in plants transformed with the repressor but also identified variable levels of *GUS* expression in the control plants. (Light intensity indicates fluorescence of 4-MU produced by GUS catalysis of 4-MUG.)

In an attempt to circumvent these difficulties, I transformed the *Ler* reporter line with *tCUP::TPL-Gal4BD* constructs with or with the K282R mutation. I isolated RNA from pooled T2 seedlings and measured the expression of the reporter and repressor by quantitative PCR. The data indicate weaker repression by the SUMOylation-deficient repressor than the wild type repressor, even when controlling for expression of the repressors (Figure 3-16). However, the standard errors for each treatment must limit confidence in the data. Furthermore, there is substantial variation in the expression of the repression constructs for each treatment. The transformants therefore do not give us a clear indication that mutation of the candidate SUMOylation sites decreases TPL's ability to repress the reporter.

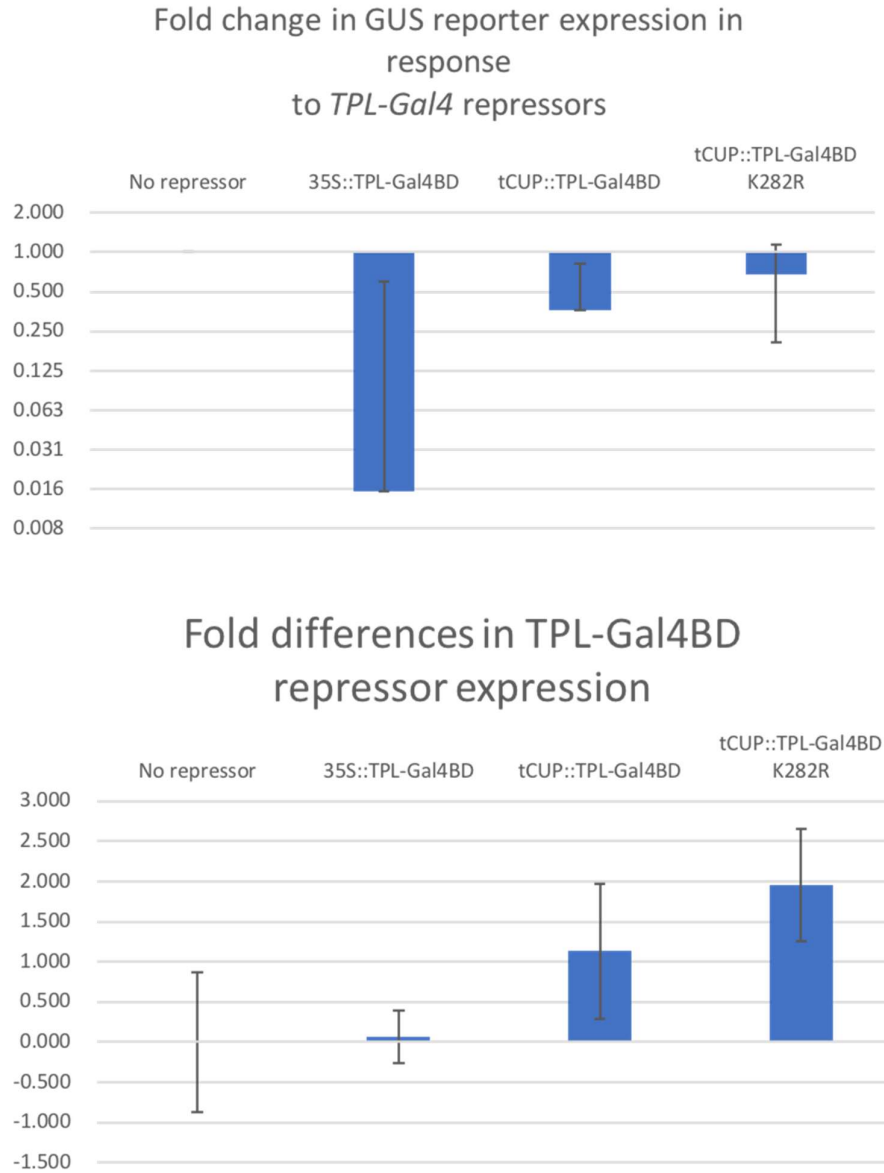


Figure 3-15. QPCR for reporter expression in the TPL-Gal4BD/GUS repression assay. Expression of the TPL-Gal4BD repressor (top chart) with the strong constitutive promoter *35S* reduces expression *UAS-UAS-35S::GUS* ('No repressor'). Use of a weaker constitutive promoter, *tCUP*, decreases reporter expression to a lesser extent. A non-synonymous mutation at a candidate SUMOylation site in TPL (K282R) reduces the ability of TPL-Gal4BD to act as a repressor. Intensity of repression was not dependent of the level of expression of the repressor (bottom chart). In fact, an inverse relationship was observed, indicating that an increased dose of TPL-Gal4BD K282R is insufficient to compensate for its reduced ability to repress.

3.4 Discussion

3.4.1 Partial complementation of *tpl-1* by reduction in SUMO turnover supports a model of stabilisation or enhancement of activity for TPL SUMOylation

The increased severity of the *tpl-1* floral phenotype in the *siz1-2* mutant background is a strong indicator that SUMOylation enhances TPL/TPR-mediated repression. Moreover, the absence of severe floral defects in *ots1 ots2 tpl-1* suggests that loss of deSUMOylation activity (which may allow TPL to remain SUMOylated when attached SUMOs might otherwise be removed) enhances TPL/TPR function, with the implication that SUMOylation is necessary for the activity or stability of these proteins.

3.4.2 Transient expression assays produce consistent results but may indicate sequestration of repressors

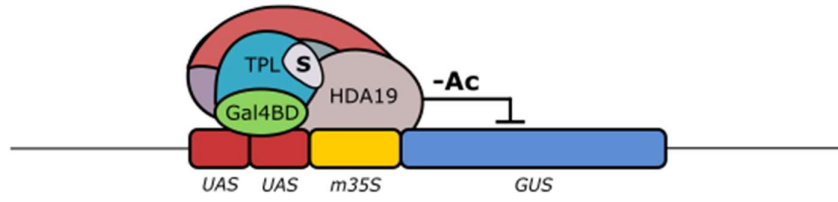
The transient expression assays generated unexpected results. Superficially, the data present TOPLESS as a co-activator. TPL interacts with a diverse collection of transcription factors and some (e.g. WUSCHEL) possess activating as well as repressive characteristics. It is possible that TPL activates gene expression via an unknown interaction with a transcription factor or other components of the transcriptional regulatory machinery. Another possible scenario is that direct recruitment of TPL in the absence of a transcription factor or other essential co-factors interferes with local regulatory processes that limit expression of the reporter. Both hypotheses are improbable, as Szemenyei et al. (2008) reported that *pTPL::TPL-Gal4BD* efficiently represses expression of a similar reporter, *UAS-UAS-tCUP::GUS*. Differences in methodology may explain the new data. Protoplast transformation deliver high concentrations of plasmid to cells. Overexpression of *AtTPL* may interfere with the regulation of gene expression. *AtTPL* could be acting as a sink for endogenous TPL/TPR interacting partners (Figure 3-14B and C), sequestering them from other regulatory complexes. This does not explain the consistency between leaf infiltration and protoplast transformation experiments, however, as leaf infiltration does not achieve a high number of transformation (and co-transformation) events, as demonstrated by the dose dependent

transformation efficiency for GUS. Another consideration is the interaction between TPL-Gal4BD and endogenous TPL/TPRs. Cross-species differences in TPL interactions and functions may interfere with TPL-mediated repression. In particular, *Nicotiana* species possess an additional subclass of TPL-like gene which is related to *Oryza sativa* ASP1 and *Zea mays* REL2 that has been lost in the Brassicaceae. The functions of this gene have not been fully characterised and thus we have limited information with which to predict how *Arabidopsis* TPL will behave when expressed alongside it.

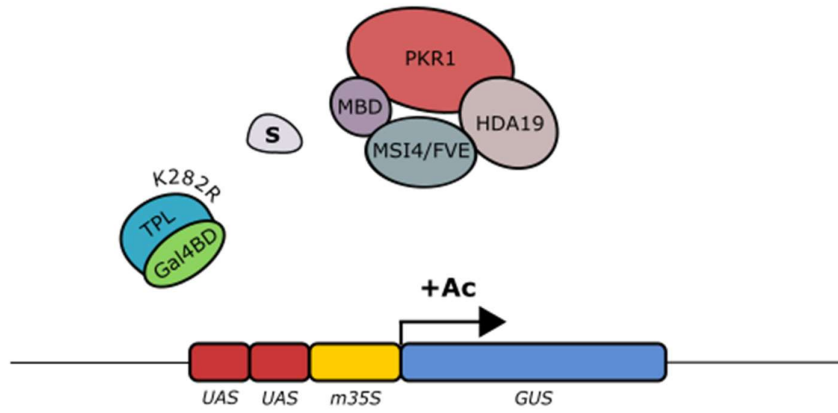
3.4.3 The *Arabidopsis* repression assay system shows that the conserved candidate SUMOylation site, K282, is functionally important for TPL-mediated repression

qPCR supports the hypothesis that SUMOylation at K282 is functionally important as the K282R mutation decreases the ability of TPL-Gal4BD to repress the GUS reporter. This difference is statistically significant. qPCR was used as protein-based assays (i.e. GUS and 4-MUG assays) generated inconsistent data between biological replicates. Protein expression in *Arabidopsis* is reported to be less consistent than in *Nicotiana*, however, it would be preferable to establish a reliable, functional system in *Arabidopsis* for comparability to other experiments, most notably crosses between mutants of TOPLESS and components of the SUMO cycle machinery. An optional approach to extend this assay would be to determine the dose response curve for TPL (i.e. roughly estimate kinetics by measuring how reporter expression correlates with repressor expression), which would test the validity of the sequestration hypothesis (Figure 3-14C).

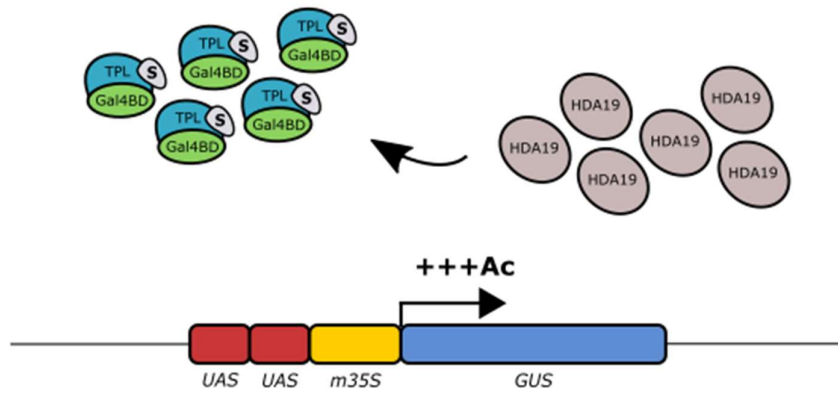
A



B



C



D

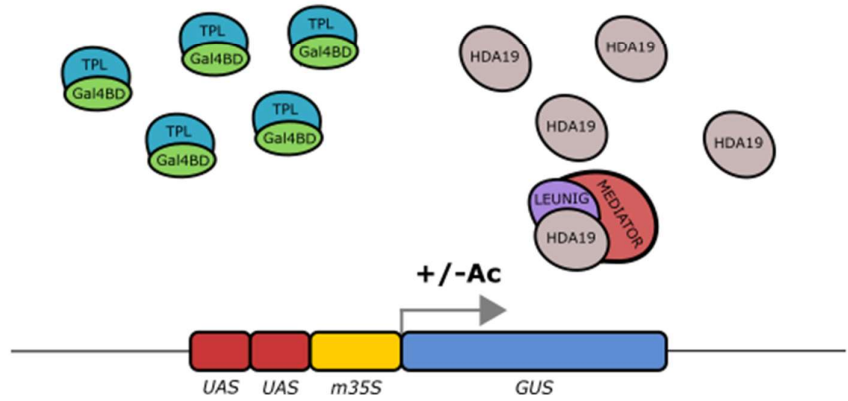


Figure 3-16. Models of interactions in the repression assay and potential problems. (A) Wild type TPL-Gal4BD suppresses expression of the *GUS* reporter. (B) Predicted abolition of SUMOylation at K282 decreases the ability of TPL to repress targets. (C) Saturation of HDA19 with excess TPL-Gal4BD interferes with baseline chromatin regulation, leading to a general increase in histone acetylation ('Ac') and gene expression. (D) Reducing SUMOylation of TPL-Gal4BD (e.g. by mutating SUMOylation sites) decreases its affinity for histone deacetylases, allowing them to participate in other regulatory interactions (e.g. binding the co-repressor LEUNIG and the MEDIATOR regulatory complex).

3.4.4 TOPLESS may be SUMOylated at multiple positions

Previous studies of the SUMOylated co-repressors Groucho and Tup1 have revealed multiple SUMOylation sites that have regulatory importance. TOPLESS and TOPLESS-RELATED proteins may undergo SUMOylation at multiple residues. Identification of these sites by bioinformatic approaches is undermined by the prevalence of non-canonical SUMOylation sites in plant proteins; as many as 40% of sites do not follow the ψ -K-x-D/E sequence. Additionally, not all apparently viable SUMOylation sites will be SUMOylated. Other factors, e.g. proximal phosphorylation sites, can potentially alter the likelihood of SUMOylation at canonical and non-canonical sites. Secondary, tertiary and quaternary structure can obstruct access to potential SUMOylation sites, as can PTMs made at, or adjacent to, the target lysine residue. Although Miller et al. (2010) identified TOPLESS as a SUMOylated protein, they did not report where TOPLESS was SUMOylated. Experimental optimisation and improvements in mass spectrometry technology allowed Rytz et al. (2018) to show that TOPLESS is SUMOylated at K689 (amino acid sequence SKPA). No crystal structure is available for the whole TPL protein, but modelling with Phyre2 would allow us to map the amino acid sequence of TPL to known structures that derive from similar sequences. The SUMOylated residue is situated on an exposed loop protruding from the face of the first beta-propeller, which is formed by repeated WD40 domains. Limited information is available regarding the effects of SUMOylation in the context of the beta-propeller, but the RACK1b protein provides an example of what may be occurring. Rack1 is a conserved eukaryotic protein that forms a single beta-propeller (Ruiz Carrillo et al., 2012). *Arabidopsis* RACK1b has been demonstrated to be SUMOylated at four positions within

and between WD40 repeats. SUMOylation is enhanced by abscisic acid, increasing the stability of RACK1b. SUMOylation prevents degradation by out-competing ubiquitylation (Guo and Sun, 2017). SUMOylation may have a similar role in TOPLESS. SUMOs can induce or promote a variety of effects, but the concept of SUMO promoting stabilisation of TPL is supported by the evidence from the *siz1-2 tpl-1* and *ots1 ots2 tpl-1* mutant. Loss of *SIZ1* enhances the *tpl-1* floral phenotype, and all *Arabidopsis* TPL/TPR proteins show reduced SUMOylation (TPL and TPR2 significantly so) in *siz1-2* (Rytz et al., 2018). Loss of SUMOylation could enhance aggregation of TPL-1 mutant protein itself; however, we might expect that parallel enhancement of TPR1-4 would compensate for this.

Future work is necessary to understand the exact impact of SUMOylation of TOPLESS. Further protein analysis is required to confirm that the lysine residues examined in this chapter are in fact SUMOylated. Optimisation of Western blots using anti-SUMO1/2 antibody (Figure 3-3 versus Figure 3-2) will allow for this. We have yet to explore the role of SUMO interacting motifs in TOPLESS, if indeed they are present. SUMO-SIM interactions are critical for SUMO-mediated interactions between some proteins (Ahn et al., 2009). TOPLESS contains seven SIM-like motifs [I/L/V] [I/L/V]x[I/L/V] at residues 94, 144, 417, 440, 629, 715 and 891. Further analysis and modelling may allow us to identify a subset of these sites for functional studies. The effects of SUMOylation on the stability or turnover of TOPLESS is another area of interest. It would be informative to compare the stability of SUMOylation-competent, wild type TOPLESS with SUMO-null versions, for example by quantifying protein levels along a time course after inhibiting protein translation. Lastly, SUMOylation could hypothetically facilitate protein-protein interactions, but we have identified only a small number of direct interactors. In the future it may be possible to describe a 'TOPLESS complex' akin to repressive complexes such as the Sin3 and Nucleosome Remodelling and histone Deacetylation complexes found in animals.

4 TOPLESS interacts with TOPLESS-RELATED proteins and chromatin regulators

4.1 Introduction

4.1.1.1 TOPLESS may act a component of the histone deacetylation complex

Histone modification is an important mechanism for regulating gene expression (Liu et al., 2014; Wang et al., 2014). Modification is orchestrated by multi-protein complexes (Baymaz et al., 2015). These complexes assemble proteins that provide enzymatic activity, pattern recognition (i.e. specificity for DNA sequences, histones or histone marks), passive structural support and other abilities (Baymaz et al., 2015). Complexes can be an aggregate of several functional modules, allowing core structural or regulatory units to combine with modules that provide other functions, e.g. target specificity. Co-regulators perform an important role in transcriptional regulation by coupling the sequence specificity of transcription factors to the enzymatic activity of chromatin remodellers and histone modifiers (Baymaz et al., 2015). Some co-repressors, such as the TOPLESS (TPL) family of plant co-repressors, facilitate histone modification by indirectly recruiting histone deacetylases to target loci (Szemenyei et al., 2008; Krogan et al., 2012; Wang et al., 2013). TOPLESS lacks histone-modifying activity itself (Krogan et al., 2012). TPL locates target sites in the chromatin by binding to a diverse range of transcription factors (*Arabidopsis* Interactome Mapping Consortium, 2011; Causier et al., 2012b). These transcription factors contain short consensus sequences known as Repression Domains (RDs) (Causier et al., 2012b; Kagale and Rozwadowski, 2011b). Transcription factors provide specificity for gene regulatory elements such as promoters and untranslated regions, and modifications to histones within these regions can influence transcriptional initiation (Liu et al., 2014). Interactomes published for the TPL family demonstrate how a general co-repressor can be recruited to regulate many targets (*Arabidopsis* Interactome Mapping Consortium,

2011; Causier et al., 2012b). Switching a modular component of the complex (the transcription factor) allows TPL to regulate many biological processes, including development, metabolism and defence (Causier et al., 2012b). TPL-transcription factor interaction has been demonstrated *in vitro* and *in vivo* (Ke et al., 2015; Martin-Arevalillo et al., 2017; Wang et al., 2013). Furthermore, fusions of TPL and RD-deficient transcription factors have been used to complement mutants lacking those transcription factors, and addition of RDs to transcription factors allows recruitment of TPL to new targets (Xu et al., 2017).

Interactions between TPL and transcription factors are well understood and have been structurally characterised (Ke et al., 2015; Martin-Arevalillo et al., 2017). Less well understood are the interactions between TPL and other chromatin regulators involved in transcriptional repression. TPL monomers assemble spontaneously to form dimers of dimers (Ke et al., 2015). This process occurs independently of transcription factor binding (Ke et al., 2015; Martin-Arevalillo et al., 2017), although the binding of some transcription factors may stabilise tetramers (Ma et al., 2017, 53).

Although TPL-mediated repression is dependent on the activity of histone deacetylases, evidence for a direct interaction is limited. Histone deacetylase HDA19 co-localises with TPL and can be precipitated in semi-*in vivo* pulldowns (Krogan et al., 2012); however yeast two-hybrid assays to test for direct physical interaction are unconvincing and HDA19 was not recovered in yeast two-hybrid library screens (Cheng et al., 2018; Causier et al., 2012b; *Arabidopsis* Interactome Mapping Consortium, 2011). The repressive activity of histone deacetylases may make it impossible to test for interaction reliably with this type of assay. Similarly, HDA6 co-precipitates with TOPLESS (Long et al., 2006; Wang et al., 2013) but was not recovered in yeast two-hybrid screens for interacting proteins (Causier et al., 2012a). Interaction *ex planta* may be weak for several reasons. Direct interaction may not occur; instead other proteins may be required to bridge TPL and HDA19. These bridging proteins may not interact with both TPL and HDA19. Instead, they may induce conformational changes that enable or stabilise a direct interaction between the two. Other essential factors, e.g. post-translational modifications, may not be correctly added or removed in the

yeast system, or may induce aberrant interactions with endogenous proteins. Proteins may not be correctly folded and may be targeted for degradation. Studies published over the last decade have begun to address these limitations by identifying interaction partners and post-translational modifications (PTMs) associated with TPL.

TOPLESS associates with proteins found in chromatin modifying complexes. Yeast two-hybrid assays by Causier et al. showed that TPL can interact with PICKLE-RELATED 1 (PKR1) and MULTICOPY SUPPRESSOR OF IRA 4 (MSI4)/FVE (Causier et al., 2012b), relatives of the Nucleosome Remodelling and histone Deacetylation (NuRD) complex (see Chapter 1, Figure 1-2) components Mi-2/Chromodomain Helicase Domain (CHD) 3/4 and Retinoblastoma Binding Protein 4/7 (RBBP4/7), respectively.

Immunoprecipitation of MSI4/FVE from *Triticum aestivum* (TaFVE) also co-precipitates TPL alongside histone acetylases and deacetylases, chromatin remodellers, DNA and histone methyltransferases, DNA and RNA helicases and transcription factors (Zheng et al., 2017). Additionally, *Arabidopsis* TPL has been co-precipitated alongside METHYL BINDING DOMAIN (MBD) 10 (homologue of NuRD components MBD2/3), MSI4/FVE, HDA19 and the histone methyltransferase PROTEIN ARGININE N-METHYLTRANSFERASE (PRMT) 4B as part of a complex thought to repress transposable elements (Clavel et al., 2015). The prevalence of proteins homologous to subunits of the NuRD complex is conspicuous. Plants cannot form a canonical NuRD complex as they lack Metastasis Associated (MTA) 1 and p66 α and p66 β . Other components of the complex may be retained due to their involvement in multiple chromatin-regulating complexes or, potentially, due to involvement in undescribed transcriptionally repressive complexes. The interaction between these proteins and TOPLESS, a co-repressor that interacts with a broad range of transcription factors (Causier et al., 2012a), raises the possibility that they form an as-yet undescribed complex that is recruited by transcription factors to silence gene expression.

TOPLESS is post-translationally modified by phosphorylation and SUMOylation. Phosphorylation is a common post-translational modification and is perhaps the most widely studied. It has emerged as an important

regulator of repressive complexes. At least one co-repressor complex, SMRT, depends on co-repressor phosphorylation for complex assembly and function (Varlakhanova et al., 2011). Phosphorylation has been reported to directly regulate sub-nuclear localisation of histone deacetylases (Latrasse et al., 2017b) as well as their dimerisation (Khan et al., 2013), enzymatic activity and protein-protein interactions (Yu et al., 2017) including association with co-repressors in the NuRD and Sin3 complexes (Sun et al., 2007). Mass spectrometric analysis has revealed that TPL is phosphorylated on at least nine residues (Reiland et al., 2009). Seven of these sites lie between T286 and S304 in the central region region of the protein which has not been structurally modelled. However, the role of phosphorylation in the activity of TPL is unknown. Turning to SUMOylation, TPL and TOPLESS-RELATED (TPR) proteins were identified as “highly SUMOylated” proteins (Miller et al., 2010). A recent analysis by Rytz et al. (2018) discovered that TPL is SUMOylated at a non-consensus attachment site (K689), sixteen residues upstream of a phosphorylation site (Reiland et al., 2009). This site is within the WD40 domains at the C-terminus of the protein. No clear role has been established for SUMOylation in TPL and it is unknown if SUMOylation occurs at other sites. However, in related co-repressors such as Groucho in *Drosophila melanogaster* and Tup1 in *Saccharomyces cerevisiae*, SUMOylation plays an important role in enabling interaction with histone deacetylases. As numerous components of histone-modifying complexes are reported to be SUMOylated, SUMO been posited as the ‘glue’ that binds together these complexes (Mazur and van den Burg, 2012).

Our existing knowledge of the modifications and protein-protein interactions of TOPLESS presents us many open questions. TOPLESS appears to act as general co-repressor, interacting with many transcription factors directly (Causier et al., 2012b) or via adaptor proteins (Pauwels et al., 2010) to repress the expression of target genes. Does TOPLESS act as part of a single repressive complex recruited by all transcription factors, is the complex modular with some fixed components and some variable components, or could TOPLESS act as an adaptor to join transcription factors to various different repressive complexes? Furthermore, how do post-translational modifications made to TOPLESS and associated proteins,

e.g. HDA19, influence their ability to participate in regulatory complexes? One approach that can be taken to address these questions is to isolate TOPLESS and its interactors using TOPLESS as 'bait'. While several aforementioned studies have identified indirect interactions or have observed TOPLESS as a co-precipitant with other proteins, TOPLESS has not been used as bait to capture its interactors *in planta*. I attempted to do this with the aim of establishing the core components of the putative 'TOPLESS complex' and to investigate post-translational modifications of TOPLESS and its interacting partners that may influence protein-protein interactions.

Aims:

- To establish the core components of the putative 'TOPLESS complex'.
- To investigate post-translational modifications of TOPLESS and its interacting partners that may influence protein-protein interactions.

4.2 Methods

4.2.1 Cross-linking with formaldehyde and disuccinyl suberate

Formaldehyde (FA): Formaldehyde forms covalent cross-links between amide groups approximately 2Å apart (Hoffman et al., 2015) and is therefore suitable for capturing closely-associated proteins. Harvested tissues were vacuum-infiltrated with 0.1% (volume) formaldehyde (FA) in FA cross-linking buffer (50mM sodium hydrogen phosphate, 150mM sodium chloride) for fifteen minutes. Cross-linking was quenched by slowly adding tris-HCl to a final concentration of 100mM, followed by vacuum infiltration for ten minutes. The tissue was then washed twice with sterile distilled water, dried and flash-frozen with liquid nitrogen.

Disuccinimidyl suberate (DSS): DSS is a hydrophobic cross-linker that forms covalent bonds between amide groups. It was selected as an alternative to formaldehyde as its bond length (approximately 11.4Å) allows for capture of

distal proteins that may be interacting as part of a larger complex. Immediately prior to the experiment, a 1M DSS stock solution was prepared using dimethyl formamide due to DSS insolubility in water. Harvested tissues were vacuum-infiltrated with 1mM DSS in DSS cross-linking buffer (100mM sodium phosphate, 150mM sodium chloride, 20mM HEPES) for fifteen minutes. Cross-linking was quenched by slowly adding tris-HCl to a final concentration of 100mM, followed by vacuum infiltration for ten minutes. The tissue was then washed twice with sterile distilled water, dried and flash-frozen with liquid nitrogen.

4.2.2 Protein extraction to preserve SUMOylation

For denaturing extractions, tissue was flash frozen in liquid nitrogen, ground with a pestle and mortar and resuspended in an extraction buffer described by Bailey et al. with high concentrations of detergent and reducing agent. The buffer consisting of 50mM tris-HCl, 4% (volume) sodium dodecyl sulphate, 2% (volume) β -mercaptoethanol and 10mM EDTA (Bailey et al., 2016), supplemented with 1x "cOmplete" EDTA-free protease inhibitor cocktail (Roche). and 100 μ m N-ethylmaleimide cysteine protease inhibitor (Sigma-Aldrich). This inhibitor has been reported to increase recovery of high-molecular weight SUMO conjugates. Frozen, powdered tissue was resuspended in extraction buffer and incubated at 16°C for 30 minutes. To deplete SDS from the extract, a buffer exchange was performed on 10kDa molecular weight cut-off columns (Pierce) using the buffer described above with the SDS content reduced to 0.1%. This increased compatibility with downstream protocols for capturing tagged proteins.

4.2.3 SDS-PAGE and Western blotting

For SDS-polyacrylamide gel electrophoresis (SDS-PAGE), protein samples were added to an equal volume of Laemmli buffer supplemented with β -mercaptoethanol (5 μ l per 100 μ l buffer) and mixed by pipetting. Samples were then denatured by heating on a heat block to 95°C for five minutes, then were kept at 4°C until loading. 50 μ l was loaded per sample into an

AnyKd or 4-20% gradient precast TGX Stain Free gel (Bio-Rad) alongside 5µl molecular weight marker (Color Prestained Protein Ladder, Broad Range (New England Biolabs) or Pageruler Plus (Thermo Scientific)). Gels were run in tris-glycine running buffer (Geneflow) at 200V for 30 minutes using the Mini-Protein SDS-PAGE system (Bio-Rad). For gel extraction of protein bands, gels were stained with Instant Blue Coomassie stain (Expedeon) for one hour followed by washing twice in distilled water (20 minutes per wash). For Western blotting, gels were blotted onto PVDF 0.2µm pore membranes using a Trans-blot Turbo system using settings optimised for high-molecular-weight proteins (1.3A, 25V, 10-minute run time). Membranes were transferred to blot boxes (Appleton Woods) reserved for use with the antibody of interest. The membranes were covered with a solution of tris-buffered saline containing 0.5% Tween-20 (TBS-T) and milk powder (5% mass:volume). After five minutes equilibration, antibody was added to a dilution of 1:5000 (volume) for HRP-conjugated anti-HA antibody (Miltenyi Biotec), 1:5000 HRP-conjugated anti-DDDDK (functionally equivalent to anti-FLAG; Abcam, ab122902) or 1:7500 for rabbit *Arabidopsis* anti-SUMO1/2 antibody (Abcam ab5316). Blots were incubated for one hour at room temperature on an orbital shaker, then washed in TBS-T five times for ten minutes per wash. Anti-SUMO1/2 blots were then probed with an HRP-conjugated goat anti-rabbit secondary antibody (Abcam, ab6721) at a 1:10000 dilution. Blots were assayed for activity of conjugated HRP using a SuperSignal West Pico chemiluminescent substrate kit (Thermo Scientific) and viewed with a G:Box gel-doc imaging system (Syngene) using the WestPico dye chemiluminescence preset.

4.2.4 Peptide analysis by mass spectrometry

Samples were processed at the Mass Spectrometry Facility at the University of Leeds. Non-cross-linked HA-TPL samples were ionised by electrospray ionisation (ESI) followed by separation by tandem MS using linear ion traps. Cross-linked HA-TPL and His-SUMO in-solution digests were ionised by MALDI then separated by tandem MS using an Orbitrap/linear trap setup.

4.3 Results

4.3.1 TOPLESS-RELATED proteins co-precipitate with TOPLESS

To establish a plant-based system from which I could isolate TPL and its interaction partners, I transformed wild type Landsberg erecta (Ler) and the semi-dominant mutant *tpl-1* with *35S::3xHA-TPL* (where HA encodes the haemagglutinin peptide tag). Flowering T2 plants were harvested (excluding root and stem tissue) for protein extraction and HA-TPL was captured by immunoprecipitation. Western blotting of electrophoresed protein presents a fragmentation pattern (see Chapter 1). The majority of HA-TPL is not recovered intact. This fragmentation has since been reported by other investigators (Rytz et al., 2018), but it is unclear if it occurring as an artefact of the preparation of the protein. The Western blots did not provide sufficient resolution to accurately determine the masses of the fragments. The number and relative sizes of the fragments suggest that cleavage has occurred within the linker regions between the structurally defined regions (the LisH-CTLH-CRA region and the two clusters of WD40 repeats).

Protein	Confidence (-10lgP)	Sequence coverage (%)	Total peptides	Unique peptides	Average mass
TOPLESS	162.61	24	25	10	124298
RBCL	141.47	30	13	13	52955
TOPLESS-RELATED 1	125.42	15	17	3	124089
TOPLESS-RELATED 4	92.39	9	11	3	124103

Table 4-1. Proteins co-precipitating with HA-TOPLESS. Results were filtered to retain those with confidence values above a 1% false discovery rate (-10lgP \geq 20.4 for proteins, \geq 8 for peptides) represented by \geq 3 unique peptides. Peptides covering the reported phosphorylation site at serine 214 (Reiland et al., 2009) also indicated phosphorylation.

Having verified the expression of the 35S::3xHA-TPL construct, I repeated the protein extraction using the same weakly denaturing extraction conditions, with the reasoning that proteins closely bound may also be captured. I submitted the immunoprecipitation to the Mass Spectrometry Facility (University of Leeds) for peptide identification. Peptides were recovered from TPL and from its relatives TOPLESS-RELATED (TPR) 1 and 4 with minimal non-specific interactions (Table 4-1). TPL family proteins demonstrate a high degree of peptide conservation. This can lead to peptides being assigned erroneously to different TPL/TPR proteins. The majority of peptides recovered matching TOPLESS are conserved between all family members. Fortunately, peptides unique to TPL, TPR1 and TPR4 were also recovered (Table 4-2 and Figure 4-1). Co-precipitation of TPR1 and TPR4 alongside TPL indicates a close association between the proteins (potentially multimerisation) *in planta*. Replicates of this experiment recovered peptides from TPRs but included increased background interactions. Increased stringency by addition of detergent (SDS) eliminated background interactions but also excluded TPRs.

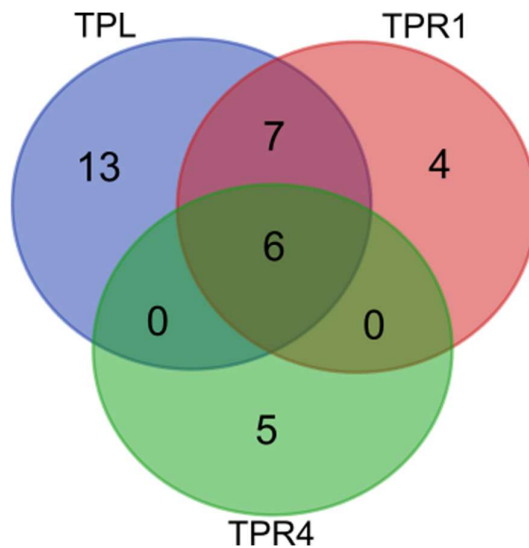


Figure 4-1. Unique peptides representing TOPLESS-RELATED proteins co-elute with HA-TOPLESS. Some peptides overlap between TPL family proteins due to sequence conservation but unique peptides were identified for TPL, TPR1 and TPR4.

4.3.2 TOPLESS associates with histones and chromatin regulators

Attempts to yield TPL/TPR-interacting proteins returned few results. A preliminary cross-linking experiment using 0.1% formaldehyde recovered TPL, TPR3 and histone H4 (Table 4-2; negative control results shown in Table 4-3). After cross-linking with 1% formaldehyde, TOPLESS co-immunoprecipitates with the chromatin regulator SPLAYED (Tables 4-4 and 4-5). Numerous recovered peptides were below the False Discovery Rate threshold. This list included BRAHMA (a close relative of SPLAYED), DDB1- and CUL4-associated factor homolog (DCAF) 1, CHROMATIN REMODELLING 8, HISTONE ACETYLTRANSFERASE (HAC) 12. A parallel co-immunoprecipitation of proteins cross-linked with 1mM DSS instead of formaldehyde recovered peptides for ATP-dependent RNA helicases DEAH11/12 and SPLAYED with BRAHMA, HAC12, SIN3-LIKE (SNL) 3 and PICKLE as subthreshold matches, but crucially, peptides from TPL were not recovered. While it is possible that we are observing non-specific interactions, it is more likely that TOPLESS is absent due to poor peptide recovery.

Protein	Confidence (-10lgP)	Sequence coverage (%)	Total peptides	Unique peptides	Average mass
TOPLESS	226.09	22	21	17	124298
RBCL	193.85	28	12	12	52955
TOPLESS-RELATED 3	128.56	5	5	1	122657
Histone H4	62.72	17	2	2	11409

Table 4-2. Proteins co-precipitating with HA-TOPLESS after cross-linking with 0.1% FA. Results were filtered to retain those with confidence values above a 1% false discovery rate (-10lgP \geq 20.4 for proteins, \geq 8 for peptides) represented by >1 peptide. N.b. RBCL is a commonly appearing contaminating protein due to its cellular abundance.

Protein	Confidence (-10lgP)	Sequence coverage (%)	Total peptides	Unique peptides	Average mass
RBCL large chain	128.79	27	9	9	52955
RBCL large chain	45.63	2	1	1	51981
Glyceraldehyde-3-phosphate dehydrogenase GAPCP2	44.02	4	1	1	44846
Glyceraldehyde-3-phosphate dehydrogenase GAPCP1	44.02	4	1	1	44831
Elongation factor Tu, mitochondrial	43.29	3	1	1	49410
Elongation factor Tu, chloroplastic	43.29	3	1	1	51630

Table 4-3. Proteins precipitating from anti-HA immunoprecipitation from untransformed wild type *Arabidopsis thaliana*. Results were filtered to retain those with confidence values above a 1% false discovery rate (-10lgP \geq 20.4 for proteins, \geq 8 for peptides) represented by \geq 1 peptide.

Protein	Confidence (-10lgP)	Sequence coverage (%)	Total peptides	Unique peptides	Average mass
TPL/TPR1/TPR2/ TPR3/TPR4	56.86	2	2	2	122657
RBCL	48.63	3	1	1	52955
MPK16	30.79	1	1	1	64912
Pentatricopeptide repeat protein At5g13230	24.59	1	1	1	91439
GAPA1	24.44	4	1	1	42490
WRKY19	16.93	0	1	1	210320
ASPARTOKINASE 3	16.32	5	1	1	61216
EUKARYOTIC TRANSLATION INITIATION FACTOR 3B	15.79	3	2	2	81876
VACUOLAR PROTEIN SORTING-ASSOCIATED PROTEIN 35C	15.30	2	1	1	89405
SPLAYED	15.03	1	1	1	389866

Table 4-4. Proteins co-precipitating with HA-TOPLESS cross-linked with 1% FA. Results were filtered to retain those with confidence values above a 1% false discovery rate (-10lgP \geq 20 for proteins, \geq 8 for peptides) with multiple identifying peptides. Peptides for TPL/TPR proteins are conserved between all family members. The Rubisco large subunit (RBCL), GAPDH subunit GAPA1, ASPARTOKINASE 3, VACUOLAR PROTEIN SORTING-ASSOCIATED PROTEIN 35C (VPSC35C) and At5g13230 are non-nuclear proteins and are likely to be non-specific interactors.

Protein	Confidence (-10lgP)	Sequence coverage (%)	Total peptides	Unique peptides	Average mass
ATP-dependent RNA helicase DEAH11/12	18.72	0	1	1	201361
SPLAYED	18.18	2	3	3	389866
Serine/threonine- protein kinase At4g03230	16.73	1	1	1	96200
AGD3	16.53	2	1	1	92524
Pentatricopeptide repeat protein At5g13230	15.5	1	1	1	78877
FILAMENT-LIKE PLANT PROTEIN 6	15.24	2	1	1	118540

Table 4-5. Proteins co-precipitating with DSS-cross-linked HA-TOPLESS. Results were filtered to retain those with confidence values above a 1% false discovery rate (-10lgP \geq 20 for proteins, \geq 8 for peptides).

The main potential interactor, a nucleus-localising chromatin regulator named SPLAYED (Wagner and Meyerowitz, 2002), was not recovered in non-cross-linking experiments performed on the same tissue. This suggests that SPLAYED is not appearing as a background contaminant. Additional support is provided by Collins et al., who recently reported an attempt to isolate TPL-interacting proteins by tandem affinity purification (Collins et al., 2018). They reported that they could not isolate specific interactors but did provide a list of commonly-recovered background proteins. Neither SPLAYED nor BRAHMA were among these proteins. Furthermore, chromatin regulators are not expressed in high abundance relative to other proteins, so their presence is unlikely to result from a lack of stringency as is sometimes observed with abundant proteins such as the Rubisco large chain (RBCL), which emerge as common contaminants. Also, recovery of chromatin regulators and histones rather than known interacting transcription factors is unsurprising when we consider that components of a regulatory complex may be in every functional complex, whereas an individual transcription factor type may be represented in only a few complexes per nucleus. In light of this information, the apparent interaction between the co-repressor TOPLESS and the chromatin regulator SPLAYED should be explored as it could be important to the regulatory functions of both proteins.

4.4 Discussion

4.4.1 Co-precipitation of TPRs with TPL

TOPLESS is predicted from crystallographic models and *in vitro* assays to form tetramers (dimers of dimers) with itself, with each monomer capable of binding a transcription factor via its repression domain (Ke et al., 2015; Martin-Arevalillo et al., 2017; Ma et al., 2017). Causier et al. (2012) revealed protein-protein interaction between TPL/TPR proteins (TPR1-TPR1, TPR4-TPR4 and TPR1-TPR4). The new MS data further support a model of interaction in which TPL and TPRs can interact. It is possible that TPL/TPRs form heteromers. TPL/TPR1/TPR4 proteins are close evolutionary relatives and exhibit substantial conservation across the N-terminal domains involved in dimerisation and tetramerisation (Martin-Arevalillo et al., 2017). Additionally, there is evidence for overlap in function between members of this group (Zhu et al., 2010). TPL, TPR1 and TPR4 may not act with complete redundancy. Yeast two-hybrid assays show differences in interaction range; large numbers of transcription factors interacting with TOPLESS and TPR2 in *Arabidopsis* compared to TPR1, 3 and 4 (Causier et al., 2012a, 201, 2012b). In tomato, SITPL2 has the broadest interaction range (Hao et al., 2014), an interesting characteristic given the loss of this type of TPL-like protein from *Arabidopsis* (see Chapter 3). However, having the ability to form heterogenous multimers of different TPL/TPRs could allow for partial redundancy. The data raise several questions to be addressed in the future. Firstly, what are the stochastic ratios of TPL/TPR within tetramers? The ratio of unique peptides from TPL, TPR1 and TPR4 may be indicative of their stochastic ratio but could also represent an average of different modular arrangements, e.g. preferred interaction between TPL homodimers and TPR1/TPR4 heterodimers or other combinations. We must also consider that high, constitutive expression of *HA-TPL* from the 35S promoter may not give an accurate representation of typical *in planta* interactions. Indeed, mild phenotypes including floral organ fusion have been reported to result from *TPL* overexpression (Espinosa-Ruiz et al., 2017). New *tpl/tpr* mutant combinations developed for this thesis (see Chapter 4) will allow us to examine TPL-TPR interactions in genetic backgrounds where members of the family are absent and thus determine whether interactions are dependent on particular combinations of TPL/TPRs.

4.4.2 TPL co-localises with histone H4

The recovery of histone H4 with HA-TPL supports *in vitro* assay data (Ma et al., 2017, 53). Ma et al. reported that the N-terminal domains of TOPLESS (the TOPLESS domain, or TPD) binds strongly to H3 and H4 and weakly to H2 variants. These interactions were strengthened by histone methylation (Martin-Arevalillo et al., 2017), a modification typically associated with transcriptional repression, although the H4 peptides recovered here were not methylated. Interaction between TPL and H4 is interesting from the perspective of complex assembly. In the NuRD complex, histones are recognised by Retinoblastoma Binding Proteins (RBBP) 4 and 7, while Methyl Binding Domain proteins 2 and 3 are capable of recognising methyl groups. TOPLESS can interact with the RBBP homologue MSI4/FVE (Causier et al., 2012a) and there is evidence that TOPLESS co-localises with MSI4/FVE (Zheng et al., 2017) and with MBD homologues (Clavel et al., 2015). However, as TOPLESS appears to overlap these proteins in terms of function, the dynamics of this interaction may not resemble the NuRD complex. This finding may also shed light on the assembly of a 'TOPLESS complex'. At present, we have no insight as to whether TOPLESS first binds to transcription factors and then to other transcriptional regulators (MSI4/FVE, PKR1 etc.) or vice versa. The ability to bind to histones could stabilise interaction between transcription factors, TOPLESS and the chromatin prior to recruitment of other transcriptional regulators.

4.4.3 Potential interactions between TOPLESS and chromatin remodellers

Mass spectrometry of HA-TPL co-precipitants identified few interacting proteins with any confidence; however, the low-quality peptide matches (Appendix B) offer a tantalising hint that TOPLESS interacts with SIN and NuRD-like repressive complexes through proteins such as SNL3 and PICKLE, respectively. We should be cautious in interpreting these data for several reasons. Low yields of HA-TPL reduced the potential number of interacting proteins recovered, resulting in rare, low quality peptides. Aside from the poor recovery of peptides, some proteins may co-localise with TOPLESS rather than directly interacting with it. As TOPLESS physically interacts with histones, we might expect other chromatin-associated proteins to be in close proximity. These proteins may even have common targets, promoting histone deacetylation, as part of independent complexes. To determine direct interaction, further experiments will be required to isolate

TOPLESS and any associated regulatory complex from these confounding factors.

The discovery of a potential interaction between TOPLESS and the co-regulator SPLAYED opens a new avenue of inquiry. SPLAYED is a SWI2/SNF2 family chromatin-remodelling ATPase (Wagner and Meyerowitz, 2002). SPLAYED is closely related to BRAHMA, a protein that is highly conserved across eukaryotes and also appeared as a weak peptide match in MS of HA-TPL co-precipitations (Appendix B). SPLAYED and BRAHMA have partially redundant roles in embryo development; mutants having an increased rate of embryonic lethality and seedlings exhibit slow growth and defects in cotyledon patterning (Bezhani et al., 2007). *Arabidopsis thaliana* also has two more non-canonical BRAHMA-like genes, *MINISCULE 1* and *2*, mutants of which show minor defects in seedling symmetry (Sang et al., 2012). SPLAYED and BRAHMA have also been associated with gene activation during floral development (Wu et al., 2012). They interact with the transcription factors LEAFY AND SEPALLATA3 to induce expression of APETALA3 and AGAMOUS in the inner whorls of the flower (Wu et al., 2012). Furthermore, SPLAYED promotes expression of genes targeted by the ethylene and jasmonic acid signalling pathways (Walley et al., 2008). Several of these regulatory pathways are antagonised via TOPLESS-mediated repression, and it seems contradictory that TOPLESS should interact with SPLAYED or BRAHMA; however, published data provide some support for the interaction. Firstly, SPLAYED and TOPLESS were both recovered by co-immunoprecipitation with *Triticum aestivum* MSI4/FVE (Zheng et al., 2017), suggesting that they are located within the same regulatory complexes. Secondly, SPLAYED and BRAHMA may not be restricted to regulatory complexes that activate expression. BRAHMA is required for transcriptional repression of Class I KNOX transcription factors that regulate inflorescence architecture (Zhao et al., 2015). Additionally, chromatin immunoprecipitation experiments indicate that BRAHMA associates with the promoters of genes that are upregulated in *brahma* mutants, implying its involvement in the repression of those genes (Tang et al., 2008).

Methodology and equipment are limiting factors. Recovery of high-quality peptides above the threshold defined by the false discovery rate would be improved by using more sensitive instrumentation (i.e. Orbitrap detectors). As an illustration, Rytz et al. (2018) cited technological advances as a key factor in increasing the list of known SUMOylation substrates from several

hundred (Miller et al., 2010) to over one thousand (Rytz et al., 2018). Additionally, pre-processing of any TPL-associated complexes or modules, for example by size exclusion chromatography or by electrophoretic separation on a non-denaturing gel, would enrich proteins of interest. It would also provide information regarding the minimal composition of any such complex and its order of assembly.

Direct identification of SUMOylation sites within SUMOylated proteins, e.g. TOPLESS, is technically complicated. Peptide identification by mass spectrometry is limited by peptide length. Peptides outside a typical size range of 4-30 residues are infrequently recovered by mass spectrometry. The addition of a SUMO moiety adds significantly to the mass of a peptide. Moreover, SUMOs contain few lysine and arginine residues, thus, digestion of proteins using a standard trypsin digest protocol leaves a high-molecular-weight SUMO fragment attached to the peptide of interest preventing recovery of the SUMOylated peptide during mass spectrometry. Other research groups have pioneered the use of mutated SUMO1/2 proteins, preferably expressed in a *SUMO*-deficient background (Miller et al., 2010; Rytz et al., 2018). Non-synonymous mutation of histidine 89 to arginine allows the SUMO peptide to be cleaved by trypsin, leaving a low-molecular-weight tag (-QTGG, 343.15Da or -pyroQTGG, 326.12Da) that is distinct from those generated by other ubiquitin-like proteins (Guo and Sun, 2017). The addition of histidine or other detectable tags allows precipitation of SUMO conjugates. Co-expression of this modified SUMO with HA-TPL would permit two-step purification of SUMOylated TOPLESS followed by mass spectrometry to identify SUMOylation sites. This approach may be preferable to proteomics approaches that have only captured a limited number of peptides for TOPLESS (Miller et al., 2010; Rytz et al., 2018) as it would allow for enrichment of SUMOylated TOPLESS during purification. Use of the SIM-conjugated agarose described in this chapter could be incorporated into this approach to further increase stringency. It must be noted, however, that this approach may not allow us to directly assay all candidate SUMOylation sites within TOPLESS. In a similar manner to SUMO itself, central regions of the protein lack cleavage sites for endoproteases such as trypsin and chymotrypsin that are commonly used to prepare proteins for peptide analysis by mass spectrometry. A thoughtful approach should be taken to overcome these challenges.

5 Mutants of TOPLESS and TOPLESS-RELATED 1-4 have a phenotypic range resembling *tpl-1*

5.1 Introduction

5.1.1 Individual *tpl* and *tpr1/2/3/4* mutants lack conspicuous phenotypes

TOPLESS (TPL) family co-repressors (Figure 5-1) have been implicated in the regulation of a host of important developmental processes including embryo patterning (Smith and Long, 2010), meristem maintenance (Kieffer, 2006; Causier et al., 2012a), organ boundary formation (Causier et al., 2012a), timing of flowering (Causier et al., 2012a) and floral patterning (Krogan et al., 2012), as well in modulating signalling from auxin (Szemenyei et al., 2008), ethylene (Causier et al., 2012a), jasmonic acid (Pauwels et al., 2010; Causier et al., 2012a), gibberellic acid (Fukazawa et al., 2014, 2015), brassinosteroids (Espinosa-Ruiz et al., 2017), abscisic acid (Pauwels et al., 2010) and strigolactones (Wang et al., 2015). Loss of TOPLESS/TOPLESS-RELATED-dependent gene repression in the *tpl-1* mutant (Landsberg erecta (Ler) ecotype) negatively affects growth and development (Long et al., 2002). Early embryo development is radically affected (Long et al., 2002). Mis-expression of *PLETHORA 1* and *2* can cause development of the shoot axis as a second root (Smith and Long, 2010). More frequently, cotyledons are partially or fully fused to one another, or the shoot axis is reduced to a radially symmetrical pin. In rosette leaves, the lamina may be distorted by asymmetric growth. Bolting and flowering commence earlier and floral organs display identity defects including petaloid sepals and, more rarely, formation of carpelloid sepals resembling those seen caused by mutations in the floral B-function gene *APETALA2* (Bowman et al., 1991). *tpl-1* floral phenotypes are enhanced by elevated temperatures, similarly to *apetala2* (Bowman et al., 1991).

In spite of the severe phenotype of the *tpl-1* mutant (Long et al., 2002), mutations in individual *Arabidopsis TPL/TPR* genes do not cause conspicuous phenotypic changes (Long et al., 2006). This has been attributed to redundancy between family members (Long et al., 2006). Similarity in gene expression patterns, expression levels (Schmid et al., 2005) and protein interaction partners (*Arabidopsis* Interactome Mapping

Consortium, 2011; Causier et al., 2012a) between *TPL* and its related genes supports a model of redundancy. The *tpl-1* phenotype is, however, recapitulated in a more conventional loss-of-function mutant. A quadruple mutant (***tpl tpr1 tpr3 tpr4***) displays infrequent petaloid sepals, as observed in *tpl-1* (Krogan et al., 2012). Silencing *TPR2* in this mutant by RNA inhibition (RNAi) replicates the *tpl-1* phenotype (Long et al., 2006), albeit with stronger *apetala2* (*ap2*)-like floral phenotypes (Krogan et al., 2012). While Zhu et al. (2010) reported that successive mutation of *TPR1*, *TPL* and *TPR4* increased the sensitivity of *Arabidopsis* to fungal pathogens, no conspicuous morphological phenotype has been reported in mutants lacking two or three *TPL/TPR* genes (Long et al., 2006; Krogan et al., 2012); redundancy or compensation by other *TPL/TPRs* conceals the reduction in repression caused by loss of a single gene.

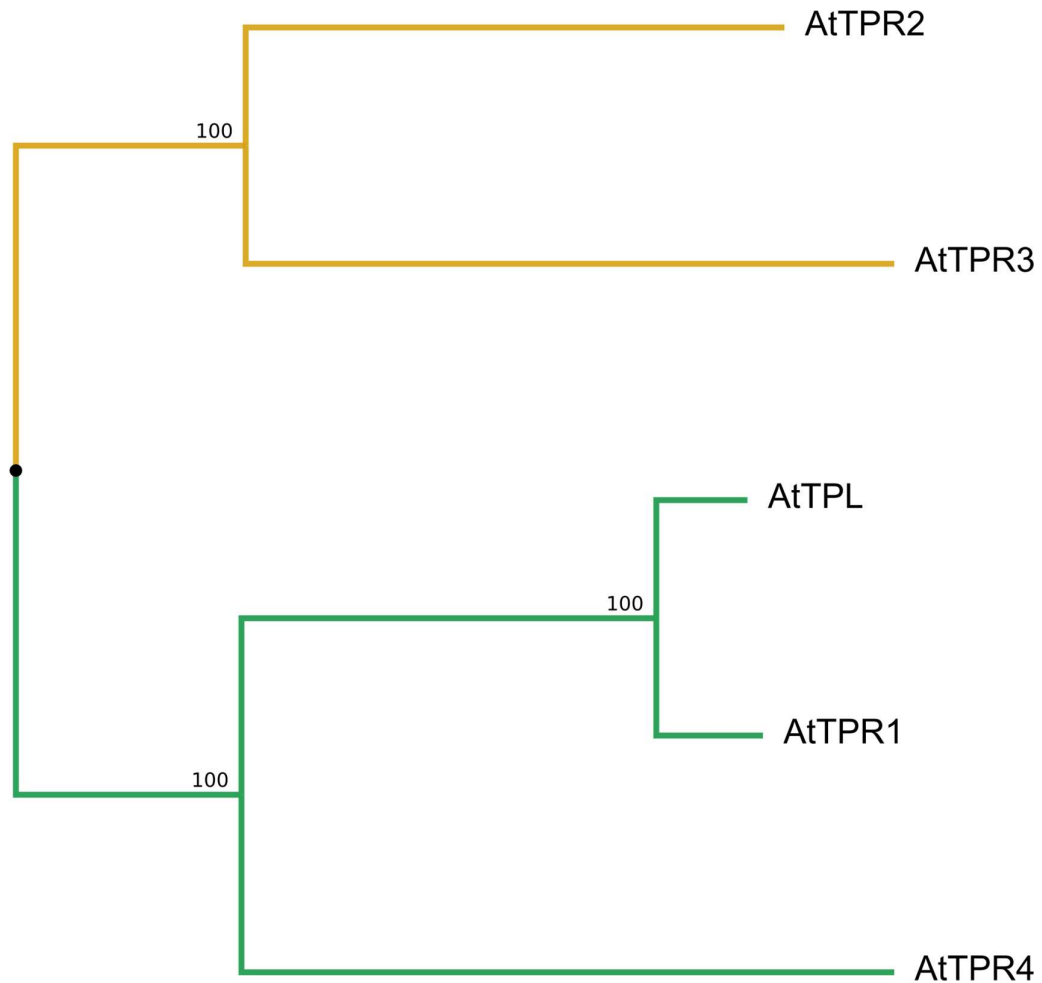


Figure 5-1. Neighbour-joining tree of *Arabidopsis* TOPLESS and TOPLESS-RELATED proteins. *Arabidopsis* TPL/TPRs form two subclades. Branch lengths indicate that AtTPL and AtTPR1 may be the products of a recent gene duplication. Node values indicate bootstrap support expressed as a percentage. Sequences aligned with L-ins-I algorithm on MAFFT 7, bootstrap run with 1000 iterations.

Yeast two-hybrid screens indicate that *Arabidopsis* TPL/TPRs have substantial redundancy in the transcription factors with which they will interact (Causier et al., 2012a), implying shared functions *in planta*. TPL family proteins can be recruited by transcription factors containing short peptide sequences described as Repression Domains (RDs) and TPL/TPR-interacting transcription factors are enriched for all known plant RDs (Causier et al., 2012a, 2012b). These include the ERF-associated Amphiphilic Repression (EAR) domain (LxLxL) (Ohta et al., 2001; Kagale et al., 2010; Kagale and Rozwadowski, 2011b) as well as LxLxPP (Causier et

al., 2012b), RLFV (Ikeda and Ohme-Takagi, 2009) and TLxLF (Cuéllar Pérez et al., 2014). Additionally, TPL/TPRs can be coupled to transcription factors that do not have RDs via adaptor proteins that contain an RD. There are four known adaptor proteins: NOVEL INTERACTOR OF JAZ (NINJA), KIX8 and 9 and TIE1. NINJA is involved in jasmonic acid signalling. While some JAZ proteins can bind to TOPLESS independently, others lack RDs. NINJA can bind to JAZ proteins its TIFY domain and can recruit TOPLESS via anEAR motif. Similarly, KIX8 and 9 enable PEAPOD1 and 2 to recruit TOPLESS (Gonzalez et al., 2015), while TIE1 bridges TOPLESS and TCP transcription factors (Tao et al., 2013).

Zhu et al. (2010) provided direct evidence for overlap in function between closely-related *TPL/TPRs* after discovering that mutations in *TPR1* suppress a gain-of-function mutant, *suppressor of npr1-1, constitutive 1 (snc1)* (Zhu et al., 2010). *SNC1* is a TIR-NB-LRR R protein involved in pathogen defense. Zhu et al. reported that *tpr1* mutants have increased pathogen susceptibility. This susceptibility is additively enhanced further by knocking out the most closely related *TPL/TPR* genes, *TPL* and *TPR4*. (Zhu et al., 2010). This effect could be mediated by a common affinity for transcription factors such as *SNC1* or by the obligate formation of multimers between specific *TPL/TPRs*. Regardless of the cause, unique functions cannot be assigned to individual *TPL* family members based on this information alone, only that all three genes are required to deliver the optimal 'dose' of repression. However, not all *TPRs* were examined. Other evidence implies functional differences between closely related *TPL/TPR* proteins. The asterid *Solanum lycopersicum* has six *TPL* orthologues. *SITPL3* and *SITPL6* proteins demonstrate a reduced interaction range when arrayed against *AUX/IAAs* compared to other *SITPLs* (Hao et al., 2014). Contrastingly, *SITPL2* has the broadest interaction range but is expressed at a low level (Hao et al., 2014). Therefore, we might yet assume differences between individual family members in terms of their capacity to function redundantly and their expression patterns.

The possible subfunctionalisation of *Arabidopsis TPL/TPRs* has not been fully explored. The discovery of phenotypic recessive mutants might reveal gene-specific functions and could also provide a platform for

complementation experiments and other studies in which the dominant action of TPL-1 would be disadvantageous. Moreover, characterisation of mutants in a single well-resourced and characterised ecotype, Columbia-0 (Col-0), instead of Landsberg erecta (*tpl-1*, *tpl-2*) (Long et al., 2002) or a combined background (*tpl tpr1 TPR2 tpr3 tpr4*) (Long et al., 2006) might reveal phenotypic traits previously masked, e.g. by heterosis. To these ends, I phenotyped the existing *tpl tpr1 tpr4* mutant (Zhu et al., 2010) and developed additional multiple mutants in a single ecotype, (Col-0), to characterise *tpl/tpr*-associated phenotypes in greater detail and to explore the possibility of subfunctionalisation in TPL/TPR proteins. Phenotyping focused on three aspects of plant development where TPL/TPRs are known or are suspected to have a regulatory role: establishment of the embryonic body plant; floral patterning and floral organ number and identity; and development and growth of primary and lateral roots.

5.2 Methods

5.2.1 Phylogenetic analysis

Sequences of known or predicted TPL-like proteins from taxa representing major plant lineages were identified and checked by reciprocal BLASTp and tBLASTx searches (Altschul et al., 1990) with *Arabidopsis thaliana* and *Physcomitrella patens* TPL/TPR sequences using the National Centre for Biotechnology Information (NCBI), Phytozome (Goodstein et al., 2012) and OneKP Transcriptome (Matasci et al., 2014) databases and annotated as follows. ***Picocystis salinarum*** (chlorophyceae) scaffold-TGNL-2001238 = PsTPL. ***Klebsormidium nitens*** (streptophytic algae) = KnTPL. ***Physcomitrella patens*** Pp1s99_260V6.1 = PpTPL1; Pp1s316_34V6.1 = PpTPL2. ***Selaginella moellendorffii*** (lycophytes) SELMODRAFT-163891 = SmTPL1; SELMODRAFT-439915 = SmTPL2; SELMODRAFT-88677 = SmTPL3. ***Amborella trichopoda*** (basal angiosperms) evm_27.model.AmTr_v1.0_scaffold00051.29 = AmTr; evm_27.model.AmTr_v1.0_scaffold00048.113 = AmTr. ***Vitis vinifera*** (basal rosids) GSVIVT01017487001 = VvTPL1; GSVIVT01015571001 = VvTPL2;

GSVIVT01017343001 = VvTPL3; GSVIVT01024440001 = VvTPL4;

GSVIVT01031186001 = VvTPL5; GSVIVT01035940001 = VvTPL6.

Arabidopsis thaliana (rosids) At1G15750 = AtTPL; AT1G80490 = AtTPR1;

AT3G16830 = AtTPR2; AT5G27030 = AtTPR3; AtAT3G15880 = TPR4.

Solanum lycopersicum (asterids) SOLYC03G117360 = SITPL1;

SOLYC08G076030 = SITPL2; SOLYC01G100050 = SITPL3;

SOLYC03G116750 = SITPL4; SOLYC07G008040 = SITPL5;

SOLYC08G029050 = SITPL6. ***Picea abies*** (gymnosperms; Pinophyta)

MA_10430083g0010 = PaTPL1; MA_10436445g0020 = PaTPL2;

MA_33469g0010 = PaTPL3; MA_60825g0010 = PaTPL4; MA_83125g0010

= PaTPL5. (Phylogenetic clade associations refer to classifications by the

Angiosperm Phylogeny Group (Stevens, 2001 onwards).) The sequences

were aligned using MAFFT 7 (Kato et al., 2017) using the L-ins-i algorithm.

A consensus tree was generated by Bayesian analysis with MrBayes 3.2.6

via the CIPRES Gateway. The analysis was performed with two runs for

5,000,000 generations or to where the topological convergence diagnostic

was less than 0.005. Chains were sampled every 25,000 generations. Trees

were summarised after a 25% burn-in. 25% of sampled parameter values

were burnt. No outgroup was specified.

Additional alga containing TPL-like BLAST hits from OneKP were obtained

by reciprocal BLASTs using PsTPL and included *Mesotaenium*

(NBYP_scaffold_2056058 *Mesotaenium_kramstei*), *Cylindrocystis*

(JOJQ_scaffold_2041843 *Cylindrocystis_cushleckae*), *Spirogyra*

(HAOX_scaffold_2025270 *Spirogyra_sp.*), *Coleochaete*

(VQBJ_scaffold_2012007 *Coleochaete_scutata*), *Interfilum*

(FPCO_scaffold_2030065 *Interfilum_paradoxum*), *Zygnema*

(WGMD_scaffold_3006813 *Zygnema_sp.*), *Entransia*

(BFIK_scaffold_2004708 *Entransia_fimbriat*) and *Chlorokybus*

(AZZW_scaffold_2021890 *Chlorokybus_atmophyticus*).

5.2.2 Assembly of *tpr2 tpr3* and additional multiple mutants

Mutant lines used in the assembly of multiple mutants are listed in Tables 5-

1 and 5-2. The *tpr1* and *tpr1 tpr4* mutants produced by Zhu et al. (2010)

were kindly provided by the corresponding author Yuelin Zhang (University of British Columbia). To obtain *tpr2 tpr3*, homozygous *tpr2* (Salk_079848C) and *tpr3* (Salk_029936C) mutants were crossed and the progeny self-pollinated to produce a homozygous double mutant. To replicate multiple mutants described by Long et al. (2006) in the Columbia ecotype, the triple (*tpl tpr1 tpr4*) and double (*tpr2 tpr3*) mutants were crossed to generate F1 quintuple heterozygotes. These heterozygotes were self-pollinated to obtain a segregating F2 population. Plants were genotyped by polymerase chain reaction using primers flanking T-DNA insertion sites and/or matching the T-DNA left border sequence (*TPL*, *TPR2*, *TPR3* and *TPR4*) or with primers within the deleted region of the gene (*TPR1*) (see Appendix C). N.b. Quadruple mutants are in bold font for clarity.

	Long et al., 2006; Krogan et al., 2012		Mutant combinations in this thesis	
Gene	Ecotype	Mutation	Ecotype	Mutation
TPL	Ler	Point mutation (<i>tpl2</i> ; Long et al., 2006)	Col-0	Salk 0792730
TPR1	Wassilewskija	T-DNA	Col-0	Deletion (Zhu et al., 2010)
TPR2	N/A	(RNAi)	Col-0	Salk 079848
TPR3	Ler	T-DNA	Col-0	Salk 029936
TPR4	Wassilewskija	T-DNA	Col-0	Salk 150008

Table 5-1. Mutants used to assemble *tpl tpr1 tpr3 tpr4* and other mutants in Krogan et al. (2012) and to create novel mutant combinations used in this thesis.

5.2.3 Embryonic and root phenotyping

Germination assays and embryonic and root phenotype screening were performed *on* sterile media. Seeds were stratified for 48 hours at 4°C in distilled water then sterilised by immersion in 0.15% sodium hypochlorite (10 minutes) then 70% ethanol (1 minute) followed by washing three times in sterile distilled water. The seeds were sown by pipetting onto sterile ½ Murashige and Skoog basal salts with Gamborg’s vitamins (Sigma), with or without 2% sucrose (Serva) in four-vent 120mm square plates (VWR). Seeds were spaced at 5mm intervals (minimum). Plates were sealed with

micropore tape. For root phenotyping, a single row of seeds was sown on each plate, 20mm from the top edge with a ± 2 mm offset to separate genotypes. Plates were placed upright in a transparent tray, approximately 80 degrees relative to the supporting surface, and maintained in long day conditions (16 hours of light, 18 hours of darkness) under fluorescent lighting.

5.2.4 Floral phenotyping

Plants were initially screened in greenhouses (20-25°C) for abnormal phenotypes alongside Col-0, Ler and *tpl-1* controls. For floral phenotype scoring, plants were grown in controlled conditions (Sanyo cabinets) at 21 or 27°C. Scoring was performed on flowers from the primary inflorescence, discarding the first five flowers.

5.3 Results

5.3.1 Embryonic and vegetative phenotypes

As *tpl-1* exhibits embryonic defects, I anticipated that partial loss of TPL/TPR genes may cause a similar but subtler phenotype. Noting that *Arabidopsis* TPL/TPR genes are divided between two clades (Figure 5-1), I examined mutants lacking genes from one or the other clade. The mutants *tpl tpr1 tpr4* and *tpr2 tpr3* mutants were grown at ~22°C (*tpl-1* exhibits more severe phenotypes at higher temperatures). The progeny of each was screened on agar plates ($\frac{1}{2}$ MS, 0% sucrose) for *tpl-1*-like embryonic phenotypes (i.e. fused or missing cotyledons, etc.). 7.8% of *tpl tpr1 tpr4* germinants displayed a strong asymmetry between cotyledons (n = 48). This phenotype was not observed in wild type controls (n = 40). Cotyledon fusion was not observed. Minor abnormalities in morphology, specifically the growth of chlorotic tissue at the tips of the cotyledons, were observed at an insignificant frequency. This is dissimilar to *tpl-1* and *tpl tpr1 tpr2^{RNAi} tpr3 tpr4*, which present cotyledon loss or fusion phenotypes (Long et al., 2006). Contrastingly, no morphological defects were observed in *tpr2 tpr3* mutant seedlings.

Ecotype	Mutant	Phenotype	Citation	TPL	TPR1	TPR2	TPR3	TPR4
Ler	<i>tpl-1</i>	Weak <i>apetala2</i> at 22°C, strong <i>apetala2</i> at 27°C; vegetative phenotype - flowering at 27°C enhances phenotype of progeny N.b. Krogan introgressed <i>tpl-1</i> from Ler into Col; no phenotypic differences reported	Long <i>et al.</i> , 2002 Krogan <i>et al.</i> , 2012	Red	Blue			Green
Ler	<i>tpl-2</i>	Morphologically wild type; from EMS screen to rescue <i>tpl-1</i>	Long <i>et al.</i> , 2006	Red				Green
Ler	<i>tpl-3</i>	Morphologically wild type; from EMS screen to rescue <i>tpl-1</i>	Long <i>et al.</i> , 2006	Red				Green
Ler	<i>tpl-4</i>	Morphologically wild type; from EMS screen to rescue <i>tpl-1</i>	Long <i>et al.</i> , 2006	Red				Green
Ler	<i>tpl-5</i>	Morphologically wild type; from EMS screen to rescue <i>tpl-1</i>	Long <i>et al.</i> , 2006	Red				Green
Ler	<i>tpl-6</i>	Morphologically wild type; from EMS screen to rescue <i>tpl-1</i>	Long <i>et al.</i> , 2006	Red				Green
Ler	<i>tpl-7</i>	Morphologically wild type; from EMS screen to rescue <i>tpl-1</i>	Long <i>et al.</i> , 2006	Red				Green
Col	<i>tpl-8</i> (Saik 0365666)	Aphenotypic; from EMS screen to rescue <i>tpl-1</i>	Long <i>et al.</i> , 2006	Red				Green
Col	<i>tpl</i> (Saik 97230)	Morphologically wild type; weakened biotic stress response	Zhu <i>et al.</i> , 2010	Red				Green
Col	<i>tplr1</i> (deletion)	Morphologically wild type; weakened biotic stress response	Zhu <i>et al.</i> , 2010	Red				Green
Col	<i>tplr4</i> (Saik 150008)	Morphologically wild type; weakened biotic stress response	Zhu <i>et al.</i> , 2010	Red				Green
Col	<i>tpl</i> <i>tplr1</i>	Morphologically wild type; weakened biotic stress response	Zhu <i>et al.</i> , 2010	Red				Green
Col	<i>tpl</i> <i>tplr1</i> <i>tplr4</i>	Reduced stamen number; infrequent floral organ identity defects; weakened biotic stress response.	Zhu <i>et al.</i> , 2010 and this thesis	Red				Green
Col	<i>tplr2</i> (Saik 079848)	Aphenotypic	Long <i>et al.</i> , 2006	Green				Red
Col	<i>tplr3</i> (Saik 029936)	Aphenotypic	Long <i>et al.</i> , 2006	Green				Red
Col	<i>tplr2</i> <i>tplr3</i>	Minor floral organ identity defects (infrequent)	Thesis	Green				Red
Ler/Ws	<i>tpl</i> <i>tplr1</i> <i>tplr3</i> <i>tplr4</i>	Petaloid sepals (<5% of flowers)	Long <i>et al.</i> , 2006	Red				Green
Ler/Ws	<i>tpl</i> <i>tplr1</i> <i>tplr2</i> ^{RNAi} <i>tplr3</i> <i>tplr4</i>	Resembles <i>tpl-1</i> but has strong <i>apetala2</i> phenotype	Long <i>et al.</i> , 2006	Red	Yellow			Green
Col	<i>tpl</i> ⁺ <i>tplr1</i> ⁺ <i>tplr2</i> ⁺ <i>tplr3</i> ⁺ <i>tplr4</i> ⁺	Aphenotypic	Thesis	Yellow				Red
Col	TPL <i>tplr1</i> <i>tplr2</i> ⁺ <i>tplr3</i> <i>tplr4</i>	Strong <i>apetala2</i> phenotype evident at 27°C; low fertility; mild early vegetative phenotype. Segregation indicates TPL-only plants not viable.	Thesis	Green				Red
Col	<i>tpl</i> <i>tplr1</i> TPR2 <i>tplr3</i> <i>tplr4</i>	Weak <i>apetala2</i> phenotype but plants viable and healthy.	Thesis	Red				Green
Col	TPL <i>tplr1</i> <i>tplr2</i> <i>tplr3</i> TPR4	No obvious phenotype. Plants viable and healthy.	Thesis	Red				Green
Col	<i>tpl</i> ⁺ <i>tplr1</i> <i>tplr2</i> <i>tplr3</i> TPR4	Strong <i>apetala2</i> phenotype evident at 27°C; low fertility; no early vegetative phenotype. Segregation indicates TPR4-only plants not viable.	Thesis	Yellow				Green

Table 5-2. Summary of *tpl//tpr* mutants described in this thesis and elsewhere. Colour-coding denotes genotype: green = homozygous wild type; red = homozygous mutant; yellow = heterozygote; orange = indicates RNA inhibition; blue = predicted loss of function at protein level. N.b. The *tplr1* mutant allele is an N-terminal deletion (Zhu *et al.*, 2010).

5.3.2 Floral phenotypes

The *tpl-1* mutant exhibits abnormal floral development. At 22°C or below, *tpl-1* flowers infrequently show organ identity defects, predominantly the conversion of sepal tissue to petaloid tissue (Krogan et al., 2012). At 27°C, the frequency of defects increases (Figure 5-2). Flowers resemble those of the *apetala2* (*ap2*) mutant (Jofuku et al., 1994). APETALA2 maintains perianth organ (A-function) identity (Irish, 2017) and in *ap2* and *tpl-1* perianth organs are converted to carpels. As in *tpl-1*, the *ap2* increases in severity with temperature (Bowman et al., 1991). AP2 and TPL interact and it is likely that together they repress ectopic expression of C-function genes (Krogan et al., 2012; Irish, 2017). Although no floral phenotype was reported for *tpl tpr1 tpr4* mutants by Zhu et al. (Zhu et al., 2010), the authors did not confirm a wild type floral phenotype, nor did they report growing these plants at elevated temperatures. I therefore screened the double, triple and quadruple *tpl/tpr* mutants for floral phenotypes.

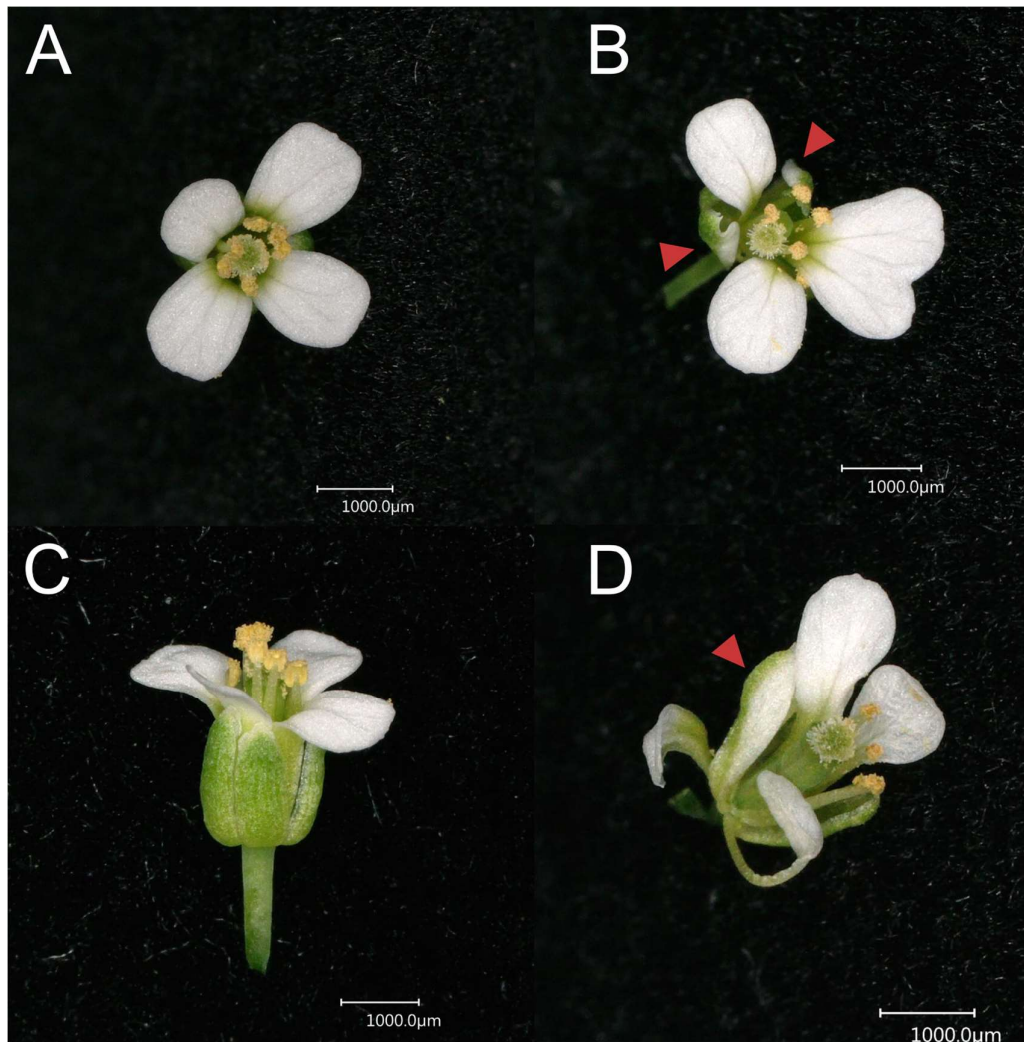


Figure 5-2. The floral phenotype of Ler wild type and *tpl-1* flowers at 27°C. Ler flowers (A, C) follow the (4, 4, 4+2, 2) floral plan associated with the wild type while *tpl-1* flowers (B, D) frequently display organ identity defects, e.g. petaloid sepals (red arrowheads); whorls are less tightly arranged and flowers appear more open.

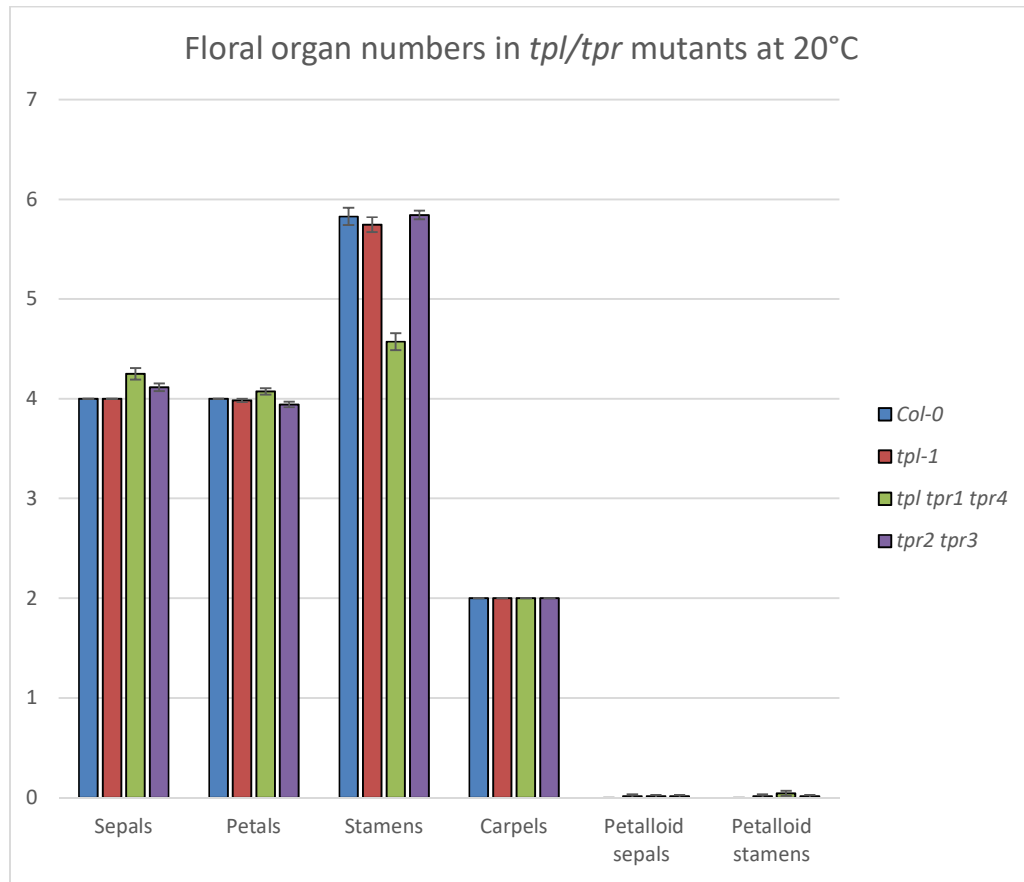


Figure 5-3. Floral organ numbers in *tpl/tpr* mutants at 20°C. Stamen number was significantly reduced in *tpl tpr1 tpr4* mutants compared to the wild type (ANOVA $f = 44.4$, $p < 0.001$; Tukey's HSD $Q = 12$, $p < 0.001$). Sepal number also increased significantly versus wild type Col-0 (ANOVA $F = 8.59$, $p < 0.001$; Tukey's HSD $Q = 5.49$, $p < 0.01$). The *tpr2 tpr3* mutants were not significantly different from wild type. The *tpl-1* mutants displayed morphological abnormalities (splayed floral organs) but did not differ significantly in organ number from other backgrounds. All mutants produced an insignificant minority of floral organs with altered identities, i.e. sepals with petaloid sectors and petaloid stamens

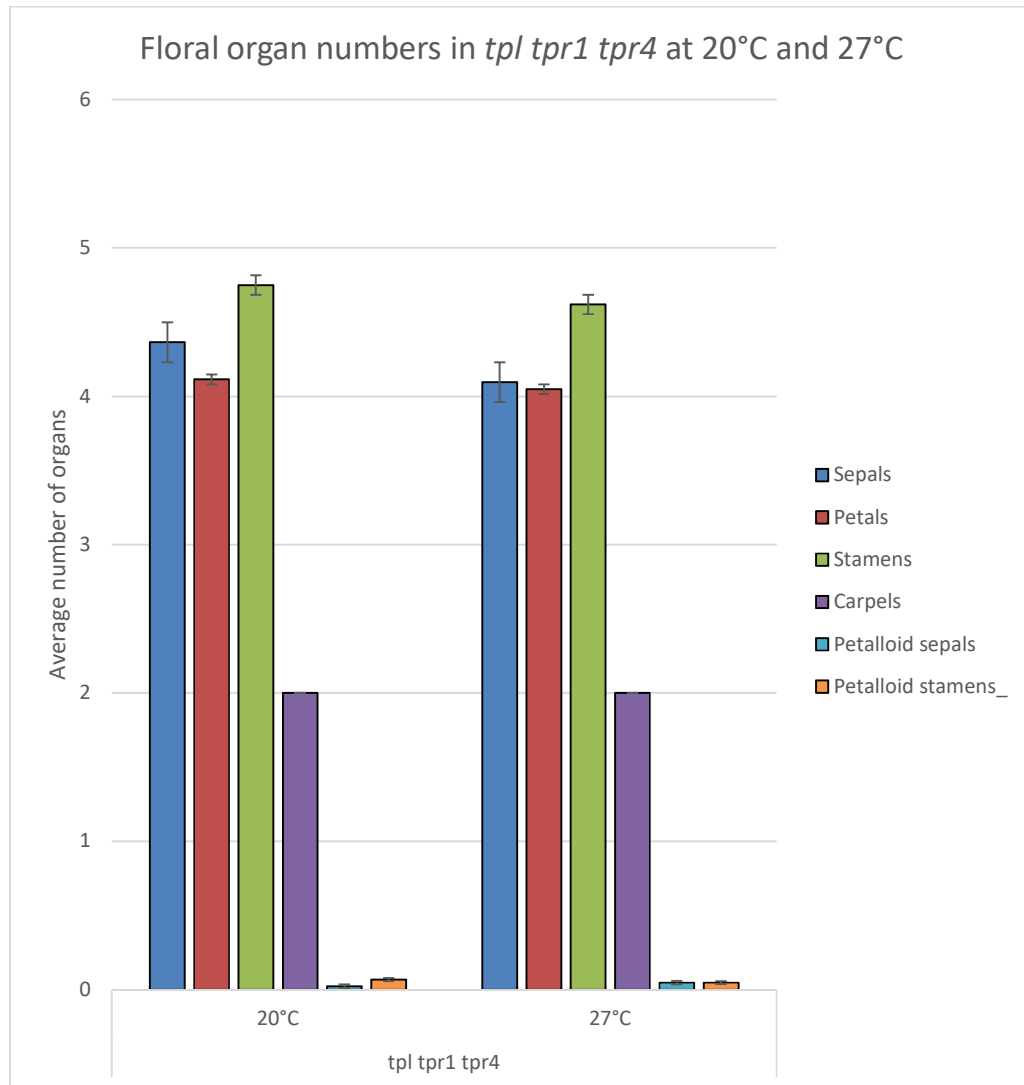


Figure 5-4. Floral organ numbers in *tpl tpr1 tpr4* at 20°C and 27°C. Flowers developing at elevated temperatures did not differ significantly in organ number from those grown at 20°C (t-tests: sepals – $t=-1.00$, $p < 0.16$; petals – $t=-.12$, $p < .67$; stamens – $p < 0.25$), suggesting that temperature sensitivity may be specific to the *tpl-1* allele.

In *tpl tpr1 tpr4* flowers produced at 20°C, stamen number was significantly reduced and, in rare instances, perianth organ number was increased and petaloid stamens were observed (Figures 5-3 and 5-4). These changes are almost never observed in wild type flowers. Surprisingly, changes in organ number and identity occurred more frequently than in *tpl-1* plants grown at 20°C. Similar abnormalities were observed in *tpr2 tpr3* but changes in organ number were not statistically significant. To test whether or not the

phenotype is enhanced by elevated temperatures as in *tpl-1*, *tpl tpr1 tpr4* plants were grown at 20°C and 27°C. In contrast to *tpl-1*, the phenotype of *tpl tpr1 tpr4* flowers developing at 27°C was not significantly different from those flowers produced at 20°C (Figure 5-5). This must be reconciled with the temperature sensitivity of *apetala2* mutants. Simple loss of *TPL/TPR*-mediated repression of genes (e.g. via *APETALA2*) should mimic loss-of-function in those genes. This suggests that the temperature sensitivity of *tpl-1* is due to the allele itself rather than a general loss of function.

5.3.3 Root phenotypes

Although published literature did not describe a root phenotype in *tpl-1*, Szemenyei et al. (2008) alluded to a potential role for TPL in lateral root development. A dominant *AUXIN/INDOLE ACETIC ACID (AUX/IAA)* mutant, *iaa14/solitary root*, produces no lateral roots, but this phenotype is rescued by inhibiting histone deacetylation (Fukaki et al., 2006). TPL interacts directly with numerous AUX/IAAs (*Arabidopsis* Interactome Mapping Consortium, 2011; Causier et al., 2012a; Szemenyei et al., 2008) and indirectly with histone deacetylases (Krogan et al., 2012). Furthermore, TPL and TPR1-3 interact with WUSCHEL-RELATED HOMEODOMAIN 5 (*WOX5*), a regulator of primary (Sarkar et al., 2007) and lateral (Tian et al., 2014) root primordia. To examine *tpl-1* for root phenotypes, Ler and *tpl-1* seeds were germinated upright on ½ MS agar plates. At six days post-germination the primary roots of *tpl-1* were significantly shorter than those of the wild type Ler control (Figure 5-6).

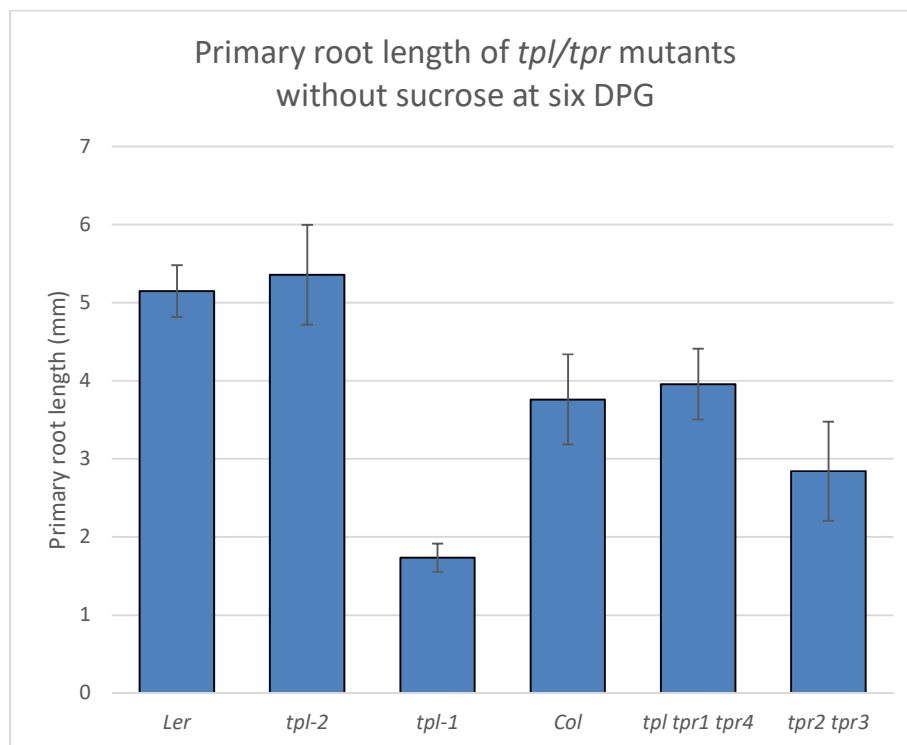


Figure 5-5. Root length of *tpl/tpr* mutants grown without sucrose at six days post-germination. Plants were grown on $\frac{1}{2}$ MS agar without sucrose. The primary root of *tpl-1* (Ler background) was shortened by a statistically significant amount (ANOVA $f = 9.03$, $p < 0.001$; Tukey's HSD $Q = 6.38$, $p < 0.01$) whereas *tpl-2* (Ler background) and the multiple *tpl/tpr* mutants (Col-0 background) do not differ significantly from their respective wild types.

The short length of the primary *tpl-1* root would be inhibitory to lateral root outgrowth and no lateral roots were observed for *tpl-1* under these conditions. This phenotype conflicted with published images of *tpl-1* and with observations of *tpl-1* grown in soil, where *tpl-1* developed a range of root lengths and produced lateral roots. Sucrose is commonly added to *in vitro* growth media as a carbon source. It increases the growth rate of primary and lateral roots, albeit through nutrition and not through signalling as part of a regulatory pathway, and weakly inhibits lateral root elongation (Roycewicz and Malamy, 2012). C. Fleming and I complemented the *tpl-1* root phenotype by supplementing the $\frac{1}{2}$ MS growth medium with 2% sucrose (Figure 5-7).

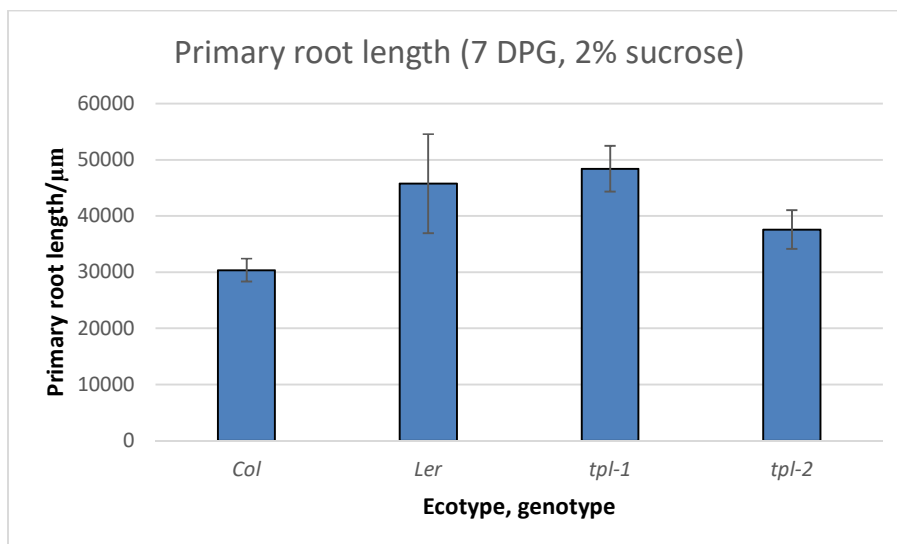


Figure 5-6. Primary root length at 7 days post germination on $\frac{1}{2}$ MS agar supplemented with 2% sucrose. The short primary root phenotype of *tpl-1* is complemented by the addition of sucrose to the medium. There is no significant difference between groups (one-way ANOVA; $f = 2.43$; $p < 0.116$; $n = 4$ for each treatment).

While examining the primary roots of *tpl-1*, we observed that *tpl-1* seedlings appeared to produce fewer elongated lateral roots than control Ler plants (Figure 5-8). Root hair production, another process regulated by auxin signalling (Salazar-Henao et al., 2016), was unaffected (Figure 5-9). Lateral root production and elongation was also significantly reduced in the quadruple ***tpl tpr1 tpr3 tpr4*** mutant (Figure 5-10). I was able to complement the primary root length phenotype of the ***tpl tpr1 tpr3 tpr4*** mutant in two independent lines by transforming the mutant with *pTPL::TPL* (Figures 5-11 and 5-12). The effect of this construct on lateral root formation in ***tpl tpr1 tpr3 tpr4*** is not known at the time of writing.

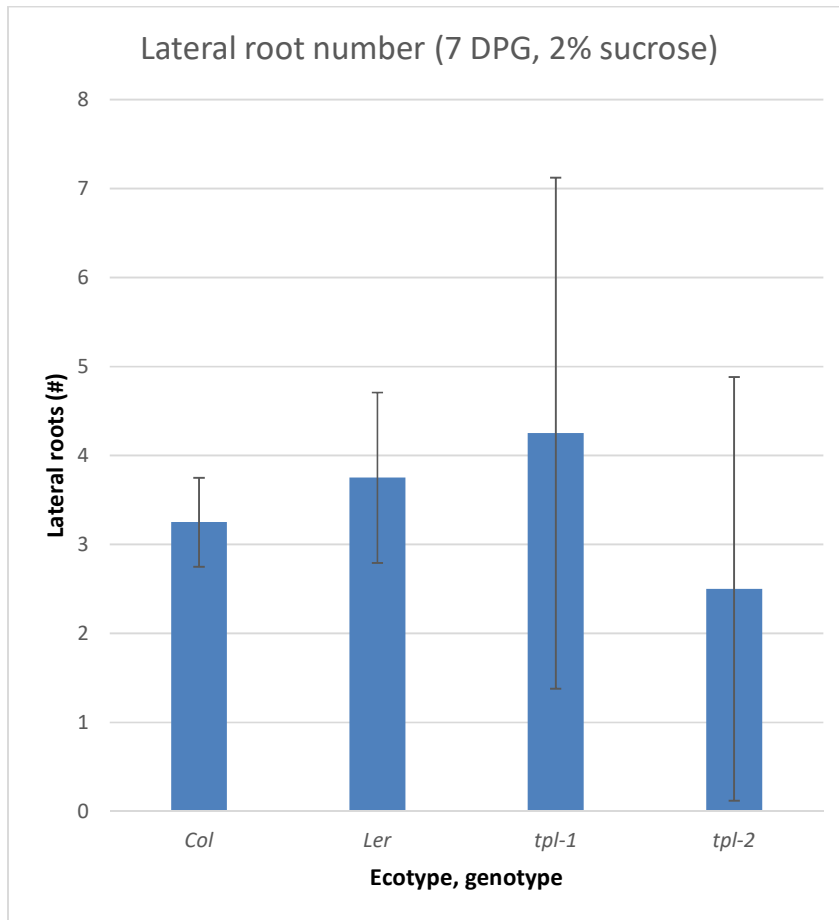


Figure 5-7. Numbers of lateral roots produced by wild type plants and *tpl* mutants at seven days post-germination. (n = 4 per treatment.) Plants were grown on $\frac{1}{2}$ MS agar supplemented with 2% sucrose. In both *tpl-1* and the non-dominant mutant *tpl-2*, lateral root number was highly variable. Significant differences between mutants were not detectable due to variance and sample size (ANOVA $f = 0.59$, $p < 0.6325$).

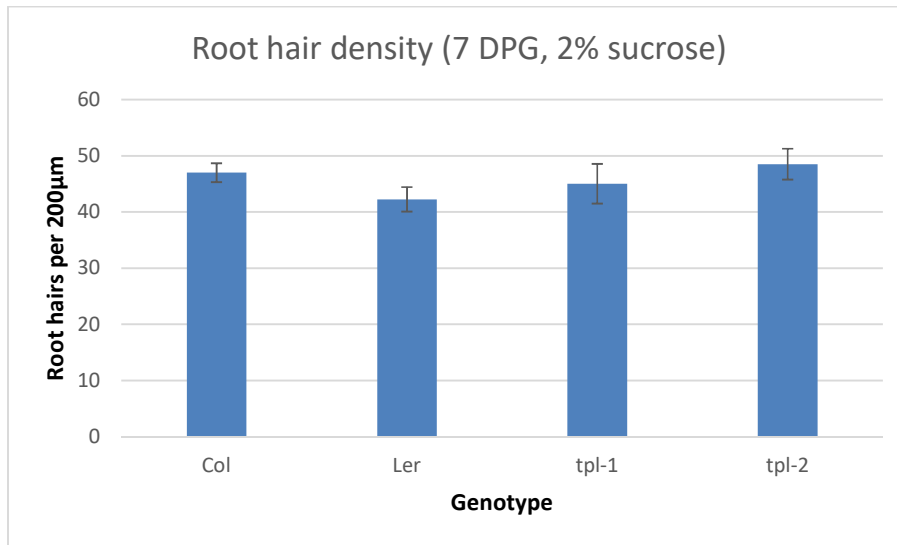


Figure 5-8. Root hair density in *tpl* mutants. Root hairs per 200µm on primary roots at 7 days post germination on ½ MS agar supplemented with 2% sucrose. No significant difference was observed between groups.

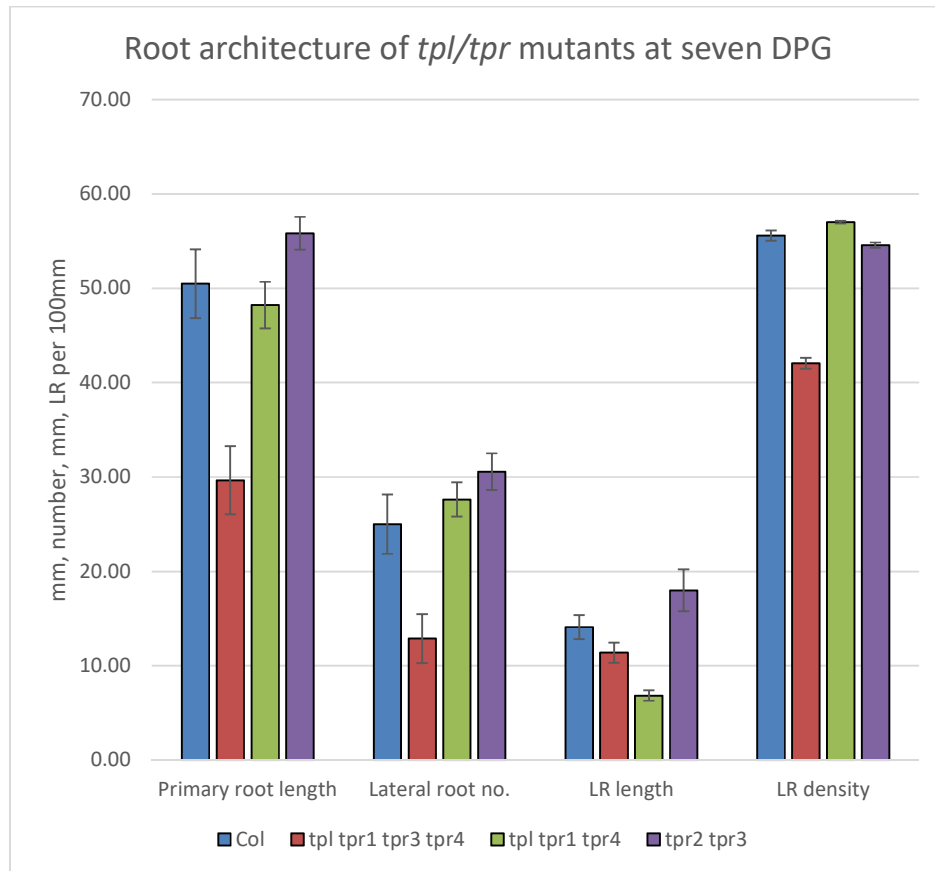


Figure 5-9. Root architecture of *tpl/tpr* mutants at seven days post-germination. Plants were grown on $\frac{1}{2}$ MS agar supplemented with 2% sucrose. The addition of sucrose increased the length of primary roots in all backgrounds, however, the quadruple mutant exhibited short primary roots and fewer lateral roots. The quadruple mutant may be less capable of founding or maintaining root meristems as its short primary root length is not rescued by the presence of sucrose in the medium, unlike *tpl-1*. Double and triple mutants do not display this characteristic, although lateral root elongation is compromised in *tpl tpr1 tpr4*.



Figure 5-10. Complementation of *tpr1 tpr3 tpr4*. The short primary root phenotype of *tpr1 tpr3 tpr4* mutants is complemented by wild type *TOPLESS* expressed from its own promoter (*pTPL::TPL*). Seedlings were grown on ½ MS agar lacking sucrose as sucrose was previously demonstrated to increase root length in *tpr-1* seedlings

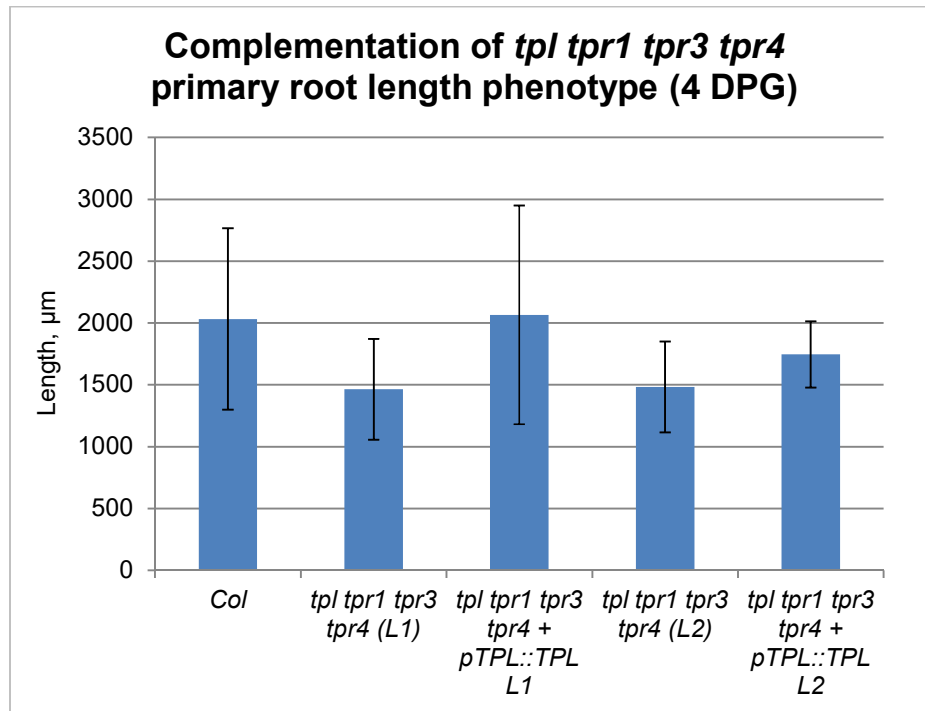


Figure 5-11. Complementation of *tpl tpr1 tpr3 tpr4*. The short primary root phenotype of *tpl tpr1 tpr3 tpr4* mutants is complemented by *pTPL::TPL*. T2 mutant seedlings in two lines (L1, L2) showed increased primary root length compared to untransformed sister seedlings at four days post-germination (DPG) on $\frac{1}{2}$ MS agar containing no sucrose. Error bars indicate standard deviation; n = 5, 4, 6, 4 and 6, respectively.

Lateral root development is responsive to auxin and cytokinin signalling, and the phenotypes of *tpl/tpr* mutants may be the result of altered auxin and cytokinin signalling. TOPLESS is known to interact with AUX/IAA transcription factors which are degraded in response to auxin signalling, but TOPLESS is not known to interact with any transcription factor associated with the cytokinin signalling pathway. To gain a preview of how auxin and cytokinin signalling changes in the roots of *tpl-1* mutants, I examined the expression of auxin/cytokinin signalling associated genes in root tissue bearing lateral roots (Figure 5-13). For auxin signalling, AUX/IAAs 12 and 14 were examined as they have been linked to lateral root initiation (Tao and Estelle, 2018; Fukaki et al., 2006; Stoeckle et al., 2018). For cytokinin signalling, expression of *ARR5*, a Type A *AUXIN RESPONSE REGULATOR*, was measured. *ARR5* expression rapidly increases in

response to cytokinin (Brandstatter, 1998). *ARR5* has previously been used as a marker for the presence of cytokinin (D'Agostino et al., 2000). The expression of AUX/IAAs 12 and 14 in wild type and mutants was similar (Figure 5-13); however, expression of the cytokinin marker *ARR5* significantly increased in the mutant. The increased expression of *ARR5* in *tpl-1* indicates elevated levels of cytokinin, a surprising result as cytokinin suppresses lateral root initiation but promotes lateral root elongation (Laplaze et al., 2007). Increased cytokinin levels may reflect some form of compensation for the constitutive auxin-like response seen in *tpl-1* (Szemenyei et al., 2008) but the underlying mechanism is not clear.

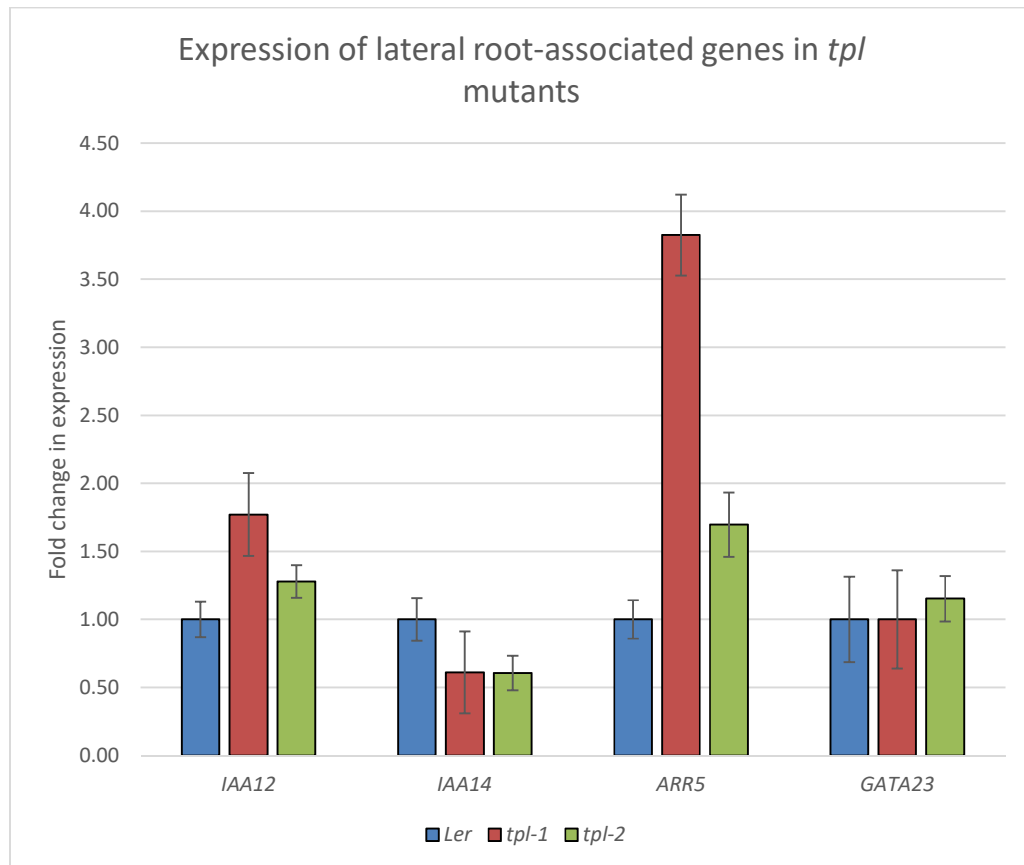


Figure 5-12. Expression of auxin and cytokinin signalling gene expression in *tpl* mutant roots by quantitative PCR. No significant difference is observed in the expression of *IAA12*, *IAA14* and *GATA23* between wild type and mutants, but expression of *ARR5*, a marker for cytokinin signalling, is significantly increased in *tpl-1*.

5.3.4 Novel mutants display *tpl-1*-like phenotypes

After crossing *tpl tpr1 tpr4* and *tpr2 tpr3*, approximately 5000 F2 seeds were screened for embryonic phenotypes. Of these, one seedling failed to develop cotyledons. No other *tpl-1*-like phenotypes were observed. 96 plants were transplanted to soil and grown under non-sterile (greenhouse) conditions. I did not expect to recover all possible genotypes due to chromosomal linkage between *TPR2* and *TPR4*, which are closely linked on the same arm of chromosome 3, reducing the likelihood of recovering a recombinant mutant lacking both genes. Genotyping did identify several mutants of interest: a quadruple ***tpl tpr1 TPR2 tpr3 tpr4*** mutant; triple mutants retaining *TPL* and either *TPR2* or *TPR4* (***TPL tpr1 TPR2 tpr3 tpr4*** and ***TPL tpr1 tpr2 tpr3 TPR4***); and a majority-heterozygous multiple mutant (***tpl^{+/-} tpr1 tpr2^{+/-} tpr3 tpr4^{+/-}***), from which a single recombinant individual with the genotype ***TPL tpr1 tpr2^{+/-} tpr3 tpr4*** was identified. Genetic and phenotypic screening also identified heterozygotes with a conspicuous floral phenotype (***tpl^{+/-} tpr1 tpr2 tpr3 TPR4***).



Figure 5-13. Floral phenotypes of *tpr2 tpr3*, *tpl tpr1 tpr4* and *tpl tpr1 tpr3 tpr4* alongside wild type Columbia. Wild type Col produces flowers with a (4, 4, 4+2, 2) floral pattern and variations in organ number are rare. Flowers of *tpr2 tpr3* mutants are typically wild type with rare changes in the numbers and identities of perianth organs and stamens (not shown). These defects, e.g. pentapetaly, are more frequent in *tpl tpr1 tpr4* mutants. Quadruple *tpl tpr1 tpr3 tpr4* mutants exhibit changes in floral morphology ranging from loss of stamens (above) to changes in organ identity (Figure 5-13).

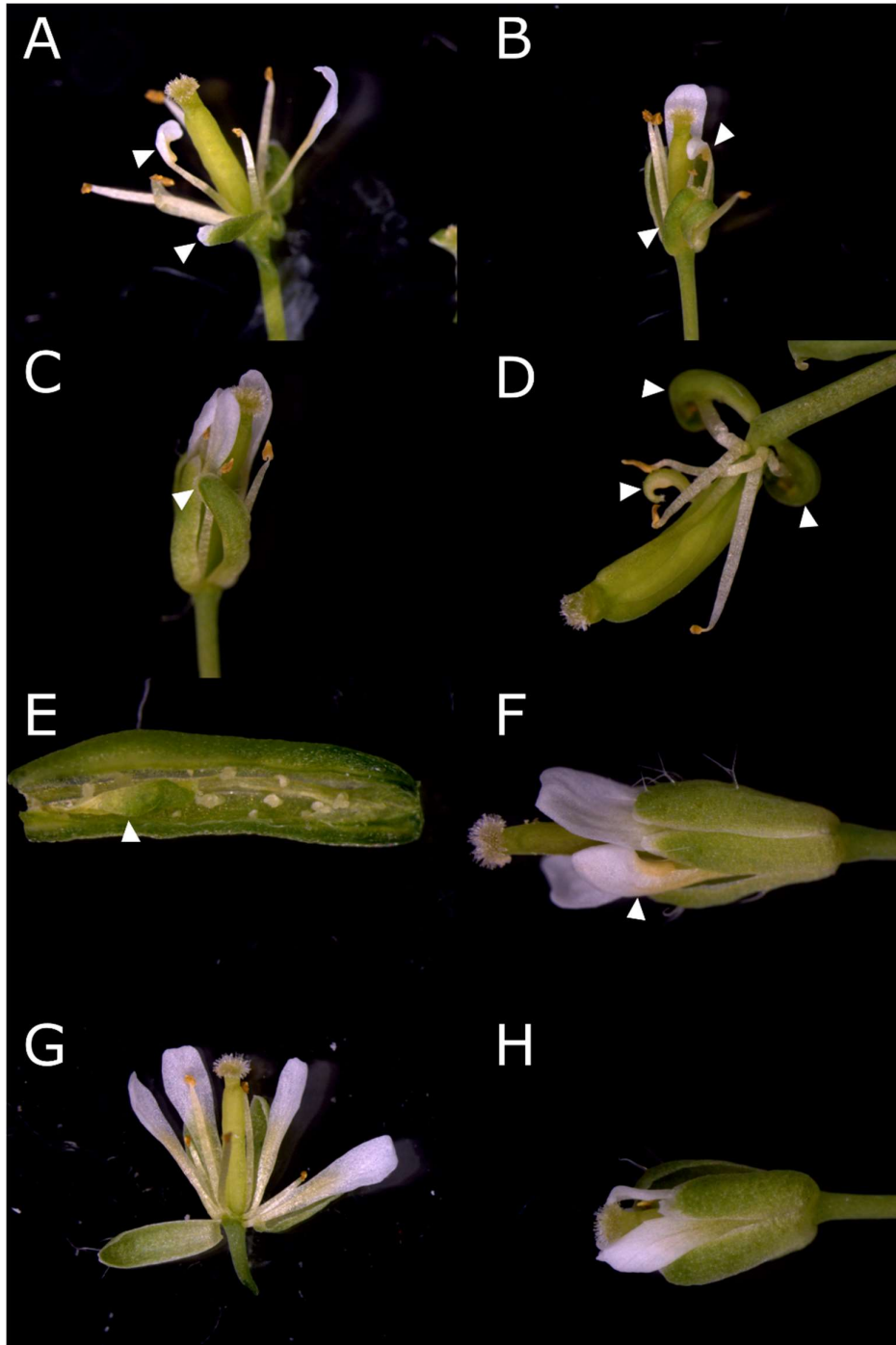


Figure 5-14. Examples of floral phenotypes in novel *tpl/tpr* mutant combinations at 27°C. A and B: *tpl tpr1 TPR2 tpr3 tpr4* flowers display developmental defects including petaloid sectors within sepals (A, arrowhead (dissected to show organs)), ectopic carpels (B, arrow) and petaloid stamens (A and B, arrows). C, D, E and F: *tpl^{+/+} tpr1 tpr2 tpr3 TPR4* flowers also present organ identity defects including ectopic carpels in place of other organs (C and D, arrows) and within the gynoecium (E, arrow) as well as petaloid stamens (F); *TPL tpr1 tpr2 tpr3 TPR4* flowers appear aphenotypic (G (dissected to show organs) and H).

The quadruple ***tpl tpr1 TPR2 tpr3 tpr4*** mutant is a novel allelic combination in the Col-0 ecotype background (Figure 5-14 and Table 5-2). During preliminary screening in a 22-27°C temperature range (greenhouse conditions), these mutants displayed floral organ identity defects as described in Long et al. (2006) and Krogan et al. (2012) in their mixed-ecotype equivalent, whereas heterozygous ***tpl^{+/-} tpr1 tpr2^{+/-} tpr3 tpr4^{+/-}*** plants did not. In addition, the quadruple mutants produced disordered rosettes with numerous axillary shoots. Other mutants allow us to compare the relative efficacy of *TPL*, *TPR2* and *TPR4* in compensating for the loss of other genes. The ***tpl^{+/-} tpr1 tpr2 tpr3 TPR4*** mutant exhibited a range of weak and strong *apetala2*-like floral phenotypes when grown in greenhouse conditions (22-27°C), resembling the *tpl-1* and the quintuple loss of function ***tpl tpr1 tpr2^{RNAi} tpr3 tpr4*** (Krogan et al., 2012). Phenotype characteristics included reduction in stamen number and replacement of perianth organs with carpelloid tissue (Figure 5-14). The mutants produced few seeds (average seed yield per plant = 60 versus >500 for wild type Columbia) and a second whorl of carpels was found to be initiated within the gynoecium of some flowers (Figure 5-14). Penetrance of the phenotype was incomplete, unlike in *apetala2-1* and related mutants (Bowman et al., 1991)) with an increase in the severity of the phenotype in flowers produced later on axillary stems. The plant was selfed and the progeny germinated at 16°C or 27°C in growth cabinets. Genotyping revealed a significant skew in segregation of the progeny: 3/35 plants were heterozygous at the *TPL* locus versus an expected frequency of 50% (18/35) and no homozygous ***tpl tpr1 tpr2 tpr3 TPR4*** were recovered. Floral phenotypes in the two plants grown at 27°C were superficially more severe than the single plant grown at 16°C.

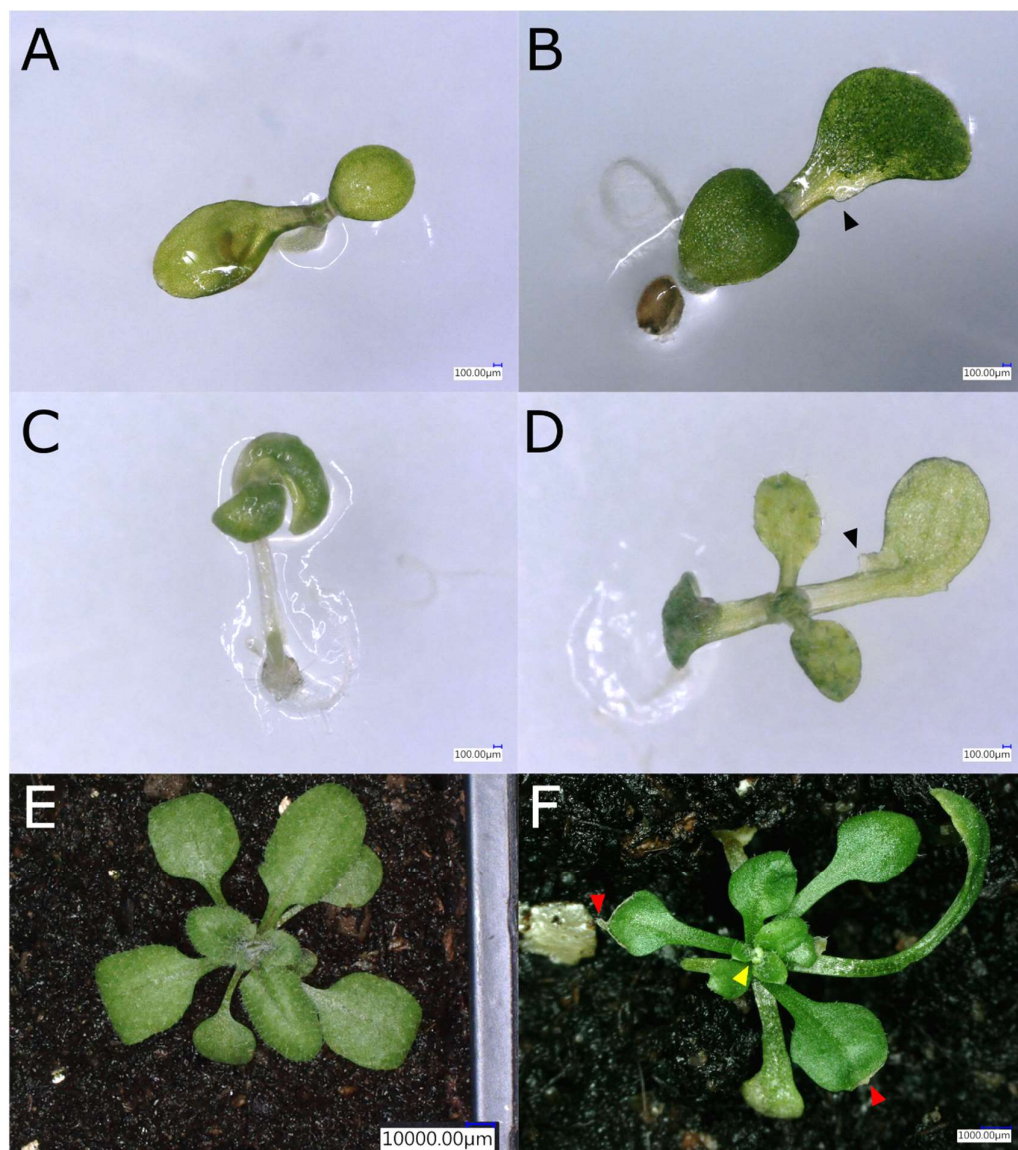


Figure 5-15. *TPL tpr1 tpr2^{+/-} tpr3 tpr4* phenotypes. Seedlings bear embryonic and early vegetative mutant phenotypes including asymmetric cotyledons (A, C), asymmetry in early leaves and outgrowth of serration or stipule-like tissue at the base of the leaf blade (B, D; black arrows). Mutants exhibited necrosis at leaf tips (F, red arrows) and produced floral buds early (F, yellow arrow) compared to wild type Col-0 (E).

TPL tpr1 tpr2^{+/-} tpr3 tpr4 mutants also present developmental defects (Figure 5-14). A single plant was obtained from a segregating parent (*tpr1^{+/-} tpr2^{+/-} tpr3 tpr4^{+/-}*). At 16°C the plant displayed no floral developmental defects. The progeny was germinated on ½ MS agar, revealing *tpr1*-like fusion of cotyledons in some germinants. At 20°C, *TPL tpr1 tpr2^{+/-} tpr3 tpr4* plants produced abnormal leaves. Outgrowth of basal teeth on the margins

of leaves in ***TPL tpr1 TPR2^{+/-} tpr3 tpr4*** (Figure 5-16) may reflect an auxin-like response where auxin-activated targets are no longer silenced, however, outgrowth was not pronounced in all leaves. The additional tissue could represent a new growth axis or a continuation of indeterminate growth. Patterning of the leaf margin is a balance between indeterminacy, which allows continued cell division, and differentiation. TPL/TPRs interact with transcription factor families that promote cell differentiation and determinacy in leaf development, including TCPs, NGATHA (NGA) and DELLAs, the latter regulating responses to gibberellic acid (Maugarny-Calès and Laufs, 2018). The mutants also flowered more than seven days earlier than wild type controls and produced *ap2*-like flowers. The segregation ratio was also skewed significantly. Two out of twenty-four plants obtained had the heterozygous ***TPL tpr1 tpr2^{+/-} tpr3 tpr4*** genotype. No homozygous mutants (***TPL tpr1 tpr2 tpr3 tpr4***) were identified. The severity of embryonic and floral phenotypes in the heterozygous ***tpl^{+/-} tpr1 tpr2 tpr3 TPR4*** and ***TPL tpr1 tpr2^{+/-} tpr3 tpr4*** (Figures 5-9 and 5-10, respectively) mutants, in addition to the absence of homozygous mutant progeny, indicates that further depletion of ***TPL/TPR*** genes in this genetic context is lethal. The failure of embryos to develop in the siliques of ***tpl^{+/-} tpr1 tpr2 tpr3 TPR4*** (Figure 5-14) suggests non-viability of female gametes or embryonic lethality as opposed to non-germination. Furthermore, as the quadruple mutant retaining ***TPR2*** is viable, we may assume a difference in either expression or functionality between ***TPR2*** and ***TPL/TPR4***.

5.3.5 Phylogenetic relationships within the TPL family

The striking phenotypes of *tpl-1* and certain multiple *tpl/tpr* mutants reveal the importance of TPL-like proteins in plant development. The presence of ***TPL***-like genes in liverworts (Flores-Sandoval et al., 2015) and moss (Causier et al., 2012b) reveals an ancient origin for these co-repressors. The evolutionary relationships between members of this family could give us insight into functional differences between individual proteins. A phylogenetic analysis of TPL-like proteins supports the broad conservation of ***TPL/TPR*** proteins across plants, including chlorophytic algae (*Picocystis salinarum*) (Lemieux et al., 2014) and streptophytic algae (*Klebsormidium nitens*) (Hori

et al., 2014) (Figure 5-17). Distinct clades emerged, indicating radiation of the family in derived lineages. Algae and basal land plants each possess a single TPL protein type. Additional reciprocal BLASTs of the OneKP transcriptome database using PsTPL reveal single *TPL*-like transcripts across streptophytic algae in *Mesotaenium*, *Mougeotia*, *Entransia*, *Spirogyra*, *Cylindrocystis* and *Coleochaete* (Figure 5-18). Chlorophyte algae possess numerous transcription factors that contain repression domains associated with TPL-mediated repression (Figure 5-19).

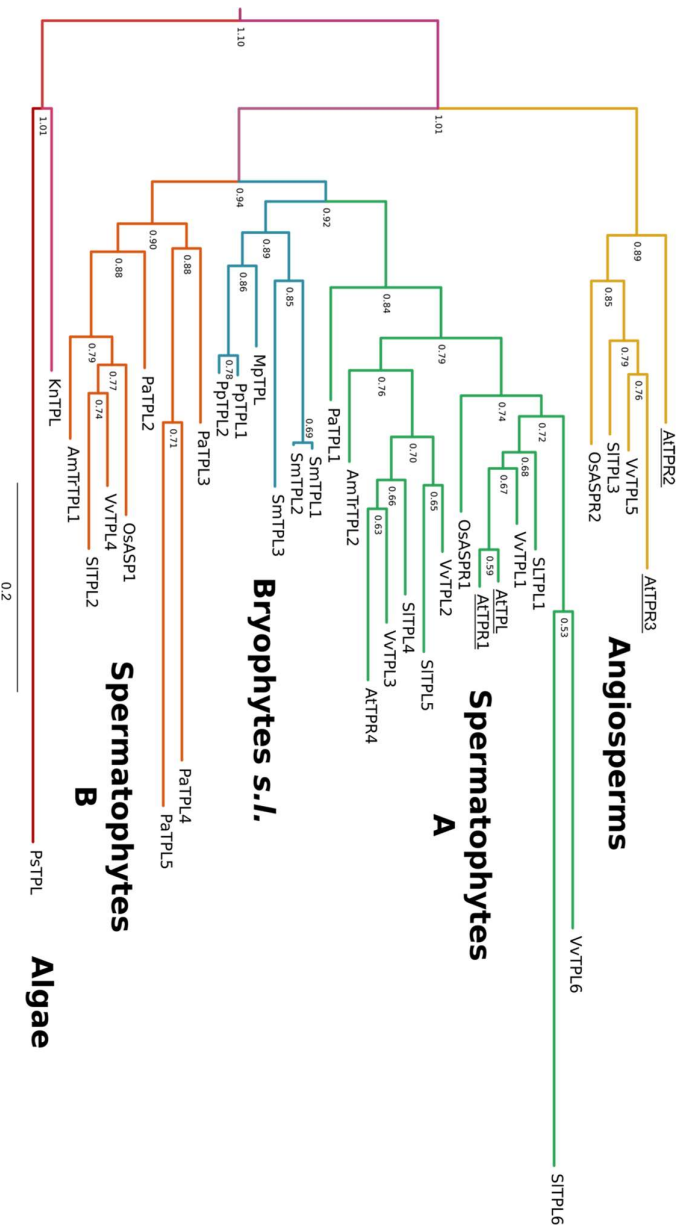


Figure 5-16. Unrooted Bayesian phylogeny of TPL-like proteins across the plant kingdom *Arabidopsis thaliana* TPL/TPRs are underlined. Clade labels denote the narrowest taxonomic group that encompasses all proteins contained therein. Node values indicate posterior probabilities expressed as percentages. Scale indicates branch length (i.e. substitutions per unit time).

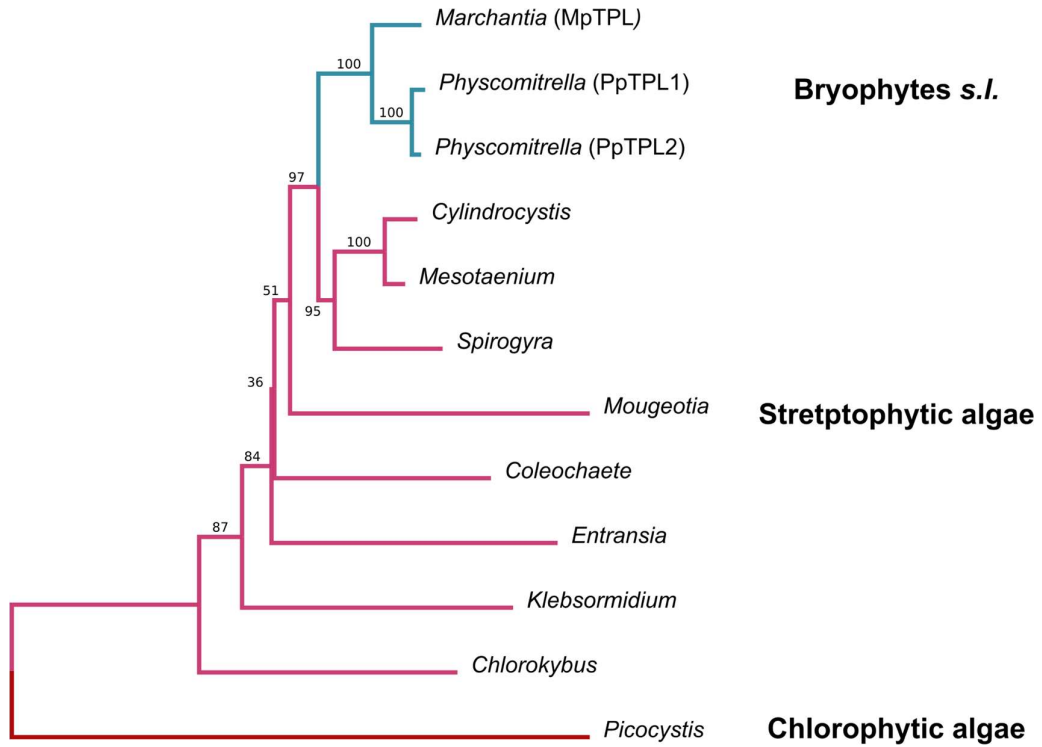


Figure 5-17. Neighbour-Joining phylogeny of TPL- like proteins from algal and basal land plant taxa. Node values indicate bootstrap support values expressed as a percentage (bootstrapped for 1,000 iterations). Sequences for MpTPL (*Marchantia polymorpha*) and PpTPL1 and 2 (*Physcomitrella patens*) were predicted from genomic open reading frames. Predicted algal TPL-like proteins were identified from the OneKP database. Sequence identifiers: *Mesotaenium* – *M. kramstei* NBYP-2056058; *Mougeotia* – *Mougeotia* sp. ZRMT-2005604; *Entransia* – *E. fimbriata*; BFIK-2004708, *Spirogyra* – *Spirogyra* sp. HAOX-2025270, *Cylindrocystis* – *C. cushleckae* JOJQ-2041843; *Coleochaete* – *C. irregularis* QPDY-2006907; *Chlorokybus* – *C. atmophyticus* AZZW-2021890.

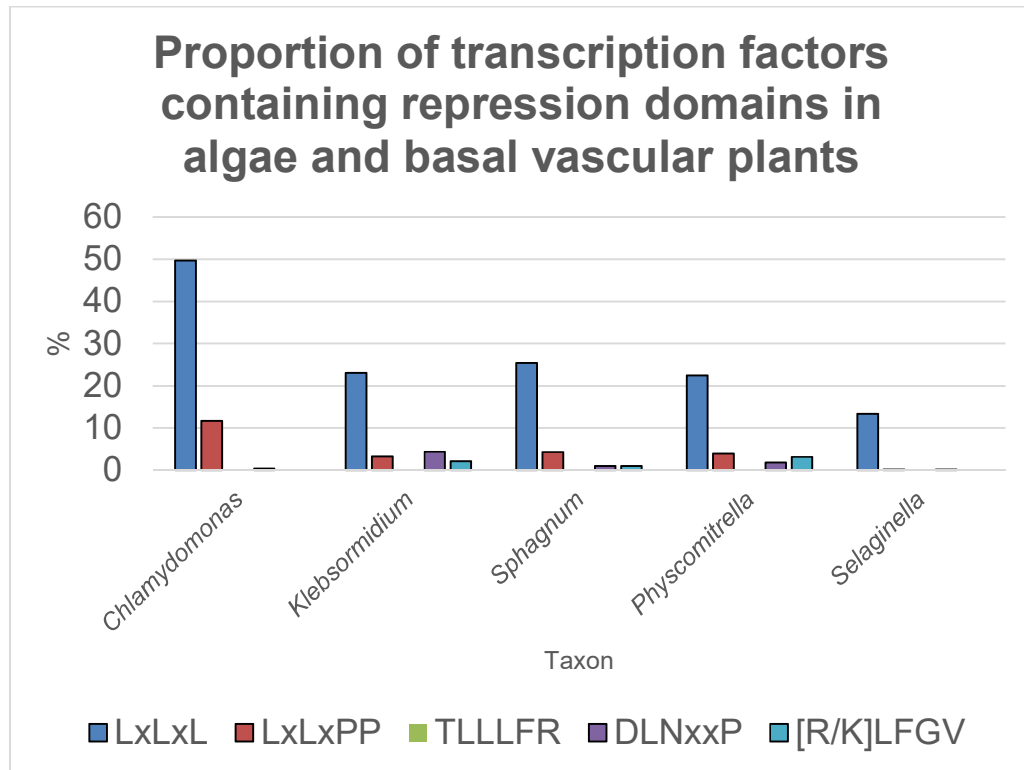


Figure 5-18. The proportion of transcription factors of all classes that contain repression domains. Motifs represent repression domains discussed by Kagale and Rozwadowski (Kagale and Rozwadowski, 2011b). Protein sequences for transcription factors from the taxa of interest from the Plant Transcription Factor Database v4.0 (Jin et al., 2017) were searched using script based on BioPython libraries (Cock et al., 2009) that identifies regular expressions matching the repression domains. Selected taxa include a chlorophyte alga that lacks TOPLESS-like proteins (*Chlamydomonas reinhardtii*), a streptophyte alga (*Klebsormidium nitens*), mosses (*Sphagnum fallax* and *Physcomitrella patens*) and a lycophyte (*Selaginella*). The appearance of DLNxxP and [R/K]LFGV motifs after the evolution of TOPLESS coincides with the expansion of gene families including APETALA, ETHYLENE RESPONSE FACTOR and LATERAL ORGAN BOUNDARY DOMAIN transcription factors in which these domains are found (Kagale et al., 2010; Kagale and Rozwadowski, 2011b).

Recent duplications have occurred in some basal vascular plants; branch lengths indicate that PpTPL1/2 (*Physcomitrella*) and SmTPL1/2 (*Selaginella*) are likely to be paralogues (Figure 15-6 – Bryophytes *s.l.*). In seed plants, three clades have emerged. All seed plants examined except *Arabidopsis thaliana* retain a close relative of the ancestral bryophyte TPL (Figure 5-16 – Spermatophytes B). Loss of the parent gene in *Oryza sativa* (*OsASP1*) and its homologue in maize (*RAMOSA 1 ENHANCER LOCUS 2, REL2*) causes

conspicuous developmental phenotypes, but *Arabidopsis* has tolerated this loss. The rosid *Vitis vinifera* retains an ASP1-like protein which suggests that it has been lost from the *Arabidopsis* lineage in a recent ancestor. By identifying the closest relative of *Arabidopsis thaliana* that retains this 'basal' *TPL* gene we can approximate the time of gene loss. Further BLAST searches in the OneKP Transcriptome database identified predicted proteins homologous to OsASP1 in basal family of the order Brassicales (Moringaceae – *Moringa oleifera*, OneKP scaffold 2004901). OsASP1-like proteins were absent from representative taxa of derived families including Brassicaceae (*Arabidopsis thaliana* and *lyrata*, *Brassica rapa* and its sister family Cleomaceae (*Tarenaya hassleriana*), implying a loss during the evolution of the Brassicales.

A second clade encompasses all spermatophytes including *Arabidopsis* (Figure 5-16 – Spermatophytes A). Inclusion of *Picea abies* PaTPL1 as the basal member of this clade provides evidence that this clade arose through gene duplication occurring prior to the separation of angiosperms and gymnosperms. Internal nodes within this clade are less informative. Eudicot taxa possess both AtTPL/TPR1 and AtTPR4-like proteins. The basal positioning of monocot (OsASPR1) and basal angiosperm (AmTrTPL2) in these respective subclades give ambiguous information regarding which of the two (if either) is ancestral. Lastly, angiosperms have a unique clade that includes AtTPR2 and AtTPR3. The position of this clade adjacent to the algal TPL-like proteins may result from long branch attraction as the taxa included are distant relatives. A truncated homologue of *AtTPR2* was identified in *Amborella trichopoda* (evm_27.model.AmTr_v1.0_scaffold00003.110) during the database search. Exploration of the upstream peptide sequence supported homology to *TPL/TPR* proteins; however, numerous stop codons had been introduced into the coding regions of the amino terminus of the protein, disrupting the open reading frame. As the predicted protein model did not include LisH, CTLH or CRA domains, I chose to exclude this protein from the analysis as inclusion of a protein lacking conserved domains would render an unrepresentative tree. Regardless, the discovery of this (pseudo) gene

allows us to place the origin of *TPR2/3* at the base of the angiosperms or earlier.

5.4 Discussion

5.4.1 Complementation and redundancy

Screening of multiple *tpl/tpr* mutants identified both phenotypic and aphenotypic mutants. The mutant phenotypes observed are consistent with the classic *tpl-1* mutant and the ***tpl tpr1 tpr2^{RNAi} tpr3 tpr4*** mutant described by Long and colleagues (2006). The absence of conspicuous phenotypes in some mutant combinations supports a model in which most TPL/TPR functions are redundant; however, differences emerge between family members in some mutant combinations. Reproduction of the quadruple mutant phenotype with an alternative collection of alleles in a uniform (Col-0) background supports earlier findings that *TPR2* is sufficient to maintain *TPL/TPR* mediated repression. The ***TPL tpr1 tpr2^{+/-} tpr3 tpr4*** and ***tpl^{+/-} tpr1 tpr2 tpr3 TPR4*** mutants provide new insight into the relative importance of TPL/TPR family members. We cannot assume complete redundancy between orthologues as the phenotype of ***tpl tpr1 TPR2 tpr3 tpr4*** is less severe than these mutants. Their phenotypes are not due only to haploinsufficiency. *TPR2* is sufficient to maintain a superficially wild type phenotype whereas *TPL* and *TPR4* cannot do so in the respective mutants. Although we lack a *tpl tpr1 tpr2 TPR3 tpr4* mutant for comparison, we can hypothesise that a difference in expression, interaction range, regulation, turnover or other factor between the TPL/TPR1/TPR4 and TPR2/TPR3 subclades renders TPL/TPR1/TPR4 less capable in this context. The appearance of mild floral phenotypes in *tpl tpr1 tpr4* but not *tpr2 tpr3* implies that the dose of TPL/TPR protein available is more impactful than subtle interaction differences with respect to at least some aspects of development (i.e. floral patterning). It is noteworthy that Long et al. (2006) did not report phenotypes for mutants other than ***tpl tpr1 tpr3 tpr4***. If the quadruple mutant was the segregated progeny of a heterozygous parent, ***tpl tpr1 tpr2^{+/-} tpr3 tpr4^{+/-}***, non-viability of ***tpl tpr1 tpr2 tpr3*** might have been

observed. No such viable mutant has been reported. Unfortunately, we have no information regarding the order of assembly of the mutant and so we cannot make direct comparisons. Furthermore, ecotype-specific differences may have concealed or complemented aspects of the Col-0 background phenotype.

It is surprising that TPL is insufficient for complementation, given the broad interaction range of the TPL protein and substantial redundancy in its interactions with TPR2 (Causier et al., 2012; *Arabidopsis* Interactome Mapping Consortium, 2011). Based on the Y2H library screen performed by Causier et al. (2012a), TPR4 has a reduced range of transcription factor interactions compared to TPL and TPR2; however, there is no mechanistic basis for reduced interaction between TPL/TPR4 and transcription factor Repression Domains as all *Arabidopsis* TPL/TPRs retain a high degree of conservation within their N-terminal protein domains (LisH, CTLH and CRA) (Martin-Arevalillo et al., 2017). Furthermore, the appearance of severe ap2-like flowers in ***TPL tpr1 tpr2^{+/-} tpr3 tpr4*** at permissive temperatures (i.e. 20°C) would indicate that TPL is less competent than TPR4 to compensate for the absence of other TPR proteins. We must exercise caution due to the small sample sizes for these mutants. Additionally, these mutants reflect a single set of mutant alleles and have not been compared to other Col-0 *tpl/tpr* mutants. Further screening of the ***TPL tpr1 tpr2^{+/-} tpr3 tpr4*** and ***tpl^{+/-} tpr1 tpr2 tpr3 TPR4*** mutants is necessary to adequately distinguish differences between the two. Given the difficulty in obtaining statistically powerful sample sizes for each mutant, this may not be feasible. The skewed segregation ratios of the progeny of the mutants indicates not only that quadruple mutants are not viable, but that heterozygous mutants are also under-represented. Homozygosity for the segregating mutant alleles may be lethal for male or female spores or may interrupt sporogenesis. TPL/TPRs are known to be involved in the genetic regulation of sporogenesis. The transcription factor SPOROCTLESS/NOZZLE recruits TPL to regulate ovule development (Chen et al., 2014; Wei et al., 2015), while DAZ1 and DAZ2 interact with TOPLESS and are required for microsporogenesis (Borg et al., 2014). The occurrence of heterozygotes demonstrates that loss of all *TPL/TPR* genes except *TPL* or *TPR4* is not

inherently lethal in either microsporogenesis or megasporogenesis, or both. Furthermore, the absence of quadruple mutants retaining only TPL or TPR4 may reflect the decreased probability of a fertilisation event involving homozygous mutant gametes due to decreased gamete viability rather than embryonic lethality.

Arabidopsis TPL/TPRs contrast with those of *Solanum lycopersicum*. In *Arabidopsis*, TPR2 appears to be necessary and sufficient for survival and has an interaction range comparable to TPL; common interactors include AUX/IAAs, TCPs, MYBs and AP2-like transcription factors (Causier et al., 2012a). In *Solanum*, the TPR2 homologue SITPL6 has a reduced range of interactions with AUX/IAA transcription factors compared to other SITPLs. This deficiency may be compensated for by *SITPL2*, which has been lost in derived families in the Brassicales. SITPL2 has a broad interaction range (Hao et al., 2014) and may represent the ancestral orthologue of the family. Mutant phenotypes have not been described for *Sitpl* mutants, but the interaction data implies that *SITPLs* have been subfunctionalised. I propose that subfunctionalisation has also occurred within *Arabidopsis* TPL/TPRs. *TPL* and *TPR4* are insufficient to maintain viability alone, due either to differences in interaction or due altered expression patterns or levels (i.e. haploinsufficiency), with the caveat that we are observing a single allelic combination.

5.4.2 Developmental phenotypes

5.4.2.1 Floral development

The floral phenotypes of *tpl-1* and other *tpl/tpr* mutants have previously been related to the MADS-box transcription factor APETALA2 (Krogan et al., 2012). *tpl-1* and *ap2* produce flowers with defects in floral organ identity that increase in severity under heat stress, although homeotic conversion of sepals and petals to carpels is more penetrant in *ap2* (Krogan et al., 2012; Bowman et al., 1991). Although it was originally identified as an A-function gene, *APETALA2* antagonises the activity of floral C-function genes *AGAMOUS* (Krogan et al., 2012; Huang et al., 2017, 2) which is required to determine organ identity in the androecium and gynoecium (Irish, 2017).

TOPLESS interacts with AP2 and with proteins from the TARGET OF EAT and SQUAMOSA-BINDING PROTEIN-LIKE families that act as upstream regulators of AP2 (Jung et al., 2014). AP2 may also interact with another related co-repressor, LEUNIG,; mutations in *LEUNIG* enhance the *ap2* phenotype and *leunig* expresses mild *ap2*-like floral defects (Liu and Meyerowitz, 1995; Conner and Liu, 2000). The ectopic development of carpelloid tissue in *tpl-1*, *TPL tpr1 tpr2^{+/-} tpr3 tpr4* and *tpl^{+/-} tpr1 tpr2 tpr3 TPR4* is consistent with this model. The loss of stamens in *tpl tpr1 tpr4* can also be ascribed to loss of AP2-mediated repression (Bowman et al., 1991). The role of TOPLESS in floral development is not limited to its interactions with AP2, however, as TOPLESS interacts with a range of transcription factors involved in development, floral meristem maintenance and general patterning of lateral organs (Causier et al., 2012a). Given the breadth of TPL/TPR transcription factor interactions involving pleiotropic pathways such as auxin signalling, a high throughput approach such as RNA-seq transcriptomics would be necessary to map all primary, secondary and downstream changes in gene expression that cause *tpl/tpr* floral phenotypes.

5.4.2.2 Root architecture

Compromised primary root growth is consistent with TPL's role in meristem maintenance. Past publications have focused on TPL's role in antagonising root specification. *TOPLESS* derives its name from *tpl-1*'s rare double root phenotype, which Smith and Long (2010) identified as a consequence of *PLETHORA (PLT) 1* and *2* being misexpressed in the shoot apical meristem. The wild type TPL protein acts as a repressor of root identity in this context. However, TPL is also employed in regulating root development. Szemenyei et al. (2008) found that TPL-mediated repression of *ARF5* by IAA12/BODENLOS may be necessary for formation of the lens-shaped cell in the early embryo. This cell gives rise to the quiescent centre of the root apical meristem. Later in root development, TPL/TPRs are recruited by WUSCHEL-LIKE HOMEBOX 5 (*WOX5*) to repress *CYCLING DOF FACTOR 4 (CDF4)* in the quiescent centre and columellar stem cells at the root tip (Pi et al., 2015). This prevents cell differentiation and allows continued division to form new root tissue. The identification of the short root

phenotype in *tpl-1* and in the quadruple mutant *tpl tpr1 tpr3 tpr4* provides us with an additional system for studying the activity of TOPLESS and TOPLESS-RELATED proteins. Whereas the early developmental phenotype *tpl-1* is defined during embryonic development, elongation of the primary root is more dependent on post-embryonic events, giving us the opportunity to manipulate the process (e.g. by altering environmental conditions). Moreover, our ability to efficiently complement this phenotype in *tpl tpr1 tpr3 tpr4* paves the way for more consistent complementation studies than can be performed in the *tpl-1* mutant background.

Lateral root formation is an equally highly-regulated developmental process (Tian et al., 2014). Lateral roots (LRs) are initiated at the root endodermis, where founder cells divide and expand to form the LR primordium. This primordium must grow through the cortex and epidermis to emerge from the primary root. The lateral root may then elongate and can initiate secondary lateral roots. The multiple steps that occur during initiation and emergence are auxin-regulated, being associated with specific AUX/IAA-ARF modules and, as such, alleviation of TPL-mediated gene repression is a common theme throughout lateral root development and emergence (Stoeckle et al., 2018). At initiation, lateral root founder cell identity is promoted by GATA23 expression (De Rybel et al., 2010). GATA23 is positively regulated by ARFs 5, 6, 7, 8 and 19, which themselves are repressed by IAA28 (De Rybel et al., 2010). Further primordium development is promoted by ARF7 (antagonised by IAA3/SHY2) (De Rybel et al., 2010). Outgrowth and emergence of the primordium from the epidermis is governed by ARF7/19 and later by ARF5/MONOPTEROS, regulated by IAA14/SOLITARY ROOT (SLR) and IAA12/BODENLOS (BDL), respectively. The ARF7/19 – IAA14/SLR module also regulates mechanical rearrangement of the cortical and epidermal cells covering the primordium during its emergence (Stoeckle et al., 2018). Developmental progression depends upon auxin signalling, which promotes the degradation of AUX/IAAs. This relieves repression of target ARFs. Conversely, LR initiation is antagonised by cytokinin signalling (Rani Debi et al., 2005). Cytokinins enhance primary root and LR elongation (Rani Debi et al., 2005; Chang et al., 2013), while auxin has an inhibitory effect of LR elongation (Chang et al., 2013; Du and Scheres, 2018). Cytokinin obstructs

cell cycle progression in primordial founder cells and also affects auxin transport by disrupting PINHEAD (PIN) protein trafficking (Du and Scheres, 2018). Overexpression of cytokinin has been found to reduce lateral root numbers (Bielach et al., 2012). The TOPLESS family of co-repressors are known to interact with some of these AUX/IAAs. TPL mediates IAA12/BDL's repression of ARF5 (Szemenyei et al., 2008), while TPL and TPR2 have been shown to bind to IAA2/SHY2 and others in yeast-two hybrid experiments (Causier et al., 2012a). Additional yeast-two hybrid experiments in *Arabidopsis* (Ito et al., 2016) and tomato (Hao et al., 2014) indicate that TPL family proteins bind to IAA14/SLR. Szemenyei et al. (2008) demonstrated that AUX/IAAs recruit TPL to repress ARFs. Loss of *TPL* family genes could reduce the efficiency of ARF repression, accelerating lateral root development or increasing the number of lateral roots initiated.

5.4.3 Evolution of TPL/TPRs

TPL family proteins were present in the last common ancestor of chlorophycean algae and flowering plants and have been conserved since that time. TPL-like proteins had been identified in the early-diverging streptophytic alga *Klebsormidium nitens* (Martin-Arevalillo et al., 2017) but might have been considered absent from chlorophytes as no homologues are present in the model species *Chlamydomonas reinhardtii* and *Volvox carteri*. The discovery of a *TPL*-like gene in the chlorophyte *Picocystis salinarum* places the evolution of the TPL significantly earlier than previously thought and raises questions regarding its retention. All surveyed vascular plant taxa expressed at least one *TOPLESS*-like gene. Transcriptome data for streptophytic algae indicate that *TPL* is retained in some families representing major branches of the algal evolutionary tree (e.g. Chlorokybophyceae and Klebsormidiophyceae) (de Vries and Archibald, 2018). In contrast, I was unable to identify *TPL*-like transcripts in the most basal streptophyte family, Mesostigmatophyceae (de Vries and Archibald, 2018), nor in the majority of chlorophytes. At present, it is unclear why *TPL*-like genes are ubiquitous in one lineage but not the other.

An interesting question raised by the phylogeny in Figure 5-16 is how has *Arabidopsis* tolerated the loss of a conserved subclade of TPL/TPRs? ASP1-like proteins appear to be conserved across land plants with the exception of late-diverging families within the Brassicales. Tolerance of this loss is all the more surprising since in monocots the loss of the gene encoding this protein radically alters inflorescence architecture (Gallavotti et al., 2010; Yoshida et al., 2012). This class of TOPLESS-like protein is evolutionarily ancient; unpublished data indicate that, as the sole class of TOPLESS protein in basal land plants, it is essential for viability for the moss *Physcomitrella patens* (personal communication, Barry Causier, University of Leeds). The relative importance of TPL family members may have changed in the *Arabidopsis* lineage and we should be careful in applying it as a model for TOPLESS-mediated gene repression in other taxa. Evidence for a shift in the importance of TPL/TPRs comes from the asterid *Solanum lycopersicum* (Solanales). SITPL3, the only homologue of *Arabidopsis* TPR2 and 3, shows reduced interactivity with AUX/IAA transcription factors (Hao et al., 2014). This apparent loss of function is surprising as *Arabidopsis* TPR2 has a broad transcription factor interaction range (Causier et al., 2012a) and is sufficient to maintain a near-wild-type phenotype in *tpl tpr1 tpr3 tpr4* (Long et al., 2006). In spite of the general sequence and structural conservation of TOPLESS family proteins (Ke et al., 2015; Martin-Arevalillo et al., 2017), it may be necessary to evaluate the importance of individual proteins on a lineage-specific basis until we fully understand the mechanics of protein-protein interactions involving TOPLESS.

6 General Discussion

6.1 SUMO as a master regulator

Over the last decade, we have begun to recognise the important roles of small ubiquitin-like modifiers (SUMOs) in post-translational regulation. The question, “can your protein be SUMOylated?” has become inescapable (Xiao et al., 2015), and with good reason, as SUMOylation is an integral regulatory mechanism. SUMOylation in plants is closely associated with its role as a mediator of stress responses and the systemic changes that occur (Augustine and Vierstra, 2018). SUMO conjugation and deconjugation occur rapidly, making SUMOylation an effective system for responding to stimuli (Miller et al., 2010). However, SUMOs regulate proteins involved in a broad range of processes (Rytz et al., 2018; Huang et al., 2009). SUMOylation can regulate protein characteristics and function in multiple ways, from stabilising protein-protein interactions via SUMO-interacting motifs (SIMs) (Song et al., 2004; Hecker et al., 2006) to promoting degradation via SUMO-targeted ubiquitin ligases (Sriramachandran and Dohmen, 2014). It has also become more difficult to predict whether or not our protein of interest is SUMOylated, as we shift from the simple model of a binding site with a single consensus sequence (Ψ KxE) (Rodriguez et al., 2001) to view that includes diverse, non-canonical motifs and the influence of cross-talk from other post-translational modifications (Hietakangas et al., 2006). Improvements in mass spectrometry and other tools are rapidly expanding the boundaries of the SUMOylome. As a result, SUMOs have been recognised as regulators of regulators (Miller et al., 2010). The enrichment of chromatin regulators in the profile of proteins SUMOylated under abiotic stress conditions strongly indicates that SUMOylation promotes changes in transcriptional regulation (Mazur and van den Burg, 2012; Elrouby et al., 2013; Rytz et al., 2018); however, as the effects of SUMOylation differ between proteins, the consequences of this ‘wave of SUMOylation’ are not completely clear. Stress and other events to which responses are regulated at the level of transcription require appropriate changes in gene expression: up-regulation,

down-regulation or homeostasis. SUMOylation may drive assembly of a complex that promotes gene activation or gene repression (Mazur and van den Burg, 2012), but it could equally induce turnover of regulatory complexes (Sriramachandran and Dohmen, 2014), allowing others to displace them. Examples exist of SUMOylation simultaneously enhancing the activity of a protein while marking it for degradation, an elegant example of self-regulation. The importance of SUMOylation in transcriptional regulation is made more apparent by data that suggest that turnover of chromatin-regulating complexes is a routine part of maintaining stable levels of transcription, as SUMOs are a flexible, inducible mechanism for altering substrate activity and interactions (Boycheva et al., 2014); Henikoff and Smith, 2015.

6.2 SUMOylation as a positive regulator of TOPLESS-mediated repression

SUMOs have many roles in regulating other proteins, but specific examples show that SUMOylation can positively regulate transcriptional co-repressors. The key discovery that SUMO-SIM interaction facilitates interaction between a co-repressor, Groucho, and the Class I histone deacetylase HDAC1 (Ahn et al., 2009) allows us to draw comparisons with an equivalent relationship in plants between the co-repressor TOPLESS and histone deacetylase HDA19. Efforts to show a direct interaction between these proteins through yeast hybrid assays have had minimal success (Cheng et al., 2018), yet complementation studies using *tpl* and *hda19* mutants support a functional relationship between the two (Long et al., 2006). Both proteins are SUMO substrates (Miller et al., 2010). Could SUMO bridge the gap between TPL and HDA19? The weak interaction observed between the TPL-SUMO fusion and HDA19 is our first indication that this is the case. Heterologous systems are practical tool but they cannot always replicate conditions (e.g. post-translational modifications) that are occurring under native conditions. The failure to detect interaction between TPL, a known SUMO substrate (Miller et al., 2010; Rytz et al., 2018) and SCE1, an essential component of the SUMOylation pathway (Saracco et al., 2007), emphasises that genuine

interactions cannot always be replicated *ex planta*. Although crude, the TPL-SUMO/HDA19 assay demonstrated that the presence of SUMO increases the potential to recruit HDA19. Subsequent experiments in the *siz1-2* and *ots1 ots2* also indicate that SUMO is a positive regulator of TOPLESS activity, possibly through recruitment of HDA19. Improvement in the *tpl-1* phenotype in *ots1 ots2*, where we would anticipate decreased turnover of SUMOs, indicates that SUMOylation enhances the function of TOPLESS and TOPLESS-RELATED proteins. Likewise, diminished SUMOylation due to loss of SUMO ligase activity enhances the *tpl-1* phenotype, suggesting that further loss of function is occurring. These results do not show that SUMOylation alters TPL/TPR activity directly as systemic changes in SUMOylation affect many SUMO substrates, including those with functions agonistic and antagonistic to TOPLESS. Consistency between results, however, point to towards SUMOylation as a positive regulator of TOPLESS-mediated repression. To obtain more direct evidence via complementation studies, it was necessary to identify SUMOylation sites within TOPLESS. The absence of canonical SUMOylation sites in TPL necessitated a bioinformatics approach to predict candidate sites. Though recently published data indicates that TPL and TPR4 are SUMOylated at unpredicted, non-consensus motifs (Rytz et al., 2018), the identification of these sites does not invalidate my predictions. Numerous proteins exhibit SUMOylation at multiple sites (Rytz et al., 2018). SUMO attachment at one site is not mutually exclusive with SUMOylation of other distal sites, and multiple sites can act synergistically (Aguilar-Martinez et al., 2015). Moreover, the SUMOylation sites identified by Rytz et al. are unusual as they are not conserved across TOPLESS-like proteins. This is difficult to reconcile with the high level of conservation within these proteins (Ke et al., 2015; Martin-Arevalillo et al., 2017), as well as with their conserved roles in transcriptional regulation (Causier et al., 2012b; Martin-Arevalillo et al., 2017), which might lead us to expect similar conservation of their mechanism of regulation. It is possible that SUMOylation is occurring opportunistically at exposed lysine residues, that this region of TOPLESS-like proteins is specifically targeted for SUMOylation, or that SUMOylation at this site is a novel development. Future experiments could explore the

relevance of these sites, for example, through complementation assays similar to those described in this thesis. SUMOylation may yet emerge as a mechanism by which TOPLESS family proteins can be differentially regulated despite their high level of sequence conservation. For example, TPR2 lacks K689 residue found to be SUMOylated by Rytz et al. (2018).

For those candidate sites examined here, the discovery of a site (K282) that is evolutionarily conserved, influences complementation efficiency and is adjacent to a known phosphorylation site (phosphorylation acts antagonistically toward SUMOylation in some plant proteins (Tomanov et al., 2018b)) is promising. An additional site found only in *Arabidopsis* TPL and TPR1, K339, has similar influence on complementation efficiency. Although we can differentiate between candidate sites based on protein function, arbitrary changes to a protein might negatively affect protein function. Fortunately, Western blotting of TOPLESS proteins with mutations at the K282 and K339 provide some clarity. The disappearance of a high-molecular-weight band suggests that K282 is a valid site for post-translational modification, and that modification (i.e. SUMOylation) cannot occur without the acceptor lysine. While this conclusion is weakened by the by the absence of a wild type TPL control, comparable published experiments indicate that wild type TOPLESS is present in multiple high-molecular-weight forms (Krogan et al., 2012). Ideally, future experiments will confirm the identity of these bands and reveal all SUMOylation sites within TOPLESS. Recent improvements in protocols for isolating SUMOylated proteins (Bailey et al., 2016) will be beneficial for the Western blotting approach used in this thesis. The 'SUMO enigma' (Hay, 2005), the low abundance of SUMOylated molecules for a given protein species continues to provide a challenge but improvements in laboratory technique may help us to overcome it. However, a modified strategy must be used if we wish to verify SUMOylation by mass spectrometry. It is not possible to recover peptides inclusive of K282 by mass spectrometry using the approach of Rytz et al. (2018). Due to the rarity of protease cleavage sites around K282, the typical approach to prepare peptides for analysis by mass spectrometry (trypsin digestion) generates extremely large (>50 residue) and small (<5 residue) peptides that cannot be recovered. Thus, a modified approach will

be needed to directly verify that SUMOylation occurs at K282. Alternatively, an *in vitro* SUMOylation approach using truncated or mutated TPL protein could also be taken to identify SUMOylated domains or residues within the protein. Looking more broadly at TOPLESS, we have benefitted from the recent publications of structures for the N-terminus (residues 1- 202) of *Oryza sativa* TPR2 and *Arabidopsis thaliana* TOPLESS (Ke et al., 2015; Martin-Arevalillo et al., 2017) but we lack any model for the central region of the protein where I predicted that SUMOylation occurs (K282). By comparison, the SUMOylated lysine identified by Rytz et al. (2018) is located on an exposed loop extending from the face of one of TPL's two C-terminal β -propeller structures, suggesting that the SUMOylated site could be exposed and available for protein-protein interactions. Additional structural information may be informative for studying SUMOylation, as it is likely that otherwise viable candidate site will be occluded by the tertiary structure of the protein.

We now know that SUMOylation is an enhancer of TOPLESS function, but to understand how this mechanism works, we need to define how SUMOylated TPL/TPR proteins interact with other components of the transcriptional regulatory machinery. Previously established interactions with MSI4/FVE and PICKLE-RELATED1 have placed TOPLESS in the context of NuRD of Sin3-like complexes (Causier et al., 2012a; Mazur and van den Burg, 2012; Clavel et al., 2015; Zheng et al., 2017). The strategy of identifying co-precipitating proteins by mass spectrometry has left this question open, but it has provided new information. TOPLESS-RELATED proteins can interact with one another in yeast two-hybrid assays (Causier et al., 2012a). Also, truncated TOPLESS proteins (residues 1-202) show the capacity to dimerise and tetramerise *in vitro* and can bind transcription factors in this state (Ke et al., 2015; Martin-Arevalillo et al., 2017). Consequently, the co-precipitation of TPL and TPRs supports the hypothesis that TPL and TPR proteins physically interact and have the potential to form functional tetramers. This hypothesis is supported by the phenotype of *tpl-1*; *tpl-1* is believed to promote aggregation of TPL tetramers, and interaction between TPL-1 and TPRs would explain TPL-1's semi-dominant mode of action (Ma et al., 2017). The possibility of heteromeric interactions is

important because interaction studies for *Arabidopsis thaliana* and *Solanum lycopersicum* TPL/TPRs indicate minor differences between proteins in the capacity to bind different transcription factors. Examination of multiple mutant combinations described in this thesis has suggested that there are functional differences between TPL, TPR2 and TPR4 with regard to maintaining viability. Different combinations or stoichiometric ratios of TPL/TPR proteins may differ in their interaction range or efficacy, providing an additional layer of regulation. On the other hand, the absence of abnormal phenotypes in most *tpl/tpr* mutants is indicative of redundancy. More information is required to determine whether or not all TPL/TPR proteins can interact with one another. Available data supports interaction between TPL, TPR and TPR4 (Causier et al., 2012a). Further work could explore this question with further co-immunoprecipitation experiments, or by attempting to complement *tpl tpr1 tpr3 tpr4* or other multiple mutant combinations using different *TPL/TPR* genes, restricting the range of possible heteromer combination that can be formed.

The co-precipitation of the chromatin regulators SPLAYED and BRAHMA with TOPLESS opens a new avenue of enquiry for our work on TOPLESS-mediated repression. SPLAYED and BRAHMA are SWI/SNF chromatin remodelling ATPases involved in transcriptional regulation (Wu et al., 2012; Wagner and Meyerowitz, 2002). Coincidentally, SPLAYED, BRAHMA and TOPLESS have been implicated in regulating several of the same biological pathways, including jasmonic acid and ethylene signalling (Walley et al., 2008), cotyledon development (Kwon et al., 2006), floral patterning (Wu et al., 2012) and maintenance of root (Yang et al., 2015) and shoot meristems (Kwon et al., 2006). However, in several of these pathways TOPLESS and SPLAYED/BRAHMA acts antagonistically, most notably in flowering where TOPLESS and APETALA2 repress the MADS-box transcription factor SEPALLATA3, while SEPALLATA 3 is involved in recruiting SPLAYED to activate expression of target genes AGAMOUS and APETALA3 (Wu et al., 2012). It is therefore unclear if SPLAYED and BRAHMA are co-precipitated due to genuine interaction or as a consequence of cross-linking between co-localising proteins. Co-immunoprecipitations using the wheat (*Triticum aestivum*) homologue of MSI4/FVE, TaFVE, recovered both SPLAYED and

TOPLESS (Zheng et al., 2017). However, MSI4/FVE (or rather, its animal homologues RBBP4 and 7) is a shared component of distinct regulatory complexes. Thus, co-precipitating proteins may derive from separate regulatory complexes. Additionally, yeast two hybrid library screens did not identify SPLAYED or BRAHMA as a TPL/TPR interactor (Causier et al., 2012a), though these assays are not exhaustive. Tests for direct interaction may answer this question. Alternatives include yeast three-hybrid assays between TOPLESS, SPLAYED or BRAHMA and potential bridging proteins such as MSI4/FVE, or performing reciprocal co-immunoprecipitations using SPLAYED and BRAHMA as bait to recover TPL/TPR proteins.

In the pursuit of new tools with which to study TPL SUMOylation, several useful discoveries have been made. Complementation studies have been handicapped by the stochastically variable and temperature sensitive phenotype of *tpl-1*, and the quadruple mutant assembled by Long et al. was not available for use (Long et al., 2006; Krogan et al., 2012). Development of a new allelic version of the quadruple ***tpl tpr1 tpr3 tpr4*** has allowed us to verify previously reported phenotypes but, more importantly, has allowed us to conduct analyses with other *TOPLESS* family mutants within a uniform ecotypic background (Col). Phenotyping of ***tpl tpr1 tpr3 tpr4***, the clade-specific mutants *tpl tpr1 tpr4* and *tpr2 tpr3* and additional mutant combinations has shed light on the relative importance of TOPLESS-like proteins. The phenotypes of *tpl tpr1 tpr4* and *tpr2 tpr3* mutants reflect substantial redundancy across the family, to the extent that an entire subclade can be lost with little impact on phenotype. On the other hand, further reduction in the number of wild type *TPL/TPR* genes can induce severe phenotypes not seen in ***tpl tpr1 tpr3 tpr4***. This implies incomplete redundancy, a factor not fully explained by our current knowledge of the structure, function and interactions (Ke et al., 2015; Martin-Arevalillo et al., 2017; Causier et al., 2012a) of family members. Furthermore, the mutant phenotypes reported in this thesis highlight unusual characteristics of the *tpl-1* mutant compared to more conventional mutants. For example, the floral phenotype of *tpl-1* is enhanced by elevated temperatures but the floral phenotype of *tpl tpr1 tpr4* is not. Also, while we can rescue aspects of the *tpl-1* root phenotype by supplementing the growth medium with sucrose, ***tpl***

tpr1 tpr3 tpr4 is seemingly unresponsive. Furthermore, though we lack some mutant combinations (e.g. *tpl tpr1 tpr2 TPR3 tpr4*), no mutant except *tpl tpr1 tpr2^{RNAI} tpr3 tpr4* has as severe an embryonic phenotype as *tpl-1* (Krogan et al., 2012). We have benefitted extensively from *tpl-1*. Data from the moss *Physcomitrella patens* indicates that loss of all *TOPLESS* genes is lethal to plants (Barry Causier, University of Leeds, personal communication) and *tpl-1* may be our only window into some aspects of development. In future we will need to disambiguate the effects of losing TPL/TPR-mediated repression and the effects of the mutant TPL-1 protein. We now have new tools to assist in this process. Further work should also be done to assemble mutant combinations not described. This will allow us to test for neofunctionalisation and/or subfunctionalisation of different family members, and to establish the minimal 'TPL system' required for viability. Differences in conservation between the *TOPLESS* family members in *Arabidopsis* and other branches of plant evolutionary tree suggest that functional differences may also have arisen. Though other authors have shown some redundancy between TPL-family genes cross-species (Gallavotti et al., 2010), with *tpl tpr1 tpr3 tpr4* (Col) we can thoroughly test complementation efficiency.

6.3 Conclusions

TOPLESS and *TOPLESS-RELATED* co-repressors are a unique and interesting group of proteins. Specific to plants (Causier et al., 2012b) but with parallels to co-repressors found across eukaryotes (Liu and Karmarkar, 2008), they have become involved in regulating almost every aspect of plant development (Zhu et al., 2010; Long et al., 2002, 2006; Gallavotti et al., 2010; Yoshida et al., 2012; Krogan et al., 2012; Causier et al., 2012a; Wang et al., 2013; Borg et al., 2014; Chen et al., 2014). The regulator must itself be regulated, and understanding how this occurs is insightful to these developmental processes. Small ubiquitin-like modifiers have shown themselves to be potent regulators of the transcriptional machinery in plants (Miller et al., 2010; Mazur and van den Burg, 2012; Augustine and Vierstra, 2018) and across the eukaryotes (Ouyang and Gill, 2009; Wotton et al.,

2017). This thesis gives us new information to support the hypothesis that SUMOylation is important for regulating the function of TOPLESS.

List of References

Abed, M., Barry, K.C., Kenyagin, D., Koltun, B., Phippen, T.M., Delrow, J.J., Parkhurst, S.M., and Orian, A. (2011). Degringolade, a SUMO-targeted ubiquitin ligase, inhibits Hairy/Groucho-mediated repression. *EMBO J.* **30**: 1289–1301.

Abgent (2018). SUMOplot analysis program.

<http://www.abgent.com/SUMOplot>

Aguilar-Martinez, E., Chen, X., Webber, A., Mould, A.P., Seifert, A., Hay, R.T., and Sharrocks, A.D. (2015). Screen for multi-SUMO-binding proteins reveals a multi-SIM-binding mechanism for recruitment of the transcriptional regulator ZMYM2 to chromatin. *Proceedings of the National Academy of Sciences* **112**: E4854–E4863.

Ahn, J.-W., Lee, Y.-A., Ahn, J.-H., and Choi, C.Y. (2009). Covalent conjugation of Groucho with SUMO-1 modulates its corepressor activity. *Biochem. Biophys. Res. Commun.* **379**: 160–165.

Alinsug, M.V., Yu, C.-W., and Wu, K. (2009). Phylogenetic analysis, subcellular localization, and expression patterns of RPD3/HDA1 family histone deacetylases in plants. *BMC Plant Biology* **9**: 37.

Alland, L., David, G., Shen-Li, H., Potes, J., Muhle, R., Lee, H.-C., Hou, H., Chen, K., and DePinho, R.A. (2002). Identification of mammalian Sds3 as an integral component of the Sin3/histone deacetylase corepressor complex. *Mol. Cell. Biol.* **22**: 2743–2750.

Altschul, S.F., Gish, W., Miller, W., Myers, E.W., and Lipman, D.J. (1990). Basic local alignment search tool. *J. Mol. Biol.* **215**: 403–410.

***Arabidopsis* Interactome Mapping Consortium** (2011). Evidence for network evolution in an *Arabidopsis* interactome map. *Science* **333**: 601–607.

Aronson, B.D., Fisher, A.L., Blechman, K., Caudy, M., and Gergen, J.P. (1997). Groucho-dependent and -independent repression activities of Runt domain proteins. *Mol. Cell. Biol.* **17**: 5581–5587.

Augustine, R.C. and Vierstra, R.D. (2018). SUMOylation: re-wiring the plant nucleus during stress and development. *Current Opinion in Plant Biology* **45**: 143–154.

Bailey, M., Srivastava, A., Conti, L., Nelis, S., Zhang, C., Florance, H., Love, A., Milner, J., Napier, R., Grant, M., and Sadanandom, A. (2016). Stability of small ubiquitin-like modifier (SUMO) proteases OVERLY TOLERANT TO SALT1 and -2 modulates salicylic acid signalling and

SUMO1/2 conjugation in *Arabidopsis thaliana*. *Journal of Experimental Botany* **67**: 353–363.

Baymaz, H.I., Karemaker, I.D., and Vermeulen, M. (2015). Perspective on unraveling the versatility of “co-repressor” complexes. *Biochim. Biophys. Acta* **1849**: 1051–1056.

Benlloch, R. and Lois, L.M. (2018). SUMOylation in plants: mechanistic insights and its role in drought stress. *Journal of Experimental Botany*.

Bensmihen, S., To, A., Lambert, G., Kroj, T., Giraudat, J., and Parcy, F. (2004). Analysis of an activated ABI5 allele using a new selection method for transgenic *Arabidopsis* seeds. *FEBS Lett.* **561**: 127–131.

Benson, D.A. (2004). GenBank. *Nucleic Acids Research* **33**: D34–D38.

Bent, A. (2006). *Arabidopsis thaliana* floral dip transformation method. *Methods Mol. Biol.* **343**: 87–103.

Bezhani, S., Winter, C., Hershman, S., Wagner, J.D., Kennedy, J.F., Kwon, C.S., Pfluger, J., Su, Y., and Wagner, D. (2007). Unique, shared, and redundant roles for the *Arabidopsis* SWI/SNF chromatin remodeling ATPases BRAHMA and SPLAYED. *Plant Cell* **19**: 403–416.

Bielach, A., Podlesáková, K., Marhavy, P., Duclercq, J., Cuesta, C., Müller, B., Grunewald, W., Tarkowski, P., and Benková, E. (2012). Spatiotemporal regulation of lateral root organogenesis in *Arabidopsis* by cytokinin. *Plant Cell* **24**: 3967–3981.

Bies, J., Markus, J., and Wolff, L. (2002). Covalent attachment of the SUMO-1 protein to the negative regulatory domain of the c-Myb transcription factor modifies its stability and transactivation capacity. *J. Biol. Chem.* **277**: 8999–9009.

Borg, M., Rutley, N., Kagale, S., Hamamura, Y., Gherghinoiu, M., Kumar, S., Sari, U., Esparza-Franco, M.A., Sakamoto, W., Rozwadowski, K., Higashiyama, T., and Twell, D. (2014). An EAR-Dependent Regulatory Module Promotes Male Germ Cell Division and Sperm Fertility in *Arabidopsis*. *Plant Cell* **26**: 2098–2113.

Bowen, A.J., Gonzalez, D., Mullins, J.G.L., Bhatt, A.M., Martinez, A., and Conlan, R.S. (2010). PAH-domain-specific interactions of the *Arabidopsis* transcription coregulator SIN3-LIKE1 (SNL1) with telomere-binding protein 1 and ALWAYS EARLY2 Myb-DNA binding factors. *J. Mol. Biol.* **395**: 937–949.

Bowman, G.D. and Poirier, M.G. (2015). Post-translational modifications of histones that influence nucleosome dynamics. *Chem. Rev.* **115**: 2274–2295.

Bowman, J.L., Smyth, D.R., and Meyerowitz, E.M. (1991). Genetic interactions among floral homeotic genes of *Arabidopsis*. *Development* **112**: 1–20.

- Boycheva, I., Vassileva, V., and Iantcheva, A.** (2014). Histone acetyltransferases in plant development and plasticity. *Curr. Genomics* **15**: 28–37.
- Bradner, J.E., West, N., Grachan, M.L., Greenberg, E.F., Haggarty, S.J., Warnow, T., and Mazitschek, R.** (2010). Chemical phylogenetics of histone deacetylases. *Nat. Chem. Biol.* **6**: 238–243.
- Brandstatter, I.** (1998). Two Genes with Similarity to Bacterial Response Regulators Are Rapidly and Specifically Induced by Cytokinin in *Arabidopsis*. *THE PLANT CELL ONLINE* **10**: 1009–1020.
- van den Burg, H.A., Kini, R.K., Schuurink, R.C., and Takken, F.L.W.** (2010). *Arabidopsis* Small Ubiquitin-Like Modifier Paralogs Have Distinct Functions in Development and Defense. *The Plant Cell* **22**: 1998–2016.
- Cai, B., Kong, X., Zhong, C., Sun, S., Zhou, X.F., Jin, Y.H., Wang, Y., Li, X., Zhu, Z., and Jin, J.B.** (2017). SUMO E3 Ligases GmSIZ1a and GmSIZ1b regulate vegetative growth in soybean: Functional characterization of soybean SUMO E3 ligase. *Journal of Integrative Plant Biology* **59**: 2–14.
- Cappadocia, L. and Lima, C.D.** (2018). Ubiquitin-like Protein Conjugation: Structures, Chemistry, and Mechanism. *Chem. Rev.* **118**: 889–918.
- Castañó-Miquel, L., Seguí, J., Manrique, S., Teixeira, I., Carretero-Paulet, L., Atencio, F., and Lois, L.M.** (2013). Diversification of SUMO-Activating Enzyme in *Arabidopsis*: Implications in SUMO Conjugation. *Molecular Plant* **6**: 1646–1660.
- de Castro, I.J., Amin, H.A., Vinciotti, V., and Vagnarelli, P.** (2017). Network of phosphatases and HDAC complexes at repressed chromatin. *Cell Cycle* **16**: 2011–2017.
- Castro, P.H., Bachmair, A., Bejarano, E.R., Coupland, G., Lois, L.M., Sadanandom, A., van den Burg, H.A., Vierstra, R.D., and Azevedo, H.** (2018). Revised nomenclature and functional overview of the ULP gene family of plant deSUMOylating proteases. *Journal of Experimental Botany*.
- Castro, P.H., Couto, D., Freitas, S., Verde, N., Macho, A.P., Huguet, S., Botella, M.A., Ruiz-Albert, J., Tavares, R.M., Bejarano, E.R., and Azevedo, H.** (2016). SUMO proteases ULP1c and ULP1d are required for development and osmotic stress responses in *Arabidopsis thaliana*. *Plant Molecular Biology* **92**: 143–159.
- Catala, R., Ouyang, J., Abreu, I.A., Hu, Y., Seo, H., Zhang, X., and Chua, N.-H.** (2007). The *Arabidopsis* E3 SUMO Ligase SIZ1 Regulates Plant Growth and Drought Responses. *THE PLANT CELL ONLINE* **19**: 2952–2966.
- Causier, B., Ashworth, M., Guo, W., and Davies, B.** (2012a). The TOPLESS interactome: a framework for gene repression in *Arabidopsis*. *Plant Physiol.* **158**: 423–438.

- Causier, B. and Davies, B.** (2002). Analysing protein-protein interactions with the yeast two-hybrid system. *Plant Mol. Biol.* **50**: 855–870.
- Causier, B., Lloyd, J., Stevens, L., and Davies, B.** (2012b). TOPLESS co-repressor interactions and their evolutionary conservation in plants. *Plant Signal Behav* **7**: 325–328.
- Chang, L., Ramireddy, E., and Schmölling, T.** (2013). Lateral root formation and growth of *Arabidopsis* is redundantly regulated by cytokinin metabolism and signalling genes. *J. Exp. Bot.* **64**: 5021–5032.
- Chen, C. et al.** (2017). Cytosolic acetyl-CoA promotes histone acetylation predominantly at H3K27 in *Arabidopsis*. *Nat Plants* **3**: 814–824.
- Chen, G.-H., Sun, J.-Y., Liu, M., Liu, J., and Yang, W.-C.** (2014). SPOROCTELESS is a novel embryophyte-specific transcription repressor that interacts with TPL and TCP proteins in *Arabidopsis*. *J Genet Genomics* **41**: 617–625.
- Chen, X., Lu, L., Mayer, K.S., Scaff, M., Qian, S., Lomax, A., Smith, L.M., and Zhong, X.** (2016). POWERDRESS interacts with HISTONE DEACETYLASE 9 to promote aging in *Arabidopsis*. *eLife* **5**.
- Cheng, X., Zhang, S., Tao, W., Zhang, X., Liu, J., Sun, J., Zhang, H., Pu, L., Huang, R., and Chen, T.** (2018). INDETERMINATE SPIKELET 1 recruits histone deacetylase and a transcriptional repression complex to regulate rice salt tolerance. *Plant Physiology*: pp.00324.2018.
- Clapier, C.R. and Cairns, B.R.** (2009). The Biology of Chromatin Remodeling Complexes. *Annual Review of Biochemistry* **78**: 273–304.
- Clark, M.D., Marcum, R., Graveline, R., Chan, C.W., Xie, T., Chen, Z., Ding, Y., Zhang, Y., Mondragón, A., David, G., and Radhakrishnan, I.** (2015). Structural insights into the assembly of the histone deacetylase-associated Sin3L/Rpd3L corepressor complex. *Proc. Natl. Acad. Sci. U.S.A.* **112**: E3669-3678.
- Clavel, M., Pélissier, T., Descombin, J., Jean, V., Picart, C., Charbonel, C., Saez-Vásquez, J., Bousquet-Antonelli, C., and Deragon, J.-M.** (2015). Parallel action of AtDRB2 and RdDM in the control of transposable element expression. *BMC Plant Biol.* **15**: 70.
- Cock, P.J.A., Antao, T., Chang, J.T., Chapman, B.A., Cox, C.J., Dalke, A., Friedberg, I., Hamelryck, T., Kauff, F., Wilczynski, B., and de Hoon, M.J.L.** (2009). Biopython: freely available Python tools for computational molecular biology and bioinformatics. *Bioinformatics* **25**: 1422–1423.
- Colignon, B., Delaive, E., Dieu, M., Demazy, C., Muhovski, Y., Wallon, C., Raes, M., and Mauro, S.** (2017a). Proteomics analysis of the endogenous, constitutive, leaf SUMOylome. *Journal of Proteomics* **150**: 268–280.

Colignon, B., Dieu, M., Demazy, C., Delaive, E., Muhovski, Y., Raes, M., and Mauro, S. (2017b). Proteomic Study of SUMOylation During *Solanum tuberosum*-*Phytophthora infestans* Interactions. *Mol. Plant Microbe Interact.* **30**: 855–865.

Collins, J., Dufresne, C., Gurley, W.B., and Chen, S. (2018). Proteomics dataset containing proteins that obscure identification of TOPLESS interactors in *Arabidopsis*. *Data in Brief* **20**: 909–916.

Cong, L., Pakala, S.B., Ohshiro, K., Li, D.-Q., and Kumar, R. (2011). SUMOylation and SUMO-interacting motif (SIM) of metastasis tumor antigen 1 (MTA1) synergistically regulate its transcriptional repressor function. *J. Biol. Chem.* **286**: 43793–43808.

Conner, J. and Liu, Z. (2000). LEUNIG, a putative transcriptional corepressor that regulates AGAMOUS expression during flower development. *Proc. Natl. Acad. Sci. U.S.A.* **97**: 12902–12907.

Conti, L., Kioumourtzoglou, D., O'Donnell, E., Dominy, P., and Sadanandom, A. (2009). OTS1 and OTS2 SUMO proteases link plant development and survival under salt stress. *Plant Signal Behav* **4**: 225–227.

Conti, L., Price, G., O'Donnell, E., Schwessinger, B., Dominy, P., and Sadanandom, A. (2008). Small ubiquitin-like modifier proteases OVERLY TOLERANT TO SALT1 and -2 regulate salt stress responses in *Arabidopsis*. *Plant Cell* **20**: 2894–2908.

Copley, R.R. (2016). The Unicellular Ancestry of Groucho-Mediated Repression and the Origins of Metazoan Transcription Factors. *Genome Biol Evol* **8**: 1859–1867.

Cuéllar Pérez, A., Nagels Durand, A., Vanden Bossche, R., De Clercq, R., Persiau, G., Van Wees, S.C.M., Pieterse, C.M.J., Gevaert, K., De Jaeger, G., Goossens, A., and Pauwels, L. (2014). The Non-JAZ TIFY Protein TIFY8 from *Arabidopsis thaliana* Is a Transcriptional Repressor. *PLoS ONE* **9**: e84891.

D'Agostino, I.B., Deruère, J., and Kieber, J.J. (2000). Characterization of the Response of the *Arabidopsis* Response Regulator Gene Family to Cytokinin. *Plant Physiology* **124**: 1706–1717.

David, G., Neptune, M.A., and DePinho, R.A. (2002). SUMO-1 modification of histone deacetylase 1 (HDAC1) modulates its biological activities. *J. Biol. Chem.* **277**: 23658–23663.

Davis, M. W. (2018). A plasmid editor.
<http://jorgensen.biology.utah.edu/wayned/ape/>

De Rybel, B. et al. (2010). A novel aux/IAA28 signaling cascade activates GATA23-dependent specification of lateral root founder cell identity. *Curr. Biol.* **20**: 1697–1706.

- Dhalluin, C., Carlson, J.E., Zeng, L., He, C., Aggarwal, A.K., and Zhou, M.M.** (1999). Structure and ligand of a histone acetyltransferase bromodomain. *Nature* **399**: 491–496.
- Du, Y. and Scheres, B.** (2018). Lateral root formation and the multiple roles of auxin. *J. Exp. Bot.* **69**: 155–167.
- Elrouby, N.** (2015). Analysis of Small Ubiquitin-Like Modifier (SUMO) Targets Reflects the Essential Nature of Protein SUMOylation and Provides Insight to Elucidate the Role of SUMO in Plant Development. *Plant Physiol.* **169**: 1006–1017.
- Elrouby, N., Bonequi, M.V., Porri, A., and Coupland, G.** (2013). Identification of *Arabidopsis* SUMO-interacting proteins that regulate chromatin activity and developmental transitions. *Proceedings of the National Academy of Sciences* **110**: 19956–19961.
- Engelhorn, J., Blanvillain, R., and Carles, C.C.** (2014). Gene activation and cell fate control in plants: a chromatin perspective. *Cell. Mol. Life Sci.* **71**: 3119–3137.
- Espinosa-Ruiz, A., Martínez, C., de Lucas, M., Fàbregas, N., Bosch, N., Caño-Delgado, A.I., and Prat, S.** (2017). TOPLESS mediates brassinosteroid control of shoot boundaries and root meristem development in *Arabidopsis thaliana*. *Development* **144**: 1619–1628.
- Fisher, A.L., Ohsako, S., and Caudy, M.** (1996). The WRPW motif of the hairy-related basic helix-loop-helix repressor proteins acts as a 4-amino-acid transcription repression and protein-protein interaction domain. *Mol. Cell. Biol.* **16**: 2670–2677.
- Flores-Sandoval, E., Eklund, D.M., and Bowman, J.L.** (2015). A Simple Auxin Transcriptional Response System Regulates Multiple Morphogenetic Processes in the Liverwort *Marchantia polymorpha*. *PLOS Genetics* **11**: e1005207.
- Foresti, O., daSilva, L.L.P., and Denecke, J.** (2006). Overexpression of the *Arabidopsis* syntaxin PEP12/SYP21 inhibits transport from the prevacuolar compartment to the lytic vacuole in vivo. *Plant Cell* **18**: 2275–2293.
- Francis, K.E. and Spiker, S.** (2005). Identification of *Arabidopsis thaliana* transformants without selection reveals a high occurrence of silenced T-DNA integrations. *Plant J.* **41**: 464–477.
- Friso, G. and van Wijk, K.J.** (2015). Posttranslational Protein Modifications in Plant Metabolism. *Plant Physiol.* **169**: 1469–1487.
- Fukaki, H., Taniguchi, N., and Tasaka, M.** (2006). PICKLE is required for SOLITARY-ROOT/IAA14-mediated repression of ARF7 and ARF19 activity during *Arabidopsis* lateral root initiation. *Plant J.* **48**: 380–389.

Fukazawa, J., Ito, T., Kamiya, Y., Yamaguchi, S., and Takahashi, Y. (2015). Binding of GID1 to DELLAs promotes dissociation of GAF1 from DELLA in GA dependent manner. *Plant Signal Behav* **10**: e1052923.

Fukazawa, J., Teramura, H., Murakoshi, S., Nasuno, K., Nishida, N., Ito, T., Yoshida, M., Kamiya, Y., Yamaguchi, S., and Takahashi, Y. (2014). DELLAs function as coactivators of GAI-ASSOCIATED FACTOR1 in regulation of gibberellin homeostasis and signaling in *Arabidopsis*. *Plant Cell* **26**: 2920–2938.

Fuks, F., Hurd, P.J., Deplus, R., and Kouzarides, T. (2003). The DNA methyltransferases associate with HP1 and the SUV39H1 histone methyltransferase. *Nucleic Acids Res.* **31**: 2305–2312.

Füßl, M., Lassowskat, I., Née, G., Koskela, M.M., Brünje, A., Tilak, P., Giese, J., Leister, D., Mulo, P., Schwarzer, D., and Finkemeier, I. (2018). Beyond Histones: New Substrate Proteins of Lysine Deacetylases in *Arabidopsis* Nuclei. *Front Plant Sci* **9**: 461.

Gallavotti, A., Long, J.A., Stanfield, S., Yang, X., Jackson, D., Vollbrecht, E., and Schmidt, R.J. (2010). The control of axillary meristem fate in the maize ramosa pathway. *Development* **137**: 2849–2856.

Gallo, P. et al. (2008). Inhibition of class I histone deacetylase with an apicidin derivative prevents cardiac hypertrophy and failure. *Cardiovascular Research* **80**: 416–424.

Garcia-Dominguez, M. and Reyes, J.C. (2009). SUMO association with repressor complexes, emerging routes for transcriptional control. *Biochim. Biophys. Acta* **1789**: 451–459.

Gershlick, D.C., Lousa, C. de M., Foresti, O., Lee, A.J., Pereira, E.A., daSilva, L.L.P., Bottanelli, F., and Denecke, J. (2014). Golgi-Dependent Transport of Vacuolar Sorting Receptors Is Regulated by COPII, AP1, and AP4 Protein Complexes in Tobacco. *The Plant Cell* **26**: 1308–1329.

Gong, Z., Brackertz, M., and Renkawitz, R. (2006). SUMO modification enhances p66-mediated transcriptional repression of the Mi-2/NuRD complex. *Mol. Cell. Biol.* **26**: 4519–4528.

Gonzalez, D., Bowen, A.J., Carroll, T.S., and Conlan, R.S. (2007). The transcription corepressor LEUNIG interacts with the histone deacetylase HDA19 and mediator components MED14 (SWP) and CDK8 (HEN3) to repress transcription. *Mol. Cell. Biol.* **27**: 5306–5315.

Gonzalez, N. et al. (2015). A Repressor Protein Complex Regulates Leaf Growth in *Arabidopsis*. *Plant Cell* **27**: 2273–2287.

Goodstein, D.M., Shu, S., Howson, R., Neupane, R., Hayes, R.D., Fazo, J., Mitros, T., Dirks, W., Hellsten, U., Putnam, N., and Rokhsar, D.S. (2012). Phytozome: a comparative platform for green plant genomics. *Nucleic Acids Res.* **40**: D1178-1186.

Gou, X. and Li, J. (2012). Activation tagging. *Methods Mol. Biol.* **876**: 117–133.

Graeff, M., Straub, D., Eguen, T., Dolde, U., Rodrigues, V., Brandt, R., and Wenkel, S. (2016). MicroProtein-Mediated Recruitment of CONSTANS into a TOPLESS Trimeric Complex Represses Flowering in *Arabidopsis*. *PLOS Genetics* **12**: e1005959.

Guo, R. and Sun, W. (2017). SUMOylation stabilizes RACK1B and enhance its interaction with RAP2.6 in the abscisic acid response. *Sci Rep* **7**: 44090.

Hammoudi, V., Fokkens, L., Beerens, B., Vlachakis, G., Chatterjee, S., Arroyo-Mateos, M., Wackers, P.F.K., Jonker, M.J., and van den Burg, H.A. (2018). The *Arabidopsis* SUMO E3 ligase SIZ1 mediates the temperature dependent trade-off between plant immunity and growth. *PLOS Genetics* **14**: e1007157.

Hall, T. (1999). Bioedit. <http://www.mbio.ncsu.edu/BioEdit/bioedit.html>

Han, Y.-C., Kuang, J.-F., Chen, J.-Y., Liu, X.-C., Xiao, Y.-Y., Fu, C.-C., Wang, J.-N., Wu, K.-Q., and Lu, W.-J. (2016). Banana Transcription Factor MaERF11 Recruits Histone Deacetylase MaHDA1 and Represses the Expression of MaACO1 and Expansins during Fruit Ripening. *Plant Physiol.* **171**: 1070–1084.

Hansen, L.L., van den Burg, H.A., and van Ooijen, G. (2017). SUMOylation Contributes to Timekeeping and Temperature Compensation of the Plant Circadian Clock. *J. Biol. Rhythms* **32**: 560–569.

Hao, Y., Wang, H., Qiao, S., Leng, L., and Wang, X. (2016). Histone deacetylase HDA6 enhances brassinosteroid signaling by inhibiting the BIN2 kinase. *Proceedings of the National Academy of Sciences* **113**: 10418–10423.

Hao, Y., Wang, X., Li, X., Bassa, C., Mila, I., Audran, C., Maza, E., Li, Z., Bouzayen, M., van der Rest, B., and Zouine, M. (2014). Genome-wide identification, phylogenetic analysis, expression profiling, and protein-protein interaction properties of TOPLESS gene family members in tomato. *J. Exp. Bot.* **65**: 1013–1023.

Hartl, M. et al. (2017). Lysine acetylome profiling uncovers novel histone deacetylase substrate proteins in *Arabidopsis*. *Molecular Systems Biology* **13**: 949.

Hay, R.T. (2005). SUMO. *Molecular Cell* **18**: 1–12.

Hazzalin, C.A. and Mahadevan, L.C. (2005). Dynamic acetylation of all lysine 4-methylated histone H3 in the mouse nucleus: analysis at c-fos and c-jun. *PLoS Biol.* **3**: e393.

Hecker, C.-M., Rabiller, M., Haglund, K., Bayer, P., and Dikic, I. (2006). Specification of SUMO1- and SUMO2-interacting motifs. *J. Biol. Chem.* **281**: 16117–16127.

- Hendriks, I.A. and Vertegaal, A.C.O.** (2016). A high-yield double-purification proteomics strategy for the identification of SUMO sites. *Nat Protoc* **11**: 1630–1649.
- Henikoff, S. and Smith, M.M.** (2015). Histone variants and epigenetics. *Cold Spring Harb Perspect Biol* **7**: a019364.
- Hermkes, R., Fu, Y.-F., Nürrenberg, K., Budhiraja, R., Schmelzer, E., Elrouby, N., Dohmen, R.J., Bachmair, A., and Coupland, G.** (2011). Distinct roles for *Arabidopsis* SUMO protease ESD4 and its closest homolog ELS1. *Planta* **233**: 63–73.
- Hietakangas, V., Anckar, J., Blomster, H.A., Fujimoto, M., Palvimo, J.J., Nakai, A., and Sistonen, L.** (2006). PDSM, a motif for phosphorylation-dependent SUMO modification. *Proc. Natl. Acad. Sci. U.S.A.* **103**: 45–50.
- Hoffman, E.A., Frey, B.L., Smith, L.M., and Auble, D.T.** (2015). Formaldehyde crosslinking: a tool for the study of chromatin complexes. *J. Biol. Chem.* **290**: 26404–26411.
- Hollender, C. and Liu, Z.** (2008). Histone deacetylase genes in *Arabidopsis* development. *J Integr Plant Biol* **50**: 875–885.
- Hori, K. et al.** (2014). *Klebsormidium flaccidum* genome reveals primary factors for plant terrestrial adaptation. *Nat Commun* **5**: 3978.
- Hua, Z., Doroodian, P., and Vu, W.** (2018). Contrasting duplication patterns reflect functional diversities of ubiquitin and ubiquitin-like protein modifiers in plants. *Plant J.* **95**: 296–311.
- Huang, L., Yang, S., Zhang, S., Liu, M., Lai, J., Qi, Y., Shi, S., Wang, J., Wang, Y., Xie, Q., and Yang, C.** (2009). The *Arabidopsis* SUMO E3 ligase AtMMS21, a homologue of NSE2/MMS21, regulates cell proliferation in the root. *Plant J.* **60**: 666–678.
- Huang, Z., Shi, T., Zheng, B., Yumul, R.E., Liu, X., You, C., Gao, Z., Xiao, L., and Chen, X.** (2017). *APETALA2* antagonizes the transcriptional activity of *AGAMOUS* in regulating floral stem cells in *Arabidopsis thaliana*. *New Phytologist* **215**: 1197–1209.
- Ikeda, M. and Ohme-Takagi, M.** (2009). A novel group of transcriptional repressors in *Arabidopsis*. *Plant Cell Physiol.* **50**: 970–975.
- Irish, V.** (2017). The ABC model of floral development. *Current Biology* **27**: R887–R890.
- Ishida, T., Yoshimura, M., Miura, K., and Sugimoto, K.** (2012). MMS21/HPY2 and SIZ1, two *Arabidopsis* SUMO E3 ligases, have distinct functions in development. *PLoS ONE* **7**: e46897.
- Ito, J., Fukaki, H., Onoda, M., Li, L., Li, C., Tasaka, M., and Furutani, M.** (2016). Auxin-dependent compositional change in Mediator in ARF7- and

ARF19-mediated transcription. *Proc. Natl. Acad. Sci. U.S.A.* **113**: 6562–6567.

Ivanov, A.V. et al. (2007). PHD domain-mediated E3 ligase activity directs intramolecular SUMOylation of an adjacent bromodomain required for gene silencing. *Mol. Cell* **28**: 823–837.

Jennings, B.H., Pickles, L.M., Wainwright, S.M., Roe, S.M., Pearl, L.H., and Ish-Horowicz, D. (2006). Molecular recognition of transcriptional repressor motifs by the WD domain of the Groucho/TLE corepressor. *Mol. Cell* **22**: 645–655.

Jin, J., Tian, F., Yang, D.-C., Meng, Y.-Q., Kong, L., Luo, J., and Gao, G. (2017). PlantTFDB 4.0: toward a central hub for transcription factors and regulatory interactions in plants. *Nucleic Acids Research* **45**: D1040–D1045.

Jin, J.B. and Hasegawa, P.M. (2008). Flowering time regulation by the SUMO E3 ligase SIZ1. *Plant Signal Behav* **3**: 891–892.

Jofuku, K.D., den Boer, B.G., Van Montagu, M., and Okamoto, J.K. (1994). Control of *Arabidopsis* flower and seed development by the homeotic gene APETALA2. *Plant Cell* **6**: 1211–1225.

Jung, J.-H., Lee, S., Yun, J., Lee, M., and Park, C.-M. (2014). The miR172 target TOE3 represses AGAMOUS expression during *Arabidopsis* floral patterning. *Plant Science* **215–216**: 29–38.

Kagale, S., Links, M.G., and Rozwadowski, K. (2010). Genome-wide analysis of ethylene-responsive element binding factor-associated amphiphilic repression motif-containing transcriptional regulators in *Arabidopsis*. *Plant Physiol.* **152**: 1109–1134.

Kagale, S. and Rozwadowski, K. (2011a). EAR motif-mediated transcriptional repression in plants: an underlying mechanism for epigenetic regulation of gene expression. *Epigenetics* **6**: 141–146.

Kagale, S. and Rozwadowski, K. (2011b). EAR motif-mediated transcriptional repression in plants: an underlying mechanism for epigenetic regulation of gene expression. *Epigenetics* **6**: 141–146.

Katoh, K., Rozewicki, J., and Yamada, K.D. (2017). MAFFT online service: multiple sequence alignment, interactive sequence choice and visualization. *Briefings in Bioinformatics*.

Ke, J., Ma, H., Gu, X., Thelen, A., Brunzelle, J.S., Li, J., Xu, H.E., and Melcher, K. (2015). Structural basis for recognition of diverse transcriptional repressors by the TOPLESS family of corepressors. *Sci Adv* **1**: e1500107.

Khan, D.H., He, S., Yu, J., Winter, S., Cao, W., Seiser, C., and Davie, J.R. (2013). Protein kinase CK2 regulates the dimerization of histone deacetylase 1 (HDAC1) and HDAC2 during mitosis. *J. Biol. Chem.* **288**: 16518–16528.

Kieffer, M. (2006). Analysis of the Transcription Factor WUSCHEL and Its Functional Homologue in Antirrhinum Reveals a Potential Mechanism for Their Roles in Meristem Maintenance. *THE PLANT CELL ONLINE* **18**: 560–573.

Klenk, C., Humrich, J., Qwitterer, U., and Lohse, M.J. (2006). SUMO-1 controls the protein stability and the biological function of phosducin. *J. Biol. Chem.* **281**: 8357–8364.

Knipscheer, P., van Dijk, W.J., Olsen, J.V., Mann, M., and Sixma, T.K. (2007). Noncovalent interaction between Ubc9 and SUMO promotes SUMO chain formation. *EMBO J.* **26**: 2797–2807.

Krogan, N.T., Hogan, K., and Long, J.A. (2012). APETALA2 negatively regulates multiple floral organ identity genes in *Arabidopsis* by recruiting the co-repressor TOPLESS and the histone deacetylase HDA19. *Development* **139**: 4180–4190.

Kurepa, J., Walker, J.M., Smalle, J., Gosink, M.M., Davis, S.J., Durham, T.L., Sung, D.-Y., and Vierstra, R.D. (2003). The small ubiquitin-like modifier (SUMO) protein modification system in *Arabidopsis*. Accumulation of SUMO1 and -2 conjugates is increased by stress. *J. Biol. Chem.* **278**: 6862–6872.

Kwak, J.S., Son, G.H., Kim, S.-I., Song, J.T., and Seo, H.S. (2016). *Arabidopsis* HIGH PLOIDY2 SUMOylates and Stabilizes Flowering Locus C through Its E3 Ligase Activity. *Frontiers in Plant Science* **7**.

Kwon, C.S., Hibara, K., Pfluger, J., Bezhani, S., Metha, H., Aida, M., Tasaka, M., and Wagner, D. (2006). A role for chromatin remodeling in regulation of CUC gene expression in the *Arabidopsis* cotyledon boundary. *Development* **133**: 3223–3230.

Lamesch, P. et al. (2012). The *Arabidopsis* Information Resource (TAIR): improved gene annotation and new tools. *Nucleic Acids Research* **40**: D1202–D1210.

Laplaze, L. et al. (2007). Cytokinins act directly on lateral root founder cells to inhibit root initiation. *Plant Cell* **19**: 3889–3900.

Latrasse, D. et al. (2017a). MAPK-triggered chromatin reprogramming by histone deacetylase in plant innate immunity. *Genome Biology* **18**.

Latrasse, D. et al. (2017b). MAPK-triggered chromatin reprogramming by histone deacetylase in plant innate immunity. *Genome Biol.* **18**: 131.

Lau, S., Slane, D., Herud, O., Kong, J., and Jürgens, G. (2012). Early Embryogenesis in Flowering Plants: Setting Up the Basic Body Pattern. *Annual Review of Plant Biology* **63**: 483–506.

Lee, J. et al. (2007). Salicylic acid-mediated innate immunity in *Arabidopsis* is regulated by SIZ1 SUMO E3 ligase. *Plant J.* **49**: 79–90.

Lejon, S., Thong, S.Y., Murthy, A., AlQarni, S., Murzina, N.V., Blobel, G.A., Laue, E.D., and Mackay, J.P. (2011). Insights into association of the NuRD complex with FOG-1 from the crystal structure of an RbAp48·FOG-1 complex. *J. Biol. Chem.* **286**: 1196–1203.

Lemieux, C., Otis, C., and Turmel, M. (2014). Six newly sequenced chloroplast genomes from prasinophyte green algae provide insights into the relationships among prasinophyte lineages and the diversity of streamlined genome architecture in picoplanktonic species. *BMC Genomics* **15**: 857.

Li, H., Torres-Garcia, J., Latrasse, D., Benhamed, M., Schilderink, S., Zhou, W., Kulikova, O., Hirt, H., and Bisseling, T. (2017). Plant-Specific Histone Deacetylases HDT1/2 Regulate *GIBBERELLIN 2-OXIDASE2* Expression to Control *Arabidopsis* Root Meristem Cell Number. *The Plant Cell* **29**: 2183–2196.

Li, S.-J. and Hochstrasser, M. (1999). A new protease required for cell-cycle progression in yeast. *Nature* **398**: 246–251.

Lin, X.-L., Niu, D., Hu, Z.-L., Kim, D.H., Jin, Y.H., Cai, B., Liu, P., Miura, K., Yun, D.-J., Kim, W.-Y., Lin, R., and Jin, J.B. (2016a). An *Arabidopsis* SUMO E3 Ligase, SIZ1, Negatively Regulates Photomorphogenesis by Promoting COP1 Activity. *PLoS Genet.* **12**: e1006016.

Lin, X.-L., Niu, D., Hu, Z.-L., Kim, D.H., Jin, Y.H., Cai, B., Liu, P., Miura, K., Yun, D.-J., Kim, W.-Y., Lin, R., and Jin, J.B. (2016b). An *Arabidopsis* SUMO E3 Ligase, SIZ1, Negatively Regulates Photomorphogenesis by Promoting COP1 Activity. *PLOS Genetics* **12**: e1006016.

Liu, X., Wei, W., Zhu, W., Su, L., Xiong, Z., Zhou, M., Zheng, Y., and Zhou, D.-X. (2017). Histone Deacetylase AtSRT1 Links Metabolic Flux and Stress Response in *Arabidopsis*. *Molecular Plant* **10**: 1510–1522.

Liu, X., Yang, S., Zhao, M., Luo, M., Yu, C.-W., Chen, C.-Y., Tai, R., and Wu, K. (2014). Transcriptional repression by histone deacetylases in plants. *Mol Plant* **7**: 764–772.

Liu, Y., Lai, J., Yu, M., Wang, F., Zhang, J., Jiang, J., Hu, H., Wu, Q., Lu, G., Xu, P., and Yang, C. (2016). The *Arabidopsis* SUMO E3 Ligase AtMMS21 Dissociates the E2Fa/DPa Complex in Cell Cycle Regulation. *The Plant Cell* **28**: 2225–2237.

Liu, Z. and Karmarkar, V. (2008). Groucho/Tup1 family co-repressors in plant development. *Trends Plant Sci.* **13**: 137–144.

Liu, Z. and Meyerowitz, E.M. (1995). LEUNIG regulates AGAMOUS expression in *Arabidopsis* flowers. *Development* **121**: 975–991.

Lois, L.M., Lima, C.D., and Chua, N.-H. (2003). Small ubiquitin-like modifier modulates abscisic acid signaling in *Arabidopsis*. *Plant Cell* **15**: 1347–1359.

- Long, J.A., Ohno, C., Smith, Z.R., and Meyerowitz, E.M.** (2006). TOPLESS regulates apical embryonic fate in *Arabidopsis*. *Science* **312**: 1520–1523.
- Long, J.A., Woody, S., Poethig, S., Meyerowitz, E.M., and Barton, M.K.** (2002). Transformation of shoots into roots in *Arabidopsis* embryos mutant at the TOPLESS locus. *Development* **129**: 2797–2806.
- Lu, L., Chen, X., Sanders, D., Qian, S., and Zhong, X.** (2015). High-resolution mapping of H4K16 and H3K23 acetylation reveals conserved and unique distribution patterns in *Arabidopsis* and rice. *Epigenetics* **10**: 1044–1053.
- Luo, M., Yu, C.-W., Chen, F.-F., Zhao, L., Tian, G., Liu, X., Cui, Y., Yang, J.-Y., and Wu, K.** (2012). Histone Deacetylase HDA6 Is Functionally Associated with AS1 in Repression of KNOX Genes in *Arabidopsis*. *PLoS Genetics* **8**: e1003114.
- Lyzenga, W.J. and Stone, S.L.** (2012). Abiotic stress tolerance mediated by protein ubiquitination. *J. Exp. Bot.* **63**: 599–616.
- Ma, H. et al.** (2017). A D53 repression motif induces oligomerization of TOPLESS corepressors and promotes assembly of a corepressor-nucleosome complex. *Sci Adv* **3**: e1601217.
- Maarifi, G., El Asmi, F., Maroui, M.A., Dianoux, L., and Chelbi-Alix, M.K.** (2018). Differential effects of SUMO1 and SUMO3 on PKR activation and stability. *Sci Rep* **8**: 1277.
- Mahajan, R., Delphin, C., Guan, T., Gerace, L., and Melchior, F.** (1997). A small ubiquitin-related polypeptide involved in targeting RanGAP1 to nuclear pore complex protein RanBP2. *Cell* **88**: 97–107.
- Martin-Arevalillo, R., Nanao, M.H., Larrieu, A., Vinos-Poyo, T., Mast, D., Galvan-Ampudia, C., Brunoud, G., Vernoux, T., Dumas, R., and Parcy, F.** (2017). Structure of the *Arabidopsis* TOPLESS corepressor provides insight into the evolution of transcriptional repression. *Proc. Natl. Acad. Sci. U.S.A.* **114**: 8107–8112.
- Matasci, N. et al.** (2014). Data access for the 1,000 Plants (1KP) project. *Gigascience* **3**: 17.
- Matic, I., Schimmel, J., Hendriks, I.A., van Santen, M.A., van de Rijke, F., van Dam, H., Gnad, F., Mann, M., and Vertegaal, A.C.O.** (2010). Site-specific identification of SUMO-2 targets in cells reveals an inverted SUMOylation motif and a hydrophobic cluster SUMOylation motif. *Mol. Cell* **39**: 641–652.
- Maugarny-Calès, A. and Laufs, P.** (2018). Getting leaves into shape: a molecular, cellular, environmental and evolutionary view. *Development* **145**: dev161646.

Mazur, M.J. and van den Burg, H.A. (2012). Global SUMO Proteome Responses Guide Gene Regulation, mRNA Biogenesis, and Plant Stress Responses. *Front Plant Sci* **3**: 215.

Mergner, J. and Schwechheimer, C. (2014). The NEDD8 modification pathway in plants. *Front Plant Sci* **5**: 103.

Merini, W., Romero-Campero, F.J., Gomez-Zambrano, A., Zhou, Y., Turck, F., and Calonje, M. (2017). The *Arabidopsis* Polycomb Repressive Complex 1 (PRC1) Components AtBMI1A, B, and C Impact Gene Networks throughout All Stages of Plant Development. *Plant Physiology* **173**: 627–641.

Millard, C.J., Varma, N., Saleh, A., Morris, K., Watson, P.J., Bottrill, A.R., Fairall, L., Smith, C.J., and Schwabe, J.W. (2016). The structure of the core NuRD repression complex provides insights into its interaction with chromatin. *eLife* **5**.

Millard, C.J., Watson, P.J., Celardo, I., Gordiyenko, Y., Cowley, S.M., Robinson, C.V., Fairall, L., and Schwabe, J.W.R. (2013). Class I HDACs share a common mechanism of regulation by inositol phosphates. *Mol. Cell* **51**: 57–67.

Miller, M.A., Pfeiffer, W., and Schwartz, T. (2011). The CIPRES science gateway: a community resource for phylogenetic analyses. In *Proceedings of the 2011 TeraGrid Conference on Extreme Digital Discovery - TG '11* (ACM Press: Salt Lake City, Utah), p. 1.

Miller, M.J., Barrett-Wilt, G.A., Hua, Z., and Vierstra, R.D. (2010). Proteomic analyses identify a diverse array of nuclear processes affected by small ubiquitin-like modifier conjugation in *Arabidopsis*. *Proc. Natl. Acad. Sci. U.S.A.* **107**: 16512–16517.

Mishra, N., Srivastava, A.P., Esmaili, N., Hu, W., and Shen, G. (2018). Overexpression of the rice gene OsSIZ1 in *Arabidopsis* improves drought-, heat-, and salt-tolerance simultaneously. *PLoS ONE* **13**: e0201716.

Mittal, A., Hobor, F., Zhang, Y., Martin, S.R., Gamblin, S.J., Ramos, A., and Wilson, J.R. (2018). The structure of the RbBP5 β -propeller domain reveals a surface with potential nucleic acid binding sites. *Nucleic Acids Res.* **46**: 3802–3812.

Miura, K., Jin, J.B., Lee, J., Yoo, C.Y., Stirm, V., Miura, T., Ashworth, E.N., Bressan, R.A., Yun, D.-J., and Hasegawa, P.M. (2007). SIZ1-Mediated SUMOylation of ICE1 Controls CBF3/DREB1A Expression and Freezing Tolerance in *Arabidopsis*. *THE PLANT CELL ONLINE* **19**: 1403–1414.

Miura, K., Lee, J., Jin, J.B., Yoo, C.Y., Miura, T., and Hasegawa, P.M. (2009). SUMOylation of ABI5 by the *Arabidopsis* SUMO E3 ligase SIZ1 negatively regulates abscisic acid signaling. *Proc. Natl. Acad. Sci. U.S.A.* **106**: 5418–5423.

Miura, K., Rus, A., Sharkhuu, A., Yokoi, S., Karthikeyan, A.S., Raghothama, K.G., Baek, D., Koo, Y.D., Jin, J.B., Bressan, R.A., Yun, D.-J., and Hasegawa, P.M. (2005). The *Arabidopsis* SUMO E3 ligase SIZ1 controls phosphate deficiency responses. *Proc. Natl. Acad. Sci. U.S.A.* **102**: 7760–7765.

Morey, L., Brenner, C., Fazi, F., Villa, R., Gutierrez, A., Buschbeck, M., Nervi, C., Minucci, S., Fuks, F., and Di Croce, L. (2008). MBD3, a component of the NuRD complex, facilitates chromatin alteration and deposition of epigenetic marks. *Mol. Cell. Biol.* **28**: 5912–5923.

Murtas, G., Reeves, P.H., Fu, Y.-F., Bancroft, I., Dean, C., and Coupland, G. (2003). A nuclear protease required for flowering-time regulation in *Arabidopsis* reduces the abundance of SMALL UBIQUITIN-RELATED MODIFIER conjugates. *Plant Cell* **15**: 2308–2319.

Murzina, N.V., Pei, X.-Y., Zhang, W., Sparkes, M., Vicente-Garcia, J., Pratap, J.V., McLaughlin, S.H., Ben-Shahar, T.R., Verreault, A., Luisi, B.F., and Laue, E.D. (2008). Structural basis for the recognition of histone H4 by the histone-chaperone RbAp46. *Structure* **16**: 1077–1085.

Negin, B., Shemer, O., Sorek, Y., and Eshed Williams, L. (2017). Shoot stem cell specification in roots by the WUSCHEL transcription factor. *PLOS ONE* **12**: e0176093.

Ng, C.H., Akhter, A., Yurko, N., Burgener, J.M., Rosonina, E., and Manley, J.L. (2015). SUMOylation controls the timing of Tup1-mediated transcriptional deactivation. *Nat Commun* **6**: 6610.

Novatchkova, M., Tomanov, K., Hofmann, K., Stuible, H.-P., and Bachmair, A. (2012). Update on SUMOylation: defining core components of the plant SUMO conjugation system by phylogenetic comparison: Research review. *New Phytologist* **195**: 23–31.

Oeser, M.L., Amen, T., Nadel, C.M., Bradley, A.I., Reed, B.J., Jones, R.D., Gopalan, J., Kaganovich, D., and Gardner, R.G. (2016). Dynamic SUMOylation of a Conserved Transcription Corepressor Prevents Persistent Inclusion Formation during Hyperosmotic Stress. *PLOS Genetics* **12**: e1005809.

Oh, E., Zhu, J.-Y., Ryu, H., Hwang, I., and Wang, Z.-Y. (2014). TOPLESS mediates brassinosteroid-induced transcriptional repression through interaction with BZR1. *Nat Commun* **5**: 4140.

Ohta, M., Matsui, K., Hiratsu, K., Shinshi, H., and Ohme-Takagi, M. (2001). Repression domains of class II ERF transcriptional repressors share an essential motif for active repression. *Plant Cell* **13**: 1959–1968.

Orosa, B., Yates, G., Verma, V., Srivasta, A.K., Srivasta, M., Campanaro, A., De Vega, D., Fernandes, A., Zhang, C., Lee, J., Bennett M.J. and Sadanandom, A. (2018). SUMO conjugation to the pattern recognition

receptor FLS2 triggers intracellular signalling in plant innate immunity. *Nat Commun.* **9** (1): 5185.

Ouyang, J. and Gill, G. (2009). SUMO engages multiple corepressors to regulate chromatin structure and transcription. *Epigenetics* **4**: 440–444.

Pauwels, L. et al. (2010). NINJA connects the co-repressor TOPLESS to jasmonate signalling. *Nature* **464**: 788–791.

Perrella, G., Lopez-Vernaza, M.A., Carr, C., Sani, E., Gosselé, V., Verduyn, C., Kellermeier, F., Hannah, M.A., and Amtmann, A. (2013). Histone deacetylase complex1 expression level titrates plant growth and abscisic acid sensitivity in *Arabidopsis*. *Plant Cell* **25**: 3491–3505.

Petricka, J.J., Winter, C.M., and Benfey, P.N. (2012). Control of *Arabidopsis* Root Development. *Annual Review of Plant Biology* **63**: 563–590.

Pi, L., Aichinger, E., van der Graaff, E., Llavata-Peris, C.I., Weijers, D., Hennig, L., Groot, E., and Laux, T. (2015). Organizer-Derived WOX5 Signal Maintains Root Columella Stem Cells through Chromatin-Mediated Repression of CDF4 Expression. *Developmental Cell* **33**: 576–588.

Rani Debi, B., Taketa, S., and Ichii, M. (2005). Cytokinin inhibits lateral root initiation but stimulates lateral root elongation in rice (*Oryza sativa*). *J. Plant Physiol.* **162**: 507–515.

Reiland, S., Messerli, G., Baerenfaller, K., Gerrits, B., Endler, A., Grossmann, J., Gruissem, W., and Baginsky, S. (2009). Large-scale *Arabidopsis* phosphoproteome profiling reveals novel chloroplast kinase substrates and phosphorylation networks. *Plant Physiol.* **150**: 889–903.

Reynolds, N., O’Shaughnessy, A., and Hendrich, B. (2013). Transcriptional repressors: multifaceted regulators of gene expression. *Development* **140**: 505–512.

Robinson, O., Dylus, D., and Dessimoz, C. (2016). *Phylo.io*: Interactive Viewing and Comparison of Large Phylogenetic Trees on the Web. *Molecular Biology and Evolution* **33**: 2163–2166.

Rodriguez, M.S., Dargemont, C., and Hay, R.T. (2001). SUMO-1 conjugation in vivo requires both a consensus modification motif and nuclear targeting. *J. Biol. Chem.* **276**: 12654–12659.

Rouvière, J.O., Bulfoni, M., Tuck, A., Cosson, B., Devaux, F., and Palancade, B. (2018). A SUMO-dependent feedback loop senses and controls the biogenesis of nuclear pore subunits. *Nat Commun* **9**: 1665.

Roycewicz, P. and Malamy, J.E. (2012). Dissecting the effects of nitrate, sucrose and osmotic potential on *Arabidopsis* root and shoot system growth in laboratory assays. *Philosophical Transactions of the Royal Society B: Biological Sciences* **367**: 1489–1500.

- Ruiz Carrillo, D., Chandrasekaran, R., Nilsson, M., Cornvik, T., Liew, C.W., Tan, S.M., and Lescar, J.** (2012). Structure of human Rack1 protein at a resolution of 2.45 Å. *Acta Crystallogr. Sect. F Struct. Biol. Cryst. Commun.* **68**: 867–872.
- Rytz, T.C., Miller, M.J., McLoughlin, F., Augustine, R.C., Marshall, R.S., Juan, Y.-T., Charng, Y.-Y., Scalf, M., Smith, L.M., and Vierstra, R.D.** (2018). SUMOylome Profiling Reveals a Diverse Array of Nuclear Targets Modified by the SUMO Ligase SIZ1 during Heat Stress. *Plant Cell* **30**: 1077–1099.
- Salazar-Henao, J.E., Vélez-Bermúdez, I.C., and Schmidt, W.** (2016). The regulation and plasticity of root hair patterning and morphogenesis. *Development* **143**: 1848–1858.
- Saleh, A., Withers, J., Mohan, R., Marqués, J., Gu, Y., Yan, S., Zavaliev, R., Nomoto, M., Tada, Y., and Dong, X.** (2015). Posttranslational Modifications of the Master Transcriptional Regulator NPR1 Enable Dynamic but Tight Control of Plant Immune Responses. *Cell Host Microbe* **18**: 169–182.
- Samanta, S. and Thakur, J.K.** (2015). Importance of Mediator complex in the regulation and integration of diverse signaling pathways in plants. *Front Plant Sci* **6**: 757.
- Sanchez, G.J., Richmond, P.A., Bunker, E.N., Karman, S.S., Azofeifa, J., Garnett, A.T., Xu, Q., Wheeler, G.E., Toomey, C.M., Zhang, Q., Dowell, R.D., and Liu, X.** (2018). Genome-wide dose-dependent inhibition of histone deacetylases studies reveal their roles in enhancer remodeling and suppression of oncogenic super-enhancers. *Nucleic Acids Res.* **46**: 1756–1776.
- Sang, Y., Silva-Ortega, C.O., Wu, S., Yamaguchi, N., Wu, M.-F., Pfluger, J., Gillmor, C.S., Gallagher, K.L., and Wagner, D.** (2012). Mutations in two non-canonical *Arabidopsis* SWI2/SNF2 chromatin remodeling ATPases cause embryogenesis and stem cell maintenance defects: *Function of MINU SWI2/SNF2 ATPases*. *The Plant Journal* **72**: 1000–1014.
- Saracco, S.A., Miller, M.J., Kurepa, J., and Vierstra, R.D.** (2007). Genetic analysis of SUMOylation in *Arabidopsis*: conjugation of SUMO1 and SUMO2 to nuclear proteins is essential. *Plant Physiol.* **145**: 119–134.
- Sarkar, A.K., Luijten, M., Miyashima, S., Lenhard, M., Hashimoto, T., Nakajima, K., Scheres, B., Heidstra, R., and Laux, T.** (2007). Conserved factors regulate signalling in *Arabidopsis thaliana* shoot and root stem cell organizers. *Nature* **446**: 811–814.
- Saunders, A., Huang, X., Fidalgo, M., Reimer, M.H., Faiola, F., Ding, J., Sánchez-Priego, C., Guallar, D., Sáenz, C., Li, D., and Wang, J.** (2017). The SIN3A/HDAC Corepressor Complex Functionally Cooperates with NANOG to Promote Pluripotency. *Cell Rep* **18**: 1713–1726.

Schmid, M., Davison, T.S., Henz, S.R., Pape, U.J., Demar, M., Vingron, M., Schölkopf, B., Weigel, D., and Lohmann, J.U. (2005). A gene expression map of *Arabidopsis thaliana* development. *Nat. Genet.* **37**: 501–506.

Seto, E. and Yoshida, M. (2014). Erasers of histone acetylation: the histone deacetylase enzymes. *Cold Spring Harb Perspect Biol* **6**: a018713.

Shen, Y., Wei, W., and Zhou, D.-X. (2015). Histone Acetylation Enzymes Coordinate Metabolism and Gene Expression. *Trends Plant Sci.* **20**: 614–621.

Shin, J., Shin, H.M., Nam, E., Kim, W.S., Kim, J., Oh, B.-H. and Yun, Y. (2012). DeSUMOylating isopeptidase: a second class of SUMO protease. *EMBO reports.* **13**. 339-46.

Silva-Alvim, F.A.L., An, J., Alvim, J.C., Foresti, O., Grippa, A., Pelgrom, A.J.E., Adams, T.L., Hawes, C., and Denecke, J. (2018). Predominant Golgi-residency of the plant K/HDEL receptor is essential for its function in mediating ER retention. *The Plant Cell: tpc.00426.2018*.

Simon, M., North, J.A., Shimko, J.C., Forties, R.A., Ferdinand, M.B., Manohar, M., Zhang, M., Fishel, R., Ottesen, J.J., and Poirier, M.G. (2011). Histone fold modifications control nucleosome unwrapping and disassembly. *Proc. Natl. Acad. Sci. U.S.A.* **108**: 12711–12716.

Sims, J.K. and Wade, P.A. (2011). Mi-2/NuRD complex function is required for normal S phase progression and assembly of pericentric heterochromatin. *Mol. Biol. Cell* **22**: 3094–3102.

Singh, K.K., Erkelenz, S., Rattay, S., Dehof, A.K., Hildebrandt, A., Schulze-Osthoff, K., Schaal, H., and Schwerk, C. (2010). Human SAP18 mediates assembly of a splicing regulatory multiprotein complex via its ubiquitin-like fold. *RNA* **16**: 2442–2454.

Skelly, M.J., Frungillo, L., and Spoel, S.H. (2016). Transcriptional regulation by complex interplay between post-translational modifications. *Curr. Opin. Plant Biol.* **33**: 126–132.

Skinner, G. (2018). Regexpr. <https://regexpr.com/>

Smith, Z.R. and Long, J.A. (2010). Control of *Arabidopsis* apical-basal embryo polarity by antagonistic transcription factors. *Nature* **464**: 423–426.

Song, C.-P. (2005). Role of an *Arabidopsis* AP2/EREBP-Type Transcriptional Repressor in Abscisic Acid and Drought Stress Responses. *THE PLANT CELL ONLINE* **17**: 2384–2396.

Song, C.-P. and Galbraith, D.W. (2006). AtSAP18, an orthologue of human SAP18, is involved in the regulation of salt stress and mediates transcriptional repression in *Arabidopsis*. *Plant Mol. Biol.* **60**: 241–257.

- Song, G. and Walley, J.W.** (2016). Dynamic Protein Acetylation in Plant-Pathogen Interactions. *Front Plant Sci* **7**: 421.
- Song, J., Durrin, L.K., Wilkinson, T.A., Krontiris, T.G., and Chen, Y.** (2004). Identification of a SUMO-binding motif that recognizes SUMO-modified proteins. *Proceedings of the National Academy of Sciences* **101**: 14373–14378.
- Soundappan, I., Bennett, T., Morffy, N., Liang, Y., Stanga, J.P., Abbas, A., Leyser, O., and Nelson, D.C.** (2015). SMAX1-LIKE/D53 Family Members Enable Distinct MAX2-Dependent Responses to Strigolactones and Karrikins in *Arabidopsis*. *Plant Cell* **27**: 3143–3159.
- Spedaletti, V., Polticelli, F., Capodaglio, V., Schininà, M.E., Stano, P., Federico, R., and Tavladoraki, P.** (2008). Characterization of a Lysine-Specific Histone Demethylase from *Arabidopsis thaliana* †. *Biochemistry* **47**: 4936–4947.
- Sriramachandran, A.M. and Dohmen, R.J.** (2014). SUMO-targeted ubiquitin ligases. *Biochimica et Biophysica Acta (BBA) - Molecular Cell Research* **1843**: 75–85.
- Srivastava, A.K., Orosa, B., Singh, P., Cummins, I., Walsh, C., Zhang, C., Grant, M., Roberts, M.R., Anand, G.S., Fitches, E., and Sadanandom, A.** (2018). SUMO Suppresses the Activity of the Jasmonic Acid Receptor CORONATINE INSENSITIVE 1. *Plant Cell*.
- Srivastava, A.K., Zhang, C., Caine, R.S., Gray, J., and Sadanandom, A.** (2017). Rice SUMO protease *Overly Tolerant to Salt 1* targets the transcription factor, OsbZIP23 to promote drought tolerance in rice. *The Plant Journal* **92**: 1031–1043.
- Srivastava, A.K., Zhang, C., and Sadanandom, A.** (2016a). Rice OVERLY TOLERANT TO SALT 1 (OTS1) SUMO protease is a positive regulator of seed germination and root development. *Plant Signal Behav* **11**: e1173301.
- Srivastava, A.K., Zhang, C., Yates, G., Bailey, M., Brown, A., and Sadanandom, A.** (2016b). SUMO Is a Critical Regulator of Salt Stress Responses in Rice. *Plant Physiol.* **170**: 2378–2391.
- Stoeckle, D., Thellmann, M., and Vermeer, J.E.** (2018). Breakout-lateral root emergence in *Arabidopsis thaliana*. *Curr. Opin. Plant Biol.* **41**: 67–72.
- Sun, J.-M., Chen, H.Y., and Davie, J.R.** (2007). Differential distribution of unmodified and phosphorylated histone deacetylase 2 in chromatin. *J. Biol. Chem.* **282**: 33227–33236.
- Szemenyi, H., Hannon, M., and Long, J.A.** (2008). TOPLESS mediates auxin-dependent transcriptional repression during *Arabidopsis* embryogenesis. *Science* **319**: 1384–1386.
- Tang, X., Hou, A., Babu, M., Nguyen, V., Hurtado, L., Lu, Q., Reyes, J.C., Wang, A., Keller, W.A., Harada, J.J., Tsang, E.W.T., and Cui, Y.** (2008).

The *Arabidopsis* BRAHMA chromatin-remodeling ATPase is involved in repression of seed maturation genes in leaves. *Plant Physiol.* **147**: 1143–1157.

Tao, Q., Guo, D., Wei, B., Zhang, F., Pang, C., Jiang, H., Zhang, J., Wei, T., Gu, H., Qu, L.-J., and Qin, G. (2013). The TIE1 transcriptional repressor links TCP transcription factors with TOPLESS/TOPLESS-RELATED corepressors and modulates leaf development in *Arabidopsis*. *Plant Cell* **25**: 421–437.

Tao, S. and Estelle, M. (2018). Mutational studies of the Aux/IAA proteins in *Physcomitrella* reveal novel insights into their function. *New Phytol.* **218**: 1534–1542.

Tasset, C., Singh Yadav, A., Sureshkumar, S., Singh, R., van der Woude, L., Nekrasov, M., Tremethick, D., van Zanten, M., and Balasubramanian, S. (2018). POWERDRESS-mediated histone deacetylation is essential for thermomorphogenesis in *Arabidopsis thaliana*. *PLOS Genetics* **14**: e1007280.

Tessarz, P. and Kouzarides, T. (2014). Histone core modifications regulating nucleosome structure and dynamics. *Nat. Rev. Mol. Cell Biol.* **15**: 703–708.

Tian, H., Jia, Y., Niu, T., Yu, Q., and Ding, Z. (2014). The key players of the primary root growth and development also function in lateral roots in *Arabidopsis*. *Plant Cell Reports* **33**: 745–753.

Tomanov, K., Nehlin, L., Ziba, I., and Bachmair, A. (2018a). SUMO chain formation relies on the amino-terminal region of SUMO-conjugating enzyme and has dedicated substrates in plants. *Biochem. J.* **475**: 61–74.

Tomanov, K., Nukarinen, E., Vicente, J., Mendiando, G.M., Winter, N., Nehlin, L., Weckwerth, W., Holdsworth, M.J., Teige, M., and Bachmair, A. (2018b). SUMOylation and phosphorylation: hidden and overt links. *Journal of Experimental Botany* **69**: 4583–4590.

Tomanov, K., Zeschmann, A., Hermkes, R., Eifler, K., Ziba, I., Grieco, M., Novatchkova, M., Hofmann, K., Hesse, H., and Bachmair, A. (2014). *Arabidopsis* PIAL1 and 2 promote SUMO chain formation as E4-type SUMO ligases and are involved in stress responses and sulfur metabolism. *Plant Cell* **26**: 4547–4560.

Torchy, M.P., Hamiche, A., and Klaholz, B.P. (2015). Structure and function insights into the NuRD chromatin remodeling complex. *Cell. Mol. Life Sci.* **72**: 2491–2507.

Townsley, B.T. and Sinha, N.R. (2012). A New Development: Evolving Concepts in Leaf Ontogeny. *Annual Review of Plant Biology* **63**: 535–562.

Ueda, M. et al. (2017). The Distinct Roles of Class I and II RPD3-Like Histone Deacetylases in Salinity Stress Response. *Plant Physiol.* **175**: 1760–1773.

- Uhrig, J.F., Huang, L.-J., Barghahn, S., Willmer, M., Thurow, C., and Gatz, C.** (2017). CC-type glutaredoxins recruit the transcriptional co-repressor TOPLESS to TGA-dependent target promoters in *Arabidopsis thaliana*. *Biochim. Biophys. Acta* **1860**: 218–226.
- Ulrich, A.K.C., Schulz, J.F., Kamprad, A., Schütze, T., and Wahl, M.C.** (2016). Structural Basis for the Functional Coupling of the Alternative Splicing Factors Smu1 and RED. *Structure* **24**: 762–773.
- Varlakhanova, N., Hahm, J.B., and Privalsky, M.L.** (2011). Regulation of SMRT corepressor dimerization and composition by MAP kinase phosphorylation. *Molecular and Cellular Endocrinology* **332**: 180–188.
- van der Veen, A.G. and Ploegh, H.L.** (2012). Ubiquitin-like proteins. *Annu. Rev. Biochem.* **81**: 323–357.
- de Vries, J. and Archibald, J.M.** (2018). Plant evolution: landmarks on the path to terrestrial life. *New Phytologist* **217**: 1428–1434.
- Wagner, D. and Meyerowitz, E.M.** (2002). SPLAYED, a novel SWI/SNF ATPase homolog, controls reproductive development in *Arabidopsis*. *Curr. Biol.* **12**: 85–94.
- Walley, J.W., Rowe, H.C., Xiao, Y., Chehab, E.W., Kliebenstein, D.J., Wagner, D., and Dehesh, K.** (2008). The Chromatin Remodeler SPLAYED Regulates Specific Stress Signaling Pathways. *PLoS Pathogens* **4**: e1000237.
- Wang, B., Smith, S.M., and Li, J.** (2018). Genetic Regulation of Shoot Architecture. *Annual Review of Plant Biology* **69**: 437–468.
- Wang, L., Kim, J., and Somers, D.E.** (2013). Transcriptional corepressor TOPLESS complexes with pseudoresponse regulator proteins and histone deacetylases to regulate circadian transcription. *Proc. Natl. Acad. Sci. U.S.A.* **110**: 761–766.
- Wang, L., Wang, B., Jiang, L., Liu, X., Li, X., Lu, Z., Meng, X., Wang, Y., Smith, S.M., and Li, J.** (2015). Strigolactone Signaling in *Arabidopsis* Regulates Shoot Development by Targeting D53-Like SMXL Repressor Proteins for Ubiquitination and Degradation. *Plant Cell* **27**: 3128–3142.
- Wang, X.D., Lapi, E., Sullivan, A., Ratnayaka, I., Goldin, R., Hay, R., and Lu, X.** (2011). SUMO-modified nuclear cyclin D1 bypasses Ras-induced senescence. *Cell Death & Differentiation* **18**: 304–314.
- Wang, Y., Hu, Q., Wu, Z., Wang, H., Han, S., Jin, Y., Zhou, J., Zhang, Z., Jiang, J., Shen, Y., Shi, H., and Yang, W.** (2017). HISTONE DEACETYLASE 6 represses pathogen defence responses in *Arabidopsis thaliana*. *Plant, Cell & Environment* **40**: 2972–2986.
- Wang, Z. et al.** (2016). *Arabidopsis* seed germination speed is controlled by SNL histone deacetylase-binding factor-mediated regulation of AUX1. *Nature Communications* **7**: 13412.

- Wang, Z., Cao, H., Chen, F., and Liu, Y.** (2014). The roles of histone acetylation in seed performance and plant development. *Plant Physiol. Biochem.* **84**: 125–133.
- Watson, A.D.** (2000). Ssn6-Tup1 interacts with class I histone deacetylases required for repression. *Genes & Development* **14**: 2737–2744.
- Watts, B.R., Wittmann, S., Wery, M., Gautier, C., Kus, K., Birot, A., Heo, D.-H., Kilchert, C., Morillon, A., and Vasiljeva, L.** (2018). Histone deacetylation promotes transcriptional silencing at facultative heterochromatin. *Nucleic Acids Res.* **46**: 5426–5440.
- Wei, B., Zhang, J., Pang, C., Yu, H., Guo, D., Jiang, H., Ding, M., Chen, Z., Tao, Q., Gu, H., Qu, L.-J., and Qin, G.** (2015). The molecular mechanism of sporocyteless/nozzle in controlling *Arabidopsis* ovule development. *Cell Res.* **25**: 121–134.
- Wotton, D., Pemberton, L.F., and Merrill-Schools, J.** (2017). SUMO and Chromatin Remodeling. *Adv. Exp. Med. Biol.* **963**: 35–50.
- Wu, M.-F., Sang, Y., Bezhani, S., Yamaguchi, N., Han, S.-K., Li, Z., Su, Y., Slewinski, T.L., and Wagner, D.** (2012). SWI2/SNF2 chromatin remodeling ATPases overcome polycomb repression and control floral organ identity with the LEAFY and SEPALLATA3 transcription factors. *Proceedings of the National Academy of Sciences* **109**: 3576–3581.
- Xiao, Y., Pollack, D., Nieves, E., Winchell, A., Callaway, M., and Vigodner, M.** (2015). Can your protein be SUMOylated? A quick summary and important tips to study SUMO-modified proteins. *Anal. Biochem.* **477**: 95–97.
- Xie, T., He, Y., Korkeamaki, H., Zhang, Y., Imhoff, R., Lohi, O., and Radhakrishnan, I.** (2011). Structure of the 30-kDa Sin3-associated protein (SAP30) in complex with the mammalian Sin3A corepressor and its role in nucleic acid binding. *J. Biol. Chem.* **286**: 27814–27824.
- Xu, Y., Li, S.F., and Parish, R.W.** (2017). Regulation of gene expression by manipulating transcriptional repressor activity using a novel CoSRI technology. *Plant Biotechnology Journal* **15**: 879–893.
- Yang, S., Li, C., Zhao, L., Gao, S., Lu, J., Zhao, M., Chen, C.-Y., Liu, X., Luo, M., Cui, Y., Yang, C., and Wu, K.** (2015). The *Arabidopsis* SWI2/SNF2 Chromatin Remodeling ATPase BRAHMA Targets Directly to *PIN*s and Is Required for Root Stem Cell Niche Maintenance. *The Plant Cell* **27**: 1670–1680.
- Yang, Y., Li, L., and Qu, L.-J.** (2016). Plant Mediator complex and its critical functions in transcription regulation. *J Integr Plant Biol* **58**: 106–118.
- Yao, Y.-L. and Yang, W.-M.** (2003). The metastasis-associated proteins 1 and 2 form distinct protein complexes with histone deacetylase activity. *J. Biol. Chem.* **278**: 42560–42568.

- Yates, G., Srivastava, A.K., and Sadanandom, A.** (2016). SUMO proteases: uncovering the roles of deSUMOylation in plants. *J. Exp. Bot.* **67**: 2541–2548.
- Yoo, C.Y., Miura, K., Jin, J.B., Lee, J., Park, H.C., Salt, D.E., Yun, D.-J., Bressan, R.A., and Hasegawa, P.M.** (2006). SIZ1 small ubiquitin-like modifier E3 ligase facilitates basal thermotolerance in *Arabidopsis* independent of salicylic acid. *Plant Physiol.* **142**: 1548–1558.
- Yoshida, A., Ohmori, Y., Kitano, H., Taguchi-Shiobara, F., and Hirano, H.-Y.** (2012). Aberrant spikelet and panicle1, encoding a TOPLESS-related transcriptional co-repressor, is involved in the regulation of meristem fate in rice. *Plant J.* **70**: 327–339.
- Yruela, I.** (2015). Plant development regulation: Overview and perspectives. *Journal of Plant Physiology* **182**: 62–78.
- Yu, C.-W., Liu, X., Luo, M., Chen, C., Lin, X., Tian, G., Lu, Q., Cui, Y., and Wu, K.** (2011). HISTONE DEACETYLASE6 Interacts with FLOWERING LOCUS D and Regulates Flowering in *Arabidopsis*. *PLANT PHYSIOLOGY* **156**: 173–184.
- Yu, C.-W., Tai, R., Wang, S.-C., Yang, P., Luo, M., Yang, S., Cheng, K., Wang, W.-C., Cheng, Y.-S., and Wu, K.** (2017). HISTONE DEACETYLASE6 Acts in Concert with Histone Methyltransferases SUVH4, SUVH5, and SUVH6 to Regulate Transposon Silencing. *Plant Cell* **29**: 1970–1983.
- Zhan, E., Zhou, H., Li, S., Liu, L., Tan, T., and Lin, H.** (2018). OTS1-dependent deSUMOylation increases tolerance to high copper levels in *Arabidopsis*: OTS1 contributes to Cu tolerance in plants. *Journal of Integrative Plant Biology* **60**: 310–322.
- Zhang, F., Wang, L., Ko, E.E., Shao, K., and Qiao, H.** (2018). Histone Deacetylases SRT1 and SRT2 Interact with ENAP1 to Mediate Ethylene-Induced Transcriptional Repression. *The Plant Cell* **30**: 153–166.
- Zhang, H.** (2006). Metastasis Tumor Antigen Family Proteins during Breast Cancer Progression and Metastasis in a Reliable Mouse Model for Human Breast Cancer. *Clinical Cancer Research* **12**: 1479–1486.
- Zhang, L., Xie, F., Zhang, J., Dijke, P.T., and Zhou, F.** (2017). SUMO-triggered ubiquitination of NR4A1 controls macrophage cell death. *Cell Death Differ.* **24**: 1530–1539.
- Zhang, Y., Iratni, R., Erdjument-Bromage, H., Tempst, P., and Reinberg, D.** (1997). Histone deacetylases and SAP18, a novel polypeptide, are components of a human Sin3 complex. *Cell* **89**: 357–364.
- Zhao, M., Yang, S., Chen, C.-Y., Li, C., Shan, W., Lu, W., Cui, Y., Liu, X., and Wu, K.** (2015). *Arabidopsis* BREVIPEDICELLUS Interacts with the SWI2/SNF2 Chromatin Remodeling ATPase BRAHMA to Regulate KNAT2

and KNAT6 Expression in Control of Inflorescence Architecture. *PLOS Genetics* **11**: e1005125.

Zheng, Y., Schumaker, K.S., and Guo, Y. (2012). SUMOylation of transcription factor MYB30 by the small ubiquitin-like modifier E3 ligase SIZ1 mediates abscisic acid response in *Arabidopsis thaliana*. *Proc. Natl. Acad. Sci. U.S.A.* **109**: 12822–12827.

Zheng, Y.-S., Lu, Y.-Q., Meng, Y.-Y., Zhang, R.-Z., Zhang, H., Sun, J.-M., Wang, M.-M., Li, L.-H., and Li, R.-Y. (2017). Identification of interacting proteins of the TaFVE protein involved in spike development in bread wheat. *Proteomics* **17**.

Zhou, Y. et al. (2013). HISTONE DEACETYLASE19 interacts with HSL1 and participates in the repression of seed maturation genes in *Arabidopsis* seedlings. *Plant Cell* **25**: 134–148.

Zhu, Z., Xu, F., Zhang, Y., Cheng, Y.T., Wiermer, M., Li, X., and Zhang, Y. (2010). *Arabidopsis* resistance protein SNC1 activates immune responses through association with a transcriptional corepressor. *Proceedings of the National Academy of Sciences* **107**: 13960–13965.

List of Abbreviations

ψ	Phi, indicating a large, hydrophobic residue
3-AT	3-Amino-1,2,4-Triazole
4-MUG	4-Methylumbelliferyl- β -D-Glucopyranosiduronic acid
AB	Antibody
AD	Activation domain
APE	A Plasmid Editor
AP2	APETALA2
ASP1	ABERRANT SPIKELET AND PANICLE 1
ASPR1	ASP1 RELATED 1
<i>At</i>	<i>Arabidopsis thaliana</i>
AUX/IAA	AUXIN/INDOLE ACETIC ACID
BD	BINDING DOMAIN
BRM	BRAHMA
bZIP	Basic leucine zipper
C-	Carboxy-
cAMP	Cyclic adenosine monophosphate
cDNA	Complementary DNA
CHD	Chromodomain helicase domain
CIPRES	Cyberinfrastructure for Phylogenetic Research
Col	Columbia
CoREST	Co-repressor of REST
CRA	CT11-RanBPM
CREB	cAMP-responsive element binding
CTLH	C-terminal to LisH
CUC	CUP-SHAPED COTYLEDONS
DNA	Deoxyribonucleic acid
DOC1	DELETED IN ORAL CANCER 1

DRB2	DOUBLE-STRANDED RNA BINDING 2
DRM2	DNA (CYTOSINE-5)-METHYLTRANSFERASE 2
DSS	Disuccinimidyl suberate
<i>E. coli</i>	<i>Escherichia coli</i>
ELM	Egl-27 and MTA1 homology
EPR1	EARLY PHYTOCHROME RESPONSIVE 1
ESD4	EARLY IN SHORT DAYS 4
FA	Formaldehyde
FOG1	Friend of GATA 1
GFP	GREEN FLUORESCENT PROTEIN
<i>Gm</i>	<i>Glycine max</i>
GUS	BETA-GLUCURONIDASE
HA	Haemagglutinin
HAC	HISTONE ACETYLTRANSFERASE
HAD/HDAC	HISTONE DEACETYLASE
HCl	Hydrochloric acid
His	Histidine
HSD	Honest Significant Difference test
JAZ	JASMONATE-ZIM DOMAIN
KDAC	Lysine deacetylase
<i>Kn</i>	<i>Klebsormidium nitens</i>
LB	Lysogeny Broth
LCH	LSD1/CoREST/HDAC
Ler	Landsberg erecta
LUG	LEUNIG
LisH	Lissencephaly homologue
LOB/LBD	LATERAL ORGAN BOUNDARIES
LSD1	Lysine-specific histone demethylase 1
MBD	METHYL CpG BINDING DOMAIN

MeCP	Methyl CpG binding protein
MED	MEDIATOR
MET1	METHYLTRANSFERASE 1
<i>Mp</i>	<i>Marchantia polymorpha</i>
MSI4	MULTICOPY SUPPRESSOR OF IRA4
MTA1	Metastasis Associated 1
MYB	MYELOBLASTOSIS
N-	Amino -
NaCl	Sodium chloride
NEDD	Neural Precursor Cell Expressed, Developmentally Down-Regulated 8
NINJA	NOVEL INTERACTOR OF JAZ
NuRD	Nucleosome Remodelling and histone Deacetylation
<i>Os</i>	<i>Oryza sativa</i>
OTS1/2	OVERLY TOLERANT TO SALT 1 / 2
<i>Pa</i>	<i>Picea abies</i>
PAGE	Polyacrylamid Gel Electrophoresis
PAH	Paired Amphipathic helix
PCR	Polymerase chain reaction
PEG	Polyethylene glycol
PIAL	PROTEIN INHIBITOR OF ACTIVATED STAT-LIKE
PKL	PICKLE
PKR1	PICKLE-RELATED 1
PNPG	1-(4-Nitrophenyl)glycerol
<i>Pp</i>	<i>Physcomitrella patens</i>
<i>Ps</i>	<i>Picocystis salinarum</i>
PTM	Post-Translational Modification
RbAP	Retinoblastoma Associated Protein
RBBP	Retinoblastoma Binding Protein
RD	Repression Domain

REL2	RAMOSA 1 ENHANCER LOCUS 2
RNA	Ribonucleic Acid
RUB	RELATED TO UBIQUITIN
<i>s.l.</i>	<i>Sensu latu</i>
SAP	Sin-Associated Protein
SD	Synthetic Defined
SDS	Sodium dodecyl sulphate
SIZ1	SAP and MIZ1 1
<i>Sl</i>	<i>Solanum lycopersicum</i>
SMG7	Suppressor with morphogenetic effect on genitalia 7
SMU	Suppressor Of Mec-8 And Unc-52
SPF	SUMO PROTEASE RELATED TO FERTILITY1
STUbl	SUMO-targeted ubiquitin ligase
SUMO	SMALL UBIQUITIN-LIKE MODIFIER
SUS3/SUDS3	Suppressor Of Defective Silencing 3
SWI3A	SWITCH/Sucrose non-fermenting 3A
SYD	SPLAYED
TBE	Tris-borate EDTA
TCA	Tricarboxylic acid
TCP	TEOSINTE BRANCHED 1, CYCLOIDEA, PCF
TF	Transcription factor
TIE1	TCP INTERACTOR CONTAINING EAR MOTIF PROTEIN 1
TLE	Transducin-linked enhancer of Split
TPL	TOPLESS
TPR	TOPLESS-RELATED
Tris	Tris(hydroxymethyl)aminomethane
TSA	Trichostatin A
UBL	Ubiquitin-like
UPGMA	Unweighted Pair Group Method with Arithmetic Mean

- 168 -

UPF1	UP Frameshift 1
WOX	WUSCHEL HOMEBOX
Ws	Wassilewskija
XSEDE	Extreme Science and Engineering Discovery Environment
YPDA	Yeast extract, peptone, (dextrose), adenine
Zm	<i>Zea mays</i>

Appendix A

Identification of Repression Domains in annotated transcription factors

Example code

```
"""Find LxLxL and LxLxPP in protein sequences
and blast sequences with motifs against Arabidopsis"""

#Import modules for regular expressions, seq handling
and Blast

import re

import csv

from Bio import SeqIO

from Bio.Seq import Seq

#We will count the number of sequences that have motifs
#The counter is initialised at zero

seqCount = 0

#Open a text file to hold the matching protein IDs and
motifs

outf = open('LxLxL.txt', 'w')

#Create a list of matches

matchList = []
```

- 170 -

```
# We will open peptide sequence data for Klebsormidium
with open("Kfl_pep.fas", "rU") as handle:
```

```
    for record in SeqIO.parse(handle, "fasta"):
        newID=str(record.id)
        newSeq=str(record.seq)
        newSeqLen=len(newSeq)
```

```
# Check for permutations of the EAR motif
motifCheck=re.search('(L.L.(L|PP)|DLN..P|RLFGV',
newSeq)
```

```
    motifCheck=re.search('(L.L.L)', newSeq)
```

```
    if motifCheck:
```

```
        motifString = motifCheck.group(0)
```

```
        print(newID," ",motifString)
```

```
        matchList.append(newID)
```

```
        seqCount = seqCount+1
```

```
#Close the files
```

```
#blastf.close()
```

```
handle.close()
```

```
matchCount=0
```

```
with open("Kfl_TF_list.csv") as pepFile:
```

```
    pepCSV = csv.reader(pepFile)
```

```
    for i in pepCSV:
```

```
        for j in matchList:
```

```
            if i[0] == j:
```

```
                print(i[0],i[2])
```

- 171 -

```
        matchCount = matchCount+1

        outf.write(i[0])

        outf.write("\t")

        outf.write(i[2])

        outf.write("\n")

    print("Match count = ",matchCount)

outf.close()

"""Repeat for the next motif"""

outf = open('DLNxxP.txt', 'w')

#Create a list of matches

matchList = []

with open("Kfl_pep.fas", "rU") as handle:

    for record in SeqIO.parse(handle, "fasta"):

        newID=str(record.id)

        newSeq=str(record.seq)

        newSeqLen=len(newSeq)

#

motifCheck=re.search('(L.L.(L|PP)|DLN..P|RLFGV',

newSeq)

        motifCheck=re.search('(DLN..P)', newSeq)

        if motifCheck:

            motifString = motifCheck.group(0)

            print(newID,"\t",motifString)

            matchList.append(newID)
```

```
seqCount = seqCount+1

#Close the files
#blastf.close()
handle.close()
matchCount=0

with open("Kfl_TF_list.csv") as pepFile:
    pepCSV = csv.reader(pepFile)
    for i in pepCSV:
        for j in matchList:
            if i[0] == j:
                print(i[0],i[2])
                matchCount = matchCount+1
                outf.write(i[0])
                outf.write("\t")
                outf.write(i[2])
                outf.write("\n")
            print("Match count = ",matchCount)
outf.close()

# with open(ListOut.txt) as csv:
#
#     for row in pepFile:
#         print(row[0])

"""Repeat for the next motif"""
```

- 173 -

```
outf = open('RLFGV.txt', 'w')

#Create a list of matches
matchList = []

with open("Kfl_pep.fas", "rU") as handle:
    for record in SeqIO.parse(handle, "fasta"):
        newID=str(record.id)
        newSeq=str(record.seq)
        newSeqLen=len(newSeq)

#
motifCheck=re.search('(L.L.(L|PP)|DLN..P|RLFGV',
newSeq)

        motifCheck=re.search('(RLFGV)', newSeq)
        if motifCheck:
            motifString = motifCheck.group(0)
            print(newID," ",motifString)
            matchList.append(newID)
            seqCount = seqCount+1

#Close the files
#blastf.close()
handle.close()
matchCount=0

with open("Kfl_TF_list.csv") as pepFile:
    pepCSV = csv.reader(pepFile)
```

- 174 -

```
    for i in pepCSV:
        for j in matchList:
            if i[0] == j:
                print(i[0],i[2])
                matchCount = matchCount+1
                outf.write(i[0])
                outf.write("\t")
                outf.write(i[2])
                outf.write("\n")
            print("Match count = ",matchCount)
outf.close()

# Optional printout
# with open(ListOut.txt) as csv:
#
#     for row in pepFile:
#         print(row[0])
```

Appendix B

Low-scoring proteins represented by peptides co-precipitating with HA-TOPLESS

Protein	Confidence (-10lgP)	Sequence coverage (%)	Total peptides	Unique peptides	Average mass
ATP-dependent RNA helicase DEAH12, chloroplastic	18.72	0	1	1	201361
ATP-dependent RNA helicase DEAH11, chloroplastic	18.72	0	1	1	202129
Chromatin structure- remodeling complex protein SPLAYED	18.18	2	3	3	389866
G-type lectin S-receptor-like S/T-protein kinase At4g03230	16.73	1	1	1	96200
ADP-ribosylation factor GTPase-activating protein AGD3	16.53	2	1	1	92524
Pentatricopeptide repeat- containing protein At5g46460, mitochondrial	15.5	1	1	1	78877
Filament-like plant protein 6	15.24	2	1	1	118540
Kinesin-like protein KIN-12D	0	1	2	2	315061
Transcription factor HBI1	0	12	2	2	37747
ATP-dependent helicase BRAHMA	0	1	2	2	245467
Type I inositol polyphosphate 5-phosphatase 5	0	5	2	2	59930
Putative ABC transporter C family member 15	0	1	1	1	117251
ABC transporter G family member 43	0	1	1	1	157642
Helicase and polymerase- containing protein TEBICHI	0	2	2	2	238521
Protein OSCA1	0	2	1	1	87607
Dihydroxy-acid dehydratase,	0	1	1	1	64914

chloroplastic					
Cytosolic sulfotransferase 13	0	2	1	1	37717
Ferrochelatase-1, chloroplastic/mitochondrial	0	3	1	1	52033
Ubiquitin carboxyl-terminal hydrolase 9	0	2	1	1	102649
BEACH domain-containing protein B	0	0	1	1	292777
Poly(A)-specific ribonuclease PARN-like	0	4	1	1	68807
Sulfoquinovosyl transferase SQD2	0	2	1	1	56630
Increased DNA methylation 1	0	2	1	1	131329
DNA repair protein UVH3	0	1	1	1	165667
SMARCA5	0	1	1	1	144332
Probable N- acetylglucosaminyltransferase	0	2	1	1	110114
RAPTOR2	0	1	1	1	147639
Transcription factor LAF1	0	5	1	1	32433
E3 ubiquitin-protein ligase UPL7	0	2	1	1	128486
Extra-large guanine nucleotide-binding protein 2	0	1	1	1	97183
DEAD-box ATP-dependent RNA helicase 28	0	3	1	1	89355
Probable inactive histone- lysine N-methyltransferase SUVR2	0	3	1	1	79363
Histone acetyltransferase HAC12	0	1	1	1	190271
Uncharacterized protein At1g65760	0	4	1	1	41105
Structural maintenance of chromosomes protein 2-2	0	1	1	1	132315
Pyrophosphate--fructose 6- phosphate 1- phosphotransferase subunit beta 2	0	3	1	1	62742
Nuclear transcription factor Y subunit B-7	0	9	1	1	24619
Probable methyltransferase	0	4	1	1	68357

PMT7					
RAN GTPase-activating protein 1	0	5	1	1	58827
Probable LRR-RLK At1g35710	0	2	1	1	124104
Eukaryotic translation initiation factor 3 subunit B	0	3	1	1	81876
Fasciclin-like arabinogalactan protein 8	0	3	1	1	43075
DEAD-box ATP-dependent RNA helicase 21	0	1	1	1	85277
Protein STABILIZED1	0	1	1	1	115576
Gamma-glutamyltranspeptidase 2	0	4	1	1	61600
Probable galacturonosyltransferase-like 8	0	4	1	1	43989
Protein WEAK CHLOROPLAST MOVEMENT UNDER BLUE LIGHT 1	0	1	1	1	89294
Protein trichome birefringence-like 16	0	3	1	1	62316
Transcription termination factor MTERF5, chloroplastic	0	4	1	1	55961
Inactive exonuclease DIS3L2	0	1	1	1	116843
Putative syntaxin-131	0	9	1	1	34720
Protein argonaute 7	0	2	1	1	113397
DDB1- and CUL4-associated factor homolog 1 (DCAF1)	0	1	1	1	205450
Glutamate receptor 3.7	0	3	1	1	103513
E3 ubiquitin-protein ligase UPL2	0	0	1	1	403618
Subtilisin-like protease SBT4.6	0	1	1	1	78802
Nuclear cap-binding protein subunit 1	0	4	1	1	96548
Probable serine/threonine-protein kinase WNK11	0	3	1	1	35531
Phosphatidate cytidyltransferase 1	0	5	1	1	48660
Protein TIC 214	0	1	1	1	213727

Protein RETICULATA-RELATED 6, chloroplastic	0	1	1	1	82252
Brefeldin A-inhibited GEF 5	0	1	1	1	192881
Putative PTR repeat-containing protein At1g28020	0	3	1	1	65310
Probable LRR RL S/T-protein kinase At1g74360	0	1	1	1	121895
Putative wall-associated receptor kinase-like 13	0	2	1	1	85212
SMR domain-containing protein At5g58720	0	3	1	1	56654
Tubby-like F-box protein 2	0	5	1	1	43878
BEACH domain-containing protein A2	0	0	1	1	393327
Origin of replication complex subunit 4	0	7	1	1	47032
Mechanosensitive ion channel protein 4	0	1	1	1	100415
Potassium transporter 9	0	1	1	1	90350
Phosphatidylinositol 4-phosphate 5-kinase 7	0	3	1	1	85955
Auxin transport protein BIG	0	0	1	1	567895
Guanylate kinase 1	0	2	1	1	42668
Probable LRR RL S/T-protein kinase At5g63710	0	3	1	1	68434
F-box protein At2g16365	0	2	1	1	88623
Polygalacturonase 1 beta-like protein 3	0	1	1	1	68060
ATPase 5, plasma membrane-type	0	2	1	1	104739
Translocase of chloroplast 159, chloroplastic	0	1	1	1	160818
Putative respiratory burst oxidase homolog protein H	0	3	1	1	100628
Probable disease resistance protein At5g47260	0	2	1	1	107732
CHD3-type chromatin-remodeling factor PICKLE	0	1	1	1	158405
Myosin-8	0	1	1	1	169493
G-type lectin S-receptor-like S/T-protein kinase SD1-1	0	2	1	1	91875

Probable LRR LRR RL S/T- protein kinase At1g53430	0	1	1	1	114945
Probable metal-nicotianamine transporter YSL5	0	1	1	1	78853

Table B-0-1. Full list of proteins represented by peptide co-immunoprecipitated by HA-TOPLESS using cross-linking with DSS. Proteins associated with chromatin level regulatory functions are highlighted.

Protein	Confidence (-10lgP)	Sequence coverage (%)	Sequence coverage (%)	Unique peptides	Average mass
Topless-related protein 3	56.86	2	2	2	122657
Topless-related protein 1	56.86	2	2	2	124089
Protein TOPLESS	56.86	2	2	2	124298
Topless-related protein 2	56.86	2	2	2	124759
Topless-related protein 4	56.86	2	2	2	124103
Ribulose biphosphate carboxylase large chain	48.63	3	1	1	52955
Mitogen-activated protein kinase 16	30.79	1	1	1	64912
Receptor protein kinase-like protein ZAR1	28.11	1	1	1	78307
Putative PTR repeat-containing protein At5g13230, mitochondrial	24.59	1	1	1	91439
GAPA1, chloroplastic	24.44	4	1	1	42490
Probable WRKY transcription factor 19	16.93	0	1	1	210320
Aspartokinase 3, chloroplastic	16.32	5	1	1	61216
Eukaryotic translation initiation factor 3 subunit B	15.79	3	2	2	81876
Extra-large guanine nucleotide- binding protein 2	15.58	1	1	1	97183
Vacuolar protein sorting- associated protein 35C	15.3	2	1	1	89405
Chromatin structure-remodeling complex protein SPLAYED	15.03	1	1	1	389866
SART-1 family protein DOT2	0	2	1	1	94142
Transcription initiation factor TFIID subunit 1b	0	2	2	2	202251
ADP-ribosylation factor GTPase- activating protein AGD3	0	2	1	1	92524
Auxin transport protein BIG	0	1	2	2	567895
DDB1- and CUL4-associated factor homolog 1 (DCAF1)	0	1	2	2	205450
S-(+)-linalool synthase, chloroplastic	0	2	1	1	65401

Exonuclease DPD1, chloroplastic/mitochondrial	0	3	1	1	35248
Protein OSCA1	0	2	1	1	87607
Disease resistance protein RPS4	0	2	1	1	137725
Putative syntaxin-131	0	9	1	1	34720
Probable pectinesterase/pectinesterase inhibitor VGDH2	0	3	1	1	62958
Chaperone protein ClpD, chloroplastic	0	3	1	1	103235
Wall-associated receptor kinase- like 17	0	2	1	1	87304
Trafficking protein particle complex II-specific subunit 120 homolog	0	1	1	1	129595
RAPTOR2	0	1	1	1	147639
Protein CHROMATIN REMODELING 8	0	1	1	1	133592
Protein PLASTID MOVEMENT IMPAIRED 1-RELATED 2	0	2	1	1	107939
Uncharacterized protein At4g38062	0	1	1	1	122709
Probable indole-3-pyruvate monooxygenase YUCCA10	0	3	1	1	42387
MAP3K epsilon protein kinase 2	0	1	1	1	151136
ATM	0	1	1	1	435117
Myosin-12	0	1	1	1	176969
Lon protease homolog 3, mitochondrial	0	3	1	1	103476
RUNKEL	0	1	1	1	152283
PHD finger protein At2g01810	0	1	1	1	79480
Nuclear pore complex protein NUP205	0	2	1	1	206727
Putative ABC transporter C family member 15	0	2	1	1	117251
1-aminocyclopropane-1- carboxylate synthase 2	0	3	1	1	55532
G-type lectin S-receptor-S/T- protein kinase At1g11280	0	2	1	1	91337
BTB/POZ domain-containing protein At3g22104	0	4	1	1	57386

Glutamate synthase 1 [NADH], chloroplastic	0	1	1	1	241897
Filament-like plant protein 6	0	2	1	1	118540
Transcription factor HBI1	0	12	1	1	37747
Probable disease resistance protein At5g47250	0	1	1	1	94801
Kinesin-like protein KIN-5C	0	2	1	1	113683
Uncharacterized protein At1g65760	0	4	1	1	41105
Histone acetyltransferase HAC12	0	1	1	1	190271
ABC transporter C family member 9	0	1	1	1	168209
Probable inactive lysine-specific demethylase JMJ19	0	3	1	1	79304
B3 domain-containing transcription factor NGA2	0	6	1	1	34270
Probable thimet oligopeptidase	0	3	1	1	80291
UTP--glucose-1-phosphate uridylyltransferase 3, chloroplastic	0	2	1	1	99043
ENHANCER OF AG-4 protein 2	0	1	1	1	151078
Transcription factor PIF4	0	4	1	1	48363
Exportin-T	0	1	1	1	111462
WPP domain-associated protein	0	2	1	1	94604
Acyl-CoA-binding domain-containing protein 4	0	3	1	1	73075
Protein QUIRKY	0	4	1	1	121413
Protein SPA1-RELATED 4	0	4	1	1	89071
Probable ubiquitin-like-specific protease 2A	0	1	1	1	87796
Kinesin-5	0	2	1	1	89194
Transcription initiation factor TFIID subunit 4	0	1	1	1	80641
PTR repeat-containing protein At1g07740, mitochondrial	0	2	1	1	52295
Cysteine-rich repeat secretory protein 26	0	11	1	1	30332
Homeobox-leucine zipper protein HDG4	0	4	1	1	79277
DEXH-box ATP-dependent RNA helicase DEXH7, chloroplastic	0	1	1	1	163599

Callose synthase 5	0	0	1	1	220659
UDP-D-xylose:L-fucose alpha-1,3-D-xylosyltransferase 1	0	5	1	1	41174
Protein SUPPRESSOR OF MAX2 1	0	2	1	1	108710
Heat shock 70 kDa protein 9, mitochondrial	0	1	1	1	73075
Acetyl-CoA carboxylase 2	0	1	1	1	262726
Glutamate receptor 2.2	0	2	1	1	102847
Nuclear pore complex protein NUP155	0	1	1	1	160013
Pentatricopeptide repeat-containing protein At2g44880	0	1	1	1	63260
Inositol oxygenase 1	0	5	1	1	36574
Paired amphipathic helix protein Sin3-like 1	0	1	1	1	156208
Probable RNA helicase SDE3	0	1	1	1	113363
Anaphase-promoting complex subunit 2	0	1	1	1	97790
NAC domain-containing protein 73	0	2	1	1	33697

Table B-2. Full list of proteins represented by peptide co-immunoprecipitated by HA-TOPLESS using cross-linking with formaldehyde. Proteins associated with chromatin level regulatory functions are highlighted in peach, while the SUMO protease ULP2A is highlighted in blue.

Appendix C

Oligonucleotides used in this thesis

Name	Sequence	Application
35S_ECORI_F_1	ATCGAGAATTCGTCCGATGTGAGACTTTTCAACA AAG	Amplification of 35S promoter from Alligator III
35S_ECORI_AT TB5R_R_1	GGGGACAACCTTTGTATACAAAAGTTGTTCTCTC CAAATGAAATGAACTTCCTTATATAG	Amplification of 35S promoter from Alligator III
EPR1_B1_F1	GGGGACAAGTTTGTACAAAAAAGCAGGCTACAT GCTCTGTTTTGTTTCGCT	Amplification of EPR1
EPR1_B2_R1	GGGGACCACTTTGTACAAGAAAGCTGGGTACTA GCATATACGTGCTCTTTGG	Amplification of EPR1
TPL_MGW_ATT B1_1	GGGGACAAGTTTGTACAAAAAAGCAGGCTACGG TGTGTGGGAAAGGAGCAAAACC	Cloning of <i>Arabidopsis pTPL::TPL</i> and <i>TPL CDS</i>
TPL_MGW_ATT B2_1	GGGGACCACTTTGTACAAGAAAGCTGGGTATCA TCTCTGAGGCTGATCAGATGC	Cloning of <i>Arabidopsis pTPL::TPL</i> and <i>TPL CDS</i>
4426 OTS1-1 LC16	CGACAAGAAGTGGTTTAGACC	Genotyping of <i>ots1 ots2</i> mutants
4427 OTS1-1 LC17	GTAACGTAACACTTATTAGATGCC	Genotyping of <i>ots1 ots2</i> mutants
4676 R_OTS2- 1_LC18	GACAGGGATGCATATTTTGTGAAG	Genotyping of <i>ots1 ots2</i> mutants
4677 F_OTS2- 1_LC15	TTAATCTGTTTGGTTACCCTTGCGG	Genotyping of <i>ots1 ots2</i> mutants
3277 LB1A	TGGTTCACGTAGTGGGCCATCG	Genotyping of <i>Salk insertion line</i> mutants
SIZ1-2_LP1	GAGCTGAAGCATCTGGTTTTG	Genotyping of <i>siz1-2</i>
SIZ1-2_RP1	CACGACAGATGAAGCATTGTG	Genotyping of <i>siz1-2</i>
TPL-092730- LP1	CAGACCCTGCTTCTAGGTGTG	Genotyping of <i>tpl</i>
TPL-092730- RP1	TTGTTCATGTACCTGGAGGC	Genotyping of <i>tpl</i>
TPR1_ZHU_F2	AAGACATGAGGCAACTTGATTTGATT	Genotyping of <i>tpr1</i> from Zhu et al. (2010)
TPR1_ZHU_R1	GTTACAACAACGCCGGTGAC	Genotyping of <i>tpr1</i> from Zhu et al. (2010)
TPR2-112730- F3	CGGTCTGCACAAACATCCAA	Genotyping of <i>tpr2</i>
TPR2-112730- R3	TTCAAAAGACCGCGCTTCAA	Genotyping of <i>tpr2</i>
TPR3-029936- F2	TCTTGTTGGATCTGCGACGG	Genotyping of <i>tpr3</i>
TPR3-029936- R2	AAAGCCAAGTCGTTACAGC	Genotyping of <i>tpr3</i>

TPR4-150008-LP1	TGTTCCACCAAAGAAAAACG	Genotyping of <i>tpr4</i>
TPR4-150008-RP1	TTAATCTCTTTCTCGGGAGCC	Genotyping of <i>tpr4</i>
2XUAS_ATT B1_ECORI	GGGGACAAGTTTGTACAAAAAAGCAGGCTCTCG GAGTACTGTCCTCCGAGCGGAGTACTGTCCTCC GG	Oligos were annealed to produce two UAS for repression assay reporter construct
2XUAS_ATT B1_ECORI_REVERSE	AATTCGGAGGACAGTACTCCGCTCGGAGGACA GTA TCCGAGAGCCTGCTTTTTGTACAAACTTG TCCCC	Oligos were annealed to produce two UAS for repression assay reporter construct
TPL-REPAIR-F1	TTCCGTGATAAATTGCAGTCCCTAC	Primers to repair non-synonymous mutation in <i>TPL</i>
TPL-REPAIR-R1	TAAAGGATTCGCCTCAATCAGC	Primers to repair non-synonymous mutation in <i>TPL</i>
QRT-ACT2_F1	GGTAACATTGTGCTCAGTGGTGG	Quantitative PCR for Actin2
QRT-ACT2_R1	CTGTGAACGATTCCTGGACC	Quantitative PCR for Actin2
ARR5_QPCR_F1	TCAGAGAACATCTTGCCTCGT	Quantitative PCR for ARR5
ARR5_QPCR_R1	ATTTACAGGCTTCAATAAGAAATC,	Quantitative PCR for ARR5
GATA23_QPCR_F1	CAATTAGGTGTTGCAGTGAGTGT	Quantitative PCR for GATA23
GATA23_QPCR_R1	TTTCTGTGTCTAATCCACATGC	Quantitative PCR for GATA23
GUS_QRT_F1	AGTCAACGGGGAAACTCAGC	Quantitative PCR for GUS reporter
GUS_QRT_R1	GCGAAATATCCCGTGCACC	Quantitative PCR for GUS reporter
IAA12_QPCR_F1	GCTTCTCCTCCTCGTTCAAGT	Quantitative PCR for IAA12
IAA12_QPCR_R1	GCTGCCTTCATAGCTTGGTT	Quantitative PCR for IAA12
IAA14_QPCR_F1	CAAAGATGGTGACTGGATGC	Quantitative PCR for IAA14
IAA14_QPCR_R1	GCATGACTCGACAAACATCG	Quantitative PCR for IAA14
TPL-GAL4_QRT_F1	GAGAACGGGTCGGCTAGC	Quantitative PCR for TPL-GAI4BD repressor
TPL-GAL4_QRT_R1	GTTCTTCAGACACTTGGCGC	Quantitative PCR for TPL-GAI4BD repressor
ATTPL_SEQF1	TTGTGTGTGTGAAAAGATACC	Sequencing of <i>Arabidopsis pTPL::TPL</i>
ATTPL_SEQF2	TTCTTGAGAGTGTATGGTGC	Sequencing of <i>Arabidopsis pTPL::TPL</i>
ATTPL_SEQF3	GGATTATCGCACAGTTACCGG	Sequencing of <i>Arabidopsis pTPL::TPL</i>
ATTPL_SEQF4	TTTGTGTGCGCTCATAACG	Sequencing of <i>Arabidopsis pTPL::TPL</i>
ATTPL_SEQF5	TTATTGCCCATCTCCATCG	Sequencing of <i>Arabidopsis pTPL::TPL</i>
ATTPL_SEQF6	CGAGAAGAAAGACGACGTAGC	Sequencing of <i>Arabidopsis pTPL::TPL</i>
ATTPL_SEQF7	CACCTCTTTCGTCTCTGTGG	Sequencing of <i>Arabidopsis pTPL::TPL</i>
ATTPL_SEQF8	TTGCTTTGTCATGTT CAGGC	Sequencing of <i>Arabidopsis pTPL::TPL</i>
ATTPL_SEQF9	AAGCTGATTGAGGCGAATCC	Sequencing of <i>Arabidopsis pTPL::TPL</i>
ATTPL_SEQF10	TTGAAGCACCCGAGA ACTCC	Sequencing of <i>Arabidopsis pTPL::TPL</i>

ATTPL_SEQF11	CCTGACGGTTCCTTGTTTGG	Sequencing of <i>Arabidopsis pTPL::TPL</i>
ATTPL_SEQF12	GGCTATTCTCTTGTGGGACG	Sequencing of <i>Arabidopsis pTPL::TPL</i>
ATTPL_SEQF13	TCGATCAGCCAATGTAGTTTCC	Sequencing of <i>Arabidopsis pTPL::TPL</i>
ATTPL_SEQF14	CATATGTAATGTCAGCCTCCGG	Sequencing of <i>Arabidopsis pTPL::TPL</i>
ATTPL_SEQF15	GCTCACTTCCTCGTTGTGC	Sequencing of <i>Arabidopsis pTPL::TPL</i>
ATTPL_SEQR1	ACCATCACACACGTAAGC	Sequencing of <i>Arabidopsis pTPL::TPL</i>
ATTPL_SEQR2	GACATCCAACCAGCAAGAGG	Sequencing of <i>Arabidopsis pTPL::TPL</i>
TPL_SDM_FKA		Site directed mutagenesis of genomic
P_F1	TCTCCGGCTTTCAGAGCACCTGACG	<i>TPL</i> at K2339
TPL_SDM_FKA		Site directed mutagenesis of genomic
P_R1	ATGACCATGGCCTGCCCTGAAAATG	<i>TPL</i> at K2339
TPL_SDM_LKH		Site directed mutagenesis of genomic
P_F1	ATAGCGGCGTTGAGGCACCCGAG	<i>TPL</i> at K282
TPL_SDM_LKH		Site directed mutagenesis of genomic
P_R1	ACCAAAGATAGGAAAGGAGTCCATTGTAAGC	<i>TPL</i> at K282
TPL_SDM_VKE		Site directed mutagenesis of genomic
P_F1	TGCTCTGGTGAGAGAACCTGTCTTC	<i>TPL</i> at K414
TPL_SDM_VKE		Site directed mutagenesis of genomic
P_R1	GCCTGAAGATACAATAATTCAGTCACTGTAG	<i>TPL</i> at K414
TPL_CDS_LRH		Site directed mutagenesis of <i>TPL</i>
P_F1	GCGGCGTTGAGGCACCCGAGA	<i>CDS</i> at K282
TPL_CDS_LRH		Site directed mutagenesis of <i>TPL</i>
P_R1	TGGGATTGATGGACCACCAAGTG	<i>CDS</i> at K282
TPL_CDS_FRA		Site directed mutagenesis of <i>TPL</i>
P_F1	CCGGCTTTCAGAGCACCTGAC	<i>CDS</i> at K339
TPL_CDS_FRA		Site directed mutagenesis of <i>TPL</i>
P_R1	AGAATGACCATGGGCCTG	<i>CDS</i> at K339
TPL_CDS_VKE		Site directed mutagenesis of <i>TPL</i>
P_F1	CTCTGGTGAAGGAACCTGTCTG	<i>CDS</i> at K414
TPL_CDS_VKE		Site directed mutagenesis of <i>TPL</i>
P_R1	CAGCCTGCAAGGGCATTG	<i>CDS</i> at K414

Table C-0-1. List of oligonucleotides used in this thesis and their applications.

Appendix D

Constructs used in this thesis

Name	Vector	Assembly method	Insert	Other elements	Antibiotic resistance
pDONR201- <i>pTPL::TPL</i>	pDONR201	Gateway BP Clonase recombination	Genomic contig including promoter region and gene (nucleotides -4951 to +5274)	None	Kanamycin resistance
pUC19- <i>TPL</i> Q164STOP	pUC19	Restriction digestion and ligation	Genomic fragment of <i>TPL</i> restricted from pDONR201- <i>pTPL::TPL</i> (-215 to +4313) that included an introduced mutation at +799 (CAG -> TAG)	None	Ampicillin resistance
pUC19- <i>TPL</i>	pUC19	Site-directed mutagenesis	Genomic fragment of <i>TPL</i> restricted from pDONR201- <i>pTPL::TPL</i> (-215 to +4313 (mutation reversed by SDM)	None	Ampicillin resistance
<i>pTPL::TPL</i>	Alligator V	Gateway LR Clonase recombination	Genomic contig including <i>TPL</i> promoter region and gene (nucleotides -4951 to +5274)	None	Spectinomycin resistance
<i>pTPL::TPL</i> K282R	Alligator V	Site-directed mutagenesis	Genomic contig including <i>TPL</i> promoter region and gene with K282R mutation	None	Spectinomycin resistance
<i>pTPL::TPL</i> K339R	Alligator V	Site-directed mutagenesis	Genomic contig including <i>TPL</i> promoter region and gene with K339R mutation	None	Spectinomycin resistance
<i>pTPL::TPL</i> K414R	Alligator V	Site-directed mutagenesis	Genomic contig including <i>TPL</i> promoter region and gene with K414R mutation	None	Spectinomycin resistance
<i>pTPL::TPL</i> K282R K339R	Alligator V	Site-directed mutagenesis	Genomic contig including <i>TPL</i> promoter region and gene with K282R and K339R mutations	None	Spectinomycin resistance
<i>pTPL::TPL</i> K282R K414R	Alligator V	Site-directed mutagenesis	Genomic contig including <i>TPL</i> promoter region and gene with K282R and K414R mutations	None	Spectinomycin resistance
<i>pTPL::TPL</i> K339R K414R	Alligator V	Site-directed mutagenesis	Genomic contig including <i>TPL</i> promoter region and gene with K339R and K414R mutations	None	Spectinomycin resistance
<i>pTPL::TPL</i> K282R K339R K414R	Alligator V	Site-directed mutagenesis	Genomic contig including <i>TPL</i> promoter region and gene with K282R, K339R and K414R mutations	None	Spectinomycin resistance
<i>35S::HA-TPL</i>	Alligator II	Gateway LR Clonase recombination	<i>TPL</i> CDS including start and stop codons cloned downstream of <i>35S</i> promoter and 5' <i>3xHA</i> tags	<i>35S</i> ; <i>3xHA</i>	Kanamycin resistance

pDONR221- 2xUAS	pDONR221	Gateway BP Clonase recombination	2 x upstream activation sequences (assembled by ligation)	N/A	Kanamycin resistance
pDONR221- 2xm35S	pDONR221	Gateway BP Clonase recombination	Minimal 35S promoter	N/A	Kanamycin resistance
2xUAS- 35S::GUS	pJAWOHL II	Gateway LR Clonase recombination	2xUAS and minimal 35S promoters cloned into pJAWOHL II Gateway cassette upstream of GUS reporter	35S	Kanamycin resistance
<i>tCUP</i>	pEX-A2	Restriction digestion and ligation	Synthesised tCUP promoter cloned into multiple cloning site	N/A	Kanamycin resistance
pDONR221- TPL_nostop	pDONR221 P1-P5r	Gateway BP Clonase recombination	TPL coding sequence lacking stop codon	N/A	Kanamycin resistance
pDONR221- Gal4BD	pDONR221 P5-P2	Gateway BP Clonase recombination	Gal4BD lacking start codon	N/A	Kanamycin resistance
Alligator III ^t	Alligator III	Restriction digestion and ligation	No insert; 35S promoter excised and replaced with <i>tCUP</i> promoter	N/A	Spectinomycin resistance
<i>tCUP</i> ::TPL- Gal4BD	Alligator III ^t	Gateway LR Clonase recombination	TPL coding sequence lacking stop codon with C-terminal Gal4BD fusion	N/A	Spectinomycin resistance
<i>tCUP</i> ::TPL- Gal4BD K282R	Alligator III ^t	Gateway LR Clonase recombination	TPL coding sequence (lacking stop codon) with K282R mutation with C- terminal Gal4BD fusion	N/A	Spectinomycin resistance
35S::TPL- Gal4BD	Alligator III	Gateway LR Clonase recombination	TPL coding sequence lacking stop codon with C-terminal Gal4BD fusion	N/A	Spectinomycin resistance
pDONR221- SUMO1	pDONR221	Gateway BP Clonase recombination	Complete SUMO1 coding sequence. Kindly provided by Barry Causier	N/A	Kanamycin resistance
BD-TPL	pGBKT7 (Gateway)	Gateway LR Clonase recombination	Complete coding sequence. Kindly provided by Barry Causier	ADH1 promoter; Gal4BD	Kanamycin resistance
AD-TPL	pGADT7 (Gateway)	Gateway LR Clonase recombination	Complete coding sequence. Kindly provided by Barry Causier	ADH1 promoter; Gal4AD	Ampicillin resistance
BD-HDA19	pGBKT7 (Gateway)	Gateway LR Clonase recombination	Complete coding sequence. Kindly provided by Barry Causier	ADH1 promoter; Gal4BD	Kanamycin resistance
AD-HDA19	pGADT7 (Gateway)	Gateway LR Clonase recombination	Complete coding sequence. Kindly provided by Barry Causier	ADH1 promoter; Gal4AD	Ampicillin resistance
BD-TPL-SUMO	pGBKT7 (Gateway)	Gateway LR Clonase recombination	TPL coding sequence with C-terminal SUMO1 coding sequence fusion	ADH1 promoter; Gal4BD	Kanamycin resistance
BD-UPF1	pGBKT7 (Gateway)	Gateway LR Clonase recombination	Complete coding sequence. Kindly provided by Barry Causier	ADH1 promoter; Gal4BD	Kanamycin resistance
AD-SMG7	pGADT7 (Gateway)	Gateway LR Clonase recombination	Complete coding sequence. Kindly provided by Barry Causier	ADH1 promoter; Gal4AD	Ampicillin resistance

<i>SCE1</i>	pTFT (Gateway)	Gateway LR Clonase recombination	Complete coding sequence. Kindly provided by Barry Causier	<i>ADH1</i> promoter	Kanamycin resistance
<i>HDA19</i>	pGADT7 (Gateway)	Gateway LR Clonase recombination	Complete coding sequence. Kindly provided by Barry Causier	<i>ADH1</i> promoter; <i>Gal4AD</i>	Ampicillin resistance
pDONR207- <i>EPR1</i>	pDONR207	Gateway BP Clonase recombination	Complete coding sequence from cDNA	N/A	Gentamycin resistance
<i>EPR1</i>	pTFT (Gateway)	Gateway LR Clonase recombination	Complete coding sequence from cDNA	Yeast constitutive promoter	Kanamycin resistance
BD- <i>TPR2</i>	pGBKT7 (Gateway)	Gateway LR Clonase recombination	Complete coding sequence from cDNA	<i>Gal4BD</i>	Kanamycin resistance
BD- <i>TPR3</i>	pGBKT7 (Gateway)	Gateway LR Clonase recombination	Complete coding sequence from cDNA	<i>Gal4BD</i>	Kanamycin resistance
BD- <i>TPR4</i>	pGBKT7 (Gateway)	Gateway LR Clonase recombination	Complete coding sequence from cDNA	<i>Gal4BD</i>	Kanamycin resistance
<i>35S::mCherry- TPL-3xFLAG</i>	pB7m34GW	Gateway LR Clonase recombination	<i>TPL</i> coding sequence lacking start and stop codons. Kindly provided by Antoine Larrieu	N-terminal <i>mCherry</i> ; C-terminal 3xFLAG	Glufosinate resistance

Table D-0-1. List of constructs used in this thesis.